ORS 46th International Sun Valley Workshop: Musculoskeletal Biology

Abstract Book

August 7 – August 10, 2016

Sun Valley, Idaho

The ORS would like to thank the following supporters

of the

46th International Sun Valley Workshop

Level 1

NIH

NSF

Level 2

Alexion Pharmaceuticals

UCB

Level 3

BIOQUANT Image Analysis Corporation

Charles River Laboratories

Micro Photonics Inc.

Novartis

OsteoMetrics

Scanco Medical

Swissray International

Ultragenyx Pharmaceutical Inc.

Zimmer-Biomet

The ORS would like to recognize the following people who participated in the mentor program and thank

BIOQUANT Image Analysis Corporation

for their support.

Mentees	Mentors
Naga Suresh Adapala	Teresita Bellido, PhD
Alessandra Carriero	David Burr, PhD
Erixa Du	Steven Cummings, PhD
Carl Gustafson	Eve Donnelly, PhD
Hadla Hariri	Matthew Drake, MD, PhD
Nilsson Holguin	Leonard Freedman, PhD
Minyi Hu	Mark Hamrick, PhD
Amira Hussein	Teppo Jarvinen, MD, PhD
Youngjae Jeong	Michaela Kneissel, PhD
Kyu San Joeng	Gary Krishnan, MSc, PhD
Courtney Karner	Nancy Lane, MD
Yohei Kawakami	Olivier Leupin, PhD
Ayse Serra Kaya	Robert Majeska
Alexander Kot	Gloria Matthews
Takamitsu Maruyama	Marjolein van der Meulen, PhD
Emily Moore	Jose Millan
Stacyann Morgan	Scott Miller
Muhammad Farooq Rai	David Mooney, PhD
Saravana Ramasamy	Jeffry Nyman, PhD
Kelly Lauter Roszko	Munro Peacock
Irene Simfia	Alex Robling
Roman Thaler	David Roodman, MD, PhD
Ryan Tomlinson	Jess Snedeker, PhD
Mustafa Unal	David Thompson
Ke Wang	Bart Williams, PhD
Daniel Whitney	Kerri Winters-Stone

ORS 46th International Sun Valley Workshop – Sun Valley, Idaho – August 7-10, 2016

Disclosure Index

Continuing Medical Education (CME) Credit

This activity has been planned and implemented in accordance with the accreditation requirements and policies of the Accreditation Council for Continuing Medical Education (ACCME) through the joint providership of the American Academy of Orthopaedic Surgeons and the Orthopaedic Research Society. The American Academy of Orthopaedic Surgeons is accredited by the ACCME to provide continuing medical education for physicians.

The American Academy of Orthopaedic Surgeons designates this live activity for a maximum of 20 ***AMA PRA Category 1 Credits™***. Physicians should claim only the credit commensurate with the extent of their participation in the activity.

Attendees will be able to claim CME from the ORS 46th International Sun Valley Workshop by completing the CME form on the ORS 46th International Sun Valley Workshop website following the meeting.

Disclosure Statement

Faculty, or a member of their immediate family, who have received something of value from any pharmaceutical, biomaterial or orthopaedic product or device company, supplier, institution, or orthopaedic publisher, which relates directly or indirectly to the subject of their presentation, are listed in the disclosure index. The Orthopaedic Research Society does not intend this identification to decrease the value of the presentation or to imply bias. It is intended solely for information.

To follow ACCME guidelines the Orthopaedic Research Society/AAOS has identified the options to disclose as follows:

Research or institutional support has been received;

Nothing to Disclose - The author (or a member of their immediate family) does not have a financial interest or other relationship with any pharmaceutical, biomaterial or orthopaedic product or device company, supplier, institution, or orthopaedic publisher.

1. Do you or a member of your immediate family receive royalties for any pharmaceutical, biomaterial or orthopaedic product or device?
2. Within the past twelve months, have you or a member of your immediate family served on the speakers bureau or have you been paid an honorarium to present by any pharmaceutical, biomaterial or orthopaedic Product or device company?

3A. Are you or a member of your immediate family a paid employee for any pharmaceutical, biomaterial or orthopaedic device or equipment company, or supplier?

3B. Are you or a member of your immediate family a paid consultant for any pharmaceutical, biomaterial or orthopaedic device or equipment company or supplier?

3C. Are you or a member of your immediate family an unpaid consultant for any pharmaceutical, biomaterial or orthopaedic device or equipment company, or supplier?

4. Do you or a member of your immediate family own stock or stock options in any pharmaceutical, biomaterial or orthopaedic device or equipment company or supplier (excluding mutual funds)?
5. Do you or a member of your immediate family receive research or institutional support as a principal investigator from any pharmaceutical, biomaterial or orthopaedic device or equipment company, or supplier?
6. Do you or a member of your immediate family receive any financial/material support from any pharmaceutical, biomaterial or orthopaedic device or equipment company, or supplier?
7. Do you or a member of your immediate family receive any royalties, financial/material support from any medical and/or orthopaedic publishers?

8. Do you or a member of your immediate family serve on the editorial or governing board of any medical and/or orthopaedic publication?
9. Do you or a member of your immediate family serve on any Board of Directors, as an owner, or officer on a relevant committee of any health care organization (e.g., hospital, surgery center, medical and/or orthopaedic professional society)?

An indication of the participant's disclosure appears after his or her name in the Disclosure Index.
For example:
Smith, J (1-Industrial Grant); Jones, M (1-Industrial Grant); Davis, S Nothing to disclose

The Orthopaedic Research Society does not view the existence of these disclosed interests or commitments as necessarily implying bias or decreasing the value of the author's participation in the course.

Sun Valley Advisory Board, Planning Committee and ORS Staff

Teresita Bellido, PhD (Nothing to disclose)

Susan Bloomfield, PhD (Nothing to disclose)

David B. Burr, PhD (8- Current Osteoporosis Reports, BONE, JBMR, Osteoporosis International, J Orthop Research, J of Bone and Mineral Metabolism, Calcified Tissue International; 9- Editorial Board, JOR)

Eve Donnelly, PhD (Nothing to disclose)

Lorena Havill, PhD (Nothing to disclose)

Mary Jo Heflin (Nothing to disclose)

Eric Hesse, MD, PhD (2- Amgen, Lilly; 8- JBMR, Gene, ECED)

Natalie Hinman (Nothing to disclose)

Laura McCabe, PhD (Nothing to disclose)

Jola Lewsza (Nothing to disclose)

Scott Miller, PhD (8- Associate Editor of The Anatomical Record; 9- Chair, Scientific Affairs Committee of the American Association of Anatomists)

Jeffrey Nyman, PhD (3c- My lab has tested mouse bones for Genzyme, and I have provided interpretation of the biomechanical properties; 6- Genzyme has paid my department for services my lab provide. ActiveLife Scientific has loaned my lab an indentation instrument for a clinical trial; 8- I am on the editorial board of the journal Bone)

Alexander G. Robling, PhD (Nothing to disclose)

Elizabeth Shane, MD (Nothing to disclose)

Matt Zuleg (Nothing to disclose)

Sun Valley Speakers and Poster Presenters

Ralf H. Adams, PhD (Nothing to disclose)

Naga Suresh Adapala, PhD (Nothing to disclose)

Adil Shahzad Ahmed, MD (Nothing to disclose)

Ozan Akkus, PhD (Nothing to disclose)

Erik Lawrence Antonsen, MD, PhD (Nothing to disclose)

Olumide Aruwajoye, PhD (Nothing to disclose)

Guniz Bas, BSc (Nothing to disclose)

Jelena Basta-Pljakic, MSc (Nothing to disclose)

Teresita Bellido, PhD (Nothing to disclose)

Kevin C. Blank, MSc (Nothing to disclose)

Susan Bloomfield, PhD, FACSM (5- MTA's from Novartis (zoledronate); from Eli Lilly (sclerostin antibody)MTA's from Novartis (zoledronate); from Eli Lilly (sclerostin antibody))

Hans Bräuner-Osborne (Nothing to disclose)

Jonathan Todd Bravman, MD (1-Shukla Medical; 3b-Smith&Nephew, DJO Global; 5-Stryker (Research/fellowship Support), Smith&Nephew (fellowship support), Depuy/Mitek (fellowship support), Stryker (Research/fellowship Support), Smith&Nephew (fellowship support), Depuy/Mitek (fellowship support); 9- Western Orthopedic Association)

Tyler J. Brenneman, BSc (Nothing to disclose)

Raquel Brown, MS Molecular Biology (Nothing to disclose)

Whitney A. Bullock, BA (Nothing to disclose)

Alessandra Carriero, PhD (Nothing to disclose)

Deven Michael Carroll, MSc (Nothing to disclose)

A. Nicole Chang, MS (Nothing to disclose)

Joseph C. Chavarria, BSc (Nothing to disclose)

Nobuaki Chinzei, MD, PhD (Nothing to disclose)

Thomas L. Clemens, PhD (8- Executive Editor, Bone Research)

Margaret E. Cooke, MD (Nothing to disclose)

Steven R. Cummings, MD (3b- Consultant on advisory boards to Amgen, Radius, and Merck)

Vishwa Deepak, PhD (Nothing to disclose)

Serkalem Demissie, PhD (Nothing to disclose)

Matthew T. Drake, MD, PhD (8- Editorial boad member of 1) Journal of Bone and Mineral Research; 2) Bone; 3) Journal of Clinical Endocrinology and Metabolism; and 4) Mayo Clinic Proceedings)

Hicham Drissi, PhD (Nothing to disclose)

Erxia Du, PhD (Nothing to disclose)

Rachel E. Embry (Nothing to disclose)

David Estrada, PhD (Nothing to disclose)

Jian Q. Feng, PhD (Nothing to disclose)

Leonard Freedman, PhD (5- ATCC and its foundation BioNexus supports GBSI.ATCC and its foundation BioNexus supports GBSI)

Kiyo Fujimoto, BS (Nothing to disclose)

Maxime A. Gallant, PhD (3b- My wife; Relypsa; 5- My wife: Relypsa)

Tom Gardella (Nothing to disclose)

Louis Gerstenfeld, PhD (8- JOR and Bone)

Daniel Evan Gibbons, BEng (Nothing to disclose)

David Anthony Gonzales, BSc (3a- My mother is an independent sales representative for Thompson Surgical Retractor; 4- I own 4 shares of Celldex Therapeutics Inc)

Carl Thomas Gustafson, BSc (Nothing to disclose)

Mark Hamrick, PhD (nothing to disclose)

Xianglong Han, DDS (Nothing to disclose)

Fadil M. Hannan, PhD (Nothing to disclose)

Hadla Mohamad Hariri, PhD (Nothing to disclose)

Mitchell R. Hoge, BS (3a- Intern at Eli Lilly and Company)

Brenna L. Hogue, MS (Nothing to disclose)

Nilsson Holguin, PhD (Nothing to disclose)

Daniel J. Horan, MS (Nothing to disclose)

Darby Adele Houck (Nothing to disclose)

Sarah A. Howles (Nothing to disclose)

Wei Hsu, PhD (8- Editorial Board; International Journal of Women's Health, Cancer Management and Research, Breast Cancer - Targets and Therapy, Human Genetics & Embryology: Current Research
Hereditary Genetics, Transcriptomics, JSM Regenerative Medicine, International Journal of Stem Cell Research and Transplantation, Associate Editor; PLOS Genetics)

Minyi Hu, PhD (Nothing to disclose)

Yuan Hui, DDS (Nothing to disclose)

Marja Hurley, MD (Nothing to disclose)

Amira I. Hussein, PhD (Nothing to disclose)

Teppo Jarvinen, MD, PhD (2- AMGEN, honorarium donated to AllTrials campaign)

Christopher R. Jacobs, PhD (Nothing to disclose)

Jaeim Jeong, BS (Nothing to disclose)

Youngjae Jeong, BSc (Nothing to disclose)

Jian Jiao, PhD (Nothing to disclose)

Kurt Matthew Johnson, MD (Nothing to disclose)

Kyung Shin Kang, PhD (Nothing to disclose)

Courtney Karner, PhD (Nothing to disclose)

Yohei Kawakami, MD, PhD (Nothing to disclose)

A. Serra Kaya, BSc (Nothing to disclose)

Harry K.W. Kim, MD (Nothing to disclose)

Michaela Kneissel, PhD (4- employee of Novartis; 7- employee of Novartis; 8- Editorial Board of BONE, Calcified Tissue International)

Everett Knudson (Nothing to disclose)

Alexander Kot, BSc (Nothing to disclose)

Matthew J. Kraeutler, MD (Nothing to disclose)

Gary Krishnan, MSc, PhD (3a –Employee of Eli Lilly and Co.; 4 –Stock symbol LLY)

Eric Krueger, PhD (Nothing to disclose)

Anjali P. Kusumbe, PhD (Nothing to disclose)

Nancy E. Lane, MD (Nothing to disclose)

Kelly Lauter Roszko, MD, PhD (Nothing to disclose)

Yu-An L. Evan Lay, MSc (Nothing to disclose)

Olivier Leupin, PhD (3a- I am employee of Novartis; 4- I have stock or stock option in Novartis)

Xiaofei Li, MEng (Nothing to disclose)

Zhi Li, PhD (Nothing to disclose)

Ying Liu, MD (Nothing to disclose)

Fanxin Long, PhD (8- JBMR Editorial Board, Bone Research Editorial Board)

Trevor J. Lujan, PhD (1- I have 1% ownership of Genesis Fracture Care, and I receive royalties from a licensing agreement for G3 technology with Zimmer; 7- I receive royalties from my 1% ownership of Genesis fracture care)

Kyle Lybrand, MD (Nothing to disclose)

Russell P. Main, PhD (Nothing to disclose)

Robert Majeska, PhD (Nothing to disclose)

Michael Mannstadt (Nothing to disclose)

Avudaiappan Maran, PhD (Nothing to disclose)

Takamitsu Maruyama, PhD (Nothing to disclose)

Heather Matheny, MSc (Nothing to disclose)

Eric C. McCarty, MD (1-Biomet, Zimmer; 3b- Biomet, Zimmer; 5- Smith Nephew, Biomet, Zimmer, Depuy Mitek; 7- Elsevier; 8- American Journal of Sports Medicine, Orthopedics; 9- Boulder Surgery Center)

Laoise Maria McNamara, PhD (Nothing to disclose)

Jose Luis Millan, PhD (2- ECTS 2016 - Alexion-sponsored symposium; 5- Grant support from AlexionGrant support from Alexion)

Freeman Miller, MD (Nothing to disclose)

Julie Ann Miller, MSc (Nothing to disclose)

Christopher Michael Modlesky, PhD (Nothing to disclose)

David Mooney, PhD (3b- Novartis, Agnovos, Samyang, Miromatrix; 4- Miromatrix, Agnovos; 5- Novartis)

Emily Moore, PhD (Nothing to disclose)

Stacyann Racine Morgan, BEng (Nothing to disclose)

Erica Morrill, MSME (Nothing to disclose)

M. Andrew Nesbit (Nothing to disclose)

Julia Oxford, PhD (Nothing to disclose)

Munro Peacock, MD (5- Ultragenyx; Amgen; Shire: PI on Pharma studies)

Robert Scott Pearsall, PhD (3a- Employee at Acceleron Pharma, Inc.; 4- I own Acceleron Stock)

Martin Pellicelli, PhD (Nothing to disclose)

Charlotte Longacre Phillips, PhD (3b- Versartis, Inc. Charlotte Phillips is a consultant for Versartis, Inc., concerning drug testing in oim mice. This consulting is independent of any aspect of the study described in the abstract; 5- Versartis, Inc is supporting a fee for service contract for Dr. Phillips Laboratory to test bones Versartis, Inc is supporting a fee for service contract for Dr. Phillips Laboratory to test bones; 9- Charlotte Phillips is the Director of Paternity Testing Corporation)

Matthew Phipps, PhD (Nothing to disclose)

Gina G. Provenzano, BSc (Nothing to disclose)

Yi-Xian Qin, PhD (4- GOOG, AMGN, AAPL; 5- NIH, DOD, NASA, Amgen; 8- J Orthop Translational)

James D. Quirk, PhD (4- Stock owner: Pfizer and Repligen from prior employment)

Muhammad Farooq Rai, PhD (9- Member of ORS Basic Science Education Committee, Ad-hoc Member of ORS Membership Committee, ORS Ambassador)

Saravana Ramasamy, PhD (Nothing to disclose)

Yinshi Ren, PhD (Nothing to disclose)

Ryan C. Riddle, PhD (8- Editorial Board, Bone Research)

G. David Roodman, MD,PhD (6- Amgen Denosumab trial. Local PI and serve on Advisory Board member)

Scott Rosenfeld, MD (2- Spoke at the International Pediatric Orthpaedic Society 12/2015 on the use of a proximal femoral locking plate for femoral osteotomies. Sponsored by OrthoPediatrics.; 3c- OrthoPediatrics; 7- Lippincott Williams and Wilkins; 9- Pediatric Orthopaedic Society of North America board of directors)

Janet Rubin, MD (Nothing to disclose)

Bi Ruiye (Nothing to disclose)

Linda J. Sandell, PhD (4- Isto Technologies, St. Louis. Stock options; 7- Editor in Chief, Journal of Orthopaedic Research)

Mitchell Schaffler, PhD (Nothing to disclose)

Jessica Schiavi, PhD (Nothing to disclose)

Eric Jon Schmidt, PhD (Nothing to disclose)

John Bradley Schrock, BA (Nothing to disclose)

Crystal Scott, MS (Nothing to disclose)

Buer Sen, MD (Nothing to disclose)

Zeynep Seref-Ferlengez, PhD (Nothing to disclose)

Tzong-Jen Sheu, PhD (Nothing to disclose)

Matthew Silva, PhD (5- Merck - Investigator Initiated GrantMerck - Investigator Initiated Grant; 8-Editorial Board: Bone, CTI, JBMR)

Irene Simfia, PhD (Nothing to disclose)

Harshvardhan Singh, PhD (Nothing to disclose)

Jordan Lee Smith, MD (Nothing to disclose)

Jess G. Snedeker, PhD (3c- ZuriMED Technologies AG; 4- ZuriMED Technologies AG; 8- Biomedizinische Technik; Technology and Healthcare; 9- European Society of Sports Traumatology, Knee Surgery & Arthroscopy; Swiss Society for Biomedical Engineering; Swiss Society of Orthopedics and Traumatology

Rene St-Arnaud, PhD (Nothing to disclose)

Kristian Strømgaard, PhD (3a- I am co-founder and CSO of a small Danish biotech company - Avilex Pharma (www.avilexpharma.com) - pursuing peptide-based inhibitors as a novel treatment for stroke. Thus, not at all related to the research described here; 4- I own shares in Avilex Pharma)

John A. Szivek, PhD (1- A University of Arizona disclosure about a cell culture procedure developed by me has resulted in payments from Tissue Genesis this year. The poster does not describe any work related to this or any other products Tissue Genesis produces; 8- I serve on the editorial board of CORR and J. of Biomedical Materials Research.; 9-I serve on the Medical Board of the Musculoskeletal Transplant Foundation (MTF). This is an unpaid position and my poster does not utilize any materials and has not had any support from MTF.)

Emily Tanasse (Nothing to disclose)

Rajesh V. Thakker, MD (2- Chairman of Astra-Xeneca Stratified Medicine Panel,Honoraria/lecture and consultancy fees from Novartis, Lilly, AstraZeneca and Ipsen; 3b- Honoraria/lecture and consultancy fees from Norvartis, Lilly, AstraZeneca and Ipsen;3c- Honoraria/lecture and consultancy fees from Norvartis, Lilly, AstraZeneca and Ipsen; 5- Medical Research Council programme grant, Wellcome Trust Investigator Award, NIHR Senior Investigator, NIHR Translational Research Collaboration, NIHR Oxford Grant - BRC funding, Wellcome Trust clinical training fellowships, EU ITN Marie Curie grant, Galaxo-SmithKline research grant, Kidney Research UK (KRUK) project grant, Novartis research grant, NPS Pharmaceuticals (USA), Marshall Smith Syndrome Research Fund; 8- Associate Editor of Journal of Bone and Mineral Research (JBMR); 9-Chairman of National Institute of Health Research/MRC- Efficacy, Mechanisms and Evaluations (EME) board)

Roman Thaler, PhD (Nothing to disclose)

David D. Thompson, PhD (3b- Alexion; 3c- perForm; 4- Karos Pharma, Azure Biotech, perForm Biotech)

Guowei Tian, PhD (Nothing to disclose)

Ryan E. Tomlinson, PhD (Nothing to disclose)

Julia P. Townsend (Nothing to disclose)

Stephanie Tuft, Biochemistry (Nothing to disclose)

Mustafa Unal, MSc (Nothing to disclose)

Gunes Uzer, PhD (Nothing to disclose)

Marjolein van der Muelen, PhD (4-Stock ownership: JNJ, NVS, PG; 9-BOD, BMES)

Deepak Vashishth, PhD (8- Board Member: Bone, Journal of Mechanical Behavior of Biomedical Materials, Academic Editor: PLoS One; 9- Member of Strategic Initiative Committee, ORS)

Ke Wang, DDS (Nothing to disclose)

Gordon Warren, PhD (Nothing to disclose)

Daniel G. Whitney, BSc (Nothing to disclose)

Michael P. Whyte, MD (2- Alexion Pharmaceuticals, Inc., New Haven, CT; 3b- Alexion Pharmaceuticals, Inc.; 4- Merck; 5- Alexion Pharmaceuticals, Inc. & Ultragenyx PharmaceuticalAlexion Pharmaceuticals, Inc. & Ultragenyx Pharmaceutical; 8- Journal of Clinical Endocrinology and Metabolism, Bone, Journal of Clinical Denistometry)

Bart Williams, PhD (2- Presented a talk at Vertex Pharmaceuticals and have scheduled a talk at Surrozen)

Kerri Winters-Stone, PhD, FACSM (Nothing to disclose)

Andrew Mark Wojtanowski, MSc (Nothing to disclose)

Liping Xiao, MD, PhD (8- Reviewer on Editorial Board of International Journal of Medicine and Health Sciences Research)

Duan Xin, MD (Nothing to disclose)

Xiaofeng Xiong, PhD (Nothing to disclose)

Shoshana Yakar, PhD (Nothing to disclose)

Ryosuke Yamaguchi, MD, PhD (Nothing to disclose)

Haisheng Yang, PhD (Nothing to disclose)

Wei Yao, PhD (Nothing to disclose)

Michael Jerome Yaszemski, MD, PhD (3b- K2M, Inc., Medtronic, Inc.; 7- Lippincott, Inc.; 8-1. Journal of Biomedical Materials Research Part A-J.Wiley, publisher; Associate Editor, 2. Techniques in Orthopaedics; Associate Editor)

Katie Yocham, MEng (Nothing to disclose)

Yilin Yu, BA (Nothing to disclose)

Hongliang Zhang, PhD (Nothing to disclose)

Zhendong A. Zhong, PhD (Nothing to disclose)

Schedule-At-A-Glance

Saturday, August 6, 2016

3:00 PM – 5:30 PM	Registration Opens	Continental Promenade

7:00 PM – 10:00 PM	Social Mixer	Dr. Burr's Lodge Apartment (inquire at the Lodge Reception Desk) Support provided by Micro Photonics Inc.

Sunday, August 7, 2016 — Continental Room

7:00 AM – 8:00 AM	Breakfast & Registration Support provided by Charles River Laboratories

8:00 AM – 9:00 AM	Mechanisms and Messengers in Osteocyte Regulation of Bone Biology and Pathophysiology RIB Awardee: Teresita Bellido, PhD *(Indiana University School of Medicine)*

9:15 AM – 9:45 AM	Blue Ribbon Sun Valley Posters Chair: Alex Robling, PhD *(Indiana University)*
	Mechanical LINC between Nucleus and Cytoskeleton Regulates βcatenin Nuclear Access Gunes Uzer, PhD *(University of North Carolina at Chapel Hill)*
	The Role of Rho-ROCK Signaling in Normal and Estrogen Deficient Bone Cells in Response to Fluid Flow Induced Shear Stress Irene Simfia, PhD *(National University of Ireland Galway)*
	Mechanobiological Modulation of In Situ and In Vivo Osteocytic Ca2+ Oscillations in Response to Acoustic Radiation Force using Black6 and Ai38/Dmp1-Cre Mice Minyi Hu, PhD *(Stony Brook University)*
	Distinct Response of Osteons at Different Locations in Response to Loading and Intermittent PTH Injections Ke Wang, DDS *(Texas A&M University, Baylor College of Dentistry)*
	Underdevelopment of Trabecular Bone Microarchitecture in the Distal Tibia and Distal Femur of Ambulatory Children with Cerebral Palsy Becomes More Pronounced with Distance from the Growth Plate Daniel Whitney, MS *(University of Delaware)*

9:45 AM – 12:00 PM	Problem: How Can We Improve Reproducibility in Pre-Clinical Models? Chair: Gary Krishnan, MSc, PhD *(Eli Lilly and Co.)*
	Overview and Historical Context – Challenges in Translating Life Sciences Research into Effective Health Care Solutions Gary Krishnan, MSc, PhD *(Eli Lilly and Co.)*
	Know Thy Cells (and Antibodies): Improving Biomedical Research Reproducibility Leonard Freedman, PhD *(President, Global Biological Standards Institute)*
	Improving the Reproducibility of Research Findings Using Mouse Models Bart Williams, PhD *(Van Andel Research Institute)*

2:00 PM – 4:00 PM	Volleyball	Volleyball Court

7:30 PM – 8:00 PM	**Blue Ribbon Sun Valley Posters** Chair: Alex Robling, PhD *(Indiana University)*
	Why We Wnt to Treat Osteosarcoma Carl Gustafson, BS *(Mayo Graduate School)*
	Role of Phosphate in the Central Ox/Phos Metabolic Processes and Its Linkage to Collagen Production Amira Hussein, PhD *(Boston University)*
	Estrogen Receptor Beta (ERβ) is Osteocytes: A Critical Regulator of Adult Bon Turnover and Mechanical Load-Induced Bone Formation Russell Main, PhD *(Purdue University)*
	Functional Adaptation of Osteocalcin and Osteopontin Deficient Mice Stacyann Morgan, BSc *(Rensselaer Polytechnic Institution)*
	Tibial Compression Overload Instigates Post-Traumatic Osteoarthritis in Mouse Knee Muhammad Farooq Rai , PhD*(Washington University in St. Louis)*

8:00 PM – 10:00 PM	**Poster Session with wine and cheese** Support provided by OsteoMetrics
	Alice L. Jee Award Winners
	Necrotic Bone Stimulates Pro-inflammatory Responses in Macrophages through the Activation of Toll-like Receptor 4 Naga Suresh Adapala, PhD *(Texas Scottish Rite Hospital for Children)*
	FGF23 Neutralizing Antibody Ameliorates Hypophosphatemia and Impaired FGF Receptor Signaling in Kidneys of FGF2 High Molecular Weight Isoform Transgenic Mice Erxia Du, PhD *(University of Connecticut Health Center)*
	Why we Wnt to Treat Osteosarcoma Carl Gustafson, BS *(Mayo Graduate School)*
	Usp53, a Novel Target Gene of the PTH-Activated αNAC Transcriptional Coregulator Hadla Hariri, PhD *(McGill University, Shriners Hospital for Children)*
	Mechanobiological Modulation of In Situ and In Vivo Osteocytic Ca2+ Oscillations in Response to Acoustic Radiation Force using Black6 and Ai38/Dmp1-Cre Mice Minyi Hu, PhD *(Stony Brook University)*
	Role of Phosphate in the Central Ox/Phos Metabolic Processes and Its Linkage to Collagen Production Amira Hussein, PhD *(Boston University)*
	The Femoral and Hindlimb Skeletal Muscle Properties of G610C Osteogenesis Imperfecta Mouse Model with Soluble Activin Receptor Type IIB Fusion Proteins (ActRIIB-mFc) Youngjae Jeong, BS *(University of Missouri)*
	Influence of Progesterone Nuclear Receptor Signaling in Osteoprogenitor Cells on Sexual Dimorphism of Trabecular Bone Mass Alexander Kot, BS *(University of California, Davis Medical Center)*
	Periosteal Osteochondroprogenitors Contribute to Development of the Appendicular Skeleton by Populating the Growth Plate and Cortical Bone Emily Moore, MS *(Columbia University)*
	Functional Adaptation of Osteocalcin and Osteopontin Deficient Mice Stacyann Morgan, BSc *(Rensselaer Polytechnic Institution)*
	Tibial Compression Overload Instigates Post-Traumatic Osteoarthritis in Mouse Knee Muhammad Farooq Rai, PhD *(Washington University in St. Louis)*
	Distinct Response of Osteons at Different Locations in Response to Loading and Intermittent PTH Injections Ke Wang, DDS *(Texas A&M University, Baylor College of Dentistry)*

8:00 PM – 10:00 PM	Underdevelopment of Trabecular Bone Microarchitecture in the Distal Tibia and Distal Femur of Ambulatory Children with Cerebral Palsy Becomes More Pronounced with Distance from the Growth Plate Daniel Whitney, MS *(University of Delaware)*
	Osteoarthritis Award Winner
	A Novel Method to Assess Articular Cartilage Hydration by Raman Spectroscopy for Early Diagnosis of Osteoarthritis Mustafa Unal, MSc *(Case Western Reserve University)*
	Charles H. Turner Young Investigator Bone Research Award Winner
	Osteoclast-selective Expression of Lrp5 HBM-causing Mutations Alters Bone Metabolism Kyung Shin Kang, PhD *(Indiana University School of Medicine)*
	Submitted Poster Presenters
	Osteoclasts are Deficient in the Expression of Osteogenic Coupling Factors Following Ischemic Osteonecrosis of the Femoral Head Naga Suresh Adapala, PhD *(Texas Scottish Rite Hospital for Children)*
	Osteogenic Induction of Human Mesenchymal Stem Cells by Cold Atmospheric Argon Plasma Adil Shahzad Ahmed, MD *(University of South Florida – Morsani College of Medicine)*
	Multiscale Mechanics and Mechano-adaptation in Mouse Bone Alessandra Carriero, PhD (*Florida Institute of Technology)*
	Lactation-Induced Changes in the Volume of the Osteocyte Lacunar-Canalicular Space Alter Local Mechanical Properties in Cortical Bone A. Serra Kaya, BSc *(The City College of New York)*
	Lesser Tuberosity Osteotomy and Subscapularis Tenotomy Repair Techniques during Total Shoulder Arthroplasty: A Meta-Analysis of Cadaveric Studies Matthew Kraeutler, MD *(University of Colorado School of Medicine)*
	The Surgical Incidence to Publication (SIP) Index: A Novel Equation used to Focus Future Research Efforts Matthew Kraeutler, MD *(University of Colorado School of Medicine)*
	Estrogen Receptor Beta (ERβ) is Osteocytes: A Critical Regulator of Adult Bon Turnover and Mechanical Load-Induced Bone Formation Russell Main, PhD *(Purdue University)*
	Three Dimensional Graphene Scaffolds for Engineering Musculoskeletal Tissue Julia Oxford, PhD *(Boise State University)*
	The Role of Rho-ROCK Signaling in Normal and Estrogen Deficient Bone Cells in Response to Fluid Flow Induced Shear Stress Irene Simfia, PhD *(National University of Ireland Galway)*
	Stem Cell Infiltrated Trabecular-Patterned Scaffolds Induce Extensive Bone Growth during Critical Sized Defect Repair John Szivek, PhD *(University of Arizona, College of Medicine)*
	Development of an In Vitro Model for Ligament Wound Healing Stephanie Tuft, BS *(Boise State University)*
	Mechanical LINC between Nucleus and Cytoskeleton Regulates βCatenin Nuclear Access Gunes Uzer, PhD *(University of North Carolina at Chapel Hill)*

Monday, August 8, 2016 — Continental Room

7:00 AM – 8:00 AM	**Breakfast & Registration** Support provided by Charles River Laboratories

8:00 AM – 9:45 AM	**Problems in Endocrinology: How Do We Treat Bone, Muscle, and Other Target Organs in Hypophosphatasia?** **Chair: David Thompson, PhD *(D. Thompson Consulting, LLC)***
	Introduction: How Do We Treat Bone, Muscle, and Other Affected Organs in Hypophosphatasia? David Thompson, PhD *(D. Thompson Consulting, LLC)*
	What We Know and Don't Know About Hypophosphatasia José Luis Millán, PhD *(Sanford-Burnham Medical Research Institute)*
	Muscle Weakness in Hypophosphatasia Michael Whyte, MD *(Washington University)*

10:00 AM – 12:00 PM	**Problems in Orthopaedics: New Materials-based and Ligand-based Strategies to Stimulate Self-Repair of Tendons and Ligaments** **Chair: Michaela Kneissel, PhD *(Novartis)***
	The Basis of Tendon Function, Homeostasis, Degeneration, and Regeneration Jess G. Snedeker, PhD *(University Hospital Belgrist)*
	Molecular Therapies to Augment Intrinsic Tendon Repair Olivier Leupin, PhD (*Novartis Institute for Biomedical Research)*
	Hydrogel-based Drug Delivery David Mooney, PhD (*Harvard University)*
	Development of an In Vitro Model for Ligament Wound Healing Stephanie Tuft, BS *(Boise State University)*
	Lesser Tuberosity Osteotomy and Subscapularis Tenotomy Repair Techniques during Total Shoulder Arthroplasty: A Meta-Analysis of Cadaveric Studies Matthew Kraeutler, MD *(University of Colorado School of Medicine)*

1:30 PM – 3:30 PM	**Career Development Workshop: Tenure and Promotion** **Chair: Marjolein van der Meulen, PhD *(Cornell University)***
	Moderator: Marjolein van der Meulen, PhD *(Cornell University)* Panelists: Teresita Bellido, PhD *(Indiana University School of Medicine)* Susan Bloomfield, PhD *(Texas A&M University)* Gary Krishnan, PhD *(Eli Lilly)* David Roodman, MD *(Indiana University School of Medicine)* The discussion will be organized around four topics: 1. Tenure & promotion policies 2. Tenure references/letter writers 3. Dossier materials: CV, statements, papers 4. Other considerations We will start each topic with comments from the panelists, followed by discussion and questions from the participants. Presenter: Gayle Lester, PhD *(Program Director, NIAMS, NIH)* Topic: Over view of recent NIH Policies: • Premise and Rigor/Reproducibility • Biosketch and annotated publications

5:30 PM – 8:00 PM	Banquet	Lodge Terrace

7:00 AM – 8:00 AM	**Breakfast & Registration** Support provided by Charles River Laboratories

8:00 AM – 9:00 AM	**ASBMR/Harold M. Frost Young Investigator Awards Presentation**
	Multiscale Mechanics and Mechano-adaptation in Mouse Bone Alessandra Carriero, PhD (*Florida Institute of Technology)*
	Inducible Deletion of β-Catenin in Nucleus Pulposus Cells Demonstrates the Degenerative Mechanism During Tail Compression of Mouse Intervertebral Discs Nilsson Holguin, PhD *(Washington University in St. Louis)*
	Glutaminase Acts in Osteoblasts to Regulate Bone Formation Courtney Karner, PhD *(Duke University)*

9:15 AM – 10:15 AM	**Debate: Is Osteoporosis Over Diagnosed?** **Chair: Steve Cummings, MD *(University of California, San Francisco)***
	Is Osteoporosis Over- or Under-diagnosed? Steve Cummings, MD *(University California, San Francisco)*
	We are Overdiagnosis Osteoporosis - For the Motion Teppo Järvinen, MD, PhD (*University of Helsinki)*
	Is Osteoporosis Over Diagnosed? - Against the Motion Munro Peacock, MD *(Indiana University)*

10:15 AM – 12:00 PM	**Poster Viewing**

2:00 PM – 4:00 PM	**Orienteering**

7:30 PM – 10:00 PM	**ASBMR/Harold M. Frost Young Investigator Awards Presentations**
	The Therapeutic Potential of Endothelial Progenitor Cells in Bone Regeneration Yohei Kawakami, MD, PhD *(Kobe University Graduate School of Medicine)*
	Stem Cells of The Suture Mesenchyme In Craniofacial Bone Development, Repair And Regeneration Takamitsu Maruyama, PhD (*University of Rochester Medical Center)*
	Blood Flow Regulates Function of Endothelium and Bone Formation in the Skeletal System Saravana Ramasamy, PhD *(Max Planck Institute for Molecular Biomedicine)*
	CRISPR/Cas9-generated Mouse Model of Autosomal-dominant Hypocalcemia Harboring the Activating G Protein Alpha 11 Mutation Arg60Cys and Use of Calcilytics and a Gαq/Gα11-specific Inhibitor Kelly Lauter Roszko, MD, PhD *(Endocrine Unit, Massachusetts General Hospital)*
	Anabolic and Anti-resorptive Modulation of Bone Homeostasis by the Epigenetic Modulator Sulforaphane, an Naturally Occurring Isothyiocyanate Roman Thaler, PhD *(Mayo Clinic)*
	Sensory Nerve Signals Mediate Skeletal Adaptation to Mechanical Loads Ryan Tomlinson, PhD *(John Hopkins Medicine)*

7:00 AM – 8:00 AM	**Breakfast & Registration** Support provided by Charles River Laboratories

8:00 AM – 11:00 AM	**Problem: How Can Bone and Muscle Health Be Maintained in Cancer Survivors?** ***Chair: G. David Roodman, MD, PhD (Indiana University)***
	The Skeletal Significance of Monoclonal Gammopathy of Undetermined Significance Matthew Drake, MD, PhD *(Mayo Clinic)*
	Problem: How Can Bone Health Be Maintained in Cancer Survivors? G. David Roodman, MD, PhD *(Indiana University)*
	Maintaining Muscle Health in Cancer Survivors: What is the Target and Is Exercise Enough? Kerri Winters-Stone, PhD, FACSM *(Oregon Health and Science University)*

11:15 AM – 12:00 PM	**Poster Viewing**

12:30 PM – 5:00 PM	**Guided Hike to Pioneer Cabin** Attendees meet at the back door or the Sun Valley Inn at 12:15 PM

7:30 PM – 10:00 PM	**Problem: How Do We Advance the Muscle-Bone Signaling Story?** ***Chair: Sue Bloomfield, PhD, FACSM (Texas A&M University)***
	Advancing the Muscle-bone Signaling Story: Using *in vivo* Models Sue Bloomfield, PhD, FACSM *(Texas A&M University)*
	How Muscle Force Production Affects Bone (or Does it?) Gordon Warren, PhD *(Georgia State University)*
	Exosomes and Microvesicles: New Candidate Mediators for Signaling between Muscle and Bone Mark Hamrick, PhD *(Georgia Regents University)*

7:00 AM – 8:00 AM	**Breakfast & Registration** Support provided by Charles River Laboratories

8:00 AM – 9:00 AM	**Mechanisms and Messengers in Osteocyte Regulation of Bone Biology and Pathophysiology** **RIB Awardee: Teresita Bellido, PhD *(Indiana University School of Medicine)***

9:15 AM – 9:45 AM	**Blue Ribbon Sun Valley Posters** Chair: Alex Robling, PhD *(Indiana University)*
	Mechanical LINC between Nucleus and Cytoskeleton Regulates βcatenin Nuclear Access Gunes Uzer, PhD *(University of North Carolina at Chapel Hill)*
	The Role of Rho-ROCK Signaling in Normal and Estrogen Deficient Bone Cells in Response to Fluid Flow Induced Shear Stress Irene Simfia, PhD *(National University of Ireland Galway)*
	Mechanobiological Modulation of In Situ and In Vivo Osteocytic Ca2+ Oscillations in Response to Acoustic Radiation Force using Black6 and Ai38/Dmp1-Cre Mice Minyi Hu, PhD *(Stony Brook University)*
	Distinct Response of Osteons at Different Locations in Response to Loading and Intermittent PTH Injections Ke Wang, DDS *(Texas A&M University, Baylor College of Dentistry)*
	Underdevelopment of Trabecular Bone Microarchitecture in the Distal Tibia and Distal Femur of Ambulatory Children with Cerebral Palsy Becomes More Pronounced with Distance from the Growth Plate Daniel Whitney, MS *(University of Delaware)*

9:45 AM – 12:00 PM	**Problem: How Can We Improve Reproducibility in Pre-Clinical Models?** **Chair: Gary Krishnan, MSc, PhD *(Eli Lilly and Co.)***
	Overview and Historical Context – Challenges in Translating Life Sciences Research into Effective Health Care Solutions Gary Krishnan, MSc, PhD *(Eli Lilly and Co.)*
	Know Thy Cells (and Antibodies): Improving Biomedical Research Reproducibility Leonard Freedman, PhD *(President, Global Biological Standards Institute)*
	Improving the Reproducibility of Research Findings Using Mouse Models Bart Williams, PhD *(Van Andel Research Institute)*

2:00 PM – 4:00 PM	Volleyball	Volleyball Court

7:30 PM – 8:00 PM	**Blue Ribbon Sun Valley Posters** Chair: Alex Robling, PhD *(Indiana University)*
	Why We Wnt to Treat Osteosarcoma Carl Gustafson, BS *(Mayo Graduate School)*
	Role of Phosphate in the Central Ox/Phos Metabolic Processes and Its Linkage to Collagen Production Amira Hussein, PhD *(Boston University)*
	Estrogen Receptor Beta (ERβ) is Osteocytes: A Critical Regulator of Adult Bon Turnover and Mechanical Load-Induced Bone Formation Russell Main, PhD *(Purdue University)*
	Functional Adaptation of Osteocalcin and Osteopontin Deficient Mice Stacyann Morgan, BSc *(Rensselaer Polytechnic Institution)*

7:30 PM – 8:00 PM	Tibial Compression Overload Instigates Post-Traumatic Osteoarthritis in Mouse Knee Muhammad Farooq Rai , PhD*(Washington University in St. Louis)*

8:00 PM – 10:00 PM	**Poster Session with wine and cheese** Support provided by OsteoMetrics
	Alice L. Jee Award Winners
	Necrotic Bone Stimulates Pro-inflammatory Responses in Macrophages through the Activation of Toll-like Receptor 4 Naga Suresh Adapala, PhD *(Texas Scottish Rite Hospital for Children)*
	FGF23 Neutralizing Antibody Ameliorates Hypophosphatemia and Impaired FGF Receptor Signaling in Kidneys of FGF2 High Molecular Weight Isoform Transgenic Mice Erxia Du, PhD *(University of Connecticut Health Center)*
	Why we Wnt to Treat Osteosarcoma Carl Gustafson, BS *(Mayo Graduate School)*
	Usp53, a Novel Target Gene of the PTH-Activated αNAC Transcriptional Coregulator Hadla Hariri, PhD *(McGill University, Shriners Hospital for Children)*
	Mechanobiological Modulation of In Situ and In Vivo Osteocytic Ca2+ Oscillations in Response to Acoustic Radiation Force using Black6 and Ai38/Dmp1-Cre Mice Minyi Hu, PhD *(Stony Brook University)*
	Role of Phosphate in the Central Ox/Phos Metabolic Processes and Its Linkage to Collagen Production Amira Hussein, PhD *(Boston University)*
	The Femoral and Hindlimb Skeletal Muscle Properties of G610C Osteogenesis Imperfecta Mouse Model with Soluble Activin Receptor Type IIB Fusion Proteins (ActRIIB-mFc) Youngjae Jeong, BS *(University of Missouri)*
	Influence of Progesterone Nuclear Receptor Signaling in Osteoprogenitor Cells on Sexual Dimorphism of Trabecular Bone Mass Alexander Kot, BS *(University of California, Davis Medical Center)*
	Periosteal Osteochondroprogenitors Contribute to Development of the Appendicular Skeleton by Populating the Growth Plate and Cortical Bone Emily Moore, MS *(Columbia University)*
	Functional Adaptation of Osteocalcin and Osteopontin Deficient Mice Stacyann Morgan, BSc *(Rensselaer Polytechnic Institution)*
	Tibial Compression Overload Instigates Post-Traumatic Osteoarthritis in Mouse Knee Muhammad Farooq Rai, PhD *(Washington University in St. Louis)*
	Distinct Response of Osteons at Different Locations in Response to Loading and Intermittent PTH Injections Ke Wang, DDS *(Texas A&M University, Baylor College of Dentistry)*
	Underdevelopment of Trabecular Bone Microarchitecture in the Distal Tibia and Distal Femur of Ambulatory Children with Cerebral Palsy Becomes More Pronounced with Distance from the Growth Plate Daniel Whitney, MS *(University of Delaware)*
	Osteoarthritis Award Winner
	A Novel Method to Assess Articular Cartilage Hydration by Raman Spectroscopy for Early Diagnosis of Osteoarthritis Mustafa Unal, MSc *(Case Western Reserve University)*
	Charles H. Turner Young Investigator Bone Research Award Winner
	Osteoclast-selective Expression of Lrp5 HBM-causing Mutations Alters Bone Metabolism Kyung Shin Kang, PhD *(Indiana University School of Medicine)*

	Submitted Poster Presenters
8:00 PM – 10:00 PM	Osteoclasts are Deficient in the Expression of Osteogenic Coupling Factors Following Ischemic Osteonecrosis of the Femoral Head Naga Suresh Adapala, PhD *(Texas Scottish Rite Hospital for Children)*
	Osteogenic Induction of Human Mesenchymal Stem Cells by Cold Atmospheric Argon Plasma Adil Shahzad Ahmed, MD *(University of South Florida – Morsani College of Medicine)*
	Multiscale Mechanics and Mechano-adaptation in Mouse Bone Alessandra Carriero, PhD (*Florida Institute of Technology)*
	Lactation-Induced Changes in the Volume of the Osteocyte Lacunar-Canalicular Space Alter Local Mechanical Properties in Cortical Bone A. Serra Kaya, BSc *(The City College of New York)*
	Lesser Tuberosity Osteotomy and Subscapularis Tenotomy Repair Techniques during Total Shoulder Arthroplasty: A Meta-Analysis of Cadaveric Studies Matthew Kraeutler, MD *(University of Colorado School of Medicine)*
	The Surgical Incidence to Publication (SIP) Index: A Novel Equation used to Focus Future Research Efforts Matthew Kraeutler, MD *(University of Colorado School of Medicine)*
	Estrogen Receptor Beta (ERβ) is Osteocytes: A Critical Regulator of Adult Bon Turnover and Mechanical Load-Induced Bone Formation Russell Main, PhD *(Purdue University)*
	Three Dimensional Graphene Scaffolds for Engineering Musculoskeletal Tissue Julia Oxford, PhD *(Boise State University)*
	The Role of Rho-ROCK Signaling in Normal and Estrogen Deficient Bone Cells in Response to Fluid Flow Induced Shear Stress Irene Simfia, PhD *(National University of Ireland Galway)*
	Stem Cell Infiltrated Trabecular-Patterned Scaffolds Induce Extensive Bone Growth during Critical Sized Defect Repair John Szivek, PhD *(University of Arizona, College of Medicine)*
	Development of an In Vitro Model for Ligament Wound Healing Stephanie Tuft, BS *(Boise State University)*
	Mechanical LINC between Nucleus and Cytoskeleton Regulates βCatenin Nuclear Access Gunes Uzer, PhD *(University of North Carolina at Chapel Hill)*

Mechanisms and Messengers in Osteocyte Regulation of Bone Biology and Pathophysiology

RIB Awardee
Teresita Bellido, PhD
Department of Anatomy and Cell Biology, Department of Medicine, Division of Endocrinology
Indiana University School of Medicine, Non clinician VA Investigator, Roudebush Veterans Administration Medical Center

For many years, osteocytes have been the forgotten bone cells and considered inactive spectators buried in the bone matrix. We now know that osteocytes detect and respond to mechanical and hormonal stimuli to coordinate bone resorption and bone formation. Osteocytes are currently considered a major source of molecules that regulate the activity of osteoclasts and osteoblasts, such as RANKL and sclerostin; and genetic and pharmacological manipulations of either molecule markedly affect bone homeostasis. Besides playing a role in physiological bone homeostasis, dysregulation of osteocyte function and alteration of osteocyte life-span underlies the pathophysiology of skeletal disorders characterized by loss bone mass and increased bone fragility, as well as the damaging effects of cancer in bone. This presentation will highlight the molecular mediators and mechanisms leading to osteocyte-driven bone formation and bone resorption under physiologic and pathological conditions, which demonstrate that osteocytes, far from being passive cells entombed in the bone, are critical for bone function and maintenance.

Mechanical LINC between Nucleus and Cytoskeleton Regulates βcatenin Nuclear Access

Gunes Uzer, PhD Guniz Bas, BS, Buer Sen, MD, Janet Rubin, MD
University of North Carolina, Chapel Hill, NC, USA

Mechanical signals generated during functional loading promote osteoblastogenesis at load bearing sites. βcatenin (βcat) signaling supports osteoblast and inhibits adipocyte recruitment from mesenchymal stem cells (MSC). βcat control of gene expression relies on non-classical nuclear shuttling involving βcat's direct interaction with nuclear pore complexes (NPCs). MSC mechanosensitivity is in-part regulated at the nuclear surface via LINC complexes (Linker of Nucleoskeleton and Cytoskeleton) that integrate the nucleus into the cytoskeleton. As LINC directly binds cytoskeletal actin filaments, NPCs and βcat, it may also have a role in βcat nuclear delivery. Here we hypothesized that LINC complexes regulate nuclear βcat availability in response to mechanical challenge.

To understand the mechanically-induced interaction of βcat with the nuclear envelope, we applied high magnitude strain (HMS, 2%, 0.17Hz) or low intensity vibration (LIV, 0.7g, 90Hz) to murine MSCs and isolated NPC-rich nucleoskeletal (NSk) fractions to probe for βcat. On average, HMS and LIV increased the βcat-NSk association by 2-fold ($p<0.01$). We next asked if LINC connectivity was critical for mechanically-induced βcat-NSk association: un-anchoring the βcat-binding element of LINC, Nesprin-2, via Sun1/2 deletion (SiSUN) decreased both basal NSk-bound βcat (50%, $p<.001$) and mechanically induced βcat-NSk association ($p<0.001$). Further, immunostaining showed that in LINC deficient MSCs where Nesprin-2 was displaced from nuclear envelope, βcat was less tightly localized to nucleus increasing its cytoplasmic staining (1.4-fold, $p<.001$). This suggests that LINC positions βcat at the nuclear envelope, thus providing access to NPC for inward transfer. We tested this possibility by measuring fluorescence recovery of GFP-βcat in the nucleus to quantify the rate of βcat nuclear entry: LINC deficient MSCs showed a 51% recovery delay ($p<.01$), indicating a LINC-dependence of βcat nuclear entry. We next considered if strengthening LINC-mediated connectivity would improve βcat-NSk association. Daily application of LIV x5d increased Nesprin-2 expression by 69% ($p<0.05$), resulting in 49% increase in HMS-induced βcat-NSk association compared to non-LIV group.
In summary, our data indicates that LINC-mediated connectivity enables βcat nuclear transfer. As such, mechanically induced adaptations of LINC complexes may represent a novel avenue for increasing βcat signaling and improving MSC fate decisions.

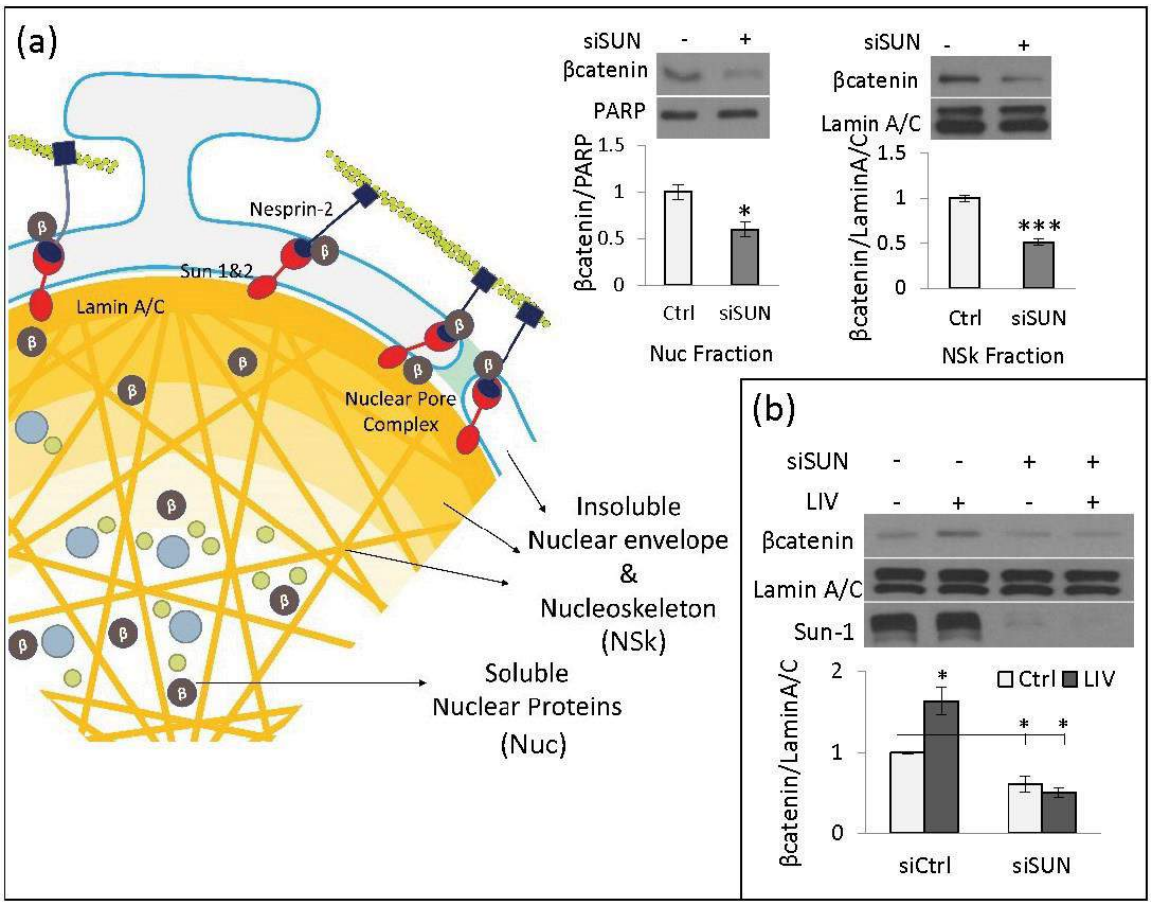

Figure1. a) Separating cell nucleus into soluble nuclear (Nuc) and insoluble nucleoskeletal (NSk) fractions revealed that the Lamin A/C nucleoskeleton and the LINC complex that integrate nucleus into the cell cytoskeleton is also associated with βcatenin. Disabling LINC function using siRNA against Nesprin anchoring protein Sun1/2 (siSUN) reduced nuclear βcatenin levels as well as NsK-βcatenin association. b) Consistent with decreased nuclear levels of βcatenin, siSUN treatment inhibited mechanically induced βcatenin-NSk association, suggesting a LINC-mediated βcatenin control at the nuclear envelope.

The Role of Rho-ROCK Signaling in Normal and Estrogen Deficient Bone Cells in Response to Fluid Flow Induced Shear Stress

Irene Simfia, PhD, Jessica Schiavi, PhD, Vishwa Deepak, PhD, Laoise M. McNamara, PhD
Mechanobiology and Medical Device Research Group, Department of Biomedical Engineering, National University of Ireland Galway, Ireland

Introduction

Osteoporosis is most commonly manifested following menopause when estrogen production is deficient. As a result, complex changes in bone composition occur leading to bone fractures. Estrogen plays an important role in the normal biology of bone cells, in particular in regulating their response to mechanical loading. Recent studies have found for the first time that complex tissue levels changes in bone composition during estrogen deficiency might be explained by alterations in bone cell biology, in particular the mechanobiological responses[1-3]. Drug treatments that target the Rho/ROCK proteins have gained interest as therapeutic targets for cancer[4, 5]. A recent study suggests that the mechanosensitivity of osteoblasts to continuous loading is regulated by activation of P2Y2R mediated Rho-ROCK signalling required for actin stress fiber formation, increasing the mechanical stiffness of the cell [6]. However, the mechanism and role of Rho-ROCK signalling in osteogenesis of mechanically stimulated osteoblasts remains unknown. This can be a useful insight into exploring the mechanisms involved in diseases like osteoporosis where bone formation by mechanically stimulated bone cells is adversely affected[7].

Specifically we seek to target the Rho/ROCK signalling pathway in estrogen deficient bone cells *in vitro* to establish changes in cell differentiation, gene expression and actin cytoskeleton when these cells are mechanically stimulated. We first, established the effect of ROCK inhibition on
PGE2synthesis by osteoblasts. We show, for the first time, that ROCK inhibition in osteoblasts reverts the effects of fluid flow induced shear stress in terms of reduction in PGE2synthesis. We also affirm with previous study [6] that ROCK inhibition of osteoblasts leads to disruption of actin cytoskeleton. All of these results will be further compared with estrogen deficient cells under similar conditions as it is fundamental to this study.

Materials and Methods

Cell Culture

Viability experiments: MC3T3-E1 osteoblast-like cells were seeded at 10,000 cells per well on 13mm coverslips and cultured in vitro for 24hours in □-Minimum Essential Medium Eagle (MEM) supplemented with 10% Fetal Bovine Serum (Sigma Aldrich), 2mM L-glutamine (Sigma Aldrich),
100U/ml Penicillin and 100ug/ml Streptomycin (Sigma Aldrich). Cells were then incubated with media supplemented with or without Y-27632 (10μM; Sigma Aldrich) for 60 min. These cells were then assessed for their viability by examining their ability to convert the Alamar Blue reagent,
Resazurin into Resorufin and were also analysed for their DNA content.
Flow study: MC3T3-E1 cells were seeded at 200,000 cells per slide on 76mm x26mm glass slides and grown for 48 hours in standard media as described above. These cells were then treated with media supplemented with the ROCK inhibitor, Y-27632, at 10μM for 60 min. This concentration was chosen as it falls in the range of concentrations of Y-27632 (1-30μM) used for ROCK inhibition in in vitro experiments [6, 8-10], which significantly affect stress fibre density, focal adhesion density and focal adhesion area. After the Y-27632 treatment, cells were washed with Dulbecco's Phosphate Buffered Saline (PBS). The control groups of cells did not receive treatment with Y-27632.

Fluid Flow

Laminar oscillatory fluid flow at a frequency of 0.5 Hz, peak flow rate of 9.2ml/min and peak shear stress of 1Pa was applied to both groups, Y-27632 and control, using custom designed parallel plate flow chambers, NE-1600 Syringe Pump (New Era Pump Systems) and 50 mL syringe (BD) following a previous study[11].

Alamar Blue Assay and DNA Hoechst Assay

To examine the viability of cells, they were incubated in 10% Alamar Blue reagent in PBS for 2hours at 37°C.Supernatant was collected and absorbance was measured at 570nm and 600nm. Cells were harvested following 3 freeze-thaw cycles in autoclaved deionized water. DNA content was quantified by mixing the cell lysate in Hoechst 33258 Solution (Sigma Aldrich) and fluorescence was measured for emission and excitation at 450nm and 365nm, respectively.

PGE2 Immunoassay

Mechanically stimulated (fluid flow applied) and static cells were allowed to synthesize PGE2 in 1ml of media under incubation at 37°C and 5%CO2 for 1hour. The supernatant was collected and assayed for PGE2 content using the Prostaglandin E2 ELISA Kit-Monoclonal. The PGE2 content was normalized to the total DNA content. Cells were harvested and DNA was quantified as described above.

Immunofluorescent staining

Alterations in the cytoskeleton due to ROCK inhibition were analysed in loaded and static groups using immunofluorescent staining to examine changes in actin stress fibres (phalloidintetramethylrhodamine Bisothiocyanate (TRITC) solution; Sigma-Aldrich; 1:1000) and nucleus (DAPI; Sigma Aldrich; 200ng/ml)

Statistical Analysis

A two-sample t-test was used to compare percentage of reduction of Alamar Blue reagent and DNA content of control cells and cells treated with Y-27632 (1010M). A one way-ANOVA test was used to compare PGE2 synthesis amongst loaded and static cells with/without ROCK inhibition.

Results

The viability of MC3T3-E1 cells was not affected when exposed to Y-27632, a pharmacological ROCK inhibitor, at 10µM for 1hr. The ability of the cells to reduce Alamar Blue reagent dye (Resazurin) did not show any statistically significant difference *(p value > 0.05)* when treated with Y-27632, Figure 1(A), indicating the non-toxic effects. Furthermore, it was also seen that DNA content of these cells was not significantly different *(p value > 0.05)* either treated or untreated with ROCK inhibitor, Figure 1(B).

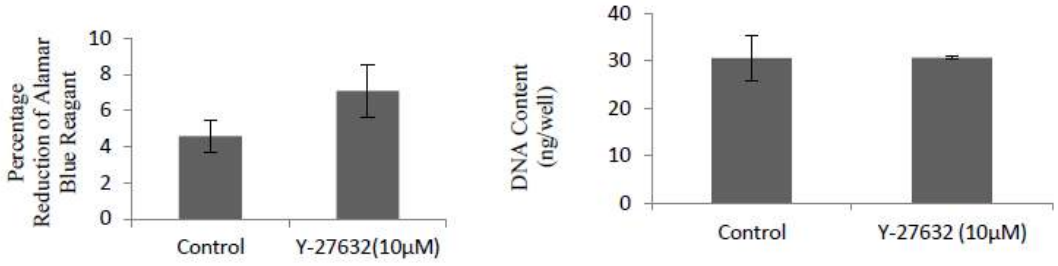

Figure 1: (A) Percentenage of reduction in Alamar Blue reagant in MC3T3-E1 cells treated with and without, pharmacological ROCK inhibitor, Y-27632 at 10µM (B) DNA content of treated and non-treated cells. No statistically significant differences seen (p value > 0.05).

When ROCK was inhibited using Y-27632 in mechanically stimulated cells, the PGE2 synthesis was highly reduced (p-value <0.05) indicating the negative effect on osteogenesis of these cells. The synthesis of PGE2 by mechanically stimulated and static control cells was also statistically significantly different from each other (p-value <0.05), Figure 2(A).
Immunofluoroscent imaging,
Figure 2(B), showed extreme disruption of cytoskeleton when flow was applied on ROCK inhibited cells. Also some disruption was visible in inhibitor exposed cells under static condition but static and flow control cells did not seem to have much difference in the development of F-actin stress-fibres as seen in a previous study[12].

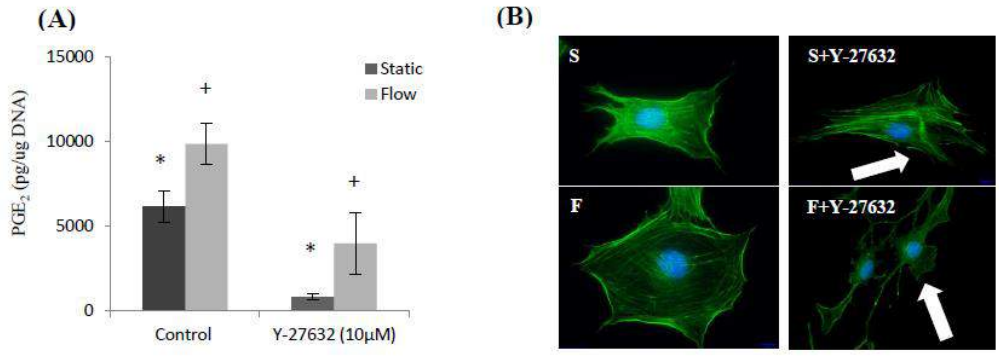

*Figure 2: (A)PGE2 synthesis by mechanically stimulated (flow) and static MC3T3-E1cells following treatment with or without Y-27632. Statistically significant differences were seen,+*p <0.05. (B) Immunofluoroscent imaging of actin-fibres (green) and nucleus (blue) for all conditions, where S is static and F is flow. White arrows indicate where disruption in actin cytoskeleton is seen*

Discussion

The results of this study for the first time, show that ROCK inhibition in osteoblasts suppresses the fluid flow induced osteogenic effects, as evident from reduction in PGE2 synthesis. Previously it was shown that ROCK activation may be necessary for fluid flow induced osteogenesis in Mesenchymal Stem Cell (MSCs) [10]. Ongoing studies are evaluating alterations in gene expressions of osteogenic markers such as COX-2, RUNX-2, ALP, RANKL and Osteocalcin. All the results will be compared to similar experiments done with estrogen deficient cells and as ROCK is an important mechanotransduction protein, further experiments are expected to shed some light on targeting the altered mechanosensitivity and mechanotransduction of osteoporotic bone cells.

References:

1. Brennan, M.A., ; McDermott, A., ; McNamara, L.M. . *The Impact of Shear Stress during Estrogen Withdrawal on Cell Viability and Mineral Production of Osteoblasts*. in *Orthopaedic Research Society*. 2012. San Francisco, USA.
2. Brennan, M.A.G., J. P.; O'Brien, F. J.; McNamara, L. M., *Effects of ageing, prolonged estrogen deficiency and zoledronate on bone tissue mineral distribution.* J Mech Behav Biomed Mater, 2014. **29**: p. 161-70.
3. Voisin, M.M., L. M., *Differential beta3 and beta1 Integrin Expression in Bone Marrow and Cortical Bone of Estrogen Deficient Rats.* Anat Rec, 2015. **298**(9): p. 1548-59.
4. Ogawa, T.T., H; Miyata, Y; Ushitora, Y; Fudaba, Y; Kobayashi, T; Arihiro, K; Okajima, M; Asahara, T, *Rho-Associated Kinase Inhibitor Reduces Tumor Recurrence After Liver Transplantation in a Rat Hepatoma Model.* American journal of transplantation, 2007. **7**(2): p. 347-355.
5. Wyckoff, J.B.P., Sophie E; Gschmeissner, Steve; Condeelis, John S; Sahai, Erik, *ROCK-and myosin-dependent matrix deformation enables protease-independent tumor-cell invasion in vivo.* Current Biology, 2006. **16**(15): p. 1515-1523.
6. Gardinier, J., et al., *P2Y2 receptors regulate osteoblast mechanosensitivity during fluid flow.* Am J Physiol Cell Physiol, 2014. **306**(11): p. C1058-67.
7. Klein-Nulend, J., et al., *Donor age and mechanosensitivity of human bone cells.* Osteoporos Int, 2002. **13**(2): p. 137-46.
8. Kazmers, N.H., et al., *Rho GTPase signaling and PTH 3–34, but not PTH 1–34, maintain the actin cytoskeleton and antagonize bisphosphonate effects in mouse osteoblastic MC3T3-E1 cells.* Bone, 2009. **45**(1): p. 52-60.
9. Street, C.A., et al., *Pharmacological inhibition of Rho-kinase (ROCK) signaling enhances cisplatin resistance in neuroblastoma cells.* International journal of oncology, 2010. **37**(5): p. 1297-1305.
10. Arnsdorf, E.J.T., Padmaja; Kwon, Ronald Y; Jacobs, Christopher R, *Mechanically induced osteogenic differentiation–the role of RhoA, ROCKII and cytoskeletal dynamics.* Journal of cell science, 2009. **122**(4): p. 546-553.
11. Haugh, M.G., T.J. Vaughan, and L.M. McNamara, *The role of integrin α V β 3 in osteocyte mechanotransduction.* Journal of the mechanical behavior of biomedical materials, 2015. **42**: p. 67-75.
12. Malone, A.M., et al., *The role of actin cytoskeleton in oscillatory fluid flow-induced signaling in MC3T3-E1 osteoblasts.* American Journal of Physiology, 2007. **292**(5): p. C1830-C1836.

Mechanobiological Modulation of In Situ and In Vivo Osteocytic Ca2+ Oscillations in Response to Acoustic Radiation Force using Black6 and Ai38/Dmp1-Cre Mice

Minyi Hu, PhD[1], Jian Jiao, MS[1], Daniel Gibbons, BS[1], Xiaofei Li, MS[1], Guowei Tian, PhD[2], Yi-Xian Qin, PhD[1]
[1]Dept of Biomedical Engineering, Stony Brook University, Stony Brook, NY 11794-5281
[2]CMIC-Two Photon Imaging Center, Stony Brook University, Stony Brook, NY 11794-5200

Clinical evidence has pointed the critical mechanotransduction in bone remodeling/regeneration. While the biological effect of ultrasound on bone healing has been well documented, the underlying mechanism is largely unknown. Our group elucidated the mechanobiological modulation of cytoskeleton and Ca^{2+} influx in in vitro osteoblastic cells by short-term focused acoustic radiation force. In greater relation to the physiological setting by solving the limitation of disconnected blood circulation, the current study aimed to visualize and quantify Ca^{2+} oscillations of real-time in situ and in vivo osteocytes in response to medium intensity focused ultrasound (MIFU). For in situ study, 3-month-old Black6 mice were used to obtain fresh calvarias. The samples were stained in Fluo-8 AM for Ca^{2+} fluorescent label and subjected to MIFU stimulation for 30sec: 0.05, 0.2, 0.3, 0.5, and 0.7W (Fig1). For in vivo study, Ai38/Dmp1-cre mice that express the Ca^{2+} indicator protein in bone cells (EGFP fluorescent GCaMP3) were under isoflurane anesthesia; the top skin of the head was cut opened, gently exposing the calvaria. The animal's head was stabilized on a custom-made bed, where its chin was placed onto the MIFU transducer (Fig2A): 0.2, 0.5 and 1W for 1min. Real-time confocal imaging was performed to capture the Ca^{2+} signal in the osteocyte cell bodies under MIFU. In situ MIFU at 0.3-0.7W led to significant Ca^{2+} oscillations: 85±16%, 80±18% and 84±17% ($p<0.01$ vs. 0.05W; $p<0.05$ vs. 0.2W) of responded cells, respectively (Fig1). MIFU at >0.3W energies led to a higher number of Ca^{2+} spikes and larger spike magnitudes. The initiation time to the first Ca^{2+} spike seemed to be relatively the same for all the energies (~18sec). In vivo MIFU at 0.2, 0.5 and 1W led to Ca^{2+} oscillations: 90%, 98% (+8% vs. 0.2W) and 100% (+11% vs. 0.2W) of responded cells, respectively (Fig2). Higher MIFU energies led to larger Ca^{2+} spike magnitudes and longer time to elicit the first spike. MIFU at 0.5 and 1W had 71% and 87% larger Ca^{2+} spike magnitude, 30% and 54% longer spike initiation time than at 0.2W, as well as 16% and 20% less Ca^{2+} spikes than at 0.2W, respectively. In conclusion, this study provided a pilot observation of in situ and in vivo osteocytic Ca^{2+} oscillations under noninvasive acoustic radiation force, which aids further exploration of the mechanosensing mechanism of controlled bone cell motility response to fluid flow loading.

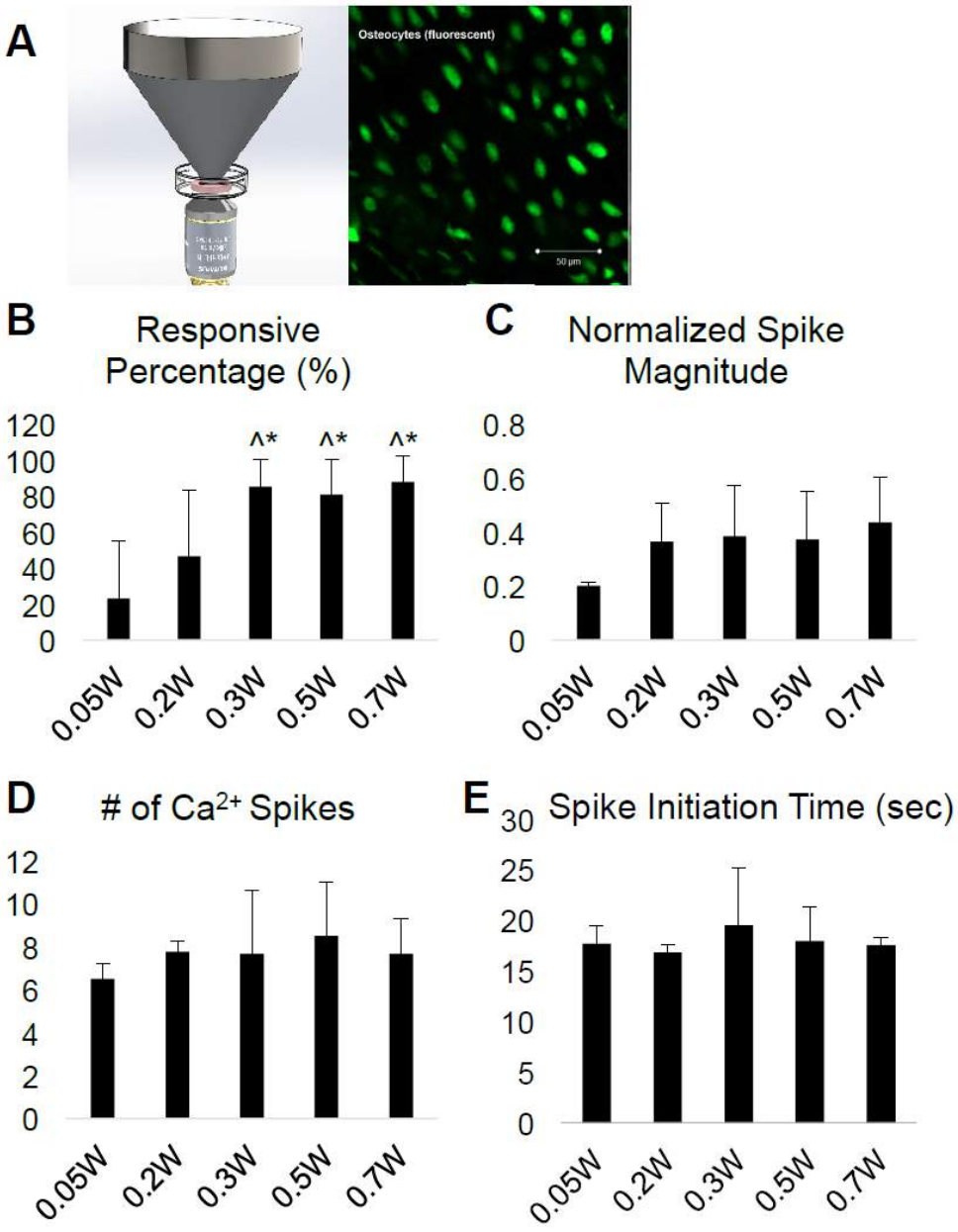

Figure 1. Experimental setup of *in situ* mouse calvaria under MIFU stimulation and Ca^{2+} imaging (A); responsive percentage (B); normalized spike magnitude (C), number of spikes (D), and spike initiation time (E) of osteocyte Ca^{2+} responses to MIFU at various energy powers. ^p<0.01 vs. 0.05W; *p<0.05 vs. 0.2W.

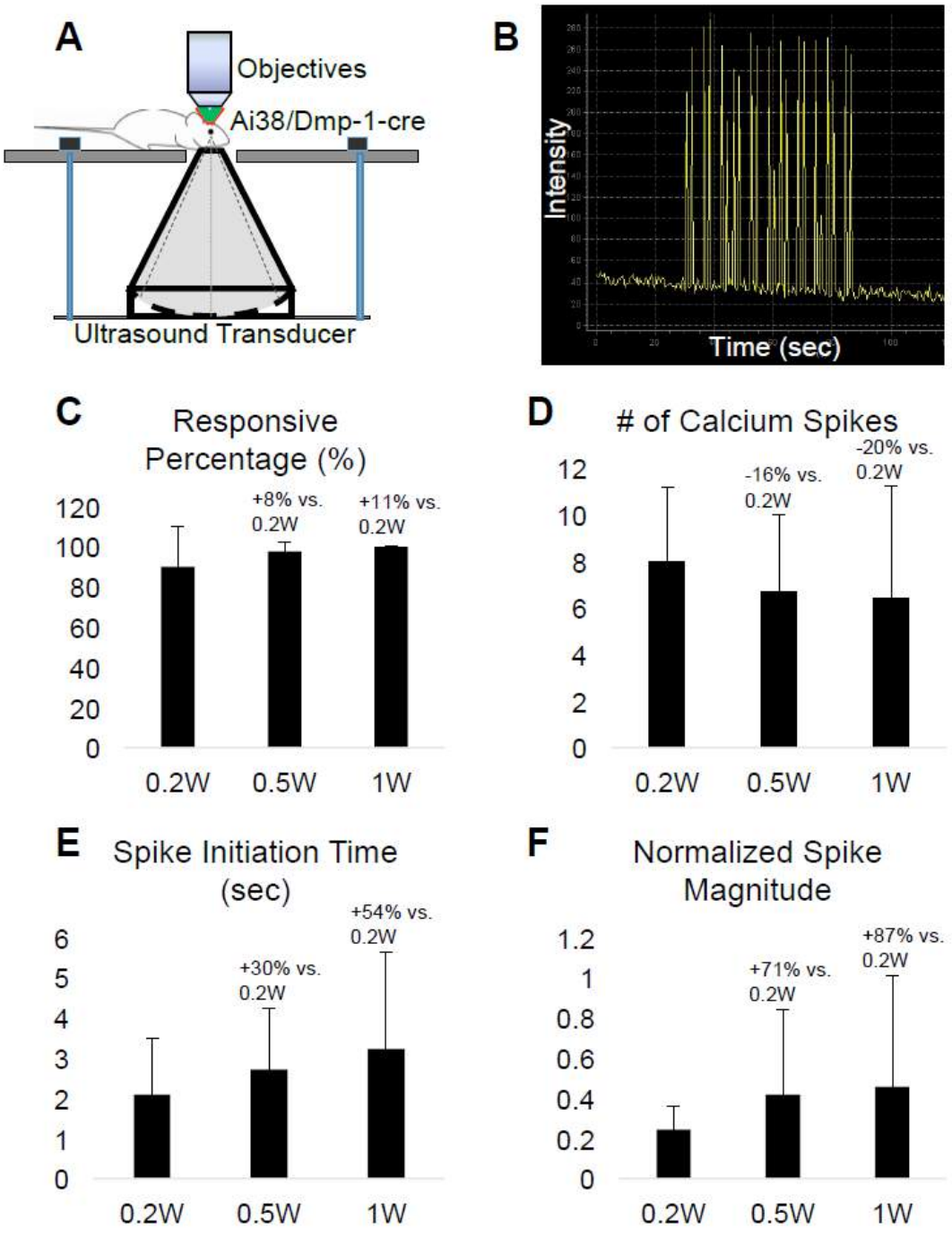

Figure 2. Experimental setup of in vivo Ai38/Dmp-1-cre mouse under MIFU stimulation and Ca^{2+} imaging on the calvaria (A); representative Ca^{2+} trace under 1W MIFU (B); responsive percentage (C); number of spikes (D); spike initiation time (E); normalized spike magnitude (F) of osteocyte Ca^{2+} responses to MIFU at various energy powers.

Distinct Response of Osteons at Different Locations in Response to Loading and Intermittent PTH Injections

Ke Wang DDS[1], Yuan Hui, DDS[2], Yinshi Ren, PhD[3], Ying Liu, MD[1], Xianglong Han, DDS[4], and Jing Q. Feng, PhD[1]
[1]Department of Biomedical Science, Texas A&M Health Science Center, Baylor College of Dentistry, Dallas, TX;
[2]Department of Orthodontics, Fourth Military Medical of University, China;
[3]Cellular, Developmental, and Genome Laboratories, Musculoskeletal Research Center, Duke University, Durham, NC;
[4]State Key Laboratory of Oral Diseases, West China Hospital of Stomatology, Sichuan University, China.

Currently, most, if not all, bone studies focus on rodents, which do not have an osteon structure, the *basic unit of bone formation and remodeling in large mammalians.* Interestingly, recent studies discovered an astonish defect in Harversian-canal-osteon structures in patients with osteoporosis. *Because studies of large animal bones have fallen out of favor since the molecular biology era*, we basically *know very little about how osteons are formed.* In this study, we first demonstrated that primary osteons in the embryonic dog femur bone are originated from both periosteum and endosteum layers proportionally (Fig 1). Next, we asked whether constant
forces, which were generated for 5-weeks by open-coil springs anchored on miniscrew implants in the tibia with a force 0, and 200 g (right tibia) separately, would affect osteon formation (Fig 2a). In the loading groups (6 adult dogs), there were sharp increases in Haversian canals by uCT (Fig 2b). The images of backscattered SEM and triple labeling (with 10 day apart) displayed many newly formed osteons, which were mainly derived from the expanded periosteum layer (Fig 3). These newly formed osteons expressed high levels of endothelial and bone markers, including VEGF, periostin, OSX and BSP (Fig 4). This asymmetric contribution of osteon formation from the periosteum prompted us to initiate a different set of experiments, in which we tested the impact of intermittent injections of PTH on wild type mice and 4 young adult dogs (10 ug/kg per day for four weeks). Interestingly, the increased bone volume was associated with the expanded endosteum layer in mice (Fig 5, left). Similarly, bone volume expansions occurred in the PTH treated dogs, in which the lamellar structures on the endosteum side were replaced by the newly formed osteons (Fig 5, right). We then asked whether similar events would occur in intramembranous bone in response to mechanical loading. Using tooth movement model, we observed numerous newly formed osteons by backscattered SEM and triple labeling images (Fig 6). This newly formed bone was originated from the periodontal ligaments (PDL). Collectively, these data for the first time revealed that 1) osteons are formed from both periosteum and endosteum layers during embryonic dog bone formation; 2) the mechanical loading initiates osteon formation from the periosteum layer; 3) the PTH induced osteon formation is mainly originated from the endosteum side; and 4) the osteon formation stimulated by tooth movement is from the PDL (Fig 7). Based on these exciting data, we conclude
that there are different progenitor cell pools, which are responsible for osteon formation in different physiological status.

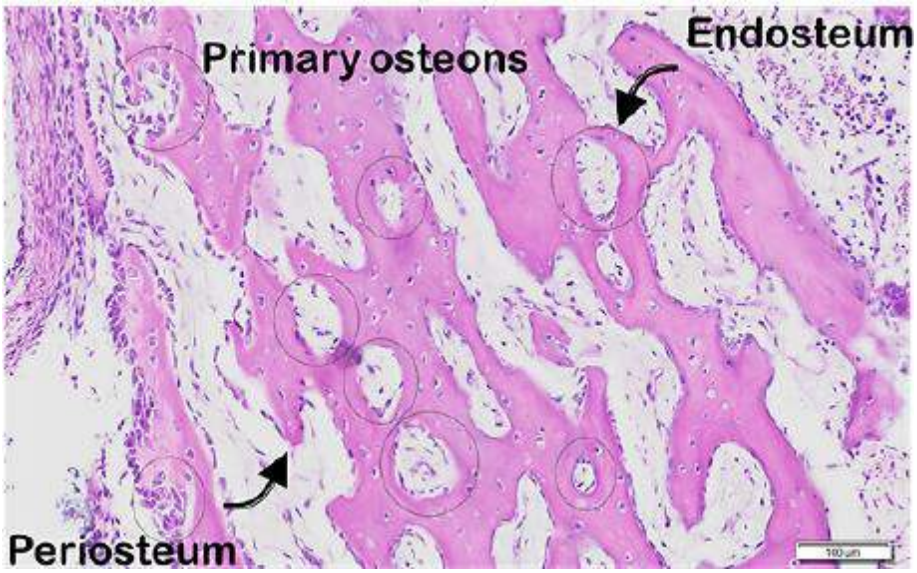

Fig 1. The dog primary osteons are formed from both periosteum and endosteum layers during embryonic development.

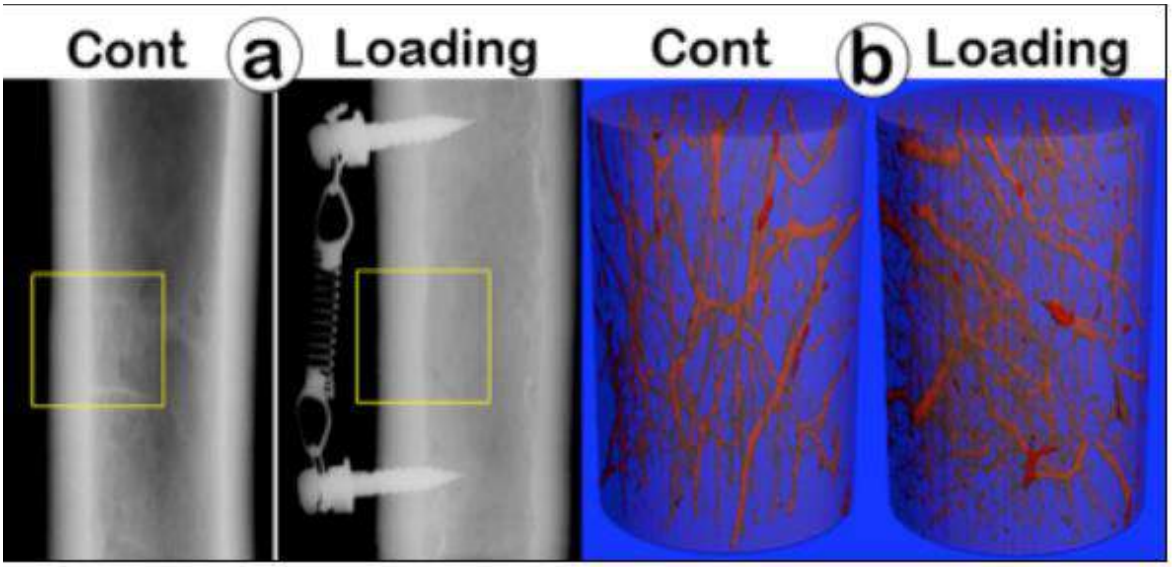

Fig 2. The loading increases the bone volume by radiograph (**a,** right) and Haversian canals by uCT (**b**, right)

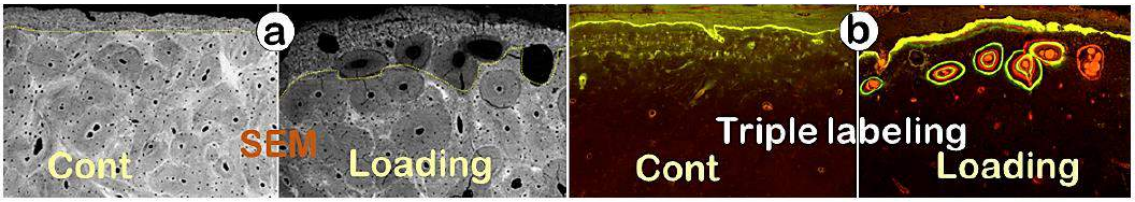

Fig 3. The loading increases the osteon formation by backscattered SEM (**a**, right) and mineralization by the triple labeling (calcein first, alizarin red second and calcein last with a 10 day gap with each injections (**b**, right).

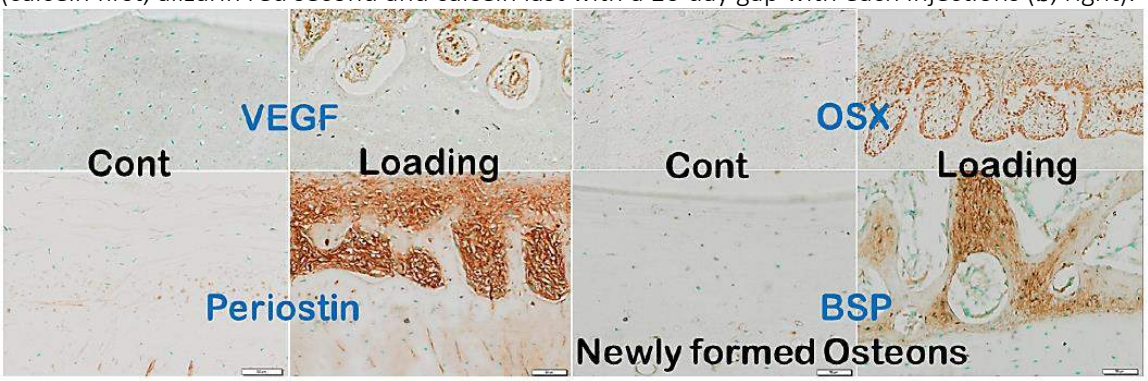

Fig 4. The loading increases expressions of markers critical for vessels and bone formation (right panels), including VEGF for endothelial cells (Upper left), osterix (OSX, an essential transcription factor for bone formation, upper right), periostin (a marker for periosteum, lower left), and BSP (a marker for bone cells, lower right).

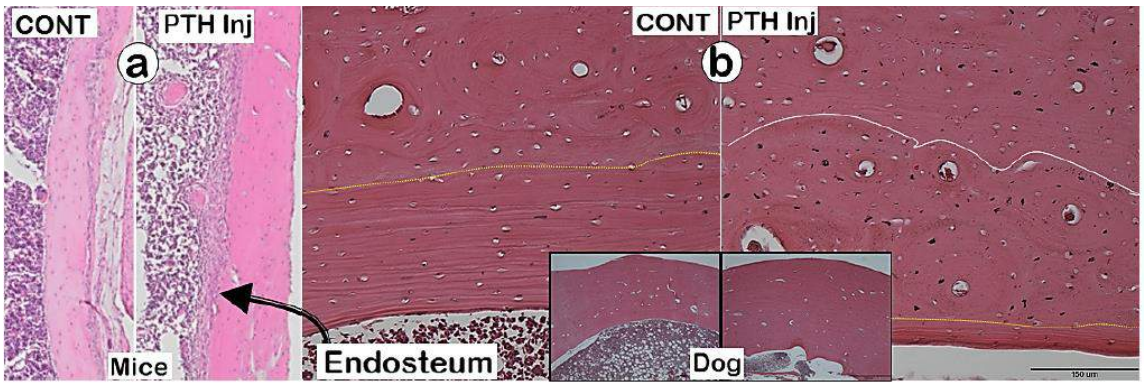

Fig 5. The intermittent PTH injections for 4-weeks result in increases in bone volumes originated from the endosteum in both mice and dogs. **a**. Injections of PTH in mice lead to increases in the endosteum layer and cortical bone (left panel); and **b**. Injections of PTH in dogs lead to increases in osteon formation, which is derived from the endosteum (right panel).

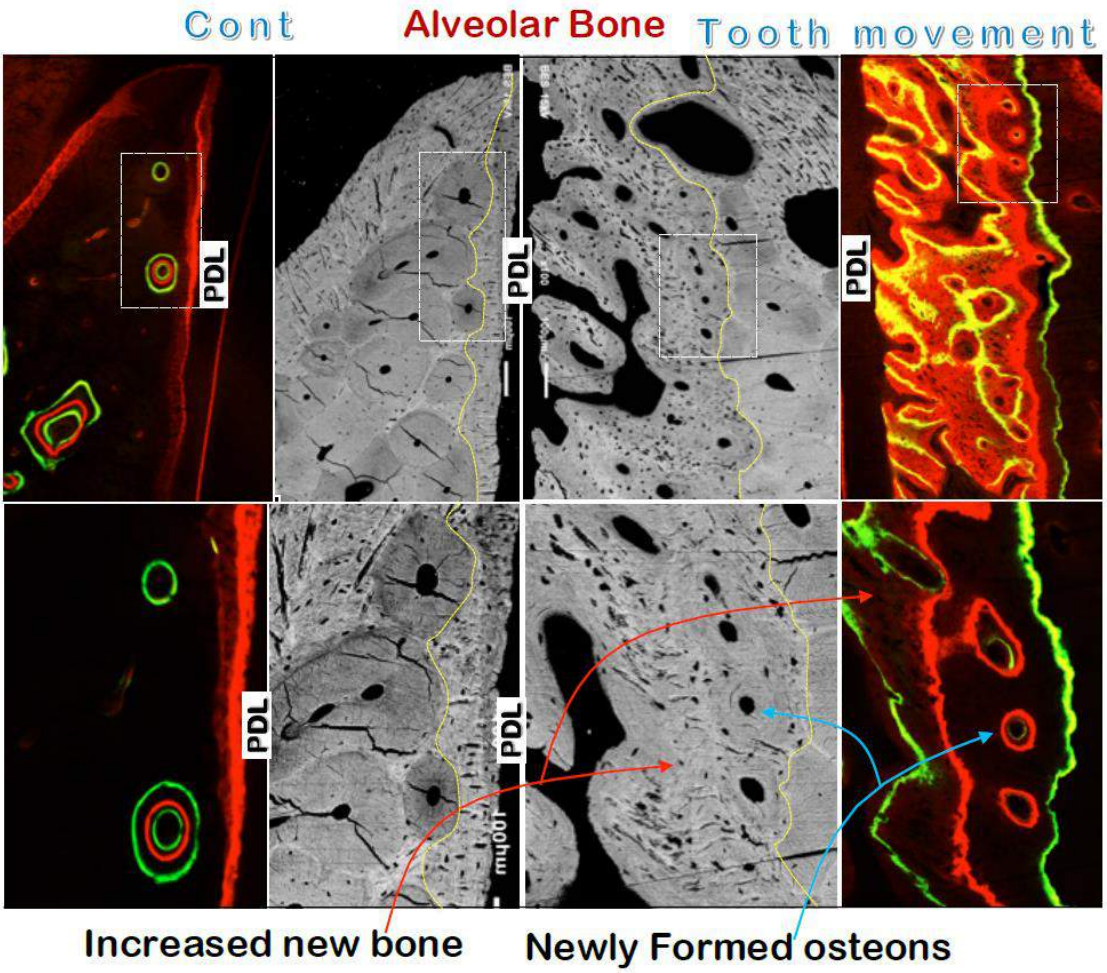

Fig 6. The tooth movement for 5-weeks results in increases in alveolar bone formation in dogs (right) as documented by the backscattered SEM techniques and the double labelling. The increased bone was originated from the periodontal ligament (PDL) layer in the movement group (right), in which there are numerous newly formed osteons in response to tooth movement.

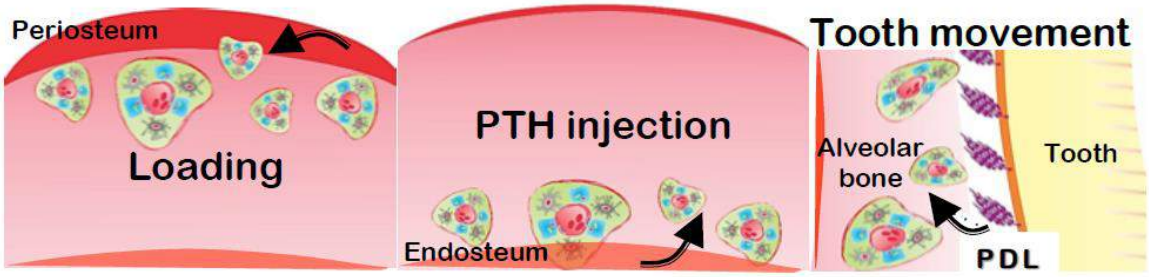

Fig 7. The three different models to show the variations in osteon formation: 1) the periosteum is responsible for osteon formation in loading (left); 2) The endosteum progenitor cells are critical for osteon formation in PTH response (middle); and 3) The PDL is responsible for osteon formation in tooth movement (right).

Underdevelopment of Trabecular Bone Microarchitecture in the Distal Tibia and Distal Femur of Ambulatory Children with Cerebral Palsy Becomes More Pronounced with Distance from the Growth Plate

Daniel G. Whitney, MS[a], Harshvardhan Singh, PhD[a], Freeman Miller, MD[b], Christopher M. Modlesky, PhD[a]
[a]Department of Kinesiology and Applied Physiology, University of Delaware, Newark, DE, USA, [b]Department of Orthopedics, AI duPont Hospital for Children, Wilmington, DE, USA.

Background: Children with cerebral palsy (CP) have impaired motor function [1, 2], an underdeveloped musculoskeletal system [3, 4] and low levels of physical activity [5] which are associated with a high incidence of low-energy fractures occurring primarily at the femur and tibia in this pediatric population [6]. Nonambulatory children with more severe forms of CP have an underdeveloped trabecular bone microarchitecture (TBM) in the distal femur, their primary fracture site [6] that becomes more pronounced with distance from the growth plate [7]. The purpose of this study was determine if ambulatory children with mild CP have an underdeveloped TBM in the distal tibia and distal femur and if the pattern of TBM becomes more pronounced with distance from the growth plate.

Methods: Twelve ambulatory children with mild CP and 12 sex-, age- and race-matched controls (5 to 12 years of age) participated in this study. Twenty-six axial magnetic resonance images (175 x 175 x 700 µm3) of the distal tibia and distal femur immediately above the growth plate were collected and measures of TBM [apparent trabecular bone volume to total volume (appBV/TV), trabecular number (appTb.N), trabecular thickness (appTb.Th) and trabecular separation (appTb.Sp)] of the medial and lateral half of the distal tibia and distal femur, respectively, were obtained **(Figure 1)**. Using SPSS, regression analyses were performed for TBM and distance from the growth plate. Independent t-tests were used to compare regions of TBM and the slopes of TBM with distance from the growth plate between groups.

Results: Compared to controls, the distal tibia and distal femur in children with CP had lower appBV/TV (20% and 12%), lower appTb.N (14% and 8%) and higher appTb.Sp (30% and 16%), respectively (all $p < 0.05$), and lower appTb.Th in the distal tibia (8%, $p = 0.016$), but not in the distal femur (5%, $p = 0.174$) **(Figure 2)**. When distance from the growth plate was regressed against measures of TBM, children with CP had steeper slopes in appBV/TV, appTb.N, appTb.Th and appTb.Sp in the distal tibia and appTb.N and appTb.Sp in the distal femur (all $p < 0.05$) **(Figure 3).**

Discussion: Ambulatory children with mild CP present with an underdevelopment in TBM in the distal tibia and distal femur, their most commonly fractured bones [6], which becomes more pronounced with distance from the growth plate. Treatments that offset this compromised bone pattern are needed.

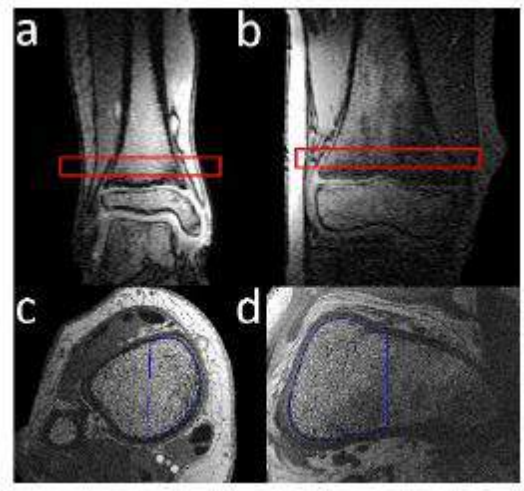

Figure 1. Regions of interest (red box) were identified using coronal magnetic resonance images of the distal tibia (a) and distal femur (b). Trabecular bone microarchitecture was analyzed using consecutive axial images of the medial half of the distal tibia (c) and the lateral half of the distal femur (d) (blue line).

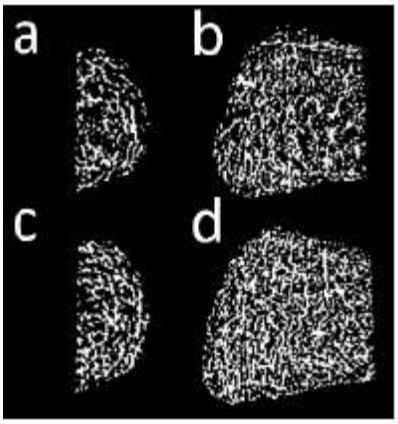

Figure 2. Representative binarized images (white is trabecular bone) from a set of twin girls (aged 5.6 yrs) show the underdevelopment of the medial half of the distal tibia (a, c) and lateral half of the distal femur (b, d) in the twin with CP (a, b) and the typically developing twin (c, d).

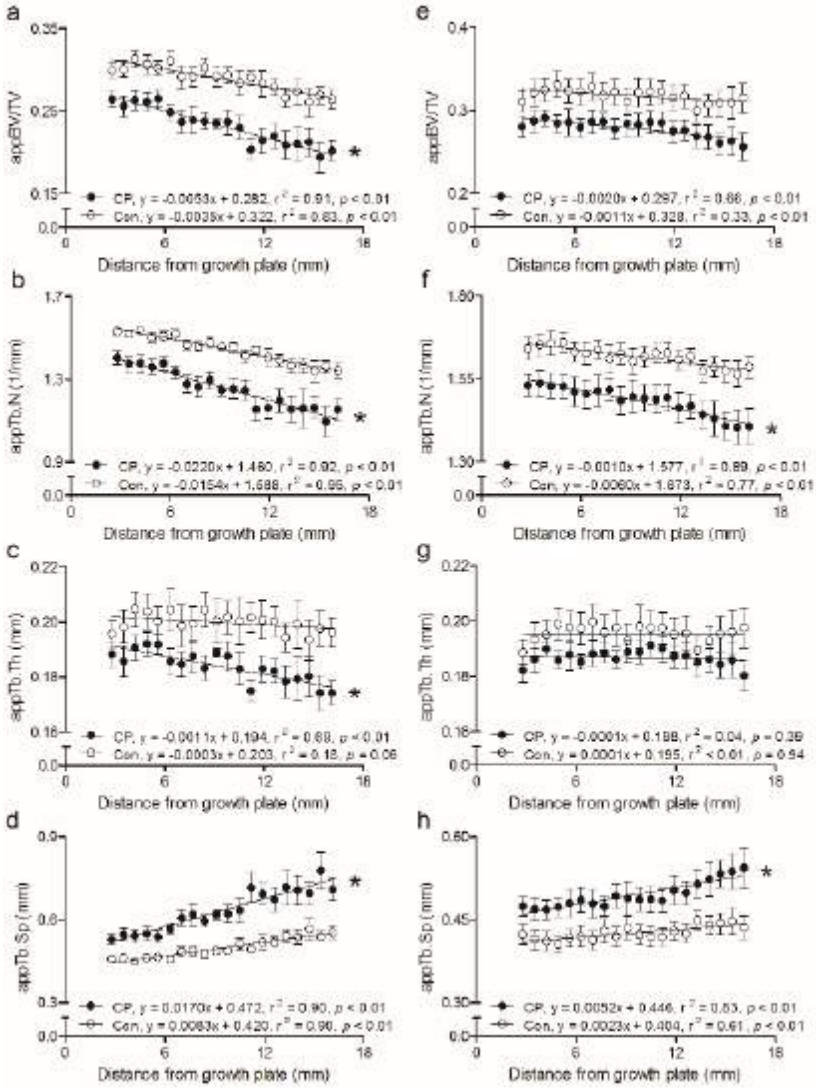

Figure 3. Scatter plots show the relationships between distance from the growth plate at the distal tibia (a–d) and distal femur (e–h) and apparent bone volume to total volume (appBV/TV) (a, e), trabecular number (appTb.N) (b, f), trabecular thickness (appTb.Th) (c, g) and trabecular separation (appTb.Sp) (d, h) in children with CP and controls. *indicates steeper slope compared to controls, $p < 0.05$.

References

[1] Stackhouse SK, Binder-Macleod SA, Lee SC. Voluntary muscle activation, contractile properties, and fatigability in children with and without cerebral palsy. Muscle & nerve 2005;31: 594-601.
[2] Moreau NG, Falvo MJ, Damiano DL. Rapid force generation is impaired in cerebral palsy and is related to decreased muscle size and functional mobility. Gait & posture 2012;35: 154-8.
[3] Johnson DL, Miller F, Subramanian P, Modlesky CM. Adipose tissue infiltration of skeletal muscle in children with cerebral palsy. The Journal of pediatrics 2009;154: 715-20.
[4] Modlesky CM, Kanoff SA, Johnson DL, Subramanian P, Miller F. Evaluation of the femoral midshaft in children with cerebral palsy using magnetic resonance imaging. Osteoporosis international : a journal established as result of cooperation between the European Foundation for Osteoporosis and the National Osteoporosis Foundation of the USA 2009;20: 609-15.
[5] Carlon SL, Taylor NF, Dodd KJ, Shields N. Differences in habitual physical activity levels of young people with cerebral palsy and their typically developing peers: a systematic review. Disability and rehabilitation 2013;35: 647-55.
[6] Presedo A, Dabney KW, Miller F. Fractures in patients with cerebral palsy. Journal of pediatric orthopedics 2007;27: 147-53.
[7] Modlesky CM, Whitney DG, Singh H, Barbe MF, Kirby JT, Miller F. Underdevelopment of trabecular bone microarchitecture in the distal femur of nonambulatory children with cerebral palsy becomes more pronounced with distance from the growth plate. Osteoporosis international : a journal established as result of cooperation between the European Foundation for Osteoporosis and the National Osteoporosis Foundation of the USA 2015;26: 505-12.

Overview and Historical Context - Challenges in Translating Life Sciences Research into Effective Health Care Solutions

Gary Krishnan, MSc, PhD
Eli Lilly and Company, Indianapolis, IN

The goal of establishing the National Institutes of Health was to enable publicly funded research initiatives to begin the process of translation as they realize their potential to provide health care solutions. The Pharmaceutical/Biotechnology Industry has built a sustainable business model that leverages public data to begin curating proprietary assets that claim to address unmet clinical need. The current model practiced over the past 350 years has generated over 7000 active medicines for use in patients. However, in the past twenty years in spite of increasing investment by the Pharmaceutical/Biotech community in research and development, it has not yielded a proportional increase in identifying novel molecular entities for patients. While there are numerous reasons for this decline, largely attributed to identifying safer and better differentiated molecules, an emerging challenge has been the inability to seed tangible drug discovery ideas from the most attractive research published in the high impact journals. For instance at Lilly, approximately 50% of targets of interests fail to measure up in terms of tractable starting points for drug discovery. Up to 70% of these attractive targets derived from high end journals fail to reproduce the biology in terms of their effect size or the claimed benefit in the context of the disease condition. Furthermore, a significant proportion (45%) of the successful targets based on rodent disease models, fail to translate in humans. This has resulted in a significant loss of opportunity and resources pursuing such targets. Root cause analysis of this reproducibility coupled with lack of relevance to human disease points to numerous systemic issues in research. The talk will focus on potential solutions for these issues and will highlight the urgency with which we should address some of the same.

Know Thy Cells (and Antibodies): Improving Biomedical Research Reproducibility

Leonard P. Freedman, PhD
Global Biological Standards Institute, Washington, DC

Irreproducible basic biological and preclinical research is a tremendously expensive and global problem. The inability to reproduce experimental data in preclinical studies has resulted in the invalidation of research breakthroughs, retraction of published papers, abrupt discontinuation of clinical studies, and reduced trust in the research and development enterprise. More importantly, valuable time and critical resources are wasted by irreproducibility as opportunities to enhance global health are delayed or simply lost. Although the causes of irreproducible preclinical research are complex, they can be traced to cumulative errors/flaws in one or more of the following areas: 1) study design, (2) biological reagents and reference materials, (3) laboratory protocols, and (4) data analysis and reporting. These sources of irreproducibility are often magnified by the explosion of high-throughput technologies, genomics, and other data-intensive disciplines. This presentation will use examples of biological materials and reagents, specifically cell lines and antibodies, on the impact of irreproducibility in basic/preclinical research and development, and how the implementation of consensus-based standards to authenticate and certify these reagents will lead to both increased rates of reproducibility and dramatic returns on research funding investments.

Improving the Reproducibility of Research Findings Using Mouse Models

Bart Williams, PhD
Van Andel Research Institute, Grand Rapids, MI

Genetically engineered mouse models (GEMMs) are a mainstay of biological research and, properly utilized and interpreted, can inform the development and optimization of therapies for human disease. The recent application of CRISPR/Cas9-mediated gene editing to the creation of GEMMs could potentially exponentially increase our ability to quickly generate mouse models even more relevant to human disease. With this in mind, it will be important to ensure accuracy in terms of reporting the results of experiments and providing access to all such GEMMs to interested investigators as soon as possible after their initial publication. Several aspects should be considered in this context. First, it will be important to report details about how such models were constructed and how the genetic alterations were validated. In addition, it is imperative that funding agencies and scientific publishers enforce NIH-mandated requirements to distribute GEMMs after publication to interested investigators as independent confirmation of experimental results is a key step towards increasing confidence in the importance of experimental advances. Finally, as we consider how to ensure that data presented from these models is accurate and reproducible, changes in how we evaluate scientific contributions should be considered. Replication and validation of published findings are critical in providing further rationale to pursue promising therapies. However, decisions on tenure, promotion, and grant funding often discount this type of work. Dealing with these systemic challenges is likely to be necessary to enhance the reproducibility of scientific findings and maintain public confidence and support for the worthiness of scientific investment by the NIH and other funding agencies.

Why we Wnt to Treat Osteosarcoma

Carl T. Gustafson, BS, Avudaiappan Maran, PhD, Michael J. Yaszemski, MD, PhD
Mayo Clinic, Rochester, MN

Osteosarcoma (OS) is the most common pediatric bone malignancy. With approximately one thousand new cases in the United States every year, 90% of OS patients are children and young adults between the ages of 10 and 30 (1, 2). During surgical resection of the primary tumor, degree of tumor necrosis is assessed and used as a litmus test to separate patients into categories of "responders" and "non-responders". Those with low tumor necrosis (necrosis <90%) after neoadjuvant chemotherapy have a dismal 5-year survival rate - nearing 20% - due to relapse and development of lung metastases. Lack of response, or resistance, to the standard chemotherapy regimen is the major cause for disease progression in OS (1, 3). While the canonical Wnt signaling pathway has been mechanistically tied to drug resistance, as well as tumor development, and poor prognosis in many cancers, including OS, Wnt signaling has largely remained untouched by our currently available chemotherapeutics (4, 5). No Wnt targeting small molecules have yet been approved for clinical use, outside of a handful of trials. In OS, a large body of work indicates overexpression of Wnt promoting factors, and correlation of Wnt expression with poor prognosis in OS (6, 7). Thus, an overwhelming consensus indicates the therapeutic appeal of Wnt signaling, while our means to effectively block Wnt have yet proved to be insufficient. In other cancers, the appeal of Wnt targeted therapies has been highlighted by the discovery of activating mutations in Wnt family member proteins. Common mutations in APC and β-catenin in colorectal cancers have historically driven cancer development, and have recently driven researchers in their efforts to develop drug candidates to address the problem of hyper-activated Wnt signaling.

Recently, a number of compounds which facilitate pharmacological inhibition of Wnt signaling have been reported. These small molecules have shown utility in applications ranging from cardiac regeneration, to diabetes, to cancer in pre-clinical models. Indeed, one newly developed compound targeting the Wnt protein modifying enzyme Porcupine has entered a Phase I dose-escalation trial (8). Among these small molecule candidates, the $^{\beta}$-catenin inhibitor FH535 has demonstrated promising fidelity to canonical Wnt inhibition in a number of reports (9, 10). Our group tested the efficacy of canonical Wnt signal blockade via FH535 in osteosarcoma. We found that FH535 effectively targets Wnt signaling, decreasing β-catenin transcriptional activity, as well as mRNA production of the β-catenin substrate Axin2. This on-target effect resulted in the inhibition of OS cell viability in all OS cell lines tested, while inducing cell cycle arrest via S-phase accumulation. Interestingly, in an *in vitro* model of doxorubicin resistant OS, we found that the doxorubicin resistant cells demonstrated greater sensitivity to FH535 as compared to the parental (wild-type) cell line (Figure 1, panels A and B). Axin2 response was pronounced in the doxorubicin resistant cells, indicating increased dependency on Wnt signaling in these cells, and susceptibility to Wnt inhibition. In the doxorubicin resistant cell line, we found that treatment with FH535 caused an accumulation of Axin2 protein (Figure 1, panel C).

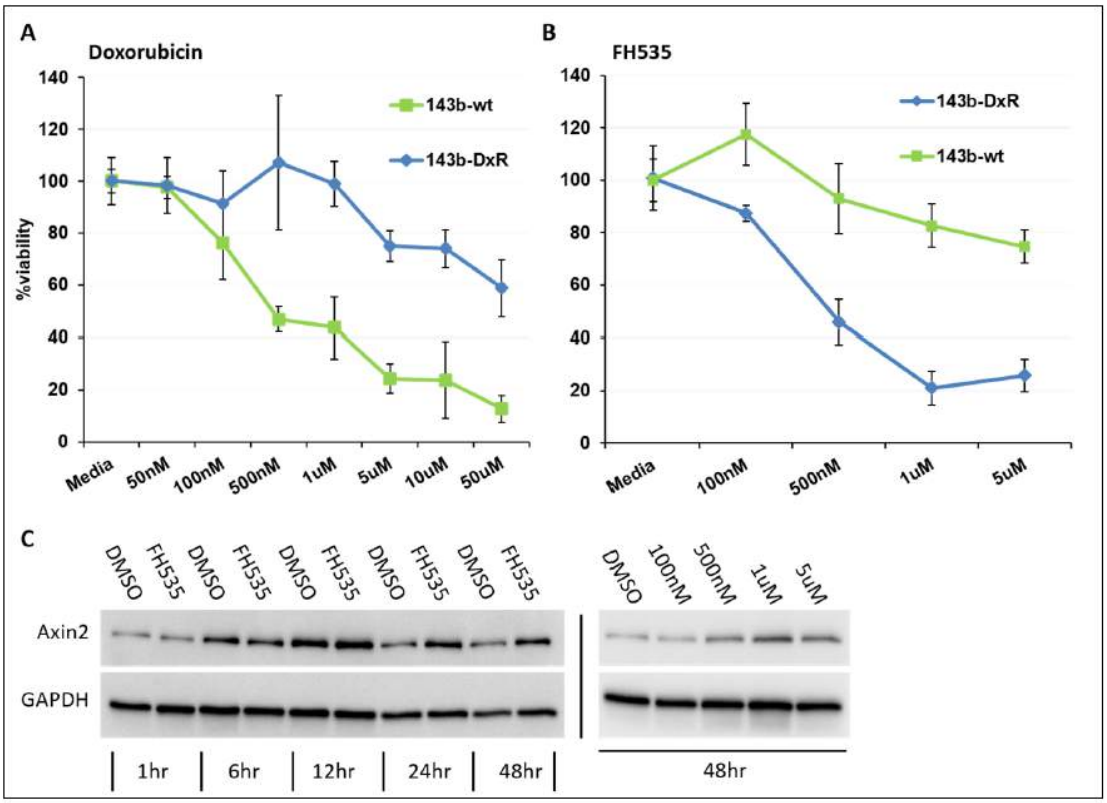

Figure 1: Cellular and molecular response to FH535. A: Response to 48 hour doxorubicin treatment in parental wild-type osteosarcoma cell line (143b-wt) and its derived doxorubicin resistant cell line (143b-DxR). B: Response to 48 hour FH535 treatment in 143b-wt and 143b-DxR cell lines. C: Effect of FH535 treatment on Axin2 protein in the 143b-DxR cell line.

This observation, though initially counter-intuitive, indicates that FH535 acts upon the Axin-regulating poly-ADP-ribose polymerase (PARP) family enzymes Tankyrase 1/2, inhibiting their function and resulting in the observed stabilization of Axin2. In recent years, Tankyrases have become the subject of much excitement and discussion within fields interested in Wnt signaling, due to the discovery of their role in regulating Axin proteins. Our study further establishes the molecular mechanism of FH535 effects on Tankyrases, while also investigating the mechanisms of cell death induced by Tankyrase inhibition in OS and doxorubicin resistant OS.

Our study is the first report of which we are aware which clarifies the specific mechanism of action of the widely published Wnt inhibitor FH535. The establishment of the mechanism of action of this drug adds significant value to its utility in Wnt, and assists in clarifying previous work done with this molecule. Additionally, our research addresses pressing questions regarding treatment options in doxorubicin resistant osteosarcoma, and the value of Wnt inhibition in this context. In sum, this work indicates potential for new treatment options for osteosarcoma patients who do not respond to the standard treatment regimen of neoadjuvant chemotherapy and surgical resection.

References:

1. Fletcher CDM, U. K., Mertens F. in *World Health Organization Classification of Tumours* (ed Sobin L Kleihues P) 415 (IARC Press, Lyon, France, 2002).
2. Ritter, J. & Bielack, S. S. *Osteosarcoma.* Ann Oncol 21 Suppl 7, vii320-325, doi:10.1093/annonc/mdq276 (2010).
3. Bacci, G. et al. *Primary chemotherapy and delayed surgery for nonmetastatic osteosarcoma of the extremities. Results in 164 patients preoperatively treated with high doses of methotrexate followed by cisplatin and doxorubicin.* Cancer 72, 3227-3238 (1993).
4. Correa, S. et al. *Wnt/beta-catenin pathway regulates ABCB1 transcription in chronic myeloid leukemia.* BMC Cancer 12, 303, doi:10.1186/1471-2407-12-303 (2012).
5. Anastas, J. N. et al. *WNT5A enhances resistance of melanoma cells to targeted BRAF inhibitors.* J Clin Invest 124, 2877-2890, doi:10.1172/JCI70156 (2014).
6. Kurayoshi, M. et al. *Expression of Wnt-5a is correlated with aggressiveness of gastric cancer by stimulating cell migration and invasion.* Cancer Res 66, 10439-10448, doi:10.1158/0008-5472.CAN-06-2359 (2006).
7. Lu, B. J. et al. *Expression of WNT-5a and ROR2 correlates with disease severity in osteosarcoma.* Mol Med Rep 5, 1033-1036, doi:10.3892/mmr.2012.772 (2012).
8. Lum, L. & Clevers, H. *The Unusual Case of Porcupine.* Science, 337, 922-923, doi: 10.1126/science.1228179 (2012).
9. Bjorklund, C. C. et al. *Evidence of a role for CD44 and cell adhesion in mediating resistance to lenalidomide in multiple myeloma: therapeutic implications.* Leukemia, 28, 373-383. doi: 10.1038/leu.2013.174. (2014).
10. Wang, W.C. et al. *IL-6 augmented motility of airway epithelial cell BEAS-2B via Akt/GSK-3β signaling pathway*. J Cell Biochem, 113, 3567-3575. doi: 10.1002/jcb.24235 (2012).

Role of Phosphate in the Central Ox/Phos Metabolic Processes and Its Linkage to Collagen Production

Amira Hussein, PhD[1], Kevin Blank, MS[1], Deven Carrol, MSl[1], Kyle Lybrand, MD[1], Margaret Cooke, MD[1], Heather Matheny, MS[1], Brenna L. Hogue, MS[1], Serkalem Demissie, PhD[2], and Louis Gerstenfeld, PhD[1]
[1]Department of Orthopaedic Surgery, [2]School of Public Health, Boston University, Boston, MA, USA

Introduction: Prior studies of mice given a phosphate (Pi) deficient diet during fracture healing showed diminished skeletal progenitor commitment, delayed chondrocyte maturation and callus mineralization. Transcriptomic analysis of callus gene expression showed mitochondrial oxidative phosphorylation (ox/phos) genes were significantly down regulated ($p=3.16x10^{-23}$). The goal of this study was to determine how Pi restriction effect on ox/phos is interrelated to intermediate metabolism gene expression and functionally related to phenotype.

Methods: Femora fractures were generated in three strains of male mice. Pi deficiency was initiated 2 days prior to fracture and maintained for 14 days after which mice were returned to normal diet. Controls were fed a normal diet. Microarray analysis of total callus RNAs was carried out over 35-days of healing. Gene expression values were compared between the groups using analyses of covariance with strain and time points as covariates to examine diet effect (FDR q-value ≤0.05). Cluster analysis of ox/phos and intermediate metabolism genes was performed in JMP to identify gene groups showing common temporal responses. Functional Pi restriction studies were performed using ATDC5 chondroprogenitors cells. Growth, differentiation, protein and collagen accumulation, matrix mineralization and oxidative function were assessed.

Results: Comparison of the temporal clustering patterns identified how strain specific profiles for specific ox/phos, tricarboxylic acid cycle, and arginine and proline metabolism genes were co-regulated and coordinated with, pyruvate dehydrogenase, and two subunits of prolyl 4-hydroxylase in response to Pi conditions. In vitro studies showed that chondrocyte differentiation was associated with 2X increase in oxidative respiration. In the absence of BGP normal differentiation proceeded with 1.5X greater accumulation in total protein in the absence of mineralization. In these cultures oxidative respiration was an additional 2X higher. When differentiation was not induced with ascorbic acid and BGP oxidative respiration showed no increase and was comparable to levels seen with 25% of normal Pi levels.

Discussion: Since complex IV genes of the electron transport, arginine and proline metabolism, and prolyl 4-hydroxylase are all commonly regulated by HIF1-α, this suggests a central means by which metabolic regulation is coordinated with collagen production which would balance bone and blood vessel formation.

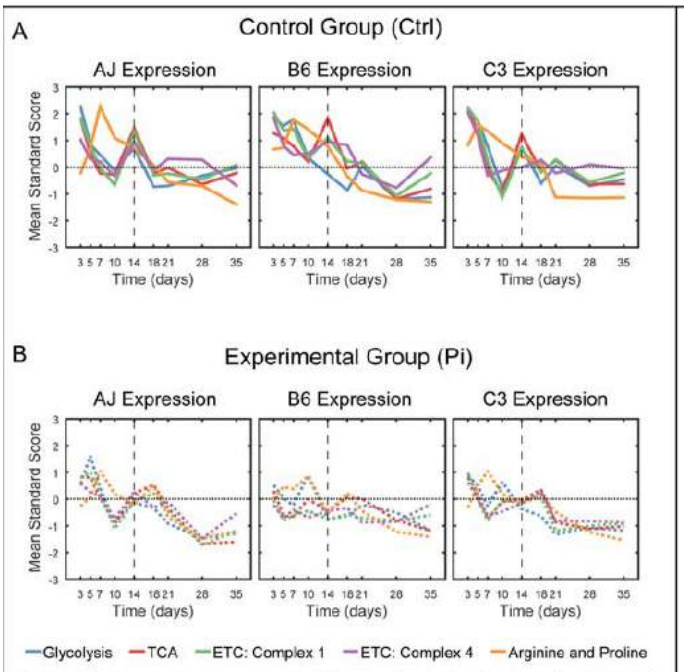

Figure 1. Average gene expression profiles for glycolysis, tricarboxylic acid (TCA), electron transport chain (ETC) and arginine and proline for: A) Control; and B) Pi groups. AJ and C3 strains had similar profiles and responded in a similar manner to Pi restriction

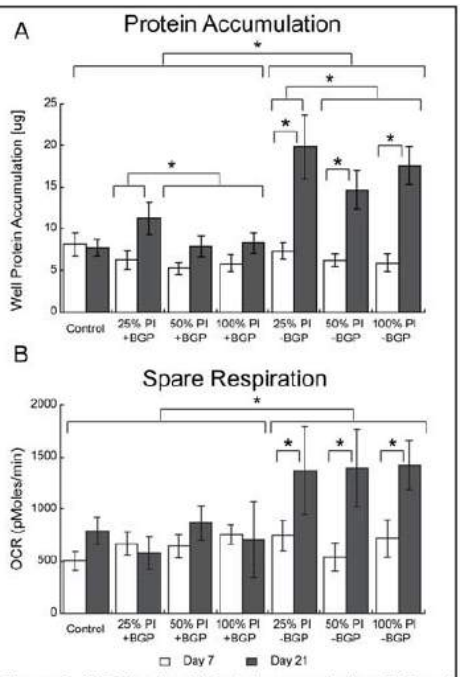

Figure 2. ATDC4 cells: A) Protein accumulation; B) Basal respiration; and C) spare respiratory capacity. All values are normalized to well DNA content. * indicates $p<0.05$.

Estrogen Receptor Beta (ERβ) is Osteocytes: A Critical Regulator of Adult Bon Turnover and Mechanical Load-Induced Bone Formation

Russell P. Main, PhD[1], Haisheng Yang, PhD[1], Julia P. Townsend[1], Rachel E. Embry[1], Mitchell R. Hoge, BS[1], Whitney A. Bullock, BA[1], Maxime A. Gallant, PhD[1], Teresita M. Bellido, PhD[2]

[1]Purdue University, West Lafayette, IN

[2]Department of Anatomy and Cell Biology, Indiana University School of Medicine & Roudebush Veterans Administration Medical Center, Indianapolis, IN

Sex hormones are key contributors to skeletal health. However, the effects of estradiol on skeletal anabolic pathways are still not well defined. While osteocytes are critical regulators of bone modeling and remodeling, osteocyte estrogen receptor alpha (ERα) has limited effects in the growing skeleton and in regulating the response to mechanical load. These results call for a better understanding of skeletal ERβ, which has previously been proposed as an inhibitor of skeletal mechanotransduction. Our goal is to characterize the role of osteocyte ERβ in regulating bone structure during growth, in adulthood, and in response to mechanical stimuli in both male and female mice. Mice lacking osteocyte ERβ were generated by Cre-LoxP recombination driven by DMP1-8kb-Cre. Male and female mice with osteocyte deletion of ERβ (KO) and littermate control mice (LC) were (i) sacrificed at 4 or 7wks old or (ii) began 2wks of unilateral tibial loading at 10 or 28wks old (12 and 30wks old at sacrifice). Serum estradiol and testosterone analyses were conducted in 4, 7, and 30wk old mice. MicroCT, dynamic histomorphometry, and histological bone resorption analyses of the tibiae and L5 vertebrae were conducted and genotypic differences tested by t-test. Load-genotype interactions were tested by linear mixed model with repeated measures.

We found no genotype-related differences in serum hormones. There were few phenotypic differences between KO and LC mice at 4, 7, or 12wks of age. Osteocyte-specific ERβ deletion had sex-dependent effects on bone mass at 30wks. Proximal tibial cancellous BV/TV (+62%) was increased in male KO relative to LC mice. By contrast, cancellous BV/TV was reduced in 30wk female KO relative to LC mice (-35%) (Figure 1). Similar cancellous patterns were seen in L5. While loading had an anabolic effect in the cancellous and cortical tissues in 12wk old tibiae, no interactive effect of genotype was found. 30wk female mice showed a strong midshaft response to load, but no genotypic interaction. At a site 37% of the tibia's length from the proximal end, 30wk female KO mice showed a greater load-induced increase in Ct.Ar than LC mice (+31% vs. +16%). This differential increase in Ct.Ar is primarily due to a greater increase in periosteal bone formation in response to load in KO relative to LC mice (Figure 2). Similarly, Tb.Th in the proximal tibia increased more in the 30wk female KO mice than in LC mice (+28% vs. +10%). 30wk old male mice did not respond strongly to tibial loading.

Osteocyte ERβ plays an important sex-specific role in regulating cancellous bone turnover in adult mice, as well as influencing the anabolic response to physical stimuli, especially in adult female mice. The cellular mechanisms and intra-cellular pathways underlying these structural outcomes are presently being investigated.

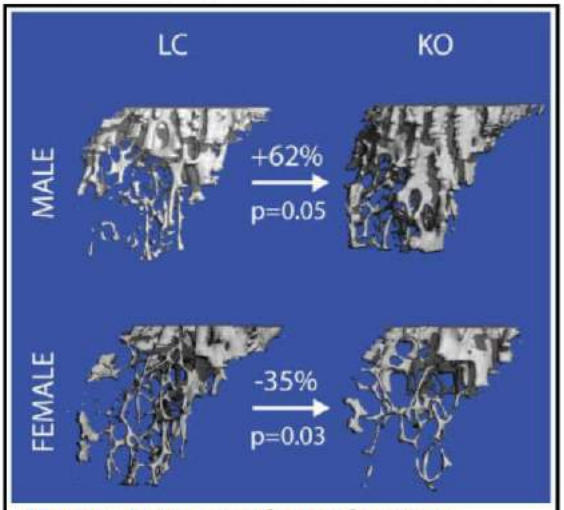

Figure 1: Bone volume fraction (BV/TV) in the proximal tibia for male and female LC and KO mice. BV/TV for the males and female Kos were increased and decreased, respectively, relative to the LC mice.

Figure 2: Periosteal and endosteal bone formation rate (BFR) for the cortical diaphysis, 37% of bone's length from the proximal end of the tibia. Load-induced periosteal BFR was elevated in KO relative to LC mice. Endosteal BFR increased similarly in response to load in both LC and KO mice.

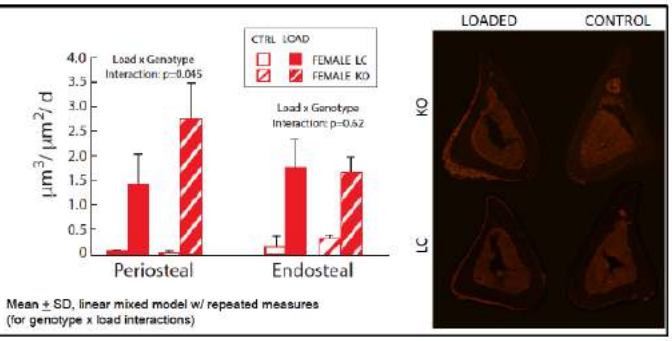

Functional Adaptation of Osteocalcin and Osteopontin Deficient Mice

Stacyann Morgan, BSc[1] and Deepak Vashishth, PhD[1]
[1]Rensselaer Polytechnic Institute, Troy, NY

Introduction

Osteocalcin (OC) is one of the most abundant non-collagenous protein (NCP) in bone [1].
It is produced during bone formation, late after mineralization by osteoblasts and forms a complex with Osteopontin (OPN) and other molecules in the extra-cellular matrix [2]. Recent studies in our laboratory showed that the OC-OPN complex regulates bone toughness through its control over matrix quality [3]. Such control may also help in determining bone size and strength. Therefore, we investigated whether these proteins play a role in regulating bone strength through morphological adaptation.

Materials and Methods

Radii from male 6 month old OC-OPN$^{-/-;-/-}$ and Wild Type mice (n=15 per group) were separated from the ulna and stored in saline soaked gauze at -80 C until use. Samples were scanned using µCT with a 10.5 µm voxel size (µCT 40; Scanco Medical) in eppendorf tubes with saline solution. Bone geometry was determined from the mid-shaft of each sample and the parameters measured were: length (Le), cortical area (Ct.Ar), cortical thickness (Ct.Th) and tissue mineral density (TMD). The mice radii were then loaded to failure in three point bending at a displacement controlled loading rate of 0.001 mm/s (Elf 3200; EnduraTEC). The resulting load-displacement curve was used to calculate the structural properties ultimate force (FU; N), yield force (FY; N), stiffness (S; N/mm), and postyield energy to failure (UPY; mJ) and ultimate strength (σU, MPa).

Statistical Analysis

Mann-Whitney Rank Sum Test was used to determine differences between the groups for all parameters measured. A path analysis was conducted to test the hypothesis that morphological and tissue quality traits are functionally related and contribute to whole bone mechanical properties. The model is constructed with bidirectional arrows representing associated variables, direct arrows indicating causal effects, and path coefficients which represent the magnitude of the relationship between traits. The structural equations were then constructed using the path coefficients. All analysis was carried out using SPSS 21 (IBM SPSS Statistics).

Results

The results showed that OC-OPN$^{-/-;-/-}$ were shorter with thicker cortices and larger cortical area (Table 1). The fracture load for OC-OPN$^{-/-;-/-}$ was also higher compared to WTs ($p<0.05$) but there were no significant differences in TMD or measures of stiffness and strength ($p>0.05$). Yield and post-yield deformation were also not different between the groups ($p >0.05$). The path diagrams indicate that cortical thickness, cortical area and TMD resulted in a good fit for both groups as determined by the chi-square and RMSEA goodness of fit indices. While 47% of the variation in stiffness was explained by these traits for WT, only 19% was explained in the OC-OPN$^{/-;-/-}$ group. These traits also explained 50-70% of the variation seen in ultimate strength for both groups.

Discussion

In the absence of both OC and OPN, the matrix quality of the bone is significantly compromised [3]. The results of this study suggests that bones of OC-OPN$^{-/-;-/-}$ adapts to loss of matrix quality by varying its length, the amount of cortical bone and thickness within the midshaft. This co-adaptation leads to a structure in the knockouts that is similar in stiffness and strength as the WT littermates but lower material level toughness [3]. In the path analysis, slenderness (Tt.Ar/Le) was chosen to determine how variability in bone size is causally related to Ct.Th and TMD. Since slender bones have a proportionate increase in Ct.Ar and whole bone stiffness depends on a measure of bone size, Ct.Ar was also added to the model. Variation in marrow expansion during growth drives subsequent adaptive changes in other traits and contributes directly to ultimate strength in WTs. Given the same set of traits, each genotype builds a mechanically functional bone but in a slightly different manner. Our study demonstrates for the first time that osteocalcin and osteopontin plays a significant role in regulating bone size (length, cortical thickness and cortical area) and bone strength.

References:

1.Sroga, Grażyna E., and Deepak Vashishth. "Effects of bone matrix proteins on fracture and fragility in osteoporosis." *Current osteoporosis reports* 10.2 (2012): 141-150.
2. Ritter, Nadine M., Mary C. Farach-Carson, and William T. Butler. "Evidence for the formation of a complex between osteopontin and osteocalcin." *Journal of Bone and Mineral Research* 7.8 (1992): 877-885.
3. Poundarik, Atharva A., et al. "Dilatational band formation in bone." *Proceedings of the National Academy of Sciences* 109.47 (2012): 19178-19183.

Parameters	WT	OC-OPN$^{-/-;-/-}$	p-value
Le (mm)	10.541±0.27	10.033±0.37	<0.001
Ct.Ar (mm^2)	0.241±0.02	0.272±0.03	0.002
Ct.Th (mm)	0.152±0.011	0.163±0.014	0.026
F_u(N)	3.409±0.63	3.907±0.84	0.056
Outer Diameter (mm)	0.642±0.04	0.688±0.05	0.026
Toughness (mJ)	0.599±0.26	0.704±0.24	0.046

Table 1: Summary of variables measured from the mid-shaft of each sample

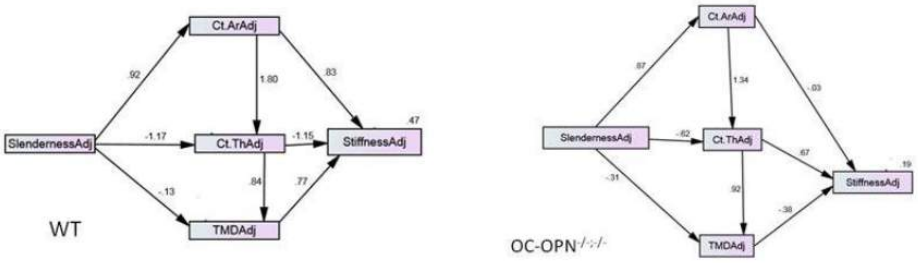

Figure 1: Path diagrams for stiffness between WT (left) and OC-OPN$^{-/-/-}$ (right)

$Stiffness_{WT} = 0.825\ Ct.Ar + 0.770\ TMD - 1.15\ Ct.Th$ $R^2 = 0.47$, $\chi^2 = 1.13$, p=0.53, df= 2, RMSEA=0.00

$Stiffness_{OC\text{-}OPN\text{-}/\text{-}/\text{-}} = -0.031\ Ct.Ar - 0.384\ TMD + 0.667\ Ct.Th$ $R^2 = 0.19$, $\chi^2 = 2.00$, p=0.37, df= 2, RMSEA=0.00

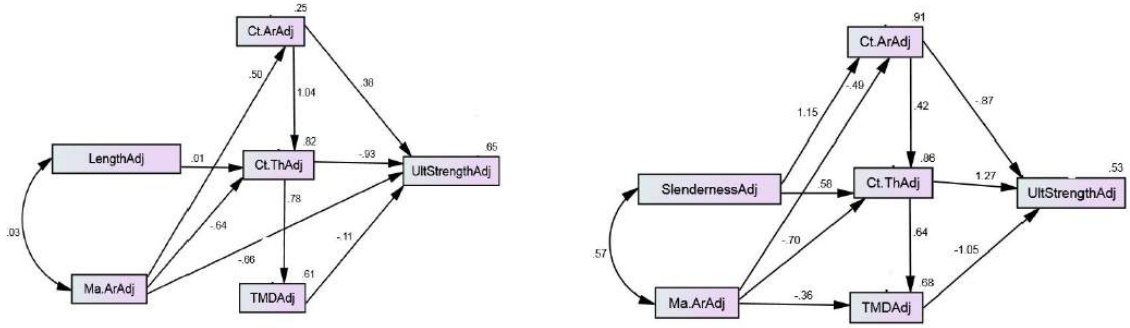

Figure 2: Path diagrams for ultimate strength between WT (left) and OC-OPN$^{-/-/-}$ (right)

$Ult.Strength_{OC\text{-}OPN\text{-}/\text{-}/\text{-}} = -0.87\ Ct.Ar - 1.05\ TMD + 1.27\ Ct.Th$ $R^2 = 0.53$, $\chi^2 = 3.93$, p=0.415, df= 4, RMSEA=0.00

$Strength_{WT} = 0.38\ Ct.Ar - 0.11\ TMD - 0.93\ Ct.Th$ $R^2 = 0.65$, $\chi^2 = 4.15$, p=0.53, df= 5, RMSEA=0.00

Tibial Compression Overload Instigates Post-Traumatic Osteoarthritis in Mouse Knee

Muhammad Farooq Rai, PhD[1], Duan Xin, MD[1], James Quirk, PhD[2], Nilsson Holguin, PhD[3], Eric Schmidt, PhD[5], Nobuaki Chinzei, MD, PhD[1], Matthew J. Silva, PhD [1,3], Linda J. Sandell, PhD[1, 3, 4]

[1]Department of Orthopaedic Surgery, Musculoskeletal Research Center, [2]Mallinckrodt Institute of Radiology, [3]Department of Biomedical Engineering, [4]Department of Cell Biology and Physiology, Washington University School of Medicine at Barnes-Jewish Hospital, MO, United States. [5]Department of Physician Assistant Medicine, School of Graduate Health Studies, Lynchburg College, Lynchburg, VA.

Objectives: Osteoarthritis (OA) is a clinical syndrome of joint pain accompanied by varying degrees of functional impairment and diminished quality of life. Primary age-related OA has unknown etiology, complex and multifaceted pathogenesis and uncertainty about the timeline of pathological events. In contrast, post-traumatic OA (PTOA) that constitutes 12% of knee OA has an injury component associated with it where disease-initiating injury event is known and sequelae of pathological footprints can be trailed. Any injury severe enough to cause anterior cruciate ligament (ACL) tear and/or meniscus destabilization frequently leads to PTOA overtime. In this study, we aim to investigate a spectrum of lesions characteristic of PTOA phenotype in the articular cartilage, meniscus, synovium, ligaments and bone in response to mechanical knee injury in an attempt to understand early and late event in PTOA. We hypothesized that alteration in knee joint stabilization recapitulates molecular and structural features of PTOA in the knee tissues depends on load intensity and time.

Methods: Eight-week old male mice from LGXSM-6 and LGXSM-33 lines were used. Axial tibial compression was applied on right knees. Three separate loading regimens were applied: 6N, 9N and 12N. The contralateral left knees served as control. Mice were scarified at 5, 9, 14, 28 and 56 days post-loading as indicated and whole knee joint changes were assessed by histology, immunostaining, micro-CT and magnetic resonance imaging.

Results: Tibial compression largely resulted in ACL tear, which disrupted the joint stabilization instigating a cascade of temporal and topographical features of PTOA. These features largely included cartilage matrix damage, chondrocyte apoptosis and altered aggrecan expression pattern, ligament and meniscus pathology, synovitis, bone loss, osteophyte formation and development of ectopic calcification.

Conclusions: This study delineates changes recapitulating morphological and anatomic features of PTOA beyond cartilage and bone after injurious mechanical injury. It provides a plausible explanation into how an ACL injury in humans leads to development of PTOA overtime. Taken together, this study provides a broad picture of pathological events in the knee following a traumatic insult strong enough to sever ACL. We observed that high mechanical loading instigated whole knee joint changes recapitulating PTOA within eight weeks. Although the actual mechanisms underlying these changes in mice and men appear to be alike, the time scale for progression to advanced PTOA is greatly accelerated in mice as compared to humans, therefore translating these findings to human PTOA should be considered with some caution. At least these studies provide a window of opportunity to treat PTOA using different therapeutic and preventive approaches. Further interrogation of the mechanism(s) of these changes is warranted to unravel the exact pathogenesis of PTOA.

Necrotic Bone Stimulates Pro-inflammatory Responses in Macrophages Through the Activation of Toll-like Receptor 4

Naga Suresh Adapala, PhD[1, 2], Ryosuke Yamaguchi, MD, PhD[1, 2], Matthew Phipps, PhD[1], Olumide Aruwajoye, PhD[1], Harry K.W. Kim, MD, MS[1, 2*]

1 *Center for Excellence in Hip Disorders, Texas Scottish Rite Hospital for Children, Dallas, TX, 75219*

2 *Department of Orthopedic Surgery, University of Texas Southwestern Medical Center, Dallas, TX, 75390-8883*

Purpose: Legg-Calvé-Perthes disease is a childhood hip disorder in which loss of blood supply results in ischemic osteonecrosis of the femoral head (ONFH). In general, macrophages sense the necrotic tissue by using pattern recognition receptors, importantly, toll-like receptors (TLRs) that activate pro-inflammatory responses. However, the role of macrophages in the inflammatory responses following ONFH has not been studied. The purpose of this study was to determine the inflammatory response of macrophages to the necrotic bone and the TLRs involved in sensing the necrotic bone.

Methods: ONFH was induced in right femoral head of 6-week old piglets (n=12), the unoperated left femoral head was used as normal control. At 8-weeks following surgery, the number of CD14+ macrophages was determined by immunohistochemistry. Macrophages were isolated from frozen sections by laser capture microdissection (LCM). The gene expression of cytokines and TLRs was determined by qRTPCR. Necrotic or normal bone was prepared from femoral head following the removal of supernatant that contains soluble factors. In vitro, bone marrow macrophages (n=5 piglets) were exposed to necrotic bone in the presence or absence of TLR4 inhibitor, TAK242. The phosphorylation of ERK1/2 and IKKα was determined by western blotting, proliferation of macrophages by MTT-based assay and migration response using transwell chambers.

Results: Quantitation of macrophages by immunohistochemistry revealed an increased number of CD14+ macrophages (4.2-fold, p=0.007) in the fibrovascular repair tissue compared to normal bone. qRTPCR analysis of the macrophages isolated by LCM showed significantly increased mRNA levels of pro-inflammatory cytokines (*IL-1β*:3.9-fold, p<0.0001; *TNF-α*:2.3-fold, p=0.0006; *IL-6*:3.6-fold, p=0.04) in the necrotic repair tissue compared to normal bone. Among the TLRs 2, 4 and 9, the gene expression of *TLR4* (5.3-fold, p=0.003) but not *TLR2* (p=0.46) and *TLR9* (p=0.9) was significantly increased in macrophages in response to ONFH. Mechanistically, necrotic bone stimulated an increased expression of TLR4 in bone marrow-derived macrophages and activated TLR4-dependent phosphorylation of ERK1/2 and IKKα. Furthermore, necrotic bone increased the proliferation, migration and inflammatory cytokine gene expression in macrophages, which were blocked by the TLR4 inhibitor, TAK242.

Conclusion: Necrotic bone stimulates pro-inflammatory responses in macrophages following ONFH through TLR4 activation.

Figure 1

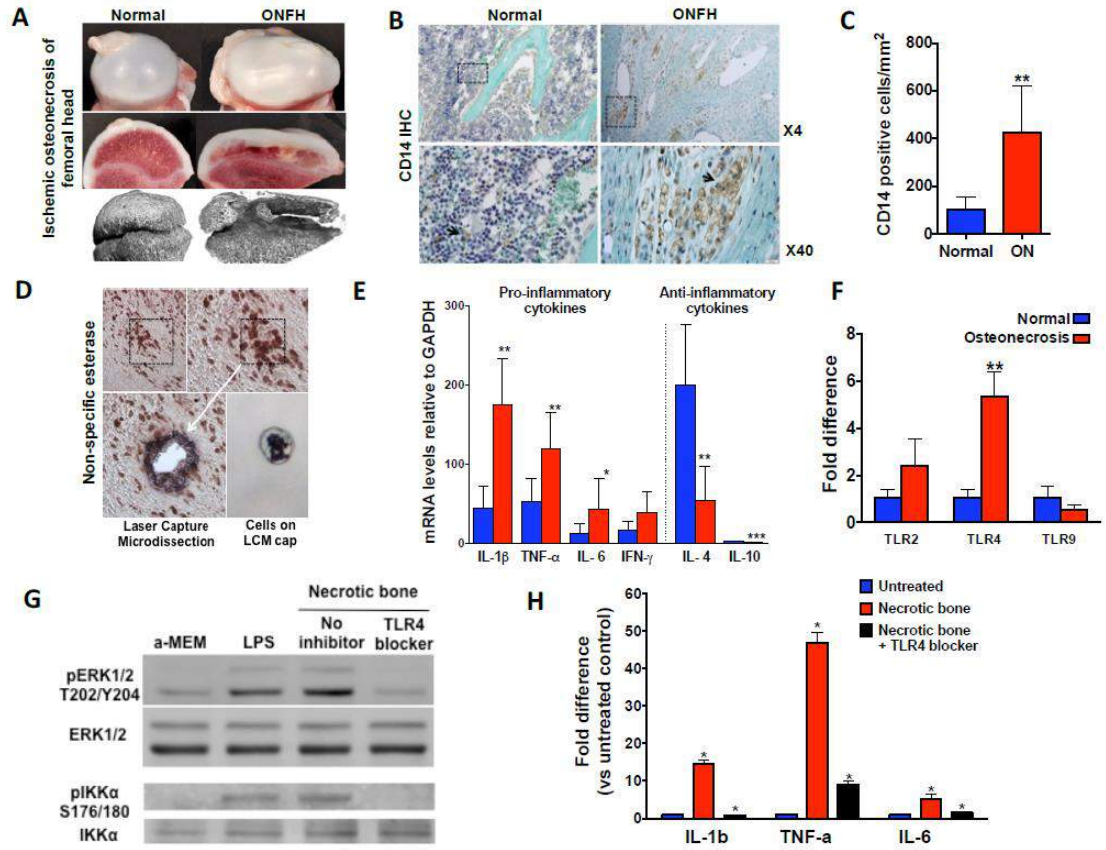

Figure 1

(A) Bone loss and femoral head deformity in ONFH in piglets (B and C) Increased number of macrophages in repair tissue (D, E and F) Laser capture microdissection method and qRTPCR analysis (G) TLR4-mediated macrophage activation by necrotic bone (H) TLR4 blocker inhibits pro-inflammatory cytokine expression in macrophages. P value *<0.05, **<0.01, ***<0.001.

FGF23 Neutralizing Antibody Ameliorates Hypophosphatemia and Impaired FGF Receptor Signaling in Kidneys of FGF2 High Molecular Weight Isoform Transgenic Mice

*Erxia Du, PhD, Liping Xiao, MD, PhD and Marja M. Hurley, MD**
Department of Medicine, UConn Health, Farmington, CT, 06030

Abstract

Transgenic mice overexpressing the high molecular weight Fibroblast Growth Factor-2 isoforms in osteoblast lineage cells (HMWFGF2Tg) phenocopy the Hyp mouse, homolog of human X-linked hypophosphatemic rickets with, phosphate wasting and abnormal fibroblast growth factor (FGF23), fibroblast growth factor receptor (FGFR), Klotho and mitogen activated protein kinases (MAPK) signaling in kidney. Since HMWFGF2Tg mice have increased expression of FGF23 in bone and serum, we assessed whether FGF23 neutralizing antibody could rescue hypophosphatemia and impaired FGFR signaling in kidneys of HMWFGF2Tg male mice. Base line bone mineral density and bone mineral content in 1 month-old HMWFGF2Tg mice were significantly reduced compared with Vector/Control. Serum FGF23 was significantly increased in HMWFGF2Tg. Vector and HMWFGF2Tg mice were intra-peritoneally injected with FGF23 neutralizing antibody (FGF23Ab) or control IgG and were euthanized 24h post treatment. Serum phosphate was significantly reduced in HMWFGF2Tg and was rescued by FGF23Ab. Serum PTH was significantly increased in HMWFGF2Tg but was not reduced by FGF23Ab. Serum 1,25(OH)2 Vitamin D was inappropriately normal in HMWFGF2Tg and was significantly increased in both Vector and HMWFGF2Tg by FGF23Ab. Analysis of HMWFGF2Tg kidneys revealed significantly increased mRNA expression of the FGF23 co-receptor Klotho, early growth response-1 transcription factor (Egr-1) mRNA, an indicator of FGF23 signaling as well as the mRNA for the transcription factor c-Fos that were all significantly decreased by FGF23Ab. A significant reduction in the phosphate transporter Npt2a mRNA was also observed in HMWFGF2Tg kidneys. FGF23Ab reduced p-FGFR1, KLOTHO, p-ERK1/2, EGR1, C-FOS and increased NPT2A protein in HMWFGF2Tg kidneys. We conclude that FGF23 blockade rescued hypophosphatemia by regulating FGF23/FGFR downstream signaling in HMWFGF2Tg kidneys. We further conclude that HMWFGF2 isoforms regulate PTH expression independent of FGF23/FGFR signaling.

Key words: HMWFGF2, FGF23Ab, phosphate, Klotho, Egr-1, PTH

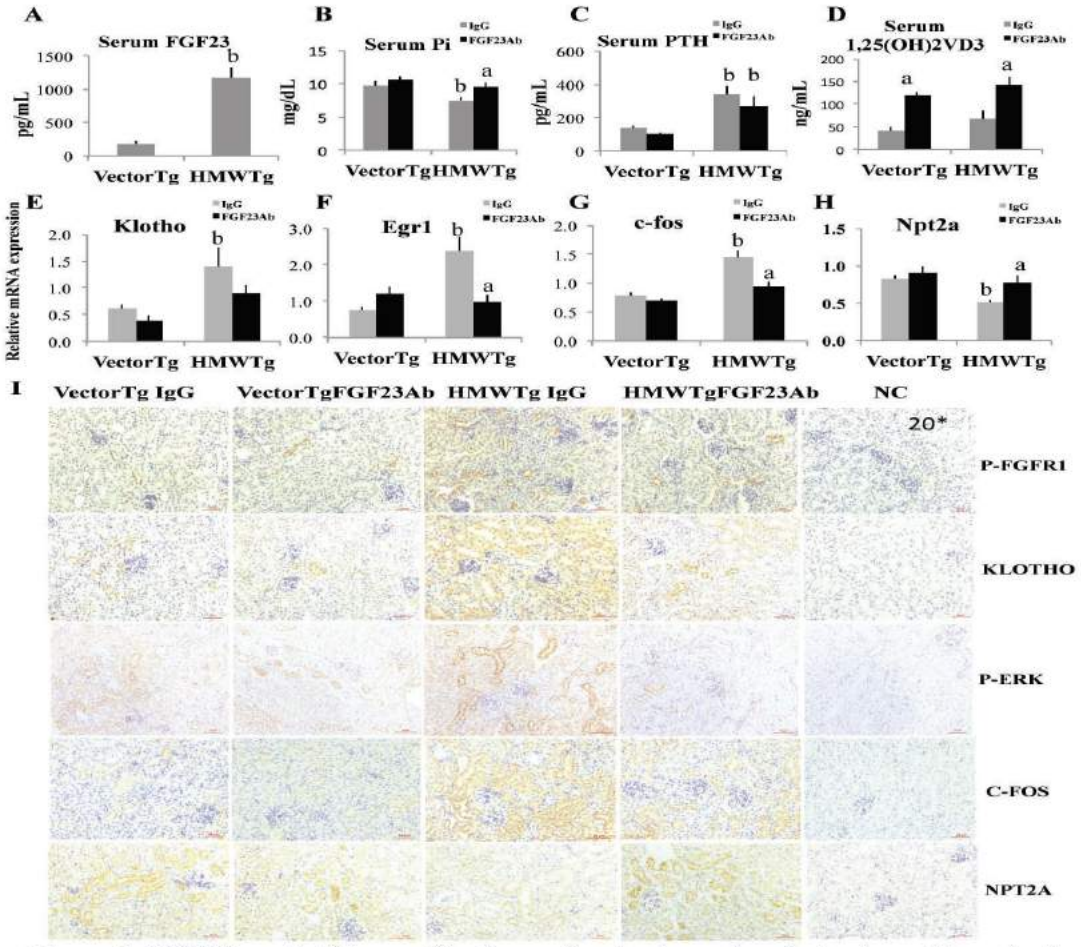

Figure 1. FGF23 neutralizing antibody ameliorates hypophosphatemia and impaired FGF23/FGFR signaling in kidneys of HMWTg mice. (A) Serum FGF23 was increased in HMWTg mice. FGF23 neutralizing antibody rescued decreased serum Pi (B) in HMWTg mice, did not effect PTH (C) and further increased 1,25(OH) 2VD3(D) both in serum of Vector and HMWTg mice. n>=6/group. To further examine signaling pathways involved in Pi regulation in kidneys of HMWTg mice, qPCR and IHC staining were performed. mRNA of klotho(E), Egr1 (F), c-Fos(G) and Npt2a (H). FGF23Ab rescued increased klotho, Egr1, c-Fos and decreased Npt2a mRNA in HMWTg mice. (I) FGF23Ab, decreased p-FGFR1, KLOTHO, p-ERK C-FOS and increased NPT2A protein. Values are mean±SE.n=3/group. a, significant effect of FGF23Ab; b, Significant effect of HMWFGF2, $p<0.05$.

REFERENCES

1. Du E, Xiao L, Hurley MM. FGFR Inhibitor Ameliorates Hypophosphatemia and Impaired Engrailed-1/Wnt Signaling in FGF2 High Molecular Weight Isoform Transgenic Mice. J Cell Biochem. 2016 Jan 13. doi: 10.1002/jcb.25493.
2. Farrow, E. G., Summers, L. J., Schiavi, S. C., McCormick, J. A., Ellison, D. H., and White, K. E. (2010) Altered renal FGF23-mediated activity involving MAPK and Wnt: effects of the Hyp mutation. *J. Endo*. ***207***, 67-75
3. Goldsweig, B. K., and Carpenter T. O. (2015) Hypophosphatemic rickets: Lessons from disrupted FGF23 control of phosphorous homeostasis. *Curr. Osteoporos*. Rep. ***13***, 88-97
4. Homer-Bouthiette, C., Doetschman, T., Xiao, L., and Hurley, M. M. (2014) Knockout of Nuclear High Molecular Weight FGF2 Isoforms in Mice Modulates Bone and Phosphate Homeostasis. *J Biol. Chem.* ***289***, 36303–36314Xiao, L.,
5. Ohata, Y., Yamazaki, M., Kawai, M., Tsugawa, N., Kanako, T., Tachikawa, K., Koinuma,T., Miyagawa, K., Kimoto, A., Nakayama, M., Namba, N., Yamamoto, H., Okano,T., Ozono, K., and Michigami ,T. (2014) Elevated Fibroblast Growth Factor 23 Exerts Its Effects on Placenta and Regulates Vitamin D Metabolism in Pregnancy of Hyp Mice. *J. Bone. Miner. Res.* ***29***,
1627-1638
6. Urakawa, I., Yamazaki, Y., Shimada, T., Iijima, K., Hasegawa, H., Okawa, K., Fujita, T., Fukumoto, S., and Yamashita, T. (2006) Klotho converts canonical FGF receptor into a specific receptor for FGF23. *Nature*. ***444***, 770–774

7. Xiao, L., Esliger, A., and Hurley, M. M. (2013) Nuclear fibroblast growth factor 2 (FGF2) isoforms inhibit bone marrow stromal cell mineralization through FGF23/FGFR/MAPK in vitro. *J. Bone. Miner. Res.* ***28***, 35-45
8. Yamashita, T., Konishi, M., Miyake, A., Inui, K., and Itoh, N. (2002) Fibroblast growth Factor (FGF)-23 inhibits renal phosphate reabsorption by activation of the mitogen-activated protein kinase pathway. *J. Biol. Chem.* ***277***, 28265–2827
9. Wöhrle, S., Bonny O, Beluch N, Hynes NE, Gaulis, S., Stamm, C., Scheibler, M., Muller, M., Kinzel, B., Theury, A., Brueggen, J., Hynes, N. E., Sellers, W. R., Hofmann, F., and Graus-Porta, D. (2011) FGF Receptors Control Vitamin D and Phosphate Homeostasis by Mediating Renal FGF-23 Signaling and Regulating FGF-23 Expression in Bone. *J Bone Miner Res*. ***26***, 2486-2497
10. Wöhrle, S. L., Henninger, C., Bonny, O., Thuery, A., Beluch, N., Hynes, N. E., Guagnano, V., Sellers, W. R, Hofmann, F., Kneissel, M., Graus Porta, D., and Wohrle, S. (2013) Pharmacological inhibition of fibroblast growth factor (FGF) receptor signaling ameliorates FGF23-mediated hypophosphatemic rickets. *J. Bone. Miner. Res.* ***28***, 899-911

Why we Wnt to Treat Osteosarcoma

Carl T. Gustafson, BS, Avudaiappan Maran, PhD, Michael J. Yaszemski, MD, PhD
Mayo Clinic, Rochester, MN

Osteosarcoma (OS) is the most common pediatric bone malignancy. With approximately one thousand new cases in the United States every year, 90% of OS patients are children and young adults between the ages of 10 and 30 (1, 2). During surgical resection of the primary tumor, degree of tumor necrosis is assessed and used as a litmus test to separate patients into categories of "responders" and "non-responders". Those with low tumor necrosis (necrosis <90%) after neoadjuvant chemotherapy have a dismal 5-year survival rate - nearing 20% - due to relapse and development of lung metastases. Lack of response, or resistance, to the standard chemotherapy regimen is the major cause for disease progression in OS (1, 3). While the canonical Wnt signaling pathway has been mechanistically tied to drug resistance, as well as tumor development, and poor prognosis in many cancers, including OS, Wnt signaling has largely remained untouched by our currently available chemotherapeutics (4, 5). No Wnt targeting small molecules have yet been approved for clinical use, outside of a handful of trials. In OS, a large body of work indicates overexpression of Wnt promoting factors, and correlation of Wnt expression with poor prognosis in OS (6, 7). Thus, an overwhelming consensus indicates the therapeutic appeal of Wnt signaling, while our means to effectively block Wnt have yet proved to be insufficient. In other cancers, the appeal of Wnt targeted therapies has been highlighted by the discovery of activating mutations in Wnt family member proteins. Common mutations in APC and β-catenin in colorectal cancers have historically driven cancer development, and have recently driven researchers in their efforts to develop drug candidates to address the problem of hyper-activated Wnt signaling.

Recently, a number of compounds which facilitate pharmacological inhibition of Wnt signaling have been reported. These small molecules have shown utility in applications ranging from cardiac regeneration, to diabetes, to cancer in pre-clinical models. Indeed, one newly developed compound targeting the Wnt protein modifying enzyme Porcupine has entered a Phase I dose-escalation trial (8). Among these small molecule candidates, the $^{\beta}$-catenin inhibitor FH535 has demonstrated promising fidelity to canonical Wnt inhibition in a number of reports (9, 10). Our group tested the efficacy of canonical Wnt signal blockade via FH535 in osteosarcoma. We found that FH535 effectively targets Wnt signaling, decreasing β-catenin transcriptional activity, as well as mRNA production of the β-catenin substrate Axin2. This on-target effect resulted in the inhibition of OS cell viability in all OS cell lines tested, while inducing cell cycle arrest via S-phase accumulation. Interestingly, in an *in vitro* model of doxorubicin resistant OS, we found that the doxorubicin resistant cells demonstrated greater sensitivity to FH535 as compared to the parental (wild-type) cell line (Figure 1, panels A and B). Axin2 response was pronounced in the doxorubicin resistant cells, indicating increased dependency on Wnt signaling in these cells, and susceptibility to Wnt inhibition. In the doxorubicin resistant cell line, we found that treatment with FH535 caused an accumulation of Axin2 protein (Figure 1, panel C).

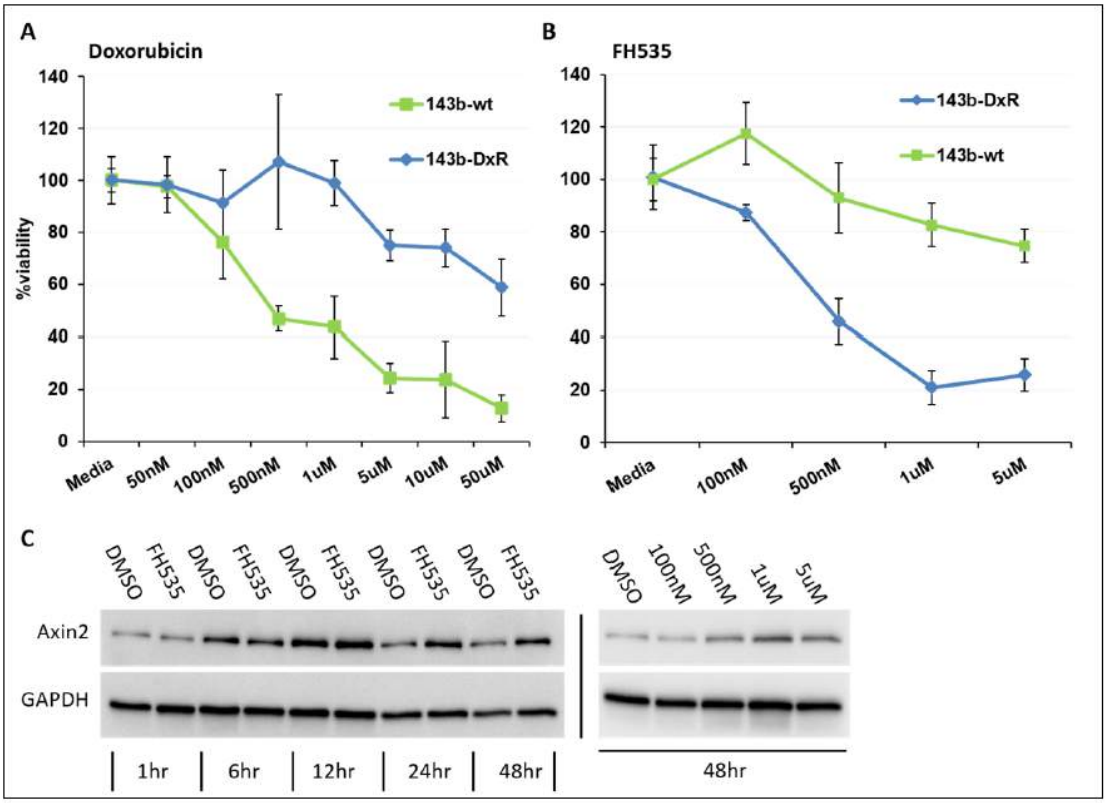

Figure 1: Cellular and molecular response to FH535. A: Response to 48 hour doxorubicin treatment in parental wild-type osteosarcoma cell line (143b-wt) and its derived doxorubicin resistant cell line (143b-DxR). B: Response to 48 hour FH535 treatment in 143b-wt and 143b-DxR cell lines. C: Effect of FH535 treatment on Axin2 protein in the 143b-DxR cell line.

This observation, though initially counter-intuitive, indicates that FH535 acts upon the Axin-regulating poly-ADP-ribose polymerase (PARP) family enzymes Tankyrase 1/2, inhibiting their function and resulting in the observed stabilization of Axin2. In recent years, Tankyrases have become the subject of much excitement and discussion within fields interested in Wnt signaling, due to the discovery of their role in regulating Axin proteins. Our study further establishes the molecular mechanism of FH535 effects on Tankyrases, while also investigating the mechanisms of cell death induced by Tankyrase inhibition in OS and doxorubicin resistant OS.

Our study is the first report of which we are aware which clarifies the specific mechanism of action of the widely published Wnt inhibitor FH535. The establishment of the mechanism of action of this drug adds significant value to its utility in Wnt, and assists in clarifying previous work done with this molecule. Additionally, our research addresses pressing questions regarding treatment options in doxorubicin resistant osteosarcoma, and the value of Wnt inhibition in this context. In sum, this work indicates potential for new treatment options for osteosarcoma patients who do not respond to the standard treatment regimen of neoadjuvant chemotherapy and surgical resection.

References:

1. Fletcher CDM, U. K., Mertens F. in *World Health Organization Classification of Tumours* (ed Sobin L Kleihues P) 415 (IARC Press, Lyon, France, 2002).

2. Ritter, J. & Bielack, S. S. *Osteosarcoma.* Ann Oncol 21 Suppl 7, vii320-325, doi:10.1093/annonc/mdq276 (2010).

3. Bacci, G. et al. *Primary chemotherapy and delayed surgery for nonmetastatic osteosarcoma of the extremities. Results in 164 patients preoperatively treated with high doses of methotrexate followed by cisplatin and doxorubicin.* Cancer 72, 3227-3238 (1993).

4. Correa, S. et al. *Wnt/beta-catenin pathway regulates ABCB1 transcription in chronic myeloid leukemia.* BMC Cancer 12, 303, doi:10.1186/1471-2407-12-303 (2012).

5. Anastas, J. N. et al. *WNT5A enhances resistance of melanoma cells to targeted BRAF inhibitors.* J Clin Invest 124, 2877-2890, doi:10.1172/JCI70156 (2014).

6. Kurayoshi, M. et al. *Expression of Wnt-5a is correlated with aggressiveness of gastric cancer by stimulating cell migration and invasion.* Cancer Res 66, 10439-10448, doi:10.1158/0008-5472.CAN-06-2359 (2006).

7. Lu, B. J. et al. *Expression of WNT-5a and ROR2 correlates with disease severity in osteosarcoma.* Mol Med Rep 5, 1033-1036, doi:10.3892/mmr.2012.772 (2012).
8. Lum, L. & Clevers, H. *The Unusual Case of Porcupine.* Science, 337, 922-923, doi: 10.1126/science.1228179 (2012).
9. Bjorklund, C. C. et al. *Evidence of a role for CD44 and cell adhesion in mediating resistance to lenalidomide in multiple myeloma: therapeutic implications.* Leukemia, 28, 373-383. doi: 10.1038/leu.2013.174. (2014).
10. Wang, W.C. et al. *IL-6 augmented motility of airway epithelial cell BEAS-2B via Akt/GSK-3β signaling pathway*. J Cell Biochem, 113, 3567-3575. doi: 10.1002/jcb.24235 (2012).

Usp53, A Novel Target Gene of the PTH-activated αNAC Transcriptional Coregulator

Hadla Hariri, PhD, Martin Pellicelli, PhD Julie A. Miller, MSc, and René St-Arnaud, PhD
Dept. of Human Genetics, McGill University and Shriners Hospitals for Children – Canada, Montreal (Quebec) Canada H4A 0A9

Nascent-polypeptide-associated complex and coregulator alpha (αNAC) was shown to be a downstream transcriptional effector of the PTH – G□s – PKA signaling cascade in bone cells. Upon PTH treatment of osteoblasts, cAMP accumulates to activate PKA, which in turn phosphorylates αNAC on residue Ser99 (Pellicelli M et al. 2014. Mol Cell Biol 34: 1622). This leads to nuclear translocation of the αNAC protein. Little is known about potential transcriptional targets of the PTHactivated, PKA-phosphorylated αNAC protein in osteoblasts.

In order to identify such targets, we performed ChIP-seq and RNA-seq experiments in PTH-treated MC3T3-E1 osteoblast-like cells. Genes showing differential responses in both data sets were further validated using conventional ChIP and qRT-PCR. These experiments identified *Usp53* as a potential αNAC target gene. Our focus was directed towards characterizing the αNAC – mediated regulation of *Usp53* expression in bone cells. Conventional ChIP assays in PTH-treated MC3T3-E1 cells confirmed a 4-fold enrichment of αNAC binding at the *Usp53* promoter region. This enrichment was further validated by Electrophoretic Mobility Shift Assay showing the promoter. PTH treatment also increased the mRNA expression of *Usp53* by 3-fold. We then established shRNA-mediated *Naca* (αNAC) knockdown in MC3T3-E1 cells. Interestingly, PTH-driven transcriptional induction of *Usp53* was completely blunted following αNAC knockdown. *Usp53* promoter fragments were then cloned upstream of a luciferase reporter vector. In transiently transfected MC3T3-E1 cells, PTH treatment stimulated transcription from the *Usp53* promoter and αNAC knockdown abrogated the response. In order to understand the role of USP53 in osteoblastic differentiation, we established shRNA- mediated *Usp53* knockdown in ST2 stromal cells and MC3T3-E1 cells. *Usp53* knockdown accelerated the rate of differentiation of ST2 cells into osteoblasts and attenuated the rate of their differentiation into adipocytes. Accelerated differentiation was also observed in *Usp53* knockdown MC3T3-E1 cells. *Usp53* knockdown up-regulated the expression level of osteoblastic differentiation markers such as: *Bglap* (*Osteocalcin*) and *Alpl* (Alkaline phosphatase) and down-regulated expression of regulators of adipogenesis such as *Pparg* and *Cebpa*. In *Usp53* knockdown ST2 cells, we measured increased mineralized nodule formation using Alizarin Red staining and reduced adipocyte differentiation (oil
Red O staining.

These experiments identify *Usp53* as a novel target for αNAC downstream of the PTH signal transduction pathway. Future studies will address the mechanism through which USP53 affects mesenchymal cell lineage-making decisions and differentiation.

Figures

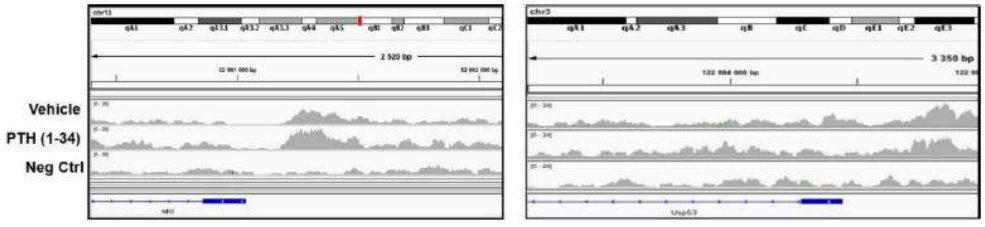

Gene	Fold Change	DESeq p value	edgeR p value	Vehicle-1 counts	Vehicle-2 counts	Vehicle-3 counts	PTH(1-34)-1 counts	PTH(1-34)-2 counts	PTH(1-34)-3 counts
Usp53	2.192	2.3E-88	8.3E-84	359	425	348	1827	1674	1674
ISY1	2.019	1.5E-48	1.2E-95	1946	1994	1974	8722	7130	8109
Nfil3	3.51	2.4e-272	1.4e-275	1363	1584	1483	16162	16489	17828
BPNT1	1.129	2.3E-31	2.7E-33	1179	1227	1259	2883	2620	2516
RELB	0.605	1.20E-10	1.50E-10	1682	1963	1769	2762	2881	2594
Dnajb4	1.488	2.20E-29	1.8E-52	1420	1490	1378	3667	4470	3890

Figure1. ChIP seq and RNA seq identification of αNAC target promoters. ChIP assay and total RNA extraction was done on MC3T3-E1 cells vehicle and PTH (1-34) treated for 2 hours. For ChIP seq, αNAC target promoters were immunoprecipitated using a rabbit anti- αNAC antibody. ChIP enriched DNA was further processed according to Illumina Inc. instructions for library preparation. For RNA seq, RNA library was prepared using poly-A tail capture technique and gene expression monitoring was presented as fold change.

Sequencing was done at McGill Genome Quebec Innovation Centre (MUGQIC).

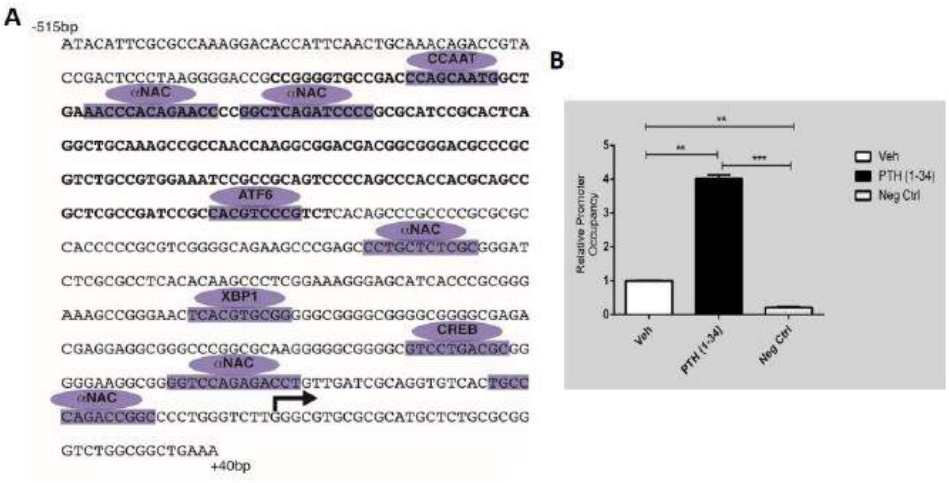

Figure2. Alpha- NAC is recruited to *Usp53* promoter in response to PTH. A, Putative binding sites (purple boxes) for αNAC and other bZIP transcription factors on *Usp53* promoter was predicted using Mat (Genomatix) Inspector matrix V$NACA1.01. Sequence in bold represents the peak identified using ChIP seq. B. Chromatin immunoprecipitation (ChIP) assay was done against endogenous αNAC in MC3T3-E1 cells vehicle and PTH (1-34) treated for 30 minutes. αNAC/*Usp53* promoter complexes were immunoprecipitated using a rabbit anti-αNAC Serine 99 (S99) antibody and a nonspecific rabbit antibody served as a negative control. ChIP products were amplified by
SYBER Green PCR using specific primers flanking the αNAC binding site in the *Usp53* promoter. Relative promoter occupancy was calculated as enrichment over vehicle treated cells, which was ascribed an arbitrary value of 1. ***, $p<0.001$ by 2- way ANOVA and Bonferroni posttest.

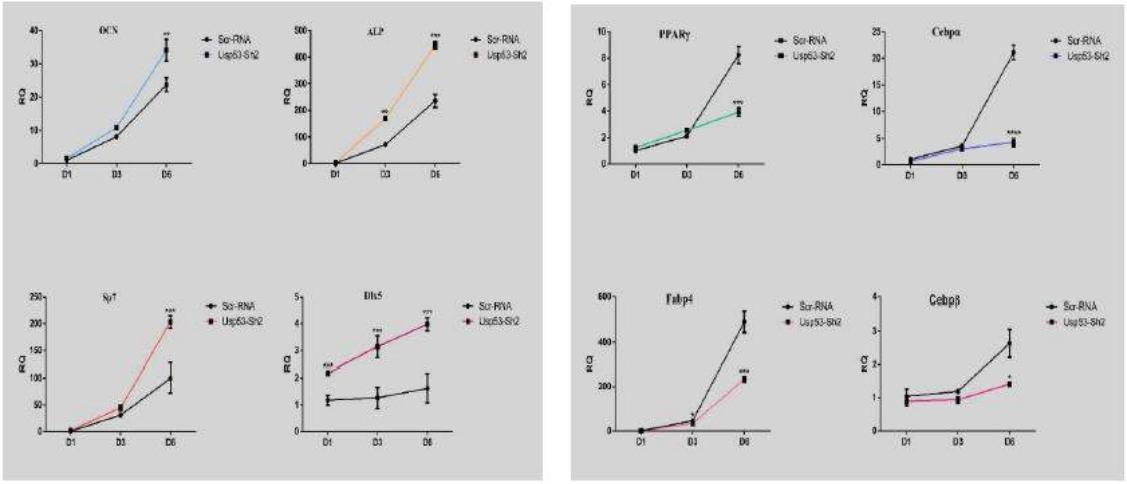

Figure3. Usp53 shRNA knockdown altered the differentiation rate of ST2 cells into osteoblasts and adipocytes. Following Usp53 shRNA RNA mediated knockdown of ST2 cells, control and Usp53 knockdown ST2 cells were grown and maintained in osteoblastic (A) and adipocytic (B) differentiation media for 6 days. RNA was collected at the indicated time points. Relative quantification of osteoblastic differentiation markers Ocn, Alp, Sp7, and Dlx5 mRNA levels (A) Usp53 (A) and adipocytic differentiation markers Pparg, Cebpa, Fabp4, and Cebpb (B) was done using real time PCR using specific TaqMan probes.

Mechanobiological Modulation of In Situ and In Vivo Osteocytic Ca2+ Oscillations in Response to Acoustic Radiation Force using Black6 and Ai38/Dmp1-Cre Mice

Minyi Hu, PhD[1], Jian Jiao, MS[1], Daniel Gibbons, BS[1], Xiaofei Li, MS[1], Guowei Tian, PhD[2], Yi-Xian Qin, PhD[1]
[1]Dept of Biomedical Engineering, Stony Brook University, Stony Brook, NY 11794-5281
[2]CMIC-Two Photon Imaging Center, Stony Brook University, Stony Brook, NY 11794-5200

Clinical evidence has pointed the critical mechanotransduction in bone remodeling/regeneration. While the biological effect of ultrasound on bone healing has been well documented, the underlying mechanism is largely unknown. Our group elucidated the mechanobiological modulation of cytoskeleton and Ca^{2+} influx in in vitro osteoblastic cells by short-term focused acoustic radiation force. In greater relation to the physiological setting by solving the limitation of disconnected blood circulation, the current study aimed to visualize and quantify Ca^{2+} oscillations of real-time in situ and in vivo osteocytes in response to medium intensity focused ultrasound (MIFU). For in situ study, 3-month-old Black6 mice were used to obtain fresh calvarias. The samples were stained in Fluo-8 AM for Ca^{2+} fluorescent label and subjected to MIFU stimulation for 30sec: 0.05, 0.2, 0.3, 0.5, and 0.7W (Fig1). For in vivo study, Ai38/Dmp1-cre mice that express the Ca^{2+} indicator protein in bone cells (EGFP fluorescent GCaMP3) were under isoflurane anesthesia; the top skin of the head was cut opened, gently exposing the calvaria. The animal's head was stabilized on a custom-made bed, where its chin was placed onto the MIFU transducer (Fig2A): 0.2, 0.5 and 1W for 1min. Real-time confocal imaging was performed to capture the Ca^{2+} signal in the osteocyte cell bodies under MIFU. In situ MIFU at 0.3-0.7W led to significant Ca^{2+} oscillations: 85±16%, 80±18% and 84±17% ($p<0.01$ vs. 0.05W; $p<0.05$ vs. 0.2W) of responded cells, respectively (Fig1). MIFU at >0.3W energies led to a higher number of Ca^{2+} spikes and larger spike magnitudes. The initiation time to the first Ca^{2+} spike seemed to be relatively the same for all the energies (~18sec). In vivo MIFU at 0.2, 0.5 and 1W led to Ca^{2+} oscillations: 90%, 98% (+8% vs. 0.2W) and 100% (+11% vs. 0.2W) of responded cells, respectively (Fig2). Higher MIFU energies led to larger Ca^{2+} spike magnitudes and longer time to elicit the first spike. MIFU at 0.5 and 1W had 71% and 87% larger Ca^{2+} spike magnitude, 30% and 54% longer spike initiation time than at 0.2W, as well as 16% and 20% less Ca^{2+} spikes than at 0.2W, respectively. In conclusion, this study provided a pilot observation of in situ and in vivo osteocytic Ca^{2+} oscillations under noninvasive acoustic radiation force, which aids further exploration of the mechanosensing mechanism of controlled bone cell motility response to fluid flow loading.

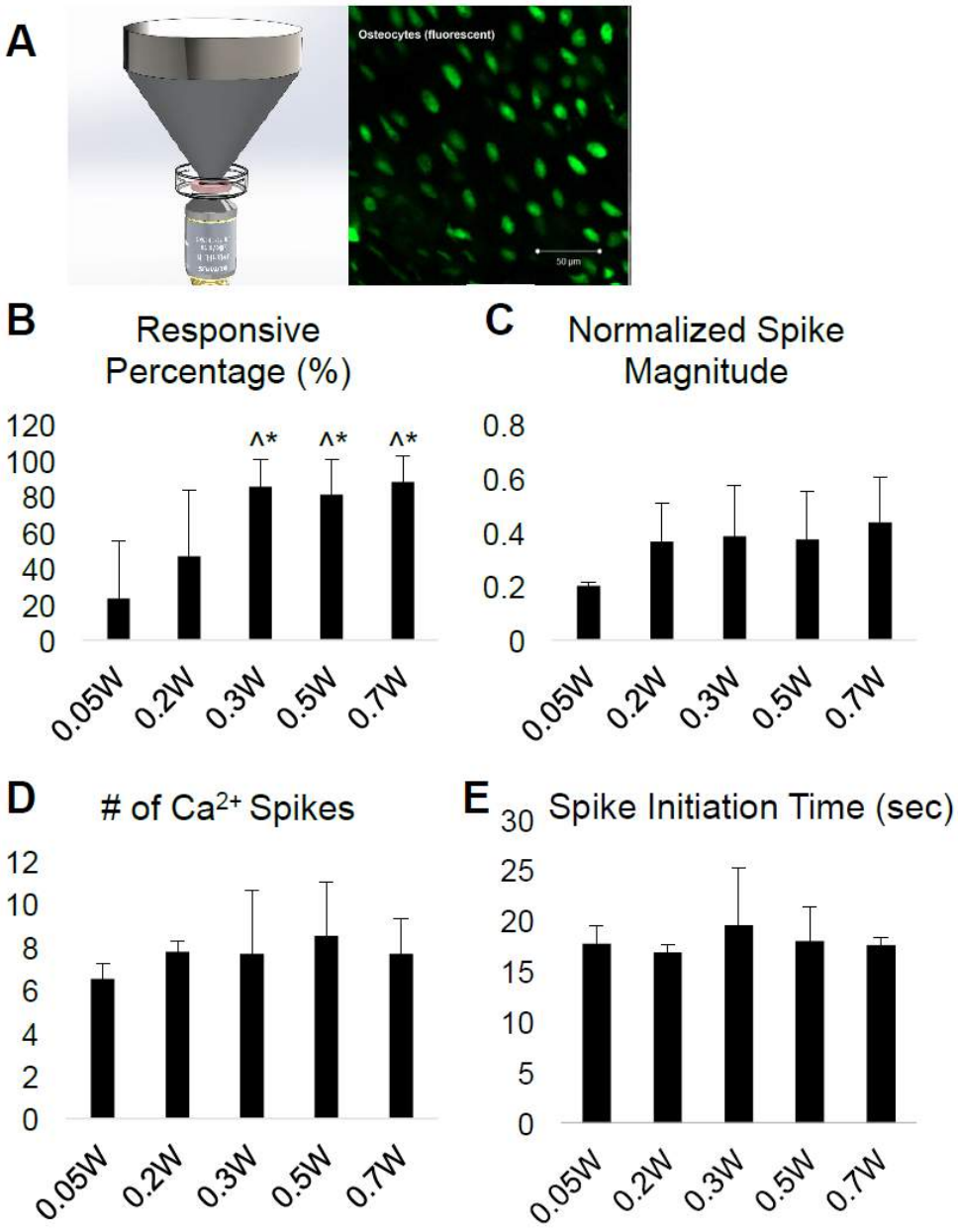

Figure 1. Experimental setup of *in situ* mouse calvaria under MIFU stimulation and Ca^{2+} imaging (A); responsive percentage (B); normalized spike magnitude (C), number of spikes (D), and spike initiation time (E) of osteocyte Ca^{2+} responses to MIFU at various energy powers. ^p<0.01 vs. 0.05W; *p<0.05 vs. 0.2W.

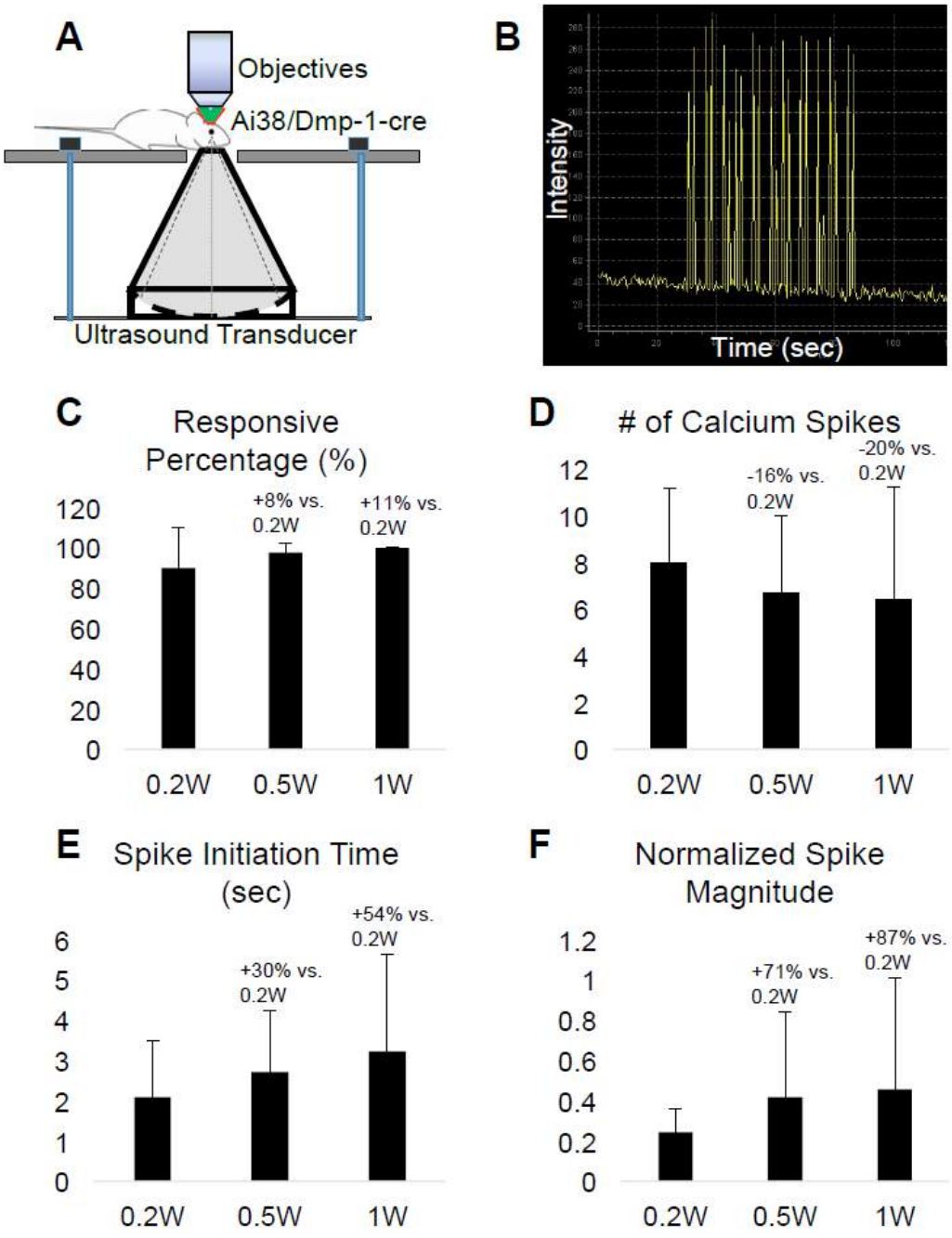

Figure 2. Experimental setup of in vivo Ai38/Dmp-1-cre mouse under MIFU stimulation and Ca^{2+} imaging on the calvaria (A); representative Ca^{2+} trace under 1W MIFU (B); responsive percentage (C); number of spikes (D); spike initiation time (E); normalized spike magnitude (F) of osteocyte Ca^{2+} responses to MIFU at various energy powers.

Role of Phosphate in the Central Ox/Phos Metabolic Processes and Its Linkage to Collagen Production

Amira Hussein, PhD[1], Kevin Blank, MS[1], Deven Carrol, MSl[1], Kyle Lybrand, MD[1], Margaret Cooke, MD[1], Heather Matheny, MS[1], Brenna L. Hogue, MS[1], Serkalem Demissie, PhD[2], and Louis Gerstenfeld, PhD[1]
[1]Department of Orthopaedic Surgery, [2]School of Public Health, Boston University, Boston, MA, USA

Introduction: Prior studies of mice given a phosphate (Pi) deficient diet during fracture healing showed diminished skeletal progenitor commitment, delayed chondrocyte maturation and callus mineralization. Transcriptomic analysis of callus gene expression showed mitochondrial oxidative phosphorylation (ox/phos) genes were significantly down regulated ($p=3.16x10^{-23}$). The goal of this study was to determine how Pi restriction effect on ox/phos is interrelated to intermediate metabolism gene expression and functionally related to phenotype.

Methods: Femora fractures were generated in three strains of male mice. Pi deficiency was initiated 2 days prior to fracture and maintained for 14 days after which mice were returned to normal diet. Controls were fed a normal diet. Microarray analysis of total callus RNAs was carried out over 35-days of healing. Gene expression values were compared between the groups using analyses of covariance with strain and time points as covariates to examine diet effect (FDR q-value ≤0.05). Cluster analysis of ox/phos and intermediate metabolism genes was performed in JMP to identify gene groups showing common temporal responses. Functional Pi restriction studies were performed using ATDC5 chondroprogenitors cells. Growth, differentiation, protein and collagen accumulation, matrix mineralization and oxidative function were assessed.

Results: Comparison of the temporal clustering patterns identified how strain specific profiles for specific ox/phos, tricarboxylic acid cycle, and arginine and proline metabolism genes were co-regulated and coordinated with, pyruvate dehydrogenase, and two subunits of prolyl 4-hydroxylase in response to Pi conditions. In vitro studies showed that chondrocyte differentiation was associated with 2X increase in oxidative respiration. In the absence of BGP normal differentiation proceeded with 1.5X greater accumulation in total protein in the absence of mineralization. In these cultures oxidative respiration was an additional 2X higher. When differentiation was not induced with ascorbic acid and BGP oxidative respiration showed no increase and was comparable to levels seen with 25% of normal Pi levels.

Discussion: Since complex IV genes of the electron transport, arginine and proline metabolism, and prolyl 4-hydroxylase are all commonly regulated by HIF1-α, this suggests a central means by which metabolic regulation is coordinated with collagen production which would balance bone and blood vessel formation.

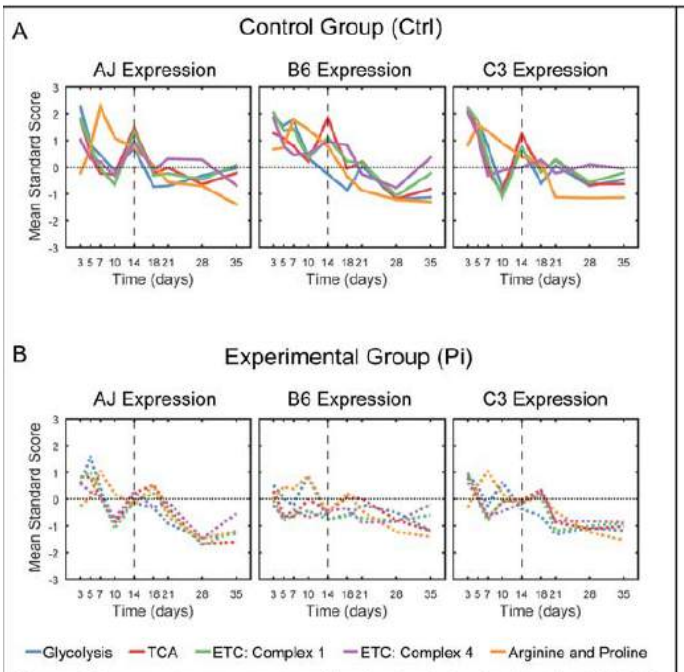

Figure 1. Average gene expression profiles for glycolysis, tricarboxylic acid (TCA), electron transport chain (ETC) and arginine and proline for: A) Control; and B) Pi groups. AJ and C3 strains had similar profiles and responded in a similar manner to Pi restriction

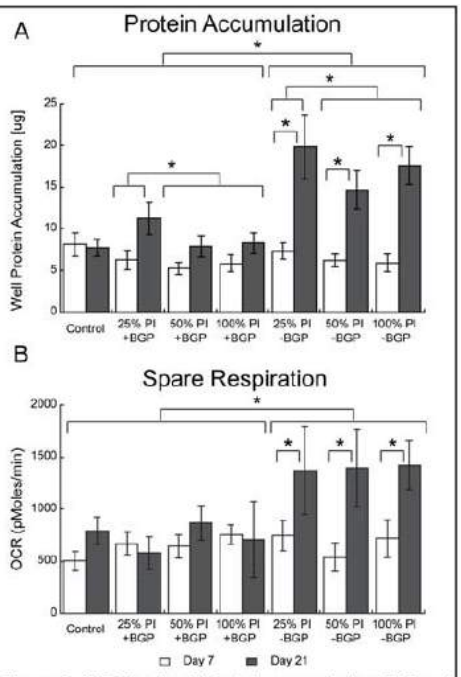

Figure 2. ATDC4 cells: A) Protein accumulation; B) Basal respiration; and C) spare respiratory capacity. All values are normalized to well DNA content. * indicates $p<0.05$.

The Femoral and Hindlimb Skeletal Muscle Properties of G610C Osteogenesis Imperfecta Mouse Model with Soluble Activin Receptor Type IIB Fusion Proteins (ActRIIB-mFc)

Youngjae Jeong BS[a], R. Scott Pearsall PhD[c], and Charlotte L. Phillips PhD[a,b]
[a]Department of Biochemistry and [b]Department of Child Health, University of Missouri, Columbia, MO 65211. [c]Acceleron Pharma, Inc., Cambridge, MA 02139

Osteogenesis Imperfecta (OI) is a rare heritable connective tissue disorder that is characterized by reduced biomechanical integrity of type I collagen containing tissues, such as bone, skin and blood vessels. OI in the majority of patients is autosomal dominant and predominantly due to mutations in the type I collagen genes (Col1a1 and Col1a2), whereas the rarer autosomal recessive forms are due to mutations in genes that code for proteins involved in type I collagen processing, such as post-translational modifications and folding (1). The autosomal dominant forms are classified into four classical subtypes depending on their phenotypic severity.
Currently more than 1500 mutations have been identified in the col1a1 or col1a2 genes (2).
There is no cure for OI and the different mutations with the high phenotypic variability make treatment difficult. In 2010, Daley et al. described 64 individuals in a large kindred of the old order Amish community that had a glycine to cysteine substitution at the 610 position of α2(I) collagen chain who exhibited reduced bone mineral density (BMD) with mild type I/IV OI phenotypes (3). The heterozygous G610C (*+/G610C*) mouse model has the same genetic mutation with similar phenotypes, such as reduced BMD and biomechanical integrity in femurs, as those in G610C OI individuals (3).

Bone strength is known to positively correlate with muscle mass and strength. This is hypothesized to be due to the mechanosensing character of bone, in which muscle mass and force represents some of the largest physiological loads on bone (4). Myostatin, a member of
TGF-β superfamily, is known to signal through activin receptor type IIs to negatively regulate muscle growth, with myostatin deficiency leading to muscle hypertrophy and hyperplasia (5, 6).
In recent studies, myostatin inhibition with soluble activin receptor type IIB [ActRIIB-mFc, Acceleron Pharma, Inc] led to improvement in muscle and bone properties of mature rodents (7).

In the following study, we investigated the effects of myostatin inhibition with ActRIIB-mFc on muscle and bone properties of the heterozygous autosomal dominant G610C OI mouse model (*+/G610C*). At 2 months of age, bi-weekly treatment of either TBS (Tris-Buffered Saline) vehicle or ActRIIB-mFc (10mg/kg) were administered for 8 weeks to wild-type (WT) and *+/G610C* mice.
At 4 months of age, mice were anesthetized and muscle contractile force was obtained by insit muscle contractile testing prior to the sacrifice. ActRIIB-mFc treated mice had increased body weight with concomitant increases in hindlimb skeletal muscle weights [soleus (Sol), plantaris, gastrocnemius (Gast), tibialis anterior (TA), and quadriceps] regardless of genotypes.
The peak tetanic force (Po) in Sol, Gast, and TA was not changed with ActRIIB-mFc treatment, however the relative Po (Po normalized to muscle wet weight) was reduced with ActRIIB-mFc treatment regardless of genotypes. µCT analyses demonstrated ActRIIB-mFc treated WT and *+/G610C* mice femur exhibited increases in cortical bone thickness and polar moment of area, suggesting the ActRIIB-mFc treatment results in greater resistance to fracture. By torsional loading to failure, we demonstrated that ActRIIB-mFc treated WT and *+/G610C* femur had increased torsional ultimate strength, as well as increased energy to failure in WT mice.

Our data demonstrate that systemic administration of ActRIIB-mFc induced increases in body weight and skeletal muscle weights without altering absolute contractile function in WT and *+/G610C* mice. The cortical bone geometry and biomechanical integrity were improved in WT and *+/G610C* mice with ActRIIB-mFc treatment. Our data suggest that ActRIIB-mFc treatment in OI mouse model induced improvement in bone properties potentially by increased muscle mass in addition to an alternative pathway impacting osteoblast and/or osteoclast functions.
Although further investigations on the mechanisms of action of ActRIIB-mFc is still required, our study suggests ActRIIB-mFc treatment can be a potential therapeutic option in OI.

1. Forlino A, Marini JC. Osteogenesis imperfecta. Lancet. 2015. Epub 2015/11/07.
2. Marini JC, Forlino A, Cabral WA, Barnes AM, San Antonio JD, Milgrom S, et al. Consortium for osteogenesis imperfecta mutations in the helical domain of type I collagen: regions rich in lethal mutations align with collagen binding sites for integrins and proteoglycans. Human mutation.
2007;28(3):209-21. Epub 2006/11/02.
3. Daley E, Streeten EA, Sorkin JD, Kuznetsova N, Shapses SA, Carleton SM, et al. Variable bone fragility associated with an Amish COL1A2 variant and a knock-in mouse model. Journal of bone and mineral research: the official journal of the American Society for Bone and Mineral Research.25(2):247-61.
4. Frost HM. Bone's mechanostat: a 2003 update. The anatomical record Part A, Discoveries in molecular, cellular, and evolutionary biology. 2003;275(2):1081-101. Epub 2003/11/13.
5. McPherron AC, Lawler AM, Lee SJ. Regulation of skeletal muscle mass in mice by a new TGF-beta superfamily member. Nature. 1997;387(6628):83-90. Epub 1997/05/01.
6. Lee SJ, McPherron AC. Regulation of myostatin activity and muscle growth. Proceedings of the
National Academy of Sciences of the United States of America. 2001;98(16):9306-11. Epub 2001/07/19.
7. Chiu CS, Peekhaus N, Weber H, Adamski S, Murray EM, Zhang HZ, et al. Increased muscle force production and bone mineral density in ActRIIB-Fc-treated mature rodents. The journals of gerontology Series A, Biological sciences and medical sciences. 2013;68(10):1181-92. Epub 2013/03/26.

Influence of Progesterone Nuclear Receptor Signaling in Osteoprogenitor Cells on Sexual Dimorphism of Trabecular Bone Mass

Alexander Kot[1], BS Zhendong Zhong, PhD[2], HongLiang Zhang, MD[1], Yu-An Lay, MS[1], Nancy E. Lane, MD[1] and Wei Yao, MD[1]
[1]University of California, Davis Medical Center, Sacramento, CA
[2]Van Adel Institute, Grand Rapids, MI

Progesterone is a sex steroid mostly known for its reproductive system effects. Its functions are largely mediated through the progesterone nuclear receptor (PR), a ligandregulated transcription factor. The PR is present in osteoblasts and osteoclasts; however, its effect on bone remains unclear. We determined that compared to 1-12 month old wild type (WT) littermates, global PR knockout (PRKO) mice had increased bone mass --female PRKO mice had increased bone formation and male PRKO mice had decreased bone resorption. We hypothesized that the PR in osteoprogenitors may be a key regulator of sexual dimorphism in bone mass acquisition.

We crossed PR-flox and Prx1-cre mice to obtain mice with the PR deleted in osteoprogenitors (Prx1;PRcKO) and WT littermates of both sexes. Bone mass acquisition, bone turnover and bone mechanical properties were evaluated in 2 and 6 month old mice by µCT, histomorphometry and 3-point bending tests respectively. To elucidate a mechanism by which the lack of osteoprogenitor PR signaling influences bone mass, we cultured MSCs from bone for RNA-seq. Two factor ANOVA was used to evaluate genotype and sex effects and their interaction for bone outcome variables. For RNA-seq, differentially expressed genes were identified using EdgeR with FDR < 0.01 after Benjamin-Hochberg correction for multiple testing. Kyoto Encyclopedia of Genes and Genomes (KEGG) pathway and gene ontology analyses were used to define functional groups of genes.

Compared to WT littermates, Prx1;PRcKO males and females had increased distal femur BV/TV and trabecular surface bone formation at 2 and 6 months of age ($p<0.05$), with greater effects in males ($p<0.05$). No significant change was observed for the cortical bone, bone strength, bone size and femur length. Preliminary results from the whole MSC transcriptome revealed that PR ablation had a sex specific effect on gene expression with more transcriptional changes observed in males (Figure). Pathways significantly overrepresented ($p<0.01$) in differentially expressed genes between the male Prx1;PRcKO and male WT groups included: osteoclast differentiation, NF-kappa B signaling, immune and inflammatory response.

These results suggest that PR signaling in osteoprogenitors is a critical regulator of bone mass acquisition and may explain sex differences. Further studies of PR signaling may provide strategies to augment bone mass.

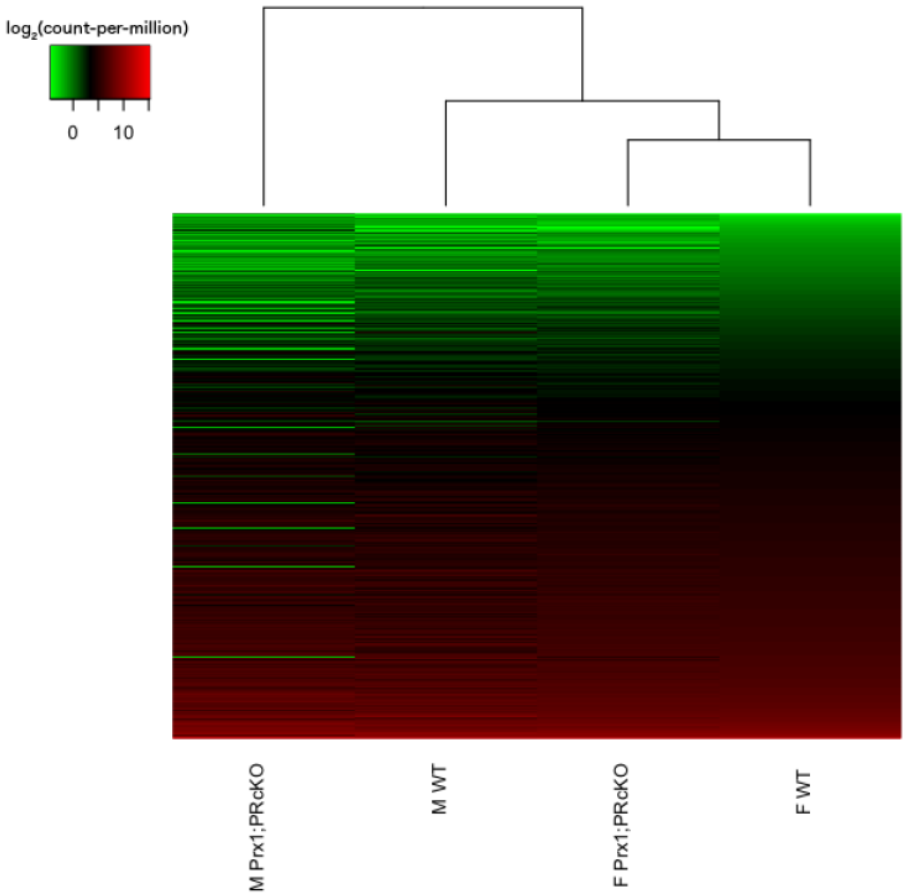
log2(count-per-million)
0
10
M Prx1;PRcKO
M WT
F Prx1;PRcKO
F WT

Periosteal Osteochondroprogenitors Contribute to Development of the Appendicular Skeleton by Populating the Growth Plate and Cortical Bone

Emily Moore, MS, Christopher Jacobs, PhD
Columbia University, New York, NY

INTRODUCTION: Periosteal progenitors continue to emerge as a promising candidate for bone and cartilage regeneration due to the ease with which the periosteum can be transplanted to affected areas and the osteochondrogenic commitment of its progenitors[1]. The periosteum's inner cambium layer contains a unique population of Prx1-expressing progenitors that demonstrate osteochondrogenic potential *in vitro* and populate the fracture callus *in vivo*[2,3]; however, investigators have to yet determine how to activate and direct these cell stores to targeted areas. The primary cilium is an extracellular sensory organelle present in most mammalian cell types and is believed to facilitate activation, migration, and differentiation of cells involved in skeletal development. For example, disruption of chondrocyte primary cilia in postnatal mice results in a lack of proliferating cells, severely altered growth plates and, ultimately, dwarfism[2]. Although periosteal progenitors and their cilia play a critical role in embryonic skeletal development[4] and fracture repair [Colnot], their roles in postnatal development are unknown due to the embryonic lethality associated with available mouse models[5]. We developed novel mouse models that allow us to temporally disrupt periosteal primary cilia and track the fate of Prx1-expressing osteochondroprogenitors in order to study their activation and migration during postnatal development. We hypothesized that primary cilia are required for migration and differentiation of Prx1-expressing osteochondroprogenitors to participate in endochondral and intramembranous ossification during juvenile skeletal development. Ultimately, this information can be used to recapitulate skeletogenesis in order to regenerate bone and cartilage *in vivo*.

METHODS: Male mice expressing tamoxifen-inducible Cre driven by the periosteum/ perichondrium-specific promoter, *Prx1*, were bred with female mice containing floxed alleles of an intraflagellar transport protein critical to proper cilium function (*Ift88*) to generate mutant *Prx1CreER-GFP;Ift88*$^{fl/fl}$ pups and *Ift88*$^{fl/fl}$ littermate controls. Littermates were injected with 33 mg/kg tamoxifen (Sigma) and 10% ethanol solution daily from postnatal day seven (P7) to P16 or P29 and sacrificed on P17 and P30, respectively. The right and left ulnae were dissected, fixed in 10% formalin, and sectioned in 5 um increments longitudinally and transversely, respectively. Hematoxylin and eosin (Sigma) stains were performed to observe morphology of the growth plate and quantify length and thickness of the ulnae. Toulidine Blue O (Sigma) stains were carried out to assess the presence of cartilage, calcified cartilage, bone, and marrow in the growth plate, trabecular and cortical bone, and secondary ossification centers. Immunohistochemistry was performed to quantify the number of proliferating cells present in the growth plate (PCNA, abcam) and differences in the hypertrophic zone (Type X Collagen, abcam). *Prx1CreER-GFP* mice were also crossed with red fluorescent reporter (*Rosa26*td^{Tomato}) mice to generate *Prx1CreER-GFP; Rosa26*td^{Tomato} pups in order to track the fate of periosteum-derived osteochondroprogenitors, which lose Prx1 expression and the GFP tag as they migrate from the periosteum. Ulnae were dissected, fixed in 4% paraformaldehyde, and cryosectioned in 5 um increments. Sections were mounted with medium containing DAPI (EMS). Statistics were performed using a student t-test with $\alpha = 0.5$ and power of 80%.

RESULTS: Mutant mice had shorter and thinner ulnae, indicative of attenuated endochondral and intramembranous ossification, compared to controls at all injection time points (Figure 1). Interestingly, the marrow area of mutants was significantly larger than that of controls except for the P17 – P30 injection group, which had areas similar to those of controls. Mutants generally had smaller growth plates and lacked the distinct columnar structure that is characteristic of proliferating chondrocytes (Figure 2). IHC revealed that mutants also had fewer proliferating chondrocytes and accelerated hypertrophy in the growth plate (Figure 3). Ossification was also severely stunted in the proximal head of mutants but this effect was less pronounced in the P17 – P30 injection group (Figure 4). In our reporter model, we found that periosteum-derived progenitors were incorporated in the growth plate as proliferating chondrocytes, surrounded both the periosteal and endocortical surfaces of the ulna, and were embedded within cortical bone as osteocytes (Figure 5). These cells were also found in secondary ossification centers and articular cartilage (data not shown).

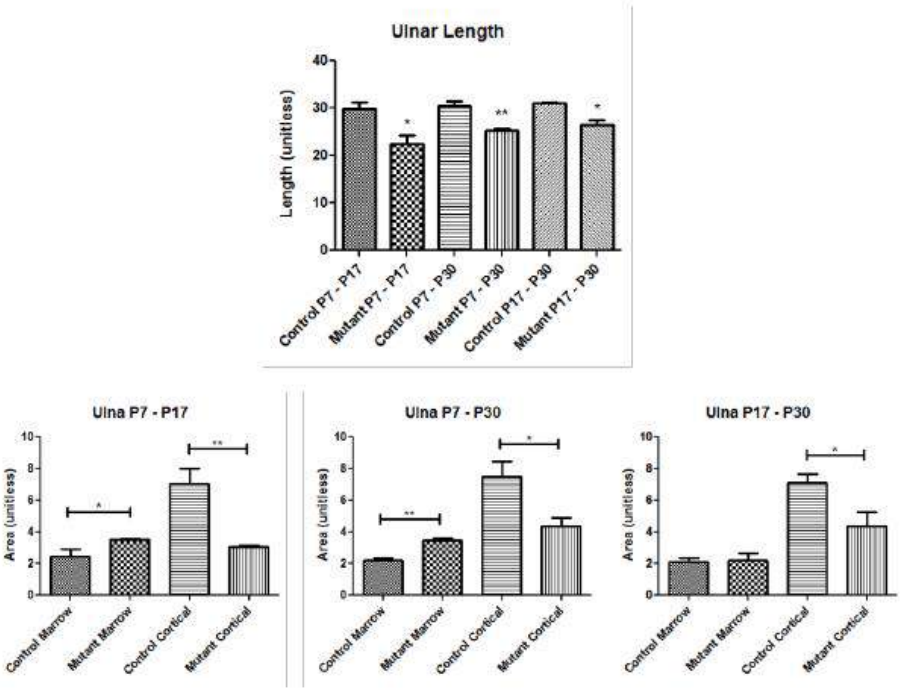

Figure 1: Juvenile mice with disrupted periosteal primary cilia have stunted endochondral (top) and intramembranous ossification (bottom).

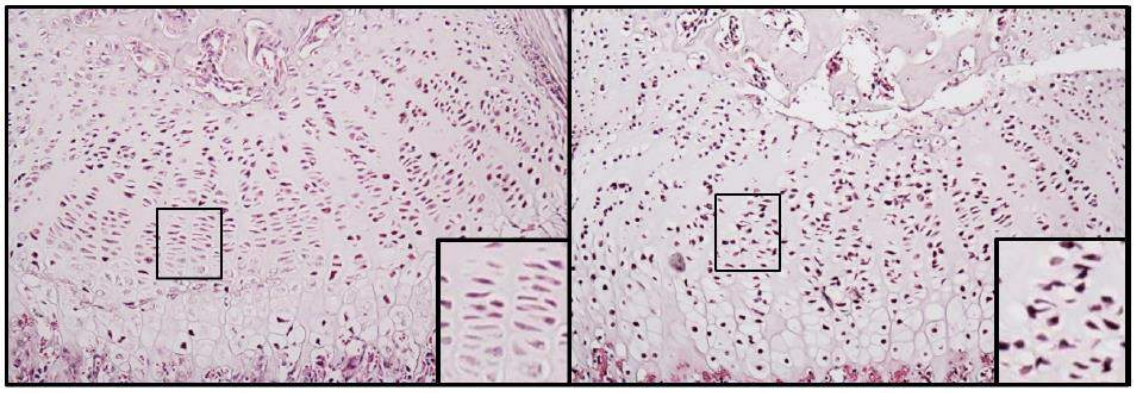

Figure 2: Proliferating chondrocytes in mutant mice injected from P7 – P30 (right) lack distinct columnar organization like that seen in the proliferation zone of control animals (left). Images collected at 20X magnification, a portion of the proliferation zone has been magnified at the bottom right of each image to better illustrate the disparity in columnar stacking.

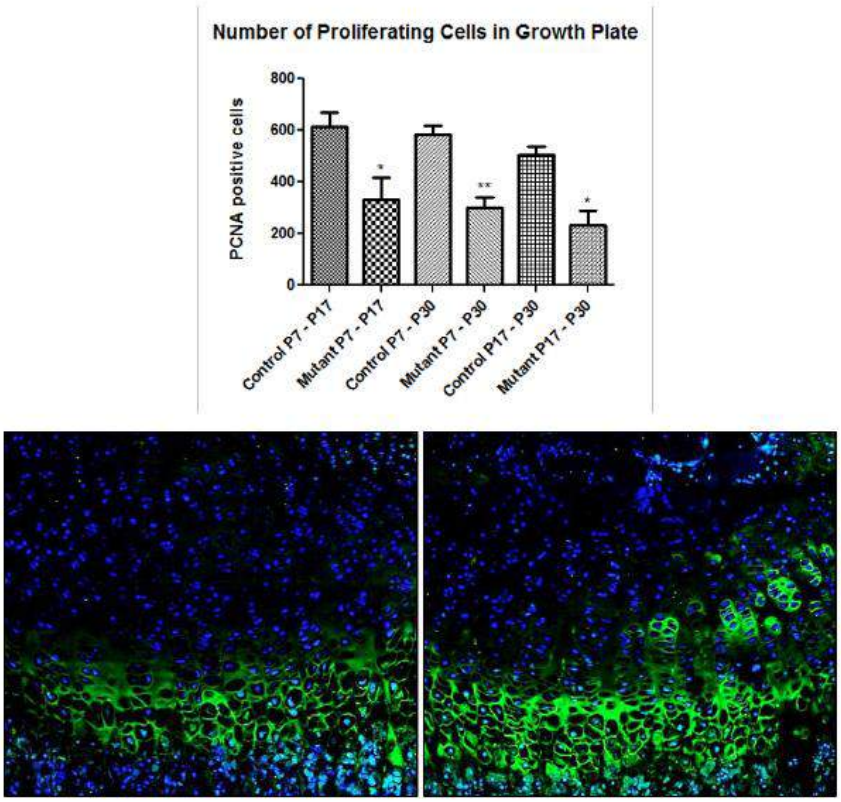

Figure 3: Mutants have significantly fewer proliferating chondrocytes than controls (top). Mutants injected from P7 – P30 (right) have larger hypertrophic zones (green) as well as premature hypertrophy in the proliferation zone.

DISCUSSION: Our results demonstrate that periosteal progenitors contribute to juvenile skeletogenesis but their role is compromised without functional primary cilia. Our tracking studies indicate these progenitors populate the growth plate and contribute to endochondral ossification, as well as generate bone at the periosteal and endocortical surfaces via intramembranous ossification. The lack of proliferating chondrocytes in mutants suggest that disrupting periosteal cilia perhaps inhibits migration of chondroprogenitors to the growth plate and impedes columnar alignment for those that do reach the proliferation zone, resulting in premature hypertrophy and stunted endochondral ossification. Chondrocyte cilia are known to align parallel to the longitudinal axis of the limb and are believed to encourage proper columnar stacking of proliferating cells[6], which facilitates migration within the growth plate and timing of hypertrophy. Indeed, we found that control proliferating chondrocytes arranged in tight columns had cilia aligned with the longitudinal axis of the growth plate, but this behavior was lost in mutants (data not shown). The significantly thinner mutant cortical cross sections indicate that periosteal cilia are necessary to generate osteoprogenitors that form bone via intramembranous ossification; however, it is rather surprising that so many tdTomato+ cells were found at the endocortical surface. We hypothesize that periosteal progenitors first invade the juvenile cartilaginous structure to form bone, which is later resorbed by osteoclasts to shape the resulting cortical marrow space. The fact that our P17 – P30 mice did not have a significantly different marrow area compared to controls supports our claim because earlier progenitors had intact cilia. In general, the less severe phenotype in the P17 – P30 injection time point indicates earlier progenitors are more important for proper marrow area and ossification at the proximal head. Currently, we are developing reporter mice with disrupted progenitor cilia in order to provide insight on how the cilium affects progenitor migration. We believe this could potentially motivate cilium-based therapeutics to activate migration and/ or differentiation of these periosteal progenitor stores for bone and cartilage regeneration in vivo.

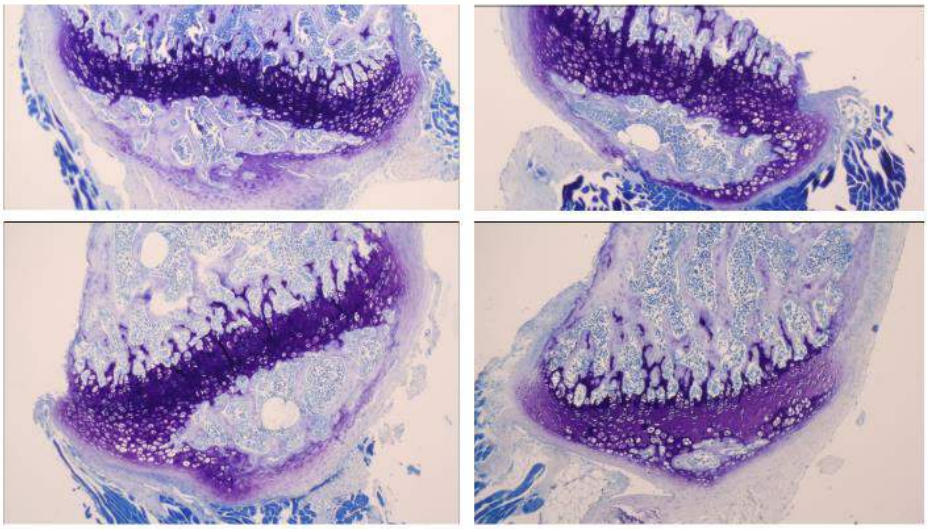

Figure 4: Mutants (left) injected from P7 – P30 (top) have significantly attenuated ossification at the proximal head compared to controls (right). Although ossification is still slightly attenuated, it is not as significant in mutants (left) injected from P17 – P30 (bottom).

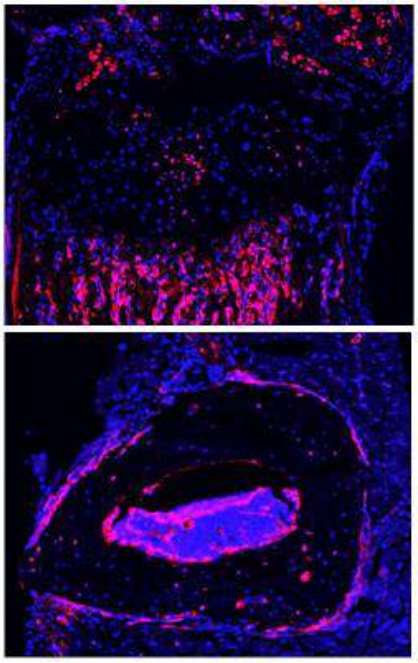

Figure 5: Periosteum derived cells (red) from P7 – P30 are incorporated in the growth plate, resting zone, and trabecular bone (top). In the transverse view, tdTomato+ cells are also found embedded in the cortical bone as well as both periosteal and endocortical surfaces (bottom).

SIGNIFICANCE: This study demonstrates for the first time that progenitor primary cilia largely contribute to juvenile bone development, potentially by triggering migration and differentiation of osteochondroprogenitors to ossify pre-existing cartilaginous structures in the appendicular skeleton. Other work performed in our lab suggests primary cilia can be pharmaceutically sensitized to enhance their sensory capabilities; thus, primary cilia are attractive candidates for therapeutics that trigger activation and recruitment of periosteal stores to regenerate cartilage and bone.

REFERENCES: 1) Castro-Silva et al. *Periosteal-derived cells for bone bioengineering: a promising candidate.* Clin Oral Imp Res. Jan 2012. 2) Kawanami et al. *Mice expressing GFP and CreER in osteochondro progenitor cells in the periosteum*. Biochem Biophys Res Commun. Aug 2009. 3) Ouyang et al. *Prx1 and 3.2kb Col1a1 promoters target distinct bone cell populations in transgenic mice*. Bone. Oct 2013. 4) Haycraft et al. *Intraflagellar transport is essential for endochondral bone formation*. Dev. Jan 2007. 5) Colnot. *Skeletal cell fate decisions within periosteum and bone marrow during bone*

regeneration. J Bone Miner Res. Feb 2009. 6) Song et al. *Development of the post-natal growth plate requires intraflagellar transport proteins*. Dev Biol. May 2007.

Functional Adaptation of Osteocalcin and Osteopontin Deficient Mice

Stacyann Morgan, BSc[1] and Deepak Vashishth, PhD[1]
[1]Rensselaer Polytechnic Institute, Troy, NY

Introduction

Osteocalcin (OC) is one of the most abundant non-collagenous protein (NCP) in bone [1]. It is produced during bone formation, late after mineralization by osteoblasts and forms a complex with Osteopontin (OPN) and other molecules in the extra-cellular matrix [2]. Recent studies in our laboratory showed that the OC-OPN complex regulates bone toughness through its control over matrix quality [3]. Such control may also help in determining bone size and strength. Therefore, we investigated whether these proteins play a role in regulating bone strength through morphological adaptation.

Materials and Methods

Radii from male 6 month old OC-OPN$^{-/-;-/-}$ and Wild Type mice (n=15 per group) were separated from the ulna and stored in saline soaked gauze at -80 C until use. Samples were scanned using µCT with a 10.5 µm voxel size (µCT 40; Scanco Medical) in eppendorf tubes with saline solution. Bone geometry was determined from the mid-shaft of each sample and the parameters measured were: length (Le), cortical area (Ct.Ar), cortical thickness (Ct.Th) and tissue mineral density (TMD). The mice radii were then loaded to failure in three point bending at a displacement controlled loading rate of 0.001 mm/s (Elf 3200; EnduraTEC). The resulting load-displacement curve was used to calculate the structural properties ultimate force (FU; N), yield force (FY; N), stiffness (S; N/mm), and postyield energy to failure (UPY; mJ) and ultimate strength (σU, MPa).

Statistical Analysis

Mann-Whitney Rank Sum Test was used to determine differences between the groups for all parameters measured. A path analysis was conducted to test the hypothesis that morphological and tissue quality traits are functionally related and contribute to whole bone mechanical properties. The model is constructed with bidirectional arrows representing associated variables, direct arrows indicating causal effects, and path coefficients which represent the magnitude of the relationship between traits. The structural equations were then constructed using the path coefficients. All analysis was carried out using SPSS 21 (IBM SPSS Statistics).

Results

The results showed that OC-OPN$^{-/-;-/-}$ were shorter with thicker cortices and larger cortical area (Table 1). The fracture load for OC-OPN$^{-/-;-/-}$ was also higher compared to WTs ($p<0.05$) but there were no significant differences in TMD or measures of stiffness and strength ($p>0.05$). Yield and post-yield deformation were also not different between the groups ($p >0.05$). The path diagrams indicate that cortical thickness, cortical area and TMD resulted in a good fit for both groups as determined by the chi-square and RMSEA goodness of fit indices. While 47% of the variation in stiffness was explained by these traits for WT, only 19% was explained in the OC-OPN$^{/-;-/-}$ group. These traits also explained 50-70% of the variation seen in ultimate strength for both groups.

Discussion

In the absence of both OC and OPN, the matrix quality of the bone is significantly compromised [3]. The results of this study suggests that bones of OC-OPN$^{-/-;-/-}$ adapts to loss of matrix quality by varying its length, the amount of cortical bone and thickness within the midshaft. This co-adaptation leads to a structure in the knockouts that is similar in stiffness and strength as the WT littermates but lower material level toughness [3]. In the path analysis, slenderness (Tt.Ar/Le) was chosen to determine how variability in bone size is causally related to Ct.Th and TMD. Since slender bones have a proportionate increase in Ct.Ar and whole bone stiffness depends on a measure of bone size, Ct.Ar was also added to the model. Variation in marrow expansion during growth drives subsequent adaptive changes in other traits and contributes directly to ultimate strength in WTs. Given the same set of traits, each genotype builds a mechanically functional bone but in a slightly different manner. Our study demonstrates for the first time that osteocalcin and osteopontin plays a significant role in regulating bone size (length, cortical thickness and cortical area) and bone strength.

References:

1.Sroga, Grażyna E., and Deepak Vashishth. "Effects of bone matrix proteins on fracture and fragility in osteoporosis." *Current osteoporosis reports* 10.2 (2012): 141-150.

2. Ritter, Nadine M., Mary C. Farach-Carson, and William T. Butler. "Evidence for the formation of a complex between osteopontin and osteocalcin." *Journal of Bone and Mineral Research* 7.8 (1992): 877-885.
3. Poundarik, Atharva A., et al. "Dilatational band formation in bone." *Proceedings of the National Academy of Sciences* 109.47 (2012): 19178-19183.

Parameters	WT	OC-OPN$^{-/-;-/-}$	p-value
Le (mm)	10.541±0.27	10.033±0.37	<0.001
Ct.Ar (mm^2)	0.241±0.02	0.272±0.03	0.002
Ct.Th (mm)	0.152±0.011	0.163±0.014	0.026
F_u(N)	3.409±0.63	3.907±0.84	0.056
Outer Diameter (mm)	0.642±0.04	0.688±0.05	0.026
Toughness (mJ)	0.599±0.26	0.704±0.24	0.046

Table 1: Summary of variables measured from the mid-shaft of each sample

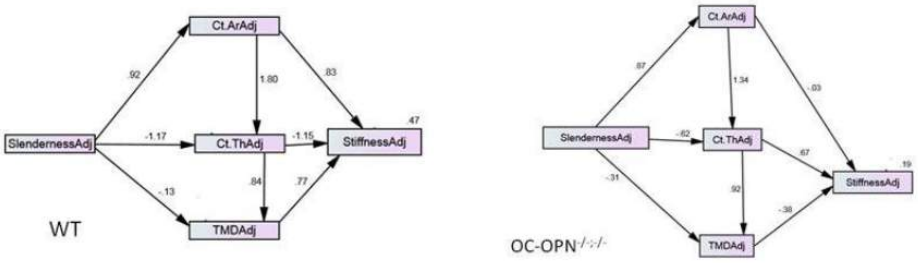

Figure 1: Path diagrams for stiffness between WT (left) and OC-OPN$^{-/-;-/-}$ (right)

$Stiffness_{WT} = 0.825\ Ct.Ar + 0.770\ TMD - 1.15\ Ct.Th$ $R^2 = 0.47$, $\chi^2 = 1.13$, p=0.53, df= 2, RMSEA=0.00

$Stiffness_{OC\text{-}OPN\text{-}/\text{-};\text{-}/\text{-}} = -0.031\ Ct.Ar - 0.384\ TMD + 0.667\ Ct.Th$ $R^2 = 0.19$, $\chi^2 = 2.00$, p=0.37, df= 2, RMSEA=0.00

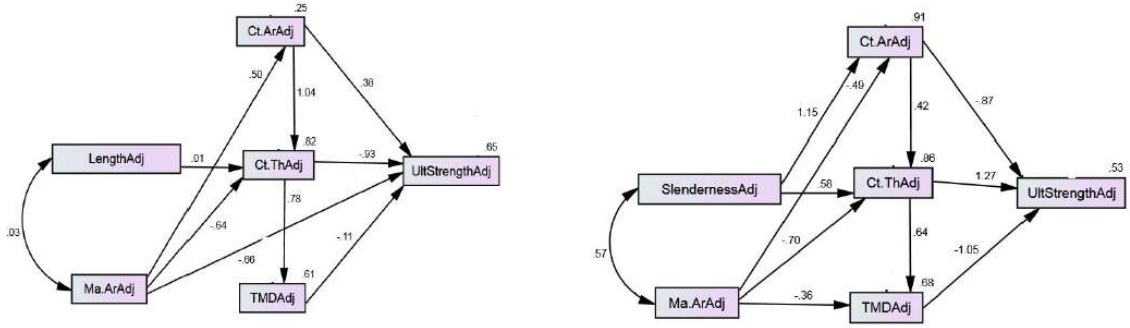

Figure 2: Path diagrams for ultimate strength between WT (left) and OC-OPN$^{-/-;-/-}$ (right)

$Ult.Strength_{OC\text{-}OPN\text{-}/\text{-};\text{-}/\text{-}} = -0.87\ Ct.Ar - 1.05\ TMD + 1.27\ Ct.Th$ $R^2 = 0.53$, $\chi^2 = 3.93$, p=0.415, df= 4, RMSEA=0.00

$Strength_{WT} = 0.38\ Ct.Ar - 0.11\ TMD - 0.93\ Ct.Th$ $R^2 = 0.65$, $\chi^2 = 4.15$, p=0.53, df= 5, RMSEA=0.00

Tibial Compression Overload Instigates Post-Traumatic Osteoarthritis in Mouse Knee

Muhammad Farooq Rai, PhD[1], Duan Xin, MD[1], James Quirk, PhD[2], Nilsson Holguin, PhD[3], Eric Schmidt, PhD[5], Nobuaki Chinzei, MD, PhD[1], Matthew J. Silva, PhD [1,3], Linda J. Sandell, PhD[1, 3, 4]

[1]Department of Orthopaedic Surgery, Musculoskeletal Research Center, [2]Mallinckrodt Institute of Radiology, [3]Department of Biomedical Engineering, [4]Department of Cell Biology and Physiology, Washington University School of Medicine at Barnes-Jewish Hospital, MO, United States. [5]Department of Physician Assistant Medicine, School of Graduate Health Studies, Lynchburg College, Lynchburg, VA.

Objectives: Osteoarthritis (OA) is a clinical syndrome of joint pain accompanied by varying degrees of functional impairment and diminished quality of life. Primary age-related OA has unknown etiology, complex and multifaceted pathogenesis and uncertainty about the timeline of pathological events. In contrast, post-traumatic OA (PTOA) that constitutes 12% of knee OA has an injury component associated with it where disease-initiating injury event is known and sequelae of pathological footprints can be trailed. Any injury severe enough to cause anterior cruciate ligament (ACL) tear and/or meniscus destabilization frequently leads to PTOA overtime. In this study, we aim to investigate a spectrum of lesions characteristic of PTOA phenotype in the articular cartilage, meniscus, synovium, ligaments and bone in response to mechanical knee injury in an attempt to understand early and late event in PTOA. We hypothesized that alteration in knee joint stabilization recapitulates molecular and structural features of PTOA in the knee tissues depends on load intensity and time.

Methods: Eight-week old male mice from LGXSM-6 and LGXSM-33 lines were used. Axial tibial compression was applied on right knees. Three separate loading regimens were applied: 6N, 9N and 12N. The contralateral left knees served as control. Mice were scarified at 5, 9, 14, 28 and 56 days post-loading as indicated and whole knee joint changes were assessed by histology, immunostaining, micro-CT and magnetic resonance imaging.

Results: Tibial compression largely resulted in ACL tear, which disrupted the joint stabilization instigating a cascade of temporal and topographical features of PTOA. These features largely included cartilage matrix damage, chondrocyte apoptosis and altered aggrecan expression pattern, ligament and meniscus pathology, synovitis, bone loss, osteophyte formation and development of ectopic calcification.

Conclusions: This study delineates changes recapitulating morphological and anatomic features of PTOA beyond cartilage and bone after injurious mechanical injury. It provides a plausible explanation into how an ACL injury in humans leads to development of PTOA overtime. Taken together, this study provides a broad picture of pathological events in the knee following a traumatic insult strong enough to sever ACL. We observed that high mechanical loading instigated whole knee joint changes recapitulating PTOA within eight weeks. Although the actual mechanisms underlying these changes in mice and men appear to be alike, the time scale for progression to advanced PTOA is greatly accelerated in mice as compared to humans, therefore translating these findings to human PTOA should be considered with some caution. At least these studies provide a window of opportunity to treat PTOA using different therapeutic and preventive approaches. Further interrogation of the mechanism(s) of these changes is warranted to unravel the exact pathogenesis of PTOA.

Distinct Response of Osteons at Different Locations in Response to Loading and Intermittent PTH Injections

Ke Wang, DDS[1], Yuan Hui, DDS[2], Yinshi Ren, PhD[3], Ying Liu[1], Xianglong Han, DDS[4], and Jing Q. Feng, PhD[1]
[1]Department of Biomedical Science, Texas A&M Health Science Center, Baylor College of Dentistry, Dallas, TX;
[2]Department of Orthodontics, Fourth Military Medical of University, China;
[3]Cellular, Developmental, and Genome Laboratories, Musculoskeletal Research Center, Duke University, Durham, NC;
[4]State Key Laboratory of Oral Diseases, West China Hospital of Stomatology, Sichuan University, China.

Currently, most, if not all, bone studies focus on rodents, which do not have an osteon structure, the *basic unit of bone formation and remodeling in large mammalians.* Interestingly, recent studies discovered an astonish defect in Harversian-canal-osteon structures in patients with osteoporosis. *Because studies of large animal bones have fallen out of favor since the molecular biology era*, we basically *know very little about how osteons are formed.* In this study, we first demonstrated that primary osteons in the embryonic dog femur bone are originated from both periosteum and endosteum layers proportionally (Fig 1). Next, we asked whether constant
forces, which were generated for 5-weeks by open-coil springs anchored on miniscrew implants in the tibia with a force 0, and 200 g (right tibia) separately, would affect osteon formation (Fig 2a). In the loading groups (6 adult dogs), there were sharp increases in Haversian canals by uCT (Fig 2b). The images of backscattered SEM and triple labeling (with 10 day apart) displayed many newly formed osteons, which were mainly derived from the expanded periosteum layer (Fig 3). These newly formed osteons expressed high levels of endothelial and bone markers, including VEGF, periostin, OSX and BSP (Fig 4). This asymmetric contribution of osteon formation from the periosteum prompted us to initiate a different set of experiments, in which we tested the impact of intermittent injections of PTH on wild type mice and 4 young adult dogs (10 ug/kg per day for four weeks). Interestingly, the increased bone volume was associated with the expanded endosteum layer in mice (Fig 5, left). Similarly, bone volume expansions occurred in the PTH treated dogs, in which the lamellar structures on the endosteum side were replaced by the newly formed osteons (Fig 5, right). We then asked whether similar events would occur in intramembranous bone in response to mechanical loading. Using tooth movement model, we observed numerous newly formed osteons by backscattered SEM and triple labeling images (Fig 6). This newly formed bone was originated from the periodontal ligaments (PDL). Collectively, these data for the first time revealed that 1) osteons are formed from both periosteum and endosteum layers during embryonic dog bone formation; 2) the mechanical loading initiates osteon formation from the periosteum layer; 3) the PTH induced osteon formation is mainly originated from the endosteum side; and 4) the osteon formation stimulated by tooth movement is from the PDL (Fig 7). Based on these exciting data, we conclude
that there are different progenitor cell pools, which are responsible for osteon formation in different physiological status.

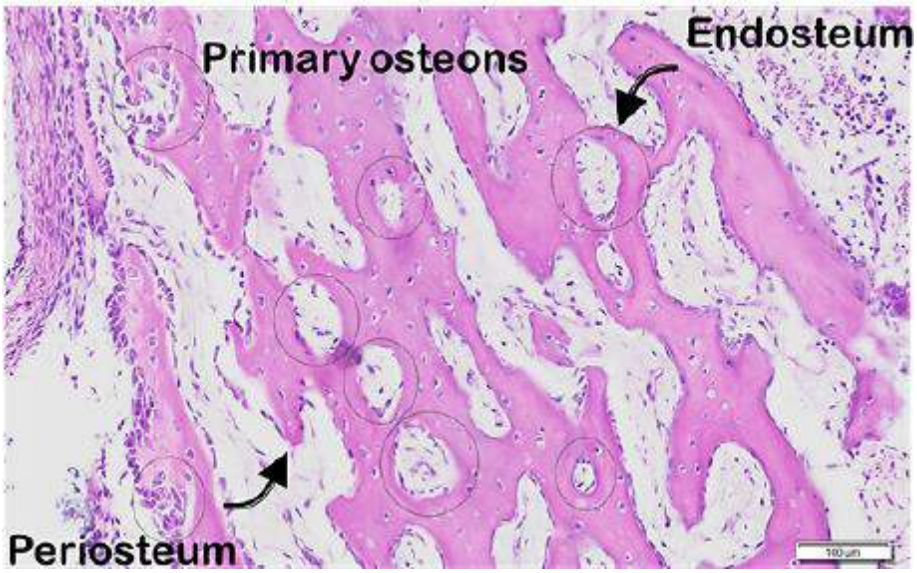

Fig 1. The dog primary osteons are formed from both periosteum and endosteum layers during embryonic development.

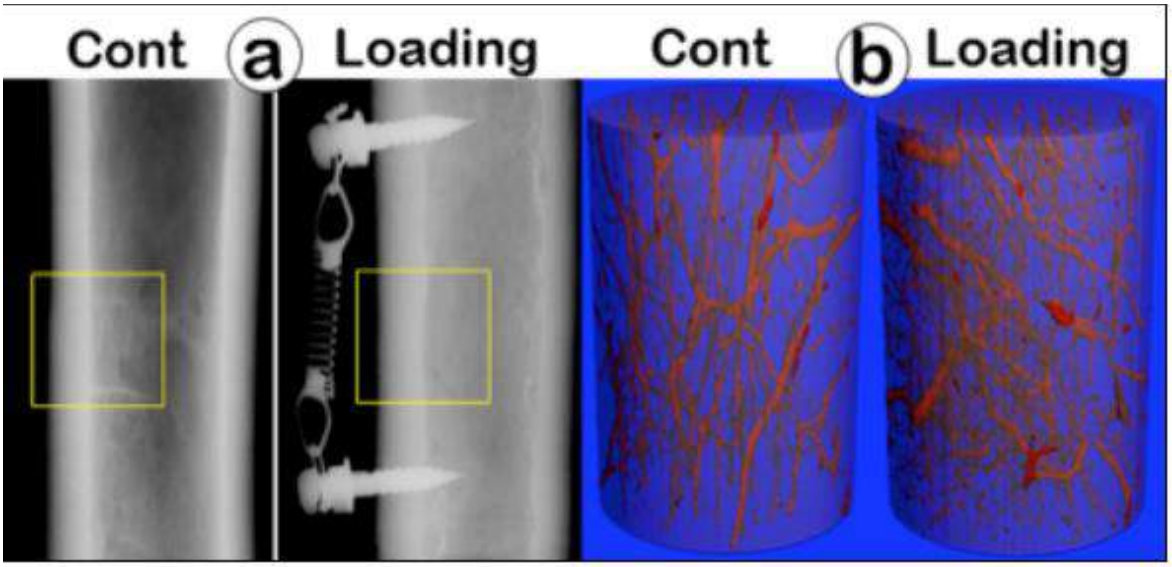

Fig 2. The loading increases the bone volume by radiograph (**a,** right) and Haversian canals by uCT (**b**, right)

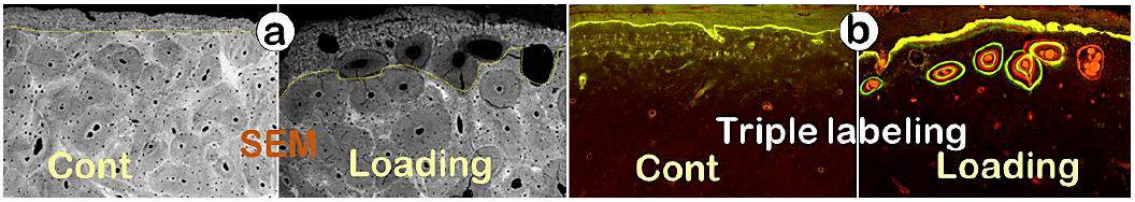

Fig 3. The loading increases the osteon formation by backscattered SEM (**a**, right) and mineralization by the triple labeling (calcein first, alizarin red second and calcein last with a 10 day gap with each injections (**b**, right).

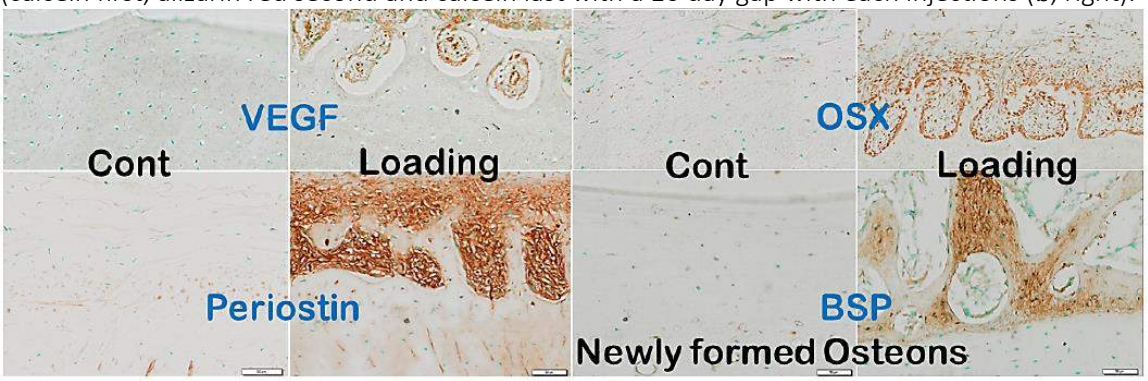

Fig 4. The loading increases expressions of markers critical for vessels and bone formation (right panels), including VEGF for endothelial cells (Upper left), osterix (OSX, an essential transcription factor for bone formation, upper right), periostin (a marker for periosteum, lower left), and BSP (a marker for bone cells, lower right).

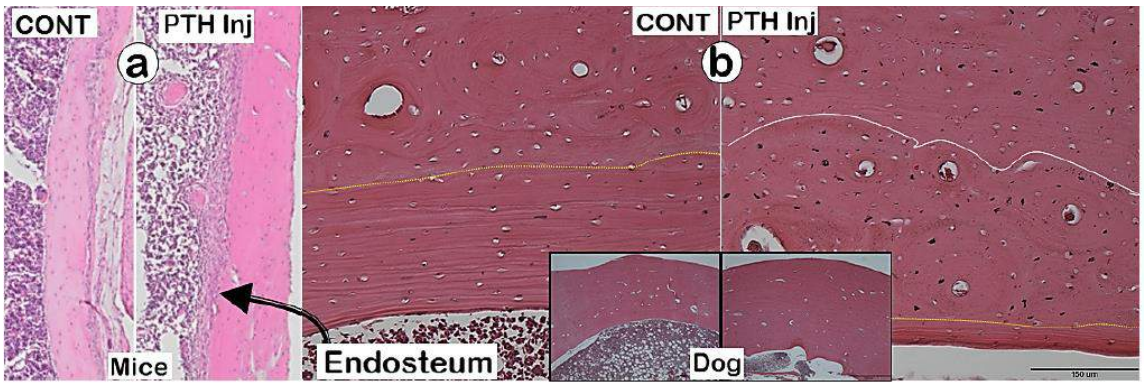

Fig 5. The intermittent PTH injections for 4-weeks result in increases in bone volumes originated from the endosteum in both mice and dogs. **a**. Injections of PTH in mice lead to increases in the endosteum layer and cortical bone (left panel); and **b**. Injections of PTH in dogs lead to increases in osteon formation, which is derived from the endosteum (right panel).

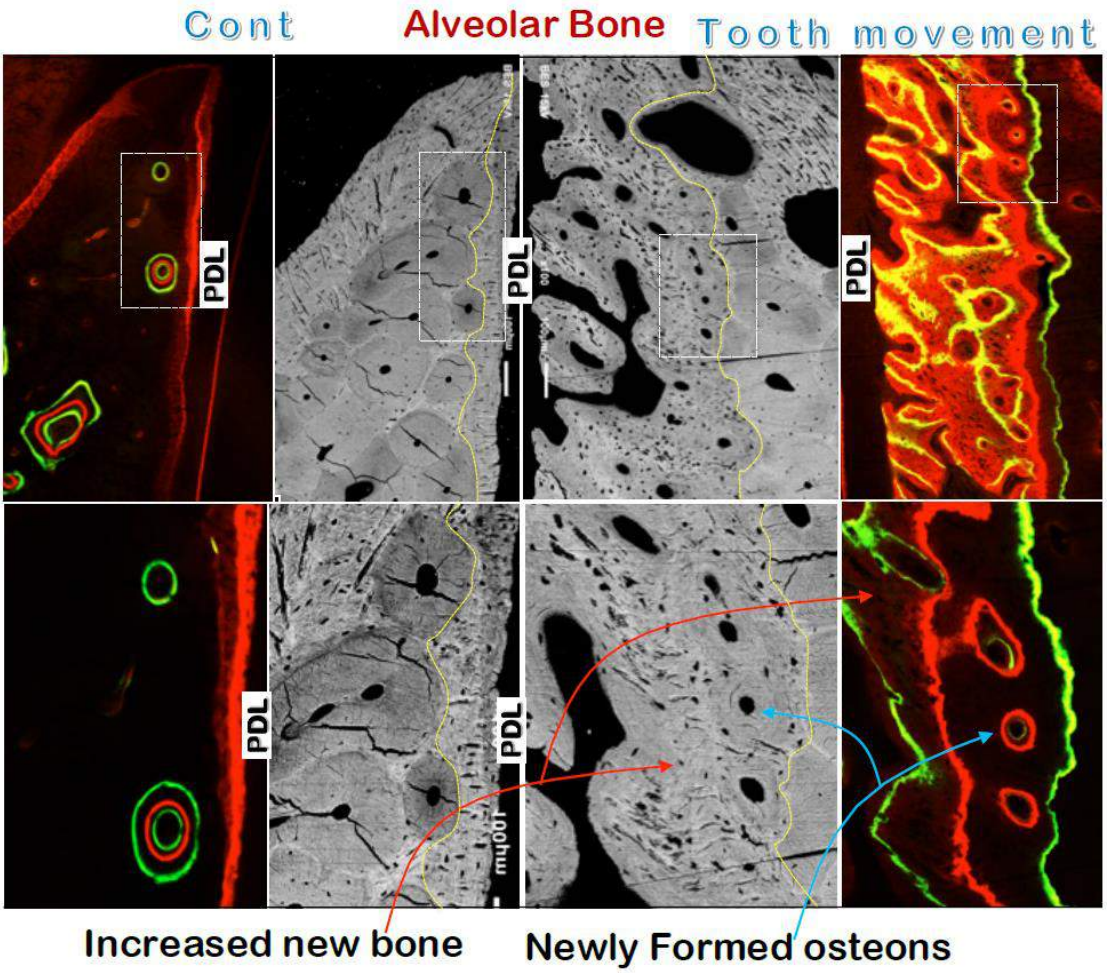

Fig 6. The tooth movement for 5-weeks results in increases in alveolar bone formation in dogs (right) as documented by the backscattered SEM techniques and the double labelling. The increased bone was originated from the periodontal ligament (PDL) layer in the movement group (right), in which there are numerous newly formed osteons in response to tooth movement.

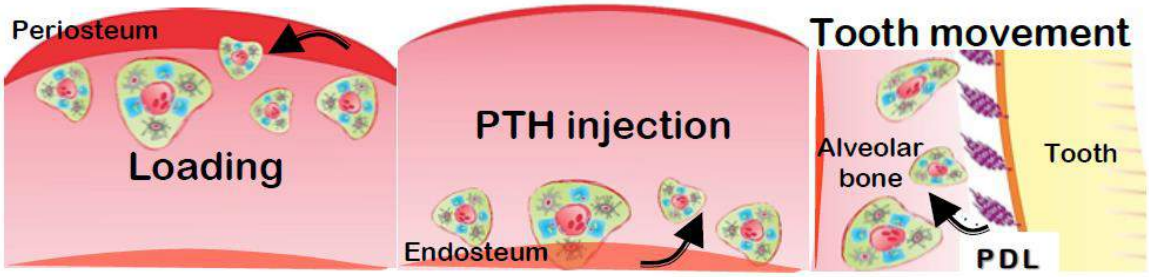

Fig 7. The three different models to show the variations in osteon formation: 1) the periosteum is responsible for osteon formation in loading (left); 2) The endosteum progenitor cells are critical for osteon formation in PTH response (middle); and 3) The PDL is responsible for osteon formation in tooth movement (right).

Underdevelopment of Trabecular Bone Microarchitecture in the Distal Tibia and Distal Femur of Ambulatory Children with Cerebral Palsy Becomes More Pronounced with Distance from the Growth Plate

Daniel G. Whitney, MS[a], Harshvardhan Singh, PhD[a], Freeman Miller, MD[b], Christopher M. Modlesky, PhD[a]
[a]Department of Kinesiology and Applied Physiology, University of Delaware, Newark, DE, USA, [b]Department of Orthopedics, AI duPont Hospital for Children, Wilmington, DE, USA.

Background: Children with cerebral palsy (CP) have impaired motor function [1, 2], an underdeveloped musculoskeletal system [3, 4] and low levels of physical activity [5] which are associated with a high incidence of low-energy fractures occurring primarily at the femur and tibia in this pediatric population [6]. Nonambulatory children with more severe forms of CP have an underdeveloped trabecular bone microarchitecture (TBM) in the distal femur, their primary fracture site [6], that becomes more pronounced with distance from the growth plate [7]. The purpose of this study was determine if ambulatory children with mild CP have an underdeveloped TBM in the distal tibia and distal femur and if the pattern of TBM becomes more pronounced with distance from the growth plate.

Methods: Twelve ambulatory children with mild CP and 12 sex-, age- and race-matched controls (5 to 12 years of age) participated in this study. Twenty-six axial magnetic resonance images (175 x 175 x 700 µm3) of the distal tibia and distal femur immediately above the growth plate were collected and measures of TBM [apparent trabecular bone volume to total volume (appBV/TV), trabecular number (appTb.N), trabecular thickness (appTb.Th) and trabecular separation (appTb.Sp)] of the medial and lateral half of the distal tibia and distal femur, respectively, were obtained **(Figure 1)**. Using SPSS, regression analyses were performed for TBM and distance from the growth plate. Independent t-tests were used to compare regions of TBM and the slopes of TBM with distance from the growth plate between groups.

Results: Compared to controls, the distal tibia and distal femur in children with CP had lower appBV/TV (20% and 12%), lower appTb.N (14% and 8%) and higher appTb.Sp (30% and 16%), respectively (all $p < 0.05$), and lower appTb.Th in the distal tibia (8%, $p = 0.016$), but not in the distal femur (5%, $p = 0.174$) **(Figure 2)**. When distance from the growth plate was regressed against measures of TBM, children with CP had steeper slopes in appBV/TV, appTb.N, appTb.Th and appTb.Sp in the distal tibia and appTb.N and appTb.Sp in the distal femur (all $p < 0.05$) **(Figure 3).**

Discussion: Ambulatory children with mild CP present with an underdevelopment in TBM in the distal tibia and distal femur, their most commonly fractured bones [6], which becomes more pronounced with distance from the growth plate. Treatments that offset this compromised bone pattern are needed.

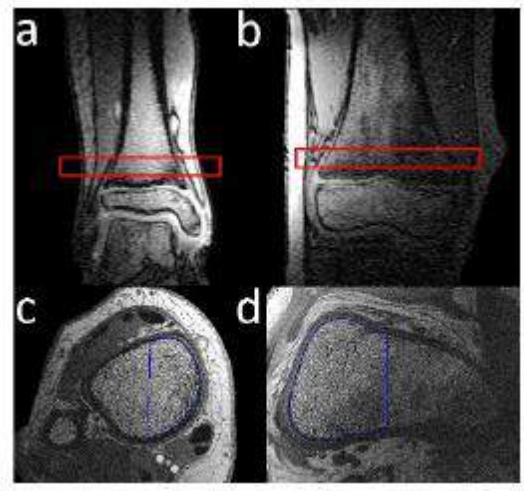

Figure 1. Regions of interest (red box) were identified using coronal magnetic resonance images of the distal tibia (a) and distal femur (b). Trabecular bone microarchitecture was analyzed using consecutive axial images of the medial half of the distal tibia (c) and the lateral half of the distal femur (d) (blue line).

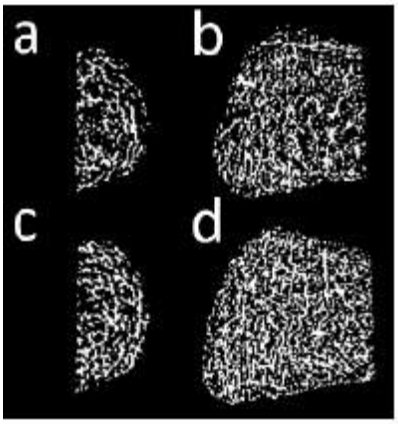

Figure 2. Representative binarized images (white is trabecular bone) from a set of twin girls (aged 5.6 yrs) show the underdevelopment of the medial half of the distal tibia (a, c) and lateral half of the distal femur (b, d) in the twin with CP (a, b) and the typically developing twin (c, d).

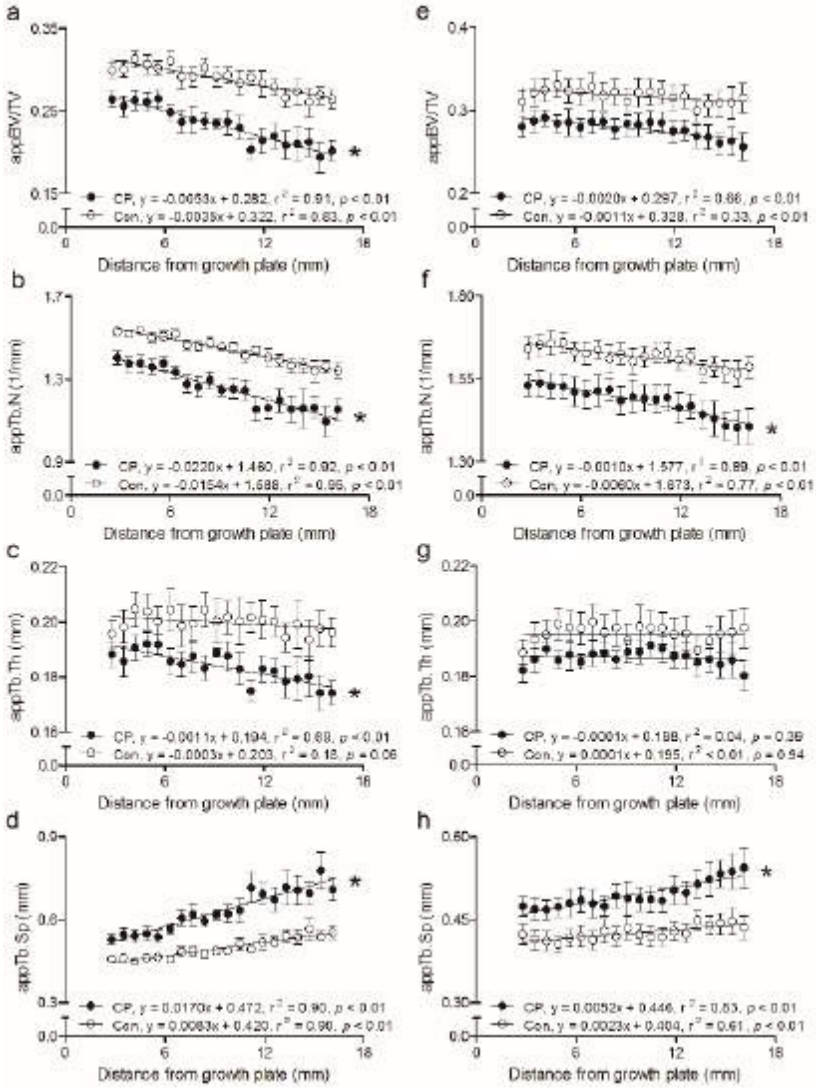

Figure 3. Scatter plots show the relationships between distance from the growth plate at the distal tibia (a–d) and distal femur (e–h) and apparent bone volume to total volume (appBV/TV) (a, e), trabecular number (appTb.N) (b, f), trabecular thickness (appTb.Th) (c, g) and trabecular separation (appTb.Sp) (d, h) in children with CP and controls. *indicates steeper slope compared to controls, $p < 0.05$.

References

[1] Stackhouse SK, Binder-Macleod SA, Lee SC. Voluntary muscle activation, contractile properties, and fatigability in children with and without cerebral palsy. Muscle & nerve 2005;31: 594-601.
[2] Moreau NG, Falvo MJ, Damiano DL. Rapid force generation is impaired in cerebral palsy and is related to decreased muscle size and functional mobility. Gait & posture 2012;35: 154-8.
[3] Johnson DL, Miller F, Subramanian P, Modlesky CM. Adipose tissue infiltration of skeletal muscle in children with cerebral palsy. The Journal of pediatrics 2009;154: 715-20.
[4] Modlesky CM, Kanoff SA, Johnson DL, Subramanian P, Miller F. Evaluation of the femoral midshaft in children with cerebral palsy using magnetic resonance imaging. Osteoporosis international : a journal established as result of cooperation between the European Foundation for Osteoporosis and the National Osteoporosis Foundation of the USA 2009;20: 609-15.
[5] Carlon SL, Taylor NF, Dodd KJ, Shields N. Differences in habitual physical activity levels of young people with cerebral palsy and their typically developing peers: a systematic review. Disability and rehabilitation 2013;35: 647-55.
[6] Presedo A, Dabney KW, Miller F. Fractures in patients with cerebral palsy. Journal of pediatric orthopedics 2007;27: 147-53.
[7] Modlesky CM, Whitney DG, Singh H, Barbe MF, Kirby JT, Miller F. Underdevelopment of trabecular bone microarchitecture in the distal femur of nonambulatory children with cerebral palsy becomes more pronounced with distance from the growth plate. Osteoporosis international : a journal established as result of cooperation between the European Foundation for Osteoporosis and the National Osteoporosis Foundation of the USA 2015;26: 505-12.

A Novel Method to Assess Articular Cartilage Hydration by Raman Spectroscopy for Early Diagnosis of Osteoarthritis

Mustafa Unal, MSc[a,b] and Ozan Akkus, PhD[a,b,c,d]
[a]Department of Mechanical and Aerospace Engineering, [b] Orthopaedic Bioengineering Laboratory, [c]Department of Biomedical Engineering, [d]Department of Orthopaedics,
Case Western Reserve University, Cleveland, OH 44106, USA

INTRODUCTION

Osteoarthritis (OA) is a debilitating musculoskeletal disease characterized by degeneration of articular cartilage and affects the lives of millions of people. Since cartilage has a limited ability naturally for self-repair, it is crucial to detect early stage of OA for the greatest possibility of successful treatment. Therefore, a great amount of effort has been focused on developing non-invasive and non-destructive method for early detection of OA. The cartilage matrix mainly contains water (65-80 wt. %), type II collagen (15-20 wt. %), and proteoglycan (PG) (3-10 wt. %) [1]. A major fraction of water in cartilage exists in the unbound state (also referred as mobile or mobile-like) as a result of electrostatic equilibrium between water molecules and glycosaminoglycan (GAG) chain(s). The rest of water is bound to collagen and PG phases of cartilage with various degrees of affinity, ranging from loosely to tightly bound states. Early stage of OA is characterized by a damaged collagen network, loss of proteoglycan and an increase in water content up to 10% [2]. It is generally thought that the water increase in the cartilage is associated with damaged collagen network that leads to decreased PG content which in turn finally increases in water content of the cartilage. Although measurement of water content in the cartilage holds the great potential for early detection of OA, there is a dearth of nondestructive methods for studying hydration status of cartilage. MRI-based methods are the few available non-destructive methods for analyzing water content in cartilage; however, the sensitivity of MRI analyses to detect small changes in cartilage matrix and water content in early stages of OA is limited due to the partial-volume averaging effects [3]. Thus, a broader range of methods is needed to infer the hydration status in cartilage. Raman spectroscopy is one of the few nondestructive methods to assess hydration status of cartilage with the unique advantages on determination of type of water with various energy levels and the moiety to which water molecules are bound to. However, to date, OH-related Raman bands of cartilage have not been studied by Raman spectroscopy since the most commercial Raman spectroscopy systems lack sensitivity into the OH-stretch range (3100-3800 cm-1). Recently, we developed a custom designed short-wave infrared (SWIR) Raman spectroscopy system to investigate the water fractions of musculoskeletal tissues with the moiety to which water molecules are attached to [4, 5]. The aim of this study was to identify novel Raman spectroscopic biomarkers which may help infer the hydration status of cartilage as early detection of OA. Towards that end, the first aim of this study was, for the first time in the literature, to characterize Raman OH-stretch band of cartilage to identify water fractions in cartilage. The second aim of this research was to assess age-related cartilage degeneration by the novel spectroscopic biomarkers identified in the first aim as a first step developing new non-destructive method for early diagnosis of OA.

METHODS

SWIR Raman Spectroscopy: A refined analysis of the water content in biological tissues is challenging with standard Raman systems because of protein related background fluorescence. Furthermore, the CCDs of most commercial Raman systems lack sensitivity in the OH-stretch range since the Raman scattered photons of the OH range shift deeper into the infrared region.

Therefore, we built a custom short-wave infrared (SWIR) Raman system to survey the OH-stretch range while accommodating the background fluorescence. The custom SWIR system involved excitation at 847 nm (Axcel Photonics) at ~40 mW on the sample and signal collection using a shortwave InGaAs IR spectrometer (BaySpec, Inc., CA, USA) optimized for 1000-1400 nm wavenumber range that is suited for OH-stretch vibrations. The collected spectra were fitted through second derivative method to identify peak locations. Raman spectra were collected in the range of 2700-4000 cm-1 to track the OH-band during dehydration. Spectra of pure collagen type II and chondroitin sulfate were also collected as standards to identify collagen and proteoglycan contributions to the OH-stretch band. Bulk water spectra were recorded as another reference.

Samples: Bovine articular cartilage plugs (diameter: 4 mm, N=6) was excised from bovine knee joints of freshly slaughtered animals. Human articular cartilage samples were prepared from two age groups: young (mean donor age: 29, 21-31 years old) and old (mean donor age: 64, 62-65 years old) (diameter: 4 mm, N=9 per group)

Serial dehydration protocol: Since Raman OH stretch band originates from the hydroxyl groups of proteins, water molecules (bound, loosely bound and unbound) and contribution from the NH stretch of proteins, a sample treatment protocol was developed so as to probe the contributions of different sources to the bands of interest. Water

compartments were interrogated by a sequential dehydration process: 1) drying in ambient conditions for 60 min, 2) oven drying at 40° C for 48 h, 3) hydrogen-deuterium exchange up to 7 days. Raman spectra were recorded immediately after each treatment. The low energy air- and oven-drying employed in this study is expected to remove the unbound water and have minimal effect on the tightly bound water compartment. The long term hydrogendeuterium oxide (H_2O/D_2O) exchange beyond oven drying provides information on the rate of dissociation of different moieties of bound water through observation of the disappearance of OH-related Raman peaks. The remaining part after H/D exchange is expected to be associated with organic matrix.

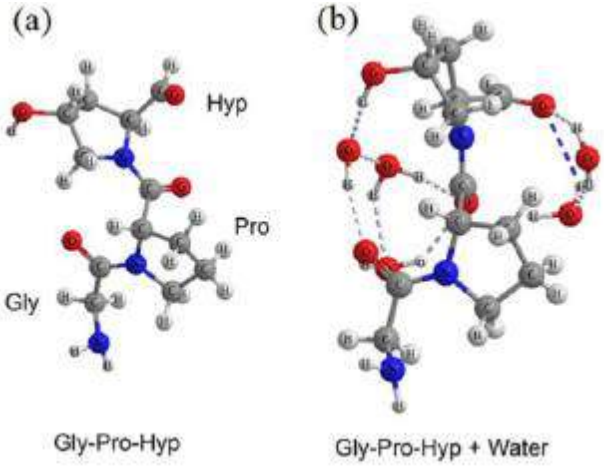

Figure 1: The optimized equilibrium structure of molecular models of (a) Gly-Pro-Hyp amino acid sequence and (b Gly-Pro - Hyp amino acid sequence of collagen with five water molecules.

Computational Prediction of Band Locations:
Raman bands pertaining to glycine-prolinehydroxyproline (Gly-Pro-Hyp) amino acid sequence of collagen were generated computationally via ChemBio 3D Ultra software (Fig. 1a). Simulations were run with and without the surrounding water molecules to further verify the assignment of the experimentally observed Raman bands (Fig. 1b). Overall, the sequential water removal protocol and computational analysis allowed the interpretation of the locations of Raman bands associated with unbound, loosely bound and tightly bound water as well as organic matrix.
Statistical Analysis: Spectroscopic biomarkers of the groups were compared using one-way ANOVA followed by Tukey's post-hoc test.

RESULTS AND DISCUSSION

Raman OH-stretch Band Assignments: The presented spectral data resulted from the average of three Raman spectra taken at different locations. The spectral range of 2700-3100 cm-1 manifest CH-stretch that is predominantly associated with the organic matrix phase of cartilage whereas the OH-stretch extends across 3100-3800 cm-1. The cartilage spectra are scaled to obtain the same intensity at the CH-stretch peak (Fig. 2a). Therefore, changes in the Raman intensities of the OH band are normalized by the amount of total organic matrix. Direct comparison of Raman spectra of bulk water with wet and oven-dried cartilage samples showed the prominence of unbound (mobile-like) water related peaks in cartilage which accounted ~90% of the Raman signal (Fig. 2a). Our H/D exchange results demonstrated that the remaining Raman signal was associated with bound water compartments and organic matrix (~10%) (Fig.2c).

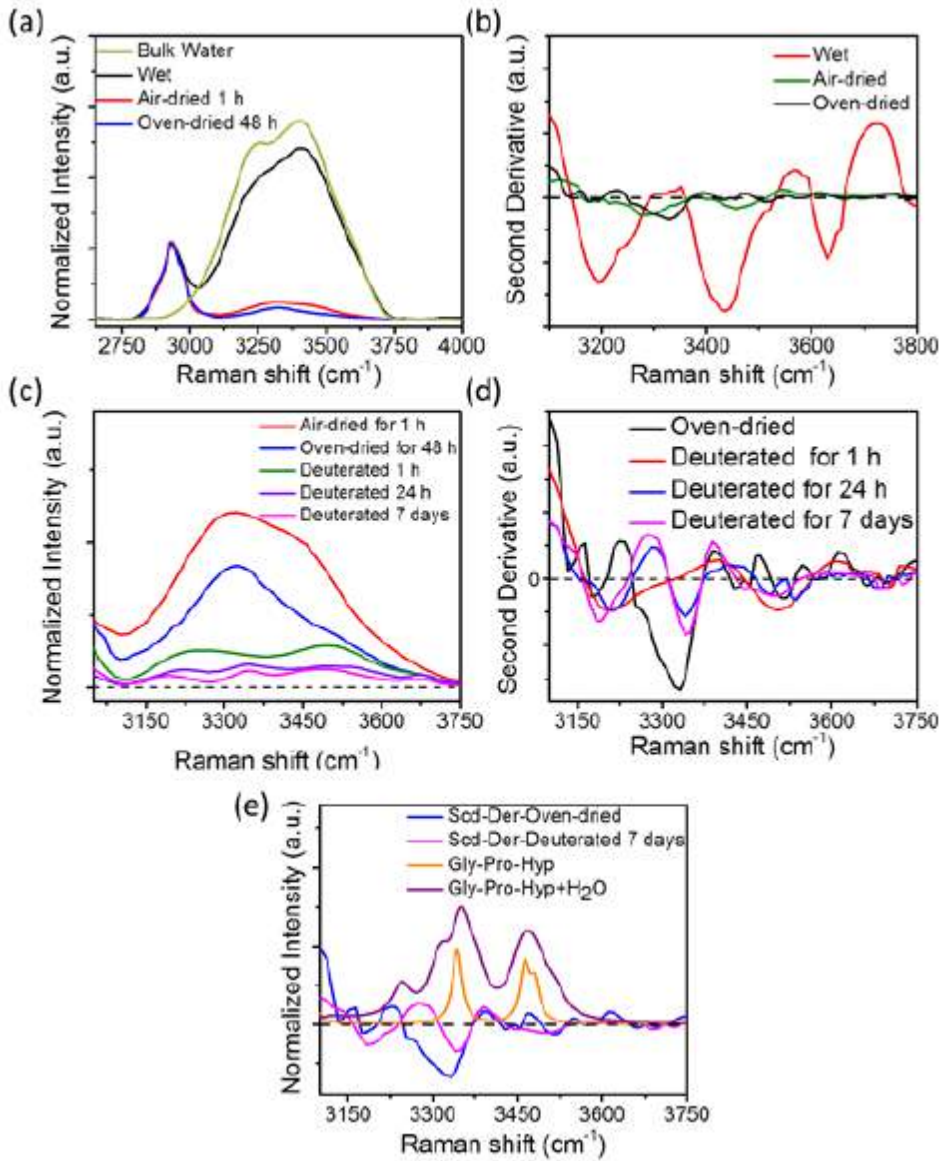

Figure 2: (a) Raman bands of wet and dehydrated samples, (b) second derivative spectra during sequential dehydration, (c) Raman bands of deuterated samples, (d) second derivative spectra as water exchanges with deuterium oxide over time, (e) comparison of computationally obtained Raman spectra with second derivative spectra of oven and deuterated samples.

Using secondary derivative and computational analyses, totally six peaks and shoulders in OH-stretch band of wet cartilage were revealed including ~3200, ~3250, ~3450, ~3520, ~3630 and ~3650 cm-1 (Fig. 2b) Direct comparison of second derivative Raman spectra of wet cartilage with oven-dried and progressively deuterated cartilage samples showed that the locations of these peaks and shoulders underwent a shift to lower or higher frequencies (Fig. 2b and 2d). Even after 7 days of deuteration treatment, there were remnant peaks in this range (Fig. 2c and 2e), indicating that these remnant peaks are associated with OH and NH groups of collagen and PG.

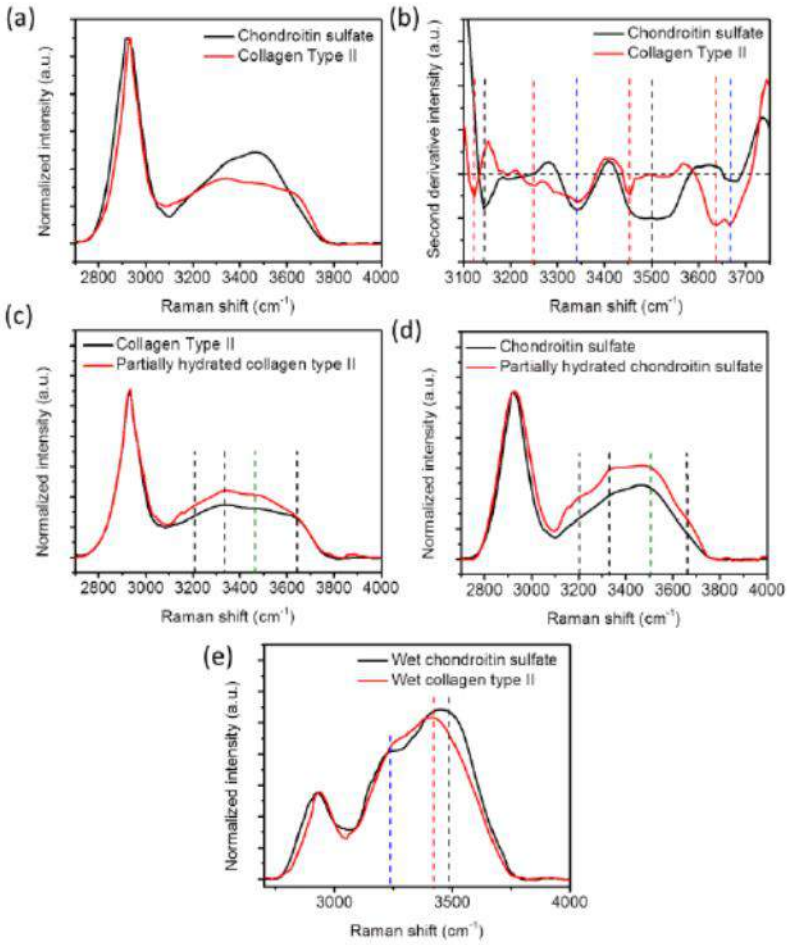

Figure 3: (a) Raman bands of collagen type II and chondroitin sulfate samples, (b) Second derivative spectra of collagen type II and chondroitin sulfate samples, (c) Raman bands of partially hydrated collagen type II, (d) Raman bands of partially hydrated chondroitin sulfate, (e) comparison of Raman spectrum of wet collagen type II with the spectrum of chondroitin sulfate.

Raman spectra of pure collagen type II and chondroitin sulfate as well as theoretically calculated spectra shed light on the identities of these remaining peaks (Fig.3a and Fig. 2e). Comparison of second derivative Raman spectra of pure collagen type II with chondroitin sulfate revealed that the peaks at ~3120 ~3250, ~3450 and ~3640 were characteristic peaks for collagen type II
(Fig. 3b), also confirmed by theoretically calculated spectra (Fig. 2e) whereas the peaks at ~3150 and a broad peak centered at ~3500 cm^{-1} were characteristic peaks for chondroitin sulfate (Fig. 3b). Furthermore, the peaks at ~3340 and ~3660 were observed in both spectra (Fig. 3b). With the help of theoretically calculated spectra, the peak at ~3340 cm^{-1} was assigned to NH-stretch band of collagen and P, and the peak at ~3450 cm^{-1} was assigned to OH group of hydroxyproline (Fig. 2e). When the collagen type II and chondroitin sulfate were gradually hydrated (Fig. 3c and 3d), several water-related peaks also emerged at the same peak locations in the Raman spectra of collagen type II and chondroitin sulfate, indicating the locations of collagen-bound water and PG-bound water.

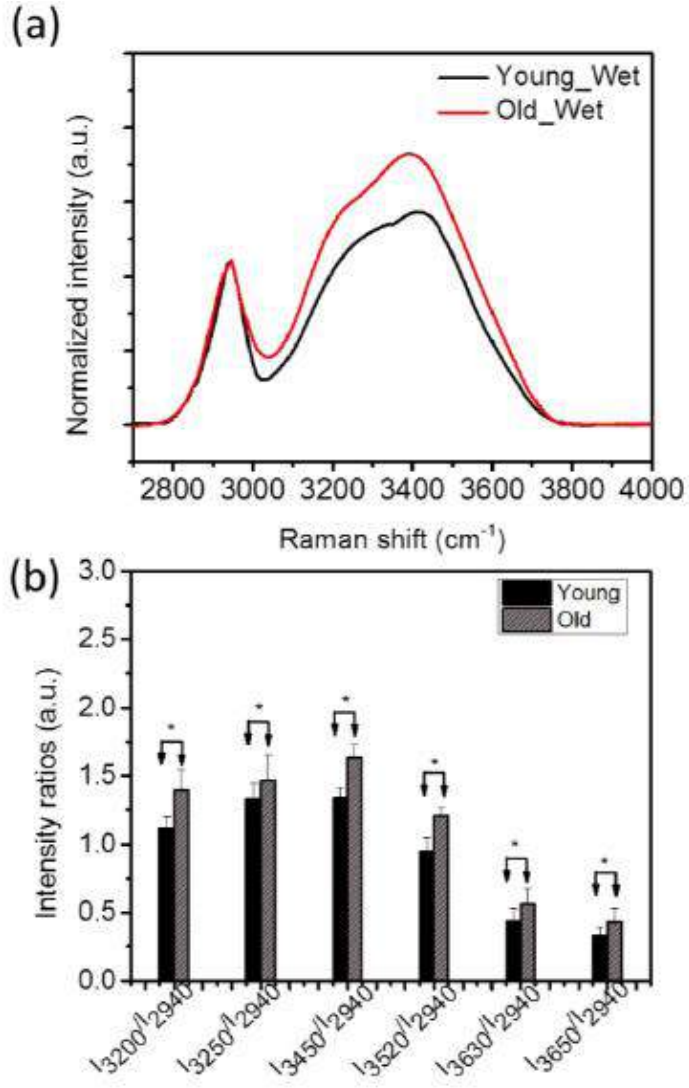

Figure 4: (a) Comparison of average Raman spectra of young cartilage samples with the average Raman spectra of old cartilage samples, (b) there are statistically significant differences between young and old cartilage sample in terms of their amount of various water compartments as shown by novel spectroscopic biomarkers identified in the first aim. *p<0.05.

Therefore, collagen-bound water peaks were located at ~3250, ~3340, ~3450 and ~3650 cm^{-1} (Fig. 3c), theoretically calculated Raman spectra further support this conclusion (Fig. 2e) such that peaks emerged at the same region after the addition of water molecules to the amino acid sequence model. On the other hands, PG-bound water peaks were located at ~3200, ~3340, ~3520 and ~3660 cm^{-1} (Fig. 3d). Another important finding of this study was that Raman peak profiles of fully hydrated collagen type II and chondroitin sulfate were different (Fig. 3e) such that for collagen type II, there was a characteristic peak centered at ~3450 cm^{-1} whereas for chondroitin sulfate, there was a characteristic peak centered at ~3500 cm^{-1} although the peak at ~3250 cm^{-1} appeared in same location at both spectra (Fig. 3e), indicating any shift at the peak in this region between ~3450 and ~3520 cm^{-1} in intake cartilage may be associated with the changes in relative amount of collagen and PG-bound water fractions. In conclusion, the peak centered at ~ 3200 with the shoulder of ~3250 cm^{-1} in intake cartilage samples seem to be the combination of unbound, collagen and PG-bound water of compartments with the contribution of solid collagen and PG matrix. The peak at 3450 cm^{-1} is associated with OH group of hydroxyproline, collagen-bound water and unbound water. The shoulder at 3520 cm^{-1} is associated with OH group of PG, PG-bound water and unbound water. The peaks at 3630 and 3650 cm^{-1} are the combination of unbound, collagen-bound and PG-bound water compartments with the contribution of solid phases of collagen and PG matrix.

Age-related hydration changes in articular cartilage:

The presented spectral data resulted from the average of 27 Raman spectra taken at different locations from two age groups (Fig. 4a). The results showed that the water amount per organic matrix significantly increased in old cartilage samples compared to young cartilage samples (Fig. 4a) as shown by increase in the intensities of the peaks identified in

the first aim of this study (Fig. 4b). Also, the Raman spectral profiles at the region between ~3400 and ~3550 indicated that the centered peak of young cartilage samples at this region may be dominated by PG-bound water whereas the centered peak at this region for old cartilage samples may be dominated by collagen-bound water (Fig. 4a), indicating age-related distinguish in hydration behavior of articular cartilage sample.

In conclusion, for the first time in the literature, OH-stretch band in cartilage was investigated to identify the water compartments which are mobile-like and loosely-bound (removable by prolonged drying at low-temperature), and semi-bound and tightly bound (removable by deuterium following prolonged drying) to the matrix of cartilage. We successfully identified six Raman peaks in the water region of cartilage spectrum. These peaks revealed that Raman spectroscopy is sensitive to changes in the amount of different water compartments (namely: free, collagen-bound and proteoglycan-bound water) in cartilage (Fig.1c and d) and we further showed that Raman spectroscopy is sensitive to distinguish age-related changes in hydration status of cartilage. Our overall results suggest that, in near future, Raman-based water measurement can potentially provide an assessment for early detection of OA *in vivo* as the recent advances in spatially offset Raman spectroscopy (SORS) [6] and Raman tomography [7].

REFERENCES

[1] N. P. Cohen, R. J. Foster, and V. C. Mow, "Composition and dynamics of articular cartilage: structure, function, and maintaining healthy state," *Journal of Orthopaedic & Sports Physical Therapy,* vol. 28, pp. 203-215, 1998.

[2] H. J. Mankin and A. Thrasher, "Water content and binding in normal and osteoarthritic human cartilage," *J Bone Joint Surg Am,* vol. 57, pp. 76-80, 1975.

[3] G. Blumenkrantz and S. Majumdar, "Quantitative magnetic resonance imaging of articular cartilage in osteoarthritis," *Eur Cell Mater,* vol. 13, 2007.

[4] M. Unal, S. Yang, and O. Akkus, "Molecular spectroscopic identification of the water compartments in bone," *Bone,* vol. 67, pp. 228-236, 2014.

[5] M. Unal and O. Akkus, "Raman spectral classification of mineral- and collagen-bound water's associations to elastic and post-yield mechanical properties of cortical bone," *Bone,* vol. 81, pp. 315-326, 2015.

[6] P. Matousek, E. R. Draper, A. E. Goodship, I. P. Clark, K. L. Ronayne, and A. W. Parker, "Noninvasive Raman spectroscopy of human tissue in vivo," *Applied spectroscopy,* vol. 60, pp. 758-763, 2006.

[7] J.-L. H. Demers, S. C. Davis, B. W. Pogue, and M. D. Morris, "Multichannel diffuse optical Raman tomography for bone characterization in vivo: a phantom study," *Biomedical optics express,* vol. 3, pp. 2299-2305, 2012.

Osteoclast-selective Expression of Lrp5 HBM-causing Mutations Alters Bone Metabolism

Kyung Shin Kang, PhD[1], Daniel J. Horan, MS[1,3], and Alexander G. Robling, PhD[1,2,3]*
[1]Department of Anatomy & Cell Biology, Indiana University School of Medicine, Indianapolis, IN
[2]Department of Biomedical Engineering, Indiana University–Purdue University at Indianapolis, Indianapolis, IN
[3]Richard L. Roudebush VA Medical Center, Indianapolis, IN

The low density lipoprotein receptor-related protein-5 (LRP5), a co-receptor in the Wnt signaling pathway, is a key protein involved in for the regulation of bone mass [1]. Mice with high bone mass (HBM)-causing point mutations in Lrp5 (Lrp5 HBM knock-in) are resistant to endogenous inhibitors such as sclerostin (Sost) and Dickkopf homolog-1 (Dkk1) [2-5]. Additionally, these mutations enhance responsiveness to mechanical loading and protect the skeleton from the bone wasting effects of mechanical disuse [6, 7]. Much of the HBM phenotype in Lrp5 HBM knockin mice has been ascribed to altered anabolic signaling in the osteoblast/osteocyte, and secondarily, to the inhibition of pro-catabolic signals that affect the osteoclast. Beyond indirect effects on the osteoclast, recent reports indicate that osteoclasts are directly responsive to Wnt stimulation [8, 9]. The most thoroughly characterized mechanism for direct osteoclast stimulation by Wnt is the Wnt5a-Ror2 pathway, which activates one of the noncanonical arms of intracellular Wnt signaling [9]. However, osteoclasts also express the molecular machinery to transduce canonical Wnt signaling (e.g., nuclear b-catenin, Gsk3b) [10]. We sought to understand whether expression of Lrp5 gain-of-function mutations (G171V, A214V) in osteoclasts would alter osteoclastogenesis and bone homeostasis in vivo.

We harvested primary bone marrow macrophages (BMMs) from the femur and tibia marrow of 6 wk-old WT mice, Lrp5 G171V knockin mice (Lrp5G/G) mice, Lrp5 A214V knockin mice (Lrp5A/A) mice, and mice harboring one of each knockin allele (Lrp5G/A). BMMs (adherent population on petri dish plastic) were plated, cultured for several days in MCSF, then replated and cultured in MCSF plus RANKL. The cultures were assayed for Trap-positive mononuclear cells per well. We repeated the experiment 5 times, with each experiment spaced several weeks apart. In 4 of the 5 experiments, BMMs from the HBM mice exhibited a 90-95% reduction ($p<0.01$) in Trap+ cells (Figure 1). Having found a significant effect of the Lrp5 HBM receptor in osteoclast-enriched cultures, we next selectively induced the HBM knockin mutation in osteoclasts *in vivo*, by recombining floxed Neo-containing (which interferes with transcription) versions of the HBM alleles (Lrp5+/Gneo and Lrp5+/Aneo) using Ctsk-Cre.

Both mutations produced significantly increased wholebody bone mineral content (BMC; 13% in female +/A, 7% in female +/G, 14% in male +/A, 15% in male +/G) and bone mineral density (BMD; 7% in female +/A, 5% in female +/G, 9% in male +/A, 12% in male +/G) in Ctsk-Cre positive (TG) compared to Ctsk-Cre negative (NTG) littermates. Trabecular BV/TV (70-80% in +/A, 31-39% in +/G), cortical thickness (11-15% in +/A, 10-16% in +/G), area (14% in females, 25% in males) were significantly increased in TG mice (compared to NTG littermates). Endocortical bone formation was higher in TG mice than in NTG littermates by at least 22%. We found that CTX levels were lower in both female +A (13%) and +/G (11%) TG roups (compared to NTG littermates), while these values were not significantly different in male TG mice.

In conclusion, heterozygous Lrp5 HBM mutations expressed in osteoclasts result in enhanced bone mass, suggesting that Wnt/Lrp5 signaling in osteoclasts might alter osteoclastogenesis and activity.

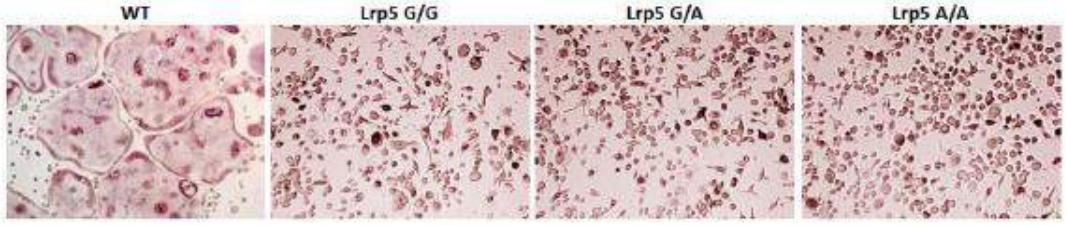

Figure 1: Trap-stained osteoclast cultures derived from WT and HBM mice show dramatically reduced osteoclastogenesis when the HBM mutations are present.

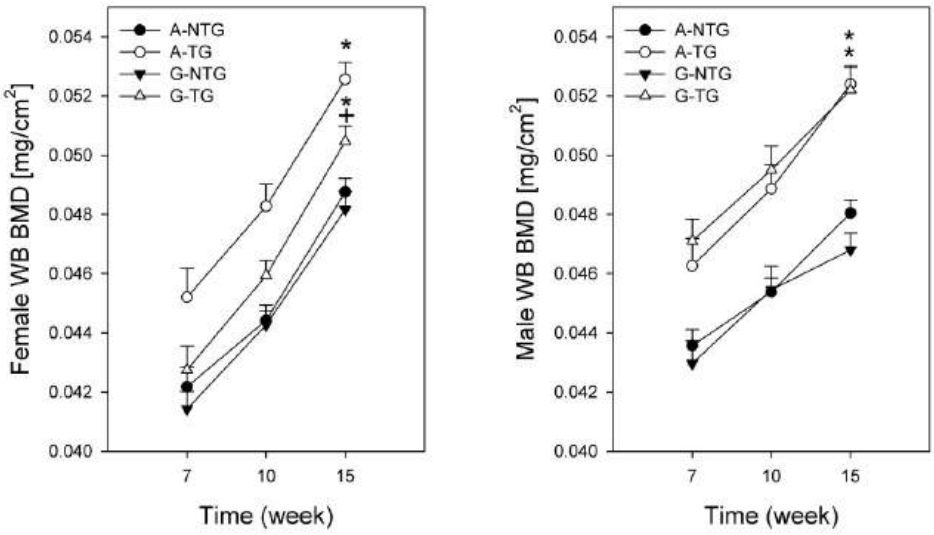

Figure 2. Bone mineral density (BMD) was obtained from DEXA at week 7, 10, 15 using an ROI that encompassed the whole body. * p<0.05 compared to the identical Lrp5 mutation NTG group, + p<0.05 compared to +/A TG group.

References

1. Kang, K.S. and A.G. Robling, *New Insights into Wnt-Lrp5/6-beta-Catenin Signaling in Mechanotransduction.* Frontiers in endocrinology, 2014. 5: p. 246.
2. Boyden, L.M., et al., *High bone density due to a mutation in LDL-receptor-related protein 5.* The New England journal of medicine, 2002. 346(20): p. 1513-21.
3. Bhat, B.M., et al., *Structure-based mutation analysis shows the importance of LRP5 betapropeller 1 in modulating Dkk1-mediated inhibition of Wnt signaling.* Gene, 2007. 391(1-2): p. 103-12.
4. Ai, M., et al., *Reduced affinity to and inhibition by DKK1 form a common mechanism by which high bone mass-associated missense mutations in LRP5 affect canonical Wnt signaling.* Molecular and cellular biology, 2005. 25(12): p. 4946-55.
5. Semenov, M.V. and X. He, *LRP5 mutations linked to high bone mass diseases cause reduced LRP5 binding and inhibition by SOST.* The Journal of biological chemistry, 2006. 281(50): p. 38276-84.
6. Niziolek, P.J., et al., *Missense Mutations in LRP5 Associated with High Bone Mass Protect the Mouse Skeleton from Disuse- and Ovariectomy-Induced Osteopenia.* PloS one, 2015. 10(11): p. e0140775.
7. Saxon, L.K., et al., *Analysis of multiple bone responses to graded strains above functional levels, and to disuse, in mice in vivo show that the human Lrp5 G171V High Bone Mass mutation increases the osteogenic response to loading but that lack of Lrp5 activity reduces it.* Bone, 2011. 49(2): p. 184-93.
8. Weivoda, M.M., et al., *Wnt Signaling Inhibits Osteoclast Differentiation by Activating Canonical and Noncanonical cAMP/PKA Pathways.* Journal of bone and mineral research : the official journal of the American Society for Bone and Mineral Research, 2016. 31(1): p. 65-75.
9. Yang, T., et al., *Wnt5a/Ror2 mediates temporomandibular joint subchondral bone remodeling.* Journal of dental research, 2015. 94(6): p. 803-12.
10. Haxaire, C., E. Hay, and V. Geoffroy, *Runx2 Controls Bone Resorption through the Downregulation of the Wnt Pathway in Osteoblasts.* The American journal of pathology, 2016.

Osteoclasts are Deficient in the Expression of Osteogenic Coupling Factors Following Ischemic Osteonecrosis of the Femoral Head

Naga Suresh Adapala, PhD[1, 2], Ryosuke Yamaguchi, MD, PhD[1, 2], Hicham Drissi, PhD[3], Harry K.W. Kim, MD, MS[1, 2]*

[1]*Center for Excellence in Hip Disorders, Texas Scottish Rite Hospital for Children, Dallas, TX 75219,* [2]*Department of Orthopedic Surgery, University of Texas Southwestern Medical Center, Dallas, TX 75390-8883,* [3]*Orthopedic Surgery, University of Connecticut Health Center, Farmington, CT, 06034*

Purpose: Legg-Calvé-Perthes disease is a childhood ischemic osteonecrosis of the femoral head (ONFH) that leads to bone loss and femoral head deformity. The mechanisms of decreased bone formation following ONFH are unknown. During normal bone remodeling, osteoclasts (OC) produce osteogenic coupling factors that can support osteoblast (OB) formation. Following ONFH, excessive bone resorption is uncoupled from OB formation. We hypothesized that OCs in ONFH are deficient in the expression of coupling factors, and in supporting OB formation. The purpose of this study was to determine (1) in vivo gene expression of coupling factors in OCs following ONFH (2) effect of NBF (necrotic bone fluid, saline flush of necrotic femoral head) on coupling factor expression (3) effect of NBF-primed OCs on OB differentiation.

Methods: ONFH was induced in right femoral heads of 6-wk old piglets (n=12) by femoral neck ligation; the left femoral head served as normal control. At 8-wks after surgery, numbers of OCs and OBs were quantified by Bioquant analysis. OCs were captured from frozen sections by laser capture microdissection (LCM), and the gene expression was analyzed by qRTPCR. In vitro, OCs were treated with NBF for 6h prior to RNA isolation. For OC-conditioned medium, OCs on pig dentine discs were primed with NBF for 12h, then cultured for 48h in fresh OC medium. The OB differentiation was assessed by *osterix* and *RUNX2* mRNA levels, alkaline phosphatase (ALP) and alizarin red staining. NBF was analyzed by ELISA and western blotting.

Results: Bioquant analysis revealed a significant increase in OC numbers in ONFH compared to normal (>4-fold,$P<0.01$) but OB numbers were significantly decreased (38-fold,$P<0.0001$). qRTPCR analysis of OCs obtained by LCM showed that, among the coupling factors tested, the gene expression of *CTHRc1, Wnt10b* and *BMP6* was significantly lower ($P<0.0001$ for each) in ONFH compared to normal. In vitro, treatment of OCs cultured on pig dentine with NBF inhibited *CTHRc1, Wnt10b and BMP6* expression. Furthermore, conditioned medium from NBF-primed OCs inhibited OB differentiation, as evidenced by decreased *osterix* and *RUNX2* gene expression in bone marrow stromal cells, ALP and alizarin red staining. NBF contained several alarmins (damaged cell and matrix factors e.g. HMGB1) and proinflammatory cytokines (e.g. IL-6) compared to normal.

Conclusion: OCs are deficient in the expression of osteogenic coupling factors following ONFH and in supporting OB formation.

Figure 1

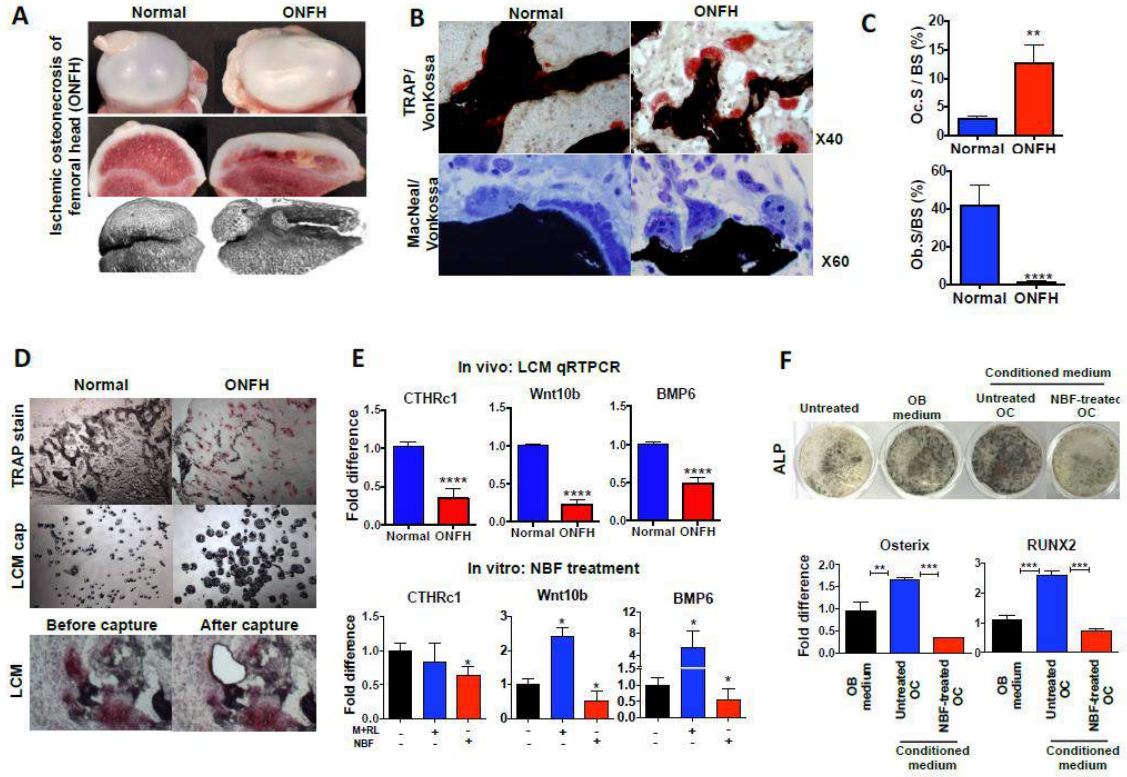

(A) Bone loss and femoral head deformity in ONFH in piglets (B and C) Increased number of osteoclasts and decreased number of osteoblasts in repair tissue (D, E top panel) Laser capture microdissection method and qRTPCR analysis (E bottom panel) In vitro effect of NBF on OC gene expression (F) Osteoclast conditioned medium from NBF-primed OCs does not support osteoblast differentiation. P value *<0.05,
<0.01, *<0.001, ****<0.0001.

Osteogenic Induction of Human Mesenchymal Stem Cells by Cold Atmospheric Argon Plasma

Adil Shahzad Ahmed, MD[1], Joseph C. Chavarria, BSc[2], Tyler J. Brenneman, BSc[2], Kurt M. Johnson, MD[2], Erik L. Antonsen, MD, PhD[2], Scott Rosenfeld, MD[2]
[1]University of South Florida – Morsani, Tampa, FL
[2]Baylor College of Medicine, Houston, TX

Introduction: Non-thermal plasmas exert broad effects on biological tissue. Induced angiogenesis, accelerated coagulation, enhanced wound healing, and selective ablation of microbes without harming eukaryotic tissue are among the reported findings. Existing work on bone tissue is minimal, but initial studies show enhanced implant osseointegration, increased osteogenic gene transcripts, and mesenchymal stem cell growth. Mesenchymal stem cell differentiation into osteoblasts is a necessary step in bone formation and healing, with significant implications for Orthopaedic Surgery. The present study employs a novel device to assess whether cold atmospheric argon plasma induces osteogenic differentiation of human mesenchymal stem cells.

Methods: Human mesenchymal stem cells were exposed to five treatment conditions: growth media, osteogenic media, non-ionized argon gas, argon plasma, and argon plasma with osteogenic media. Known markers of osteoblastic differentiation – alkaline phosphatase, osteocalcin, and RANKL – were assessed on Day 1, Day 10, and Day 28. Cellular production of DNA was measured for normalization. Plasma parameters employing a novel dielectric barrier discharge device were as follows: energy 5J, flow rate 30psig/min, distance 22mm, duration 30s.

Results: Argon plasma decreased alkaline phosphatase levels compared to other treatments, with varying levels of significance. Non-ionized argon gas significantly increased alkaline phosphatase levels ($p < 0.0014$) compared to all other groups. Osteogenic media did not result in significant differences from growth media (control). Significant changes in osteocalcin or RANKL were not observed.

Discussion: In the present study, a definitive claim regarding cold argon plasma's ability to induce osteoblastic differentiation of human mesenchymal stem cells cannot be made. Lack of addition of β-glycerophosphate on Day 14 prevented osteogenic media from responding as expected. Furthermore, non-ionized argon gas significantly increased alkaline phosphatase production by human mesenchymal stem cells. This novel finding, possibly due to phenomenon of argon shielding and/or production of shear forces, merits further study.

Multiscale Mechanics and Mechano-adaptation in Mouse Bone

Alessandra Carriero, PhD
Department of Biomedical Engineering, Florida Institute of Technology,
Melbourne FL

Composition and structure of the bone over many length-scales are responsible for its strength, toughness, and ability to adapt to mechanical loads. Aging and disease alter bone composition, disrupt its hierarchical structure and change the loads acting on it, therefore increasing bone's vulnerability to fractures and deformities. My research examines the relation between composition, structure and mechanics of mouse bone model of aging and disease with the aim to (i) develop multiscale pipelines to understand factors affecting bone mechanics and adaptation, improving reproducibility in preclinical testing, and (ii) aid in the development of new treatment for bone fragility and deformities.

Multi-scale mechanics: I developed a novel multidisciplinary approach for investigating mechanisms of fracture in murine bone. Using mouse models of osteogenesis imperfecta with genetic defects of the collagen, my research reveals how small scale molecular abnormalities ramify at larger length scales, causing whole bone fragility. Using interdisciplinary methods, I assess composition, structure, and mechanics from the molecular level to the whole-bone organ level. The use of such a multiscale study allows to detect the salient damage modes and corresponding toughening mechanisms in mouse bones. The application of this pipeline to other mouse bones, models of disease and knock-out genes, will improve our understanding of the interaction between biology and fracture, thus offering insights for more effective treatment strategies for bone frailty.

Mechano-adaptation: Bone adapts its shape and structure in response to the applied loads. My research combines clinical studies, computational modeling and animal experiments to examine how mechanical forces influence bone shape, structure, and function. Particularly, my studies on mouse bone investigate how bone mechano-adaptation is spatially coordinated in aging and disease. I developed new methods to examine 3D bone adaptation and strain mapping across the entire cortical bone surface in mouse bone. These methods will now make it possible to more precisely match strain, as well as other mechanical stimuli investigated with 3D finite element analysis, to the ensuing changes in cellular osteogenic/anti-resorptive adaptive activity between various mouse bones analyzed. Unraveling how gender, aging and disease influence bone mechanoadaptive responses will aid to develop treatment therapies focused on maintaining normal bone mass.

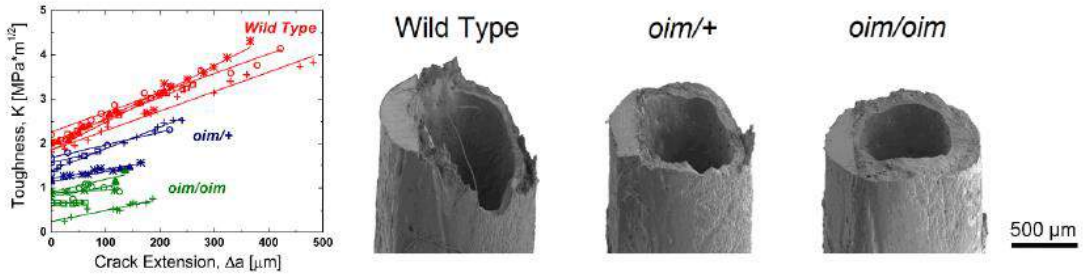

Figure 1 Right) Crack-resistance curve for WT and oim mouse bones [Carriero et al. JBMR 2014] Left) Fracture surface for WT and oim bones [Carriero et al. JBMR 2014]

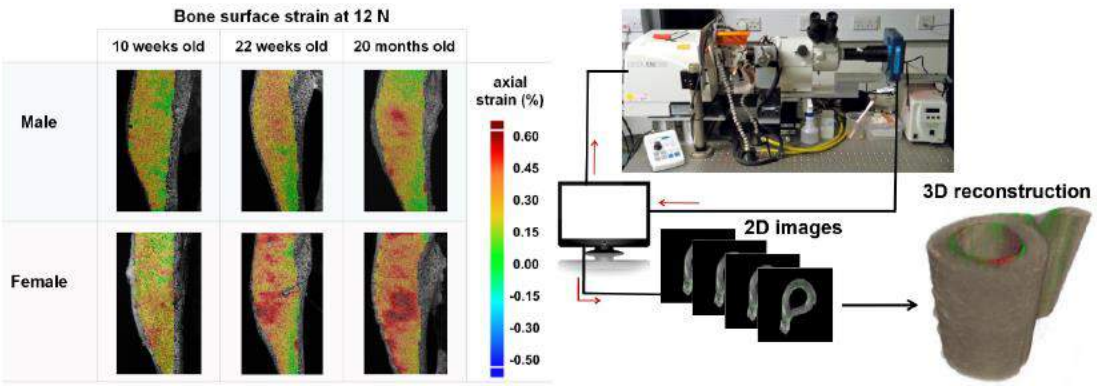

Figure 2 Right) Strain map on male and female mouse bone at 10 w.o., 22 w.o. and 20m.o. Left) Method for 3D histology of bone adptation: a microtrome and a fluorescence microscope are connected to a PC for automatic slice and view of the bone block. Images are acquired with a camera and saved on the PC. Composite images from different filters were put together in 2D first and then in 3D for the volumetric reconstruction of the bone adaptation (grey is bone, green is calcein and red is alizarin label). Resolution is 1----2 um in image 5um axial.

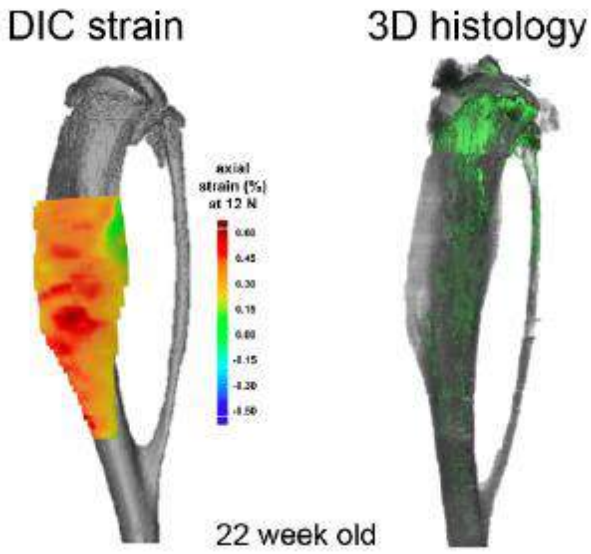

Figure 3 Axial strain map at 12 N and 3D histology reconstruction of the bone and adaptation to load (green) for a 22 w.o. mouse bone. Bone adaptation results from a loading regime of 12N for 40 cycles, 3 times a week for 2 weeks.

Lactation-Induced Changes in the Volume of the Osteocyte Lacunar-Canalicular Space Alter Local Mechanical Properties in Cortical Bone

A. Serra Kaya, BSc[1], Jelena Basta-Pljakic, MSc[1], Zeynep Seref-Ferlengez, PhD[1], Robert Majeska, PhD[1], Shoshana Yakar, PhD[2], Mitchell B. Schaffler, PhD[1]

[1]City College of New York, [2] New York University College of Dentistry

INTRODUCTION: Osteocytes can dynamically alter their surrounding bone matrix in a process known as osteocytic osteolysis, leading to increase in the volume of lacunae and canaliculi under high metabolic stress conditions such as lactation[1,2]. Moreover, these increases appear to be reversible. It is well established that cortical bone modulus is known to depend strongly and inversely on vascular porosity[3,4] and lactation does not induce intracortical remodeling in mice. Whether small changes in osteocyte pericellular space can alter the local material properties of bone is not known. In the current study, we examined how bone elastic modulus changes
at the microscopic level in response to lactation and post-lactation recovery, and assessed the contributions of changes in osteocyte lacunar-canalicular space (LCS) versus bone matrix composition in accounting for altered tissue-level mechanical properties in cortical bone with Lactation and Post-Lactation Recovery.

METHODS: *Experimental Design:* Under IACUC approval, groups of C57Bl/6 mice (3 month old, n=5/group) were mated were allowed to nurse their pups for 2 weeks. Group 1 was sacrificed immediately after 2 weeks of lactation (Lac), and the remaining mice underwent force weaning. Groups 2 and 3 mice were allowed to recover for 1 week (1W Rec) and 4 weeks (4W Rec) after forced-weaning. Litter size was fixed at 3-5 pups to normalize the lactation stress. Age-matched controls were also examined (n=5/group). Femurs were collected immediately after euthanasia; left femora were frozen at -20°C until mechanical testing and right femora were fixed in 10% formalin for tissue studies. *Mechanical Testing:* Micro-level testing allowed us to sample only matrix and LCS and avoid resorption spaces triggered by the lactation. Three transverse sections (1 mm thick) were cut from each mid-diaphysis. Sections were surface polished with graded carborundum paper and diamond paste to achieve a 0.25 µm finish. Sections were kept hydrated with Ca^{2+} supplemented PBS throughout sectioning, polishing and mechanical testing. Measurements were performed in the anterior (A) and posterior (P) quadrants of mid-diaphyses. Indents were performed using a microindenter equipped with a Vickers diamond microindenter.
Elastic modulus (Ei) values were calculated from Indentation Hardness (Hv) values measured directly from individual indent profiles[5]. *Area Measurements:* We measured LCS changes using a Structured Illumination super-resolution microscope (SIM). SIM studies were conducted on sections from the mid-diaphyseal samples stained with basic fuchsin. Sections were examined using 63x oil-immersion objective under 561 nm wavelength. All osteocytes and lacunae within anterior region were imaged with a sampling depth of 20µm (Fig 2). Single plane SIM images were analyzed using ImageJ; LCS spaces were thresholded using the Otsu's method and lacunar and canalicular areas were determined. *Compositional Measurements:* High-resolution back-scattered electron microscopy (BSE) was used to examine relative mineralization differences among control, lactation and one week recovery groups in the bone matrix between adjacent canaliculi, using coronal section of the anterior diaphysis to allow visualization of large numbers of canaliculi in cross-sectional profile (Fig 4). Enlarged images, containing 10-12 canaliculi around 8 µm away from lacuna were used for measurement. The normalized gray level profile of the bone matrix was measured radially from a canalicular edge at 80 nm increments until half the distance to an adjacent canaliculus. These data allowed us to compare mineral content distribution between canaliculi among experimental groups. Furthermore, we used a Raman microspectroscopy as complementary approach to determine mineral content and composition of the bone matrix with lactation and recovery. Raman spectra were collected using a 0.5 µm spot size. We avoided osteocyte lacunae visible on the bone surface. Spectra were sampled using a 100X magnification oil immersion objective. Raman spectra were captured from the mid-cortex of anterior quadrant of each femur cross-sections to determine: 1) mineral/matrix ratio, 2) carbonate/phosphate ratio and 3) mineral crystallinity. *Statistical Analysis:* All data are reported as mean ± sd. Differences in Ei values, lacunar and canalicular area, mineral/matrix ratio, carbonate/phosphate ratio and crystallinity index among groups were tested with a one-way ANOVA test and post hoc comparisons were performed with Fisher's least significant difference (LSD).

RESULTS: *Mechanical Testing:* Lactation caused marked reductions in bone elastic modulus (10% and 15% at posterior and anterior locations, respectively, $p<0.005$ vs age-matched control, Fig 1). With 1W Recovery, elastic modulus values returned to age-matched control levels ($p>0.6$). Furthermore, bone elastic modulus did not increase further even after four weeks (4W Recovery). Finally, there was no difference in bone elastic modulus between aged-matched nulliparous

control groups (Fig 1). *Area Measurements:* SIM studies showed an ~25% increase lacunar space with lactation compared to controls ($p<0.05$, Fig 3). Lactation also caused an increase in canalicular space (15%) but this was not significant in these studies. Moreover, lacunar and canalicular areas decreased back to control level by SIM (Fig 3). *Compositional Measurements:* Our results showed that mineralization was lowest at the canaliculus wall; it increased rapidly and exponentially over the course of 250 nm, then became asymptotic. Bone matrix mineral distribution in between adjacent canaliculi did not change with lactation compared to control (Fig 5). Moreover, the complementary Raman spectroscopy results revealed that there is no difference in mineral to matrix ratio and crystallinity between lactation, 1 week recovery and control groups ($p>0.7$). However, carbonate to phosphate ratio was decreased significantly in lactation compared to control ($p<0.05$) (Fig 6).

DISCUSSION: The current studies reveal that bone tissue-level material properties are rapidly and reversibly modulated in response to lactation and recovery. These changes occur in a manner that is independent of bone remodeling. We showed that elastic modulus of mouse femur decreases with lactation and these lactation-induced reductions in tissue modulus reverse very quickly once lactation stops. These data reveal that bone possesses an intrinsic ability for rapid dynamic regulation of its material properties. Whole bone mechanical tests from previous studies showed marked decreases in stiffness during lactation in rats compared to control bones in rat studies.[6,7] which was attributed principally to endocortical thinning. However, in the current studies we found that lactation directly decreases cortical bone tissue modulus and recovery from lactation restores bone tissue modulus. Moreover, we showed that these changes in cortical bone modulus track directly with changes in osteocyte lacunar and canalicular void space, as measured by SIM and BSE, during lactation and recovery. These are the first studies to use super-resolution microscopy (SIM) to examine osteocytes in situ. We observed similar relative changes in LCS void space with lactation and recovery to those reported previously by Qing and colleagues.1 Furthermore, our studies revealed that lactation did not alter either bone matrix mineralization or composition. Canaliculi enlarged by ~ 60 nm in diameter (15% of average 400 nm canalicular diameter), resulting from mineral loss at their walls. However, beyond that small region of loss, there was no alteration in the mineralization profile nor were there any detectable changes in mineralization or crystallinity, which are well established determinants of bone material properties[8]. The small changes observed in carbonate substitution remain unexplained at this time, but such small changes are not known to alter bone modulus[8]. These data are consistent with data reported for the canalicular network in both human and rodent bone[9,10].
Taken together, our data support the concept that the changes in tissue level mechanical properties in lactation and recovery depend on small changes in the LCS void volume. These data point to a hitherto unappreciated role for osteocytes in modulating and maintaining local bone material properties.

Significance: This is the first study to demonstrate local bone material properties are reversibly modulated in response to physiological challenge (lactation) without bone remodeling and altered microscopic mechanical properties observed in lactation and recovery can be attributed to the small changes in the LCS void volume.

Acknowledgments: Grants AR41210 and AR60445 from NIAMS.

References: [1] Qing et al, J Bone Miner Res 27(5):1018-29, 2012; [2] Wysolmerski, Bone 54:230, 2013; [3] Martin, Burr, Sharkey, Skeletal Tissue Biomechanics, 1998; [4] Cardoso et al, J Biomech 46:253-65, 2013; [5] Seref-Ferlengez et al, J Bone Miner Res 29(12):2537-44, 2014; [6] Vajda et al, Biol Reprod 65(3):689-95, 2001; [7] Liu et al, J Bone Miner Res 27(4):865-75, 2012 [8] Donnelly et al, J Biomed Mater Res A. 92(3):1048-56, 2010; [9] Hesse et al, J Bone Miner Res 30(2):346-56, 2015; [10] Nango et al, Bone 84:279-88, 2016

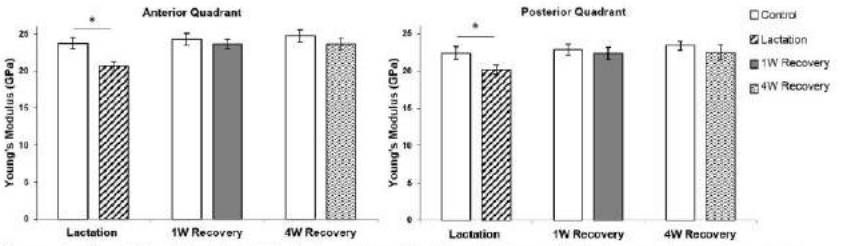

Figure 1. Microindentation Elastic Modulus values (Gpa) for Anterior and Posterior regions of mouse femur. Statistical Analysis: One-way ANOVA, LSD post-hoc *: p<0.005 vs Control

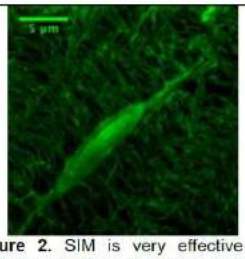

Figure 2. SIM is very effective for imaging, allowing visualization of the osteocytes, their lacunar and canalicular space

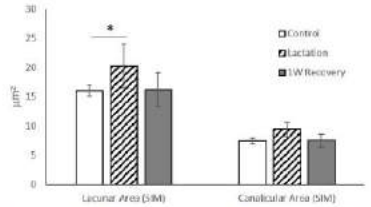

Figure 3. Super-resolution Microscopy results showing lacunar and canalicular area (μm^2) among the control, lactation and 1 week recovery groups. One-way ANOVA, LSD post-hoc *: p<0.05

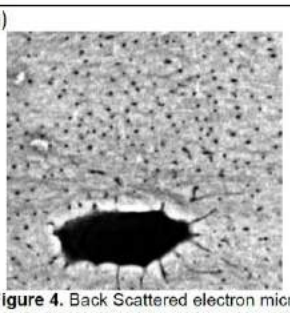

Figure 4. Back Scattered electron microscopy image of longitudinal section through a mouse femoral diaphysis. **a)** Numerous cross-sections of canaliculi are seen surrounding the single osteocyte lacuna. **b)** Cropped image showing distinct canaliculi and mean gray levels 80 nm apart from each other

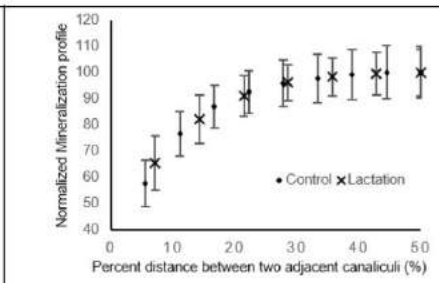

Figure 5. Back-scattered microscopy results showing normalized mineralization profile vs normalized distance from a canaliculus wall to the half way distance for control and lactation group

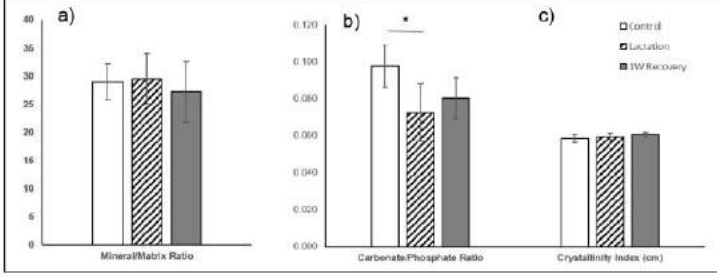

Figure 6. a) Mineral/matrix ratio, indicates the relative mineral amount b) Carbonate/Phosphate ratio, indicates carbonate substitution into phosphate in the crystal lattice c) Crystallinity Index (cm) (inverse of full width half max of phosphate band) indicates the size of the mineral crystals. One-way ANOVA, LSD post-hoc *: p<0.05

Lesser Tuberosity Osteotomy and Subscapularis Tenotomy Repair Techniques during Total Shoulder Arthroplasty: A Meta-Analysis of Cadaveric Studies

Matthew J. Kraeutler, MD, John B. Schrock, BA, Darby A. Houck, Gina G. Provenzano, BSc, Eric C. McCarty, MD, Jonathan T. Bravman, MD
University of Colorado School of Medicine, Boulder, CO

Introduction: Numerous techniques have been used to mobilize and repair the subscapularis tendon during total shoulder arthroplasty (TSA). The purpose of this study is to perform a detailed comparison of subscapularis tenotomy (Figure 1) and lesser tuberosity osteotomy (LTO) (Figure 2) repairs during TSA.

Methods: Two independent reviewers searched two databases (PubMed and the Cochrane Library) to find cadaveric studies comparing the biomechanical strength of various subscapularis repair techniques following TSA. The following search terms were used: subscapularis, subscapularis repair, arthroplasty, total shoulder, biomechanics, lesser tuberosity osteotomy, and subscapularis tenotomy. Articles that compared at least two repair techniques with similar biomechanical methods were included.

Results: An initial literature search resulted in 145 studies. A title and abstract review resulted in five studies which analyzed outcomes of subscapularis tenotomy (total n = 29) or LTO using a single- or dual-row suture technique (total n = 46). Load to failure was significantly higher in the LTO group (443 ± 231 N) than the tenotomy group (350 ± 113 N) ($p = 0.047$) (Table 1). Tenotomy (n = 19) and LTO (n = 31) had average cyclic displacements of 1.7 ± 1.3 mm and 2.1 ± 1.6 mm, respectively ($p = 0.36$). Mode of failure was significantly different between the two groups ($p < 0.0001$), with soft tissue failure accounting for most tenotomy repairs (97%) and bone failure accounting for the majority of LTO repairs (72%).

Discussion and Conclusion: Based on current biomechanical data, LTO is a stronger repair than a subscapularis tenotomy at "time-zero" in terms of load to failure. However, cyclic displacement did not differ statistically between the two techniques.

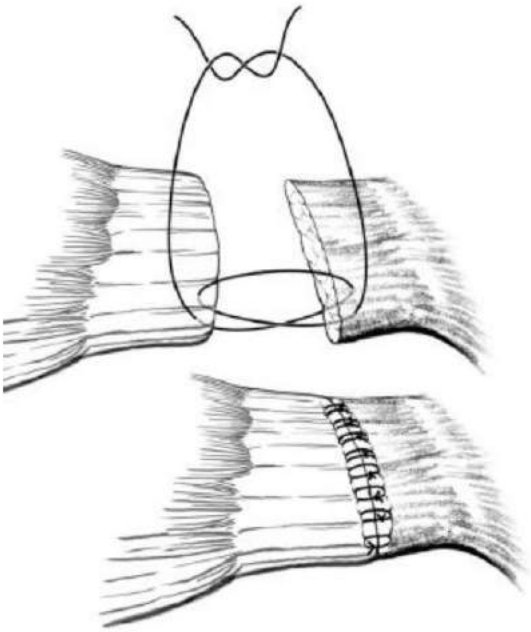

Figure 1: Subscapularis tenotomy repair technique with eight sutures placed in a figure-of-eight fashion.1 Reprinted from Giuseffi SA, Wongtriratanachai P, Omae H, Cil A, Zobitz ME, An KN, et al. Biomechanical comparison of lesser tuberosity osteotomy versus subscapularis tenotomy in total shoulder arthroplasty. J Shoulder Elbow Surg 2012;21(8):1087-1095

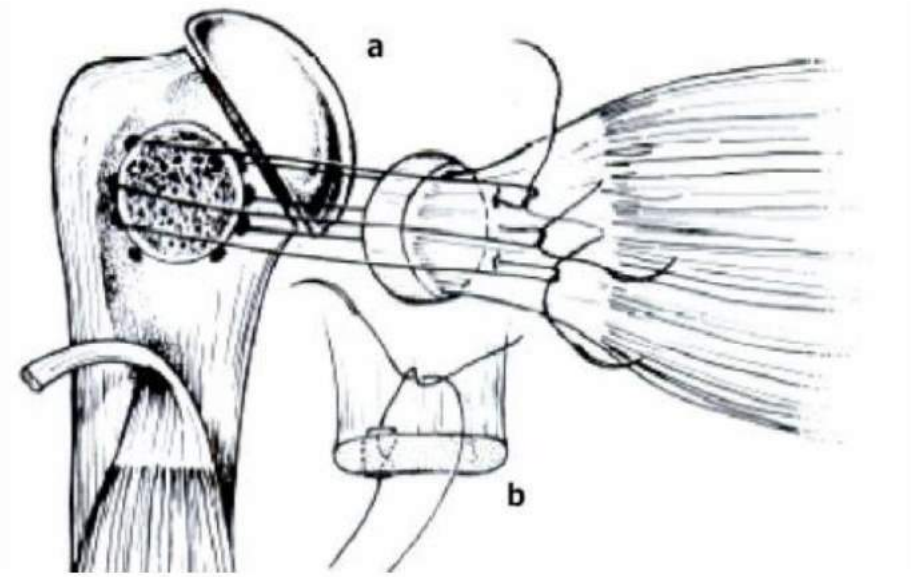

Figure 2: Lesser tuberosity osteotomy subscapularis repair technique.2 Reprinted from Ponce BA, Ahluwalia RS, Mazzocca AD, Gobezie RG, Warner JJ, Millett PJ. Biomechanical and clinical evaluation of a novel lesser tuberosity repair technique in total shoulder arthroplasty. J Bone Joint Surg Am 2005;87 suppl 2:1-8.

Table 1. Load to failure and cyclic displacement outcomes. Data are given as a mean ± SD. LTO = lesser tuberosity osteotomy. *Double-row LTO. †Single-row LTO. [α]Thick osteotomy bony wafer. [β]Thin osteotomy bony wafer.

		Load to failure (N)		Displacement (mm)	
Study	**n**	**Tenotomy (n = 29)**	**LTO (n = 46)**	**Tenotomy (n = 19)**	**LTO (n = 31)**
Fishman et al, 2014[3]	10	300 ± 92	375 ± 125	-	-
Giuseffi et al, 2012[1]	20	439 ± 96	447 ± 89	0.8 ± 0.2	1.8 ± 0.6
Krishnan et al, 2009[4*]	15	252 ± 99	466 ± 158	-	-
Krishnan et al, 2009[4†]		-	430 ± 202	-	-
Ponce et al, 2005[2]	18	334 ± 88	738 ± 261	2.7 ± 1.2	0.9 ± 0.5
Schmidt et al, 2014[5α]	12	-	249 ± 150	-	2.4 ± 1.1
Schmidt et al, 2015[5β]		-	234 ± 97	-	4.2 ± 2.3
Total	75	350 ± 113	443 ± 231	1.7 ± 1.3	2.1 ± 1.6
p-value		*0.047*		0.36	

References:

1. Giuseffi SA, Wongtriratanachai P, Omae H, Cil A, Zobitz ME, An KN, Sperling JW, Steinmann SP. Biomechanical comparison of lesser tuberosity osteotomy versus subscapularis tenotomy in total shoulder arthroplasty. J Shoulder Elbow Surg. 2012;21(8):1087-1095.
2. Ponce BA, Ahluwalia RS, Mazzocca AD, Gobezie RG, Warner JJ, Millett PJ. Biomechanical and clinical evaluation of a novel lesser tuberosity repair technique in total shoulder arthroplasty. J Bone Joint Surg Am. 2005;87 Suppl 2:1-8.
3. Fishman MP, Budge MD, Moravek JE Jr, Mayer M, Kurdziel MD, Baker KC, Wiater JM. Biomechanical testing of small versus large lesser tuberosity osteotomies: effect on gap formation and ultimate failure load. J Shoulder Elbow Surg. 2014;23(4):470-476.
4. Krishnan SG, Stewart DG, Reineck JR, Lin KC, Buzzell JE, Burkhead WZ. Subscapularis repair after shoulder arthroplasty: biomechanical and clinical validation of a novel technique. J Shoulder Elbow Surg. 2009;18(2):184-192.
5. Schmidt CC, Jarrett CD, Brown BT, DeGravelle M Jr, Sawardeker P, Weir DM, Latona CR, Miller MC. Effect of lesser tuberosity osteotomy size and repair construct during total shoulder arthroplasty. J Shoulder Elbow Surg. 2014;23(1):117-127.

The Surgical Incidence to Publication (SIP) Index: A Novel Equation used to Focus Future Research Efforts

Matthew J. Kraeutler, MD, John B. Schrock, BA, Darby A. Houck, Gina G. Provenzano, BSc, Eric C. McCarty, MD, Jonathan T. Bravman, MD
University of Colorado School of Medicine, Boulder, CO

Introduction: With increased publication rates across all fields of medicine, some research topics become heavily weighted in the literature while other, equally important topics do not receive the same exposure. The purpose of this study is to present a simple equation which can be used to measure the current level of research interest on any particular surgical procedure or medical diagnosis.
Methods: The SIP Index (surgical incidence/publications) is calculated as shown below,

$$SIP\ Index = \frac{Incidence\ of\ X}{Number\ of\ publications\ on\ X}$$

where X can be any particular surgical procedure. The numerator, utilized as a surrogate for the actual number of a particular case performed in a given time period, was estimated by the total number of cases presented during Part-II of the American Board of Orthopaedic Surgery (ABOS) certification examination from 1999-20031. The denominator was taken from a PubMed search for several of the most common orthopaedic procedures submitted to ABOS from 1999-2003.

Results: Statistically significant differences were found in the SIP Index between upper extremity procedures ($p = 0.016$) and lower extremity procedures ($p < 0.0001$) over the years 1999-2003. Within the upper extremity group (Figure 1A), the SIP Index for arthroscopic subacromial decompression was significantly greater than that of distal radius/ulna fracture repair and rotator cuff repair. Within the lower extremity group (Figure 1B), the SIP Index for arthroscopic knee chondroplasty was significantly greater than that for all other lower extremity procedures. The SIP Index for arthroscopic knee meniscectomy was also significantly greater than that of total knee arthroplasty and total hip arthroplasty. No other significant differences were found between groups.

Discussion and Conclusion: We have developed a statistic known as the SIP Index which can be used to assess national or worldwide research efforts on any particular surgical procedure or medical diagnosis, and have provided an example of how this equation can be applied to a set of incidence data on common orthopaedic surgical procedures. When used in this way, the SIP Index can provide some insight into which procedures are relatively over- or under-researched. This will be critical knowledge that we envision will ultimately be utilized in addition to population burden to help guide funding and research support moving forward.

References:
1. Garrett WE Jr, Swiontkowski MF, Weinstein JN, et al. American Board of Orthopaedic Surgery practice of the orthopaedic surgeon: Part-II, certification examination case mix. J Bone Joint Surg Am 2006;88(3):660-667.

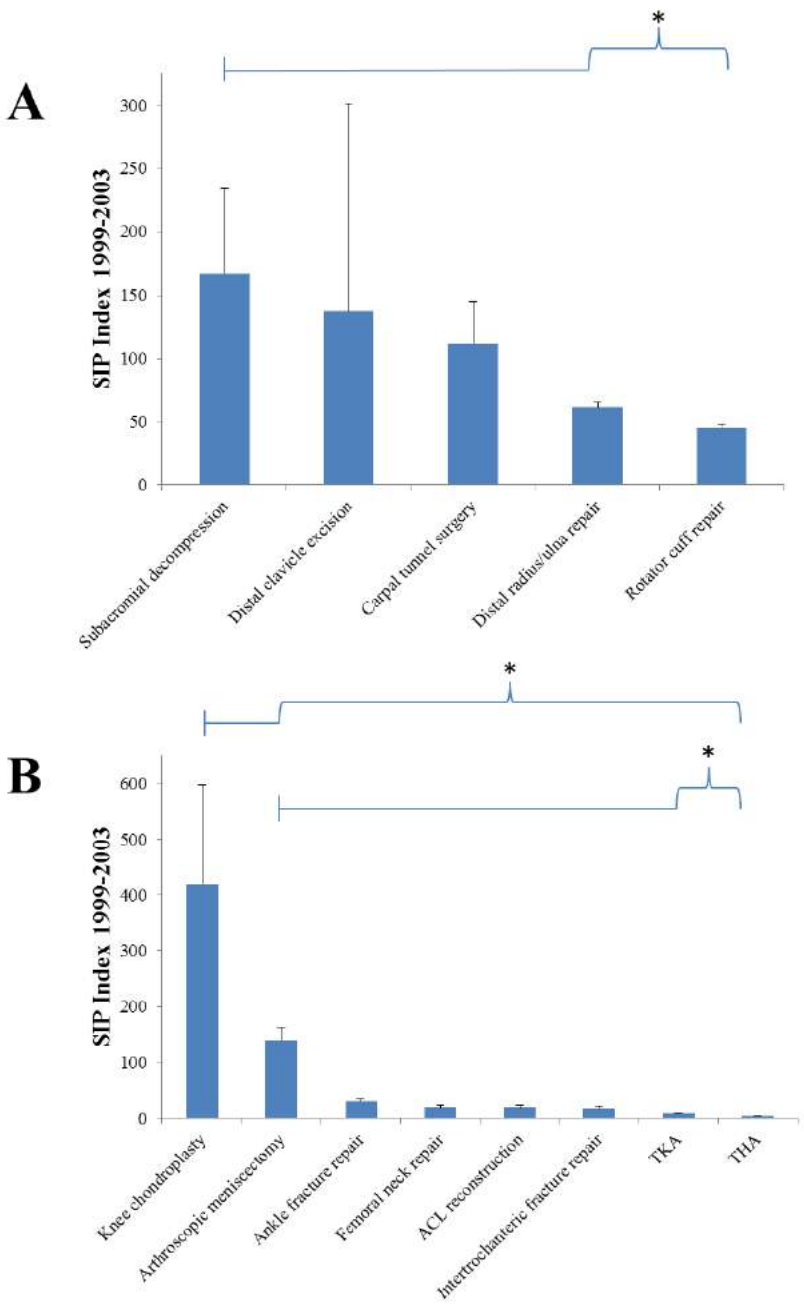

1. A) Upper extremity and B) lower extremity SIP Indexes. An average SIP Index was calculated from 1999-2003 for each procedure and compared across procedures. Error bars represent standard deviations. *Significant differences were found between paired groups using Tukey's range rest. ACL = anterior cruciate ligament, TKA = total knee arthroplasty, THA = total hip arthroplasty

Estrogen Receptor Beta (ERβ) is Osteocytes: A Critical Regulator of Adult Bon Turnover and Mechanical Load-Induced Bone Formation

Russell P. Main, PhD[1], Haisheng Yang, PhD[1], Julia P. Townsend[1], Rachel E. Embry[1], Mitchell R. Hoge, BS[1], Whitney A. Bullock, BA[1], Maxime A. Gallant, PhD[1], Teresita M. Bellido, PhD[2]
[1]Purdue University, West Lafayette, IN
[2]Department of Anatomy and Cell Biology, Indiana University School of Medicine & Roudebush Veterans Administration Medical Center, Indianapolis, IN

Sex hormones are key contributors to skeletal health. However, the effects of estradiol on skeletal anabolic pathways are still not well defined. While osteocytes are critical regulators of bone modeling and remodeling, osteocyte estrogen receptor alpha (ERα) has limited effects in the growing skeleton and in regulating the response to mechanical load. These results call for a better understanding of skeletal ERβ, which has previously been proposed as an inhibitor of skeletal mechanotransduction. Our goal is to characterize the role of osteocyte ERβ in regulating bone structure during growth, in adulthood, and in response to mechanical stimuli in both male and female mice. Mice lacking osteocyte ERβ were generated by Cre-LoxP recombination driven by DMP1-8kb-Cre. Male and female mice with osteocyte deletion of ERβ (KO) and littermate control mice (LC) were (i) sacrificed at 4 or 7wks old or (ii) began 2wks of unilateral tibial loading at 10 or 28wks old (12 and 30wks old at sacrifice). Serum estradiol and testosterone analyses were conducted in 4, 7, and 30wk old mice. MicroCT, dynamic histomorphometry, and histological bone resorption analyses of the tibiae and L5 vertebrae were conducted and genotypic differences tested by t-test. Load-genotype interactions were tested by linear mixed model with repeated measures.

We found no genotype-related differences in serum hormones. There were few phenotypic differences between KO and LC mice at 4, 7, or 12wks of age. Osteocyte-specific ERβ deletion had sex-dependent effects on bone mass at 30wks. Proximal tibial cancellous BV/TV (+62%) was increased in male KO relative to LC mice. By contrast, cancellous BV/TV was reduced in 30wk female KO relative to LC mice (-35%) (Figure 1). Similar cancellous patterns were seen in L5. While loading had an anabolic effect in the cancellous and cortical tissues in 12wk old tibiae, no interactive effect of genotype was found. 30wk female mice showed a strong midshaft response to load, but no genotypic interaction. At a site 37% of the tibia's length from the proximal end, 30wk female KO mice showed a greater load-induced increase in Ct.Ar than LC mice (+31% vs. +16%). This differential increase in Ct.Ar is primarily due to a greater increase in periosteal bone formation in response to load in KO relative to LC mice (Figure 2). Similarly, Tb.Th in the proximal tibia increased more in the 30wk female KO mice than in LC mice (+28% vs. +10%). 30wk old male mice did not respond strongly to tibial loading.

Osteocyte ERβ plays an important sex-specific role in regulating cancellous bone turnover in adult mice, as well as influencing the anabolic response to physical stimuli, especially in adult female mice. The cellular mechanisms and intra-cellular pathways underlying these structural outcomes are presently being investigated.

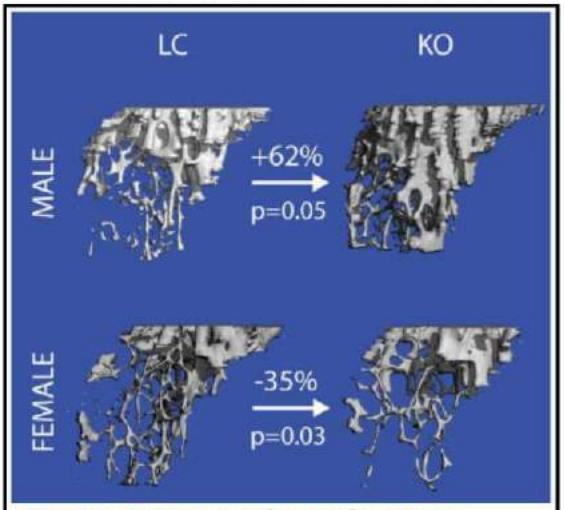

Figure 1: Bone volume fraction (BV/TV) in the proximal tibia for male and female LC and KO mice. BV/TV for the males and female Kos were increased and decreased, respectively, relative to the LC mice.

Figure 2: Periosteal and endosteal bone formation rate (BFR) for the cortical diaphysis, 37% of bone's length from the proximal end of the tibia. Load-induced periosteal BFR was elevated in KO relative to LC mice. Endosteal BFR increased similarly in response to load in both LC and KO mice.

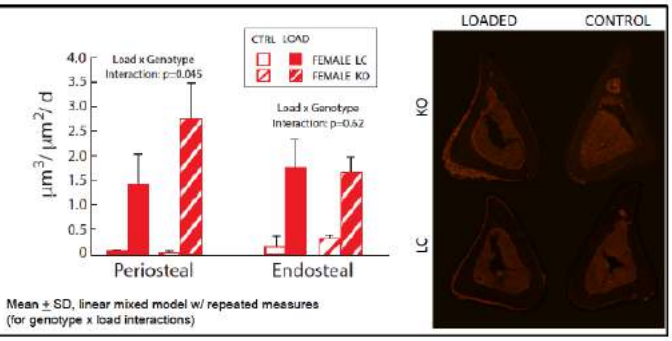

Three-dimensional Graphene Scaffolds for Engineering Musculoskeletal Tissue

Crystal Scott, MS, Raquel Brown, MS, Emily Tanasse, Kiyo Fujimoto, BS, Katie Yocham, ME, A. Nicole Chang, MS, Eric Krueger, PhD, Trevor Lujan, PhD, David Estrada, PhD, Julia T. Oxford, PhD
Boise State University, Boise, ID

Introduction: A major focus in tissue engineering is to construct biocompatible and bioresorbable scaffolds for the purpose of creating 3-dimensional (3D) structures which promote regeneration in bone, cartilage, and many other tissues. Graphene foam (GF) is a 3D form of graphene [1] – a single layer of carbon atoms arranged in a hexagonal crystal – which is emerging as a unique bioscaffold for engineering the chief components of the musculoskeletal system. [2-4] GF produced by chemical vapor deposition (CVD) creates a pure graphene scaffold which is porous, electrically conductive, and functions as a biomimetic micro environment. GF is biocompatible and cytocompatible, having been shown to support both cell adhesion and proliferation in culture conditions, as well as remain stable for up to seven months *in vivo*.[5] In this study, we compare the proliferation and differentiation of myoblasts and chondrocytes on bare GF to that on GF coated with specific extracellular matrix proteins. Specifically, we demonstrate the myogenic differentiation and the chondrogenic differentiation of pluripotent cells on GF scaffolds.

Methods:.We use well established protocols in our custom-built CVD system to synthesize GF on nickel foam substrates. Free standing GF is then obtained by selective etching of the underlying nickel substrate.[1, 4] The GF is characterized via scanning electron microscopy, Raman spectroscopy, X-ray micro-CT, and compressive mechanical testing. Freestanding GF bioscaffolds are seeded with one of two different cell lines to investigate the growth of myoblasts and chondrocytes on GF bioscaffolds with and without extracellular matrix protein coatings. For myogenic differentiation studies the GF is seeded with C2C12 myoblast cells which are then cultured and incubated in standard cell culture conditions. [4] In a similar sche, for chondrogenic differentiation studies, the GF was seeded with ATDC5 chondrocyte cells and cultured according to standard protocols. Cell adhesion and morphology is monitored via laser scanning confocal fluorescence microscopy.

Results: Raman characterization of the GF revealed regions of monolayer and few layer graphene. Imaging by X-Ray micro-CT showed the GF has a surface area to volume ratio of 323.34 mm-1 and a porosity of 84.56%. Compressive mechanical testing of the GF substrates reveals three regions of mechanical deformation: elastic, plastic, and densification, consistent with previous studies.[3] Our cell culture studies demonstrate bare and fibronectin coated GF as a feasible bioscaffold for growth and differentiation of ATDC5 cells into chondrocytes. ATDC5 cells on graphene adhere, proliferate, and are viable for more than 3 weeks. Additionally, laminin-coated GF is found to increase the rate of C2C12 differentiation into functional myotubes as compared to bare GF.[4]

Significance and Future Directions: Together, these findings provide new insight into GF as a bioscaffold for growth and differentiation of functional myogenic and chondrogenic tissue. This highlights a new path towards electrically conductive 3D bioscaffolds for developing tissue models of the musculoskeletal system. Our group is currently investigating embedding graphene electrodes in the cell culture environment to monitor the effect of electrical stimulus on cell growth, proliferation, differentiation, and gene expression. We anticipate these future studies will shed new light on the role of bioelectric cues in controlling stem cell fate.

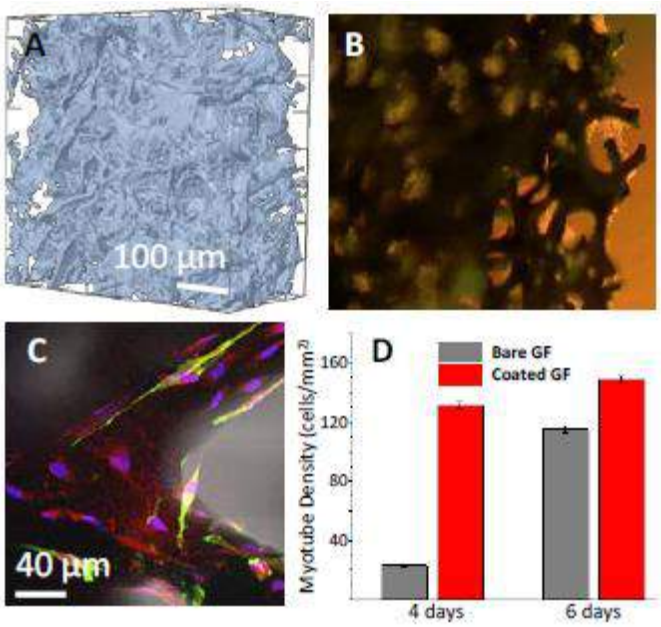

Figure 1. A) X-Ray micro-CT scan of GF revealing the internal structure of the bioscaffold. B) 100X optical image of ATDC5 cells proliferating on fibronectin-coated GF after 9 days. C) Confocal z-stack images of C2C12 cells cultured on laminin coated GF for 4 days. Blue, nuclei (Hoechst); red, actin (Alexa Fluor 546 phalloidin). D) Myotube density determined from multinucleated and MHC expressing cells and the estimated surface area for cultures on bare and laminin coated GF.

Acknowledgements: Research reported in this publication was supported by Institutional Development Awards (IDeA) from the National Institute of General Medical Sciences of the National Institutes of Health under grant numbers P20GM103408 and P20GM109095. We also acknowledge support from the Biomolecular Research Center at Boise State University with funding from the National Science Foundation, grant numbers 0619793 and 0923535, the MJ Murdock Charitable Trust, and the Idaho State Board of Education.

References: [1] Z. Chen, W. Ren, L. Gao, B. Liu, S. Pei, H. M. Cheng, *Nature Materials*, *10*(6), 424-428, 2011. [2] S. W. Crowder, D. Prasai, R. Rath, D. A. Balikov, H. Bae, K. I. Bolotin, H. J. Sung, *Nanoscale*, *5*(10), 4171-4176, 2013. [3] A. Nieto, R. Dua, C. Zhang, B. Boesl, S. Ramaswamy, A. Agarwal, *Advanced Functional Materials*, *25*(25), 3916-3924, 2015. [4] E. Krueger, A. Nicole Chang, D. Brown, J. Eixenberger, R. Brown, S. Rastegar, K. Yocham, K. D. Cantley, D. Estrada. *ACS Biomaterials Science & Engineering*, DOI: 10.1021/acsbiomaterials.6b00139, 2016. [5] Y. Zha, R. Chai, Q. Song, L. Chen, X. Wang, G. Cheng, M. Tang, M. Wang, *Journal of Nanoparticle Research*, *18*(5), 1-12, 2016.

The Role of Rho-ROCK Signaling in Normal and Estrogen Deficient Bone Cells in Response to Fluid Flow Induced Shear Stress

Irene Simfia, PhD, Jessica Schiavi, PhD, Vishwa Deepak, PhD, Laoise M. McNamara, PhD
Mechanobiology and Medical Device Research Group, Department of Biomedical Engineering, National University of Ireland Galway, Ireland

1. Introduction

Osteoporosis is most commonly manifested following menopause when estrogen production is deficient. As a result, complex changes in bone composition occur leading to bone fractures. Estrogen plays an important role in the normal biology of bone cells, in particular in regulating their response to mechanical loading. Recent studies have found for the first time that complex tissue levels changes in bone composition during estrogen deficiency might be explained by alterations in bone cell biology, in particular the mechanobiological responses[1-3]. Drug treatments that target the Rho/ROCK proteins have gained interest as therapeutic targets for cancer [4, 5]. A recent study suggests that the mechanosensitivity of osteoblasts to continuous loading is regulated by activation of P2Y2R mediated Rho-ROCK signalling required for actin stress fiber formation, increasing the mechanical stiffness of the cell [6]. However, the mechanism and role of Rho-ROCK signalling in osteogenesis of mechanically stimulated osteoblasts remains unknown. This can be a useful insight into exploring the mechanisms involved in diseases like osteoporosis where bone formation by mechanically stimulated bone cells is adversely affected[7].Specifically we seek to target the Rho/ROCK signalling pathway in estrogen deficient bone cells *in vitro* to establish changes in cell differentiation, gene expression and actin cytoskeleton when these cells are mechanically stimulated. We first, established the effect of ROCK inhibition on PGE2synthesis by osteoblasts. We show, for the first time, that ROCK inhibition in osteoblasts reverts the effects of fluid flow induced shear stress in terms of reduction in PGE2synthesis. We also affirm with previous study [6] that ROCK inhibition of osteoblasts leads to disruption of actin cytoskeleton. All of these results will be further compared with estrogen deficient cells under similar conditions as it is fundamental to this study.

2. Materials and Methods

Cell Culture

Viability experiments: MC3T3-E1 osteoblast-like cells were seeded at 10,000 cells per well on 13mm coverslips and cultured in vitro for 24hours in α-Minimum Essential Medium Eagle (MEM) supplemented with 10% Fetal Bovine Serum (Sigma Aldrich), 2mM L-glutamine (Sigma Aldrich), 100U/ml Penicillin and 100ug/ml Streptomycin (Sigma Aldrich). Cells were then incubated with media supplemented with or without Y-27632 (10μM; Sigma Aldrich) for 60 min. These cells were then assessed for their viability by examining their ability to convert the Alamar Blue reagent, Resazurin into Resorufin and were also analysed for their DNA content.

Flow study: MC3T3-E1 cells were seeded at 200,000 cells per slide on 76mm x26mm glass slides and grown for 48 hours in standard media as described above. These cells were then treated with media supplemented with the ROCK inhibitor, Y-27632, at 10μM for 60 min. This concentration was chosen as it falls in the range of concentrations of Y-27632 (1-30μM) used for ROCK inhibition in in vitro experiments [6, 8-10], which significantly affect stress fibre density, focal adhesion density and focal adhesion area. After the Y-27632 treatment, cells were washed with Dulbecco's Phosphate Buffered Saline (PBS). The control groups of cells did not receive treatment with Y-27632.

Fluid Flow

Laminar oscillatory fluid flow at a frequency of 0.5 Hz, peak flow rate of 9.2ml/min and peak shear stress of 1Pa was applied to both groups, Y-27632 and control, using custom designed parallel plate flow chambers, NE-1600 Syringe Pump (New Era Pump Systems) and 50 mL syringe (BD) following a previous study[11].

Alamar Blue Assay and DNA Hoechst Assay

To examine the viability of cells, they were incubated in 10% Alamar Blue reagent in PBS for 2hours at 37°C.Supernatant was collected and absorbance was measured at 570nm and 600nm. Cells were harvested following 3 freeze-thaw cycles in autoclaved deionized water. DNA content was quantified by mixing the cell lysate in Hoechst 33258 Solution (Sigma Aldrich) and fluorescence was measured for emission and excitation at 450nm and 365nm, respectively.

PGE2 Immunoassay

Mechanically stimulated (fluid flow applied) and static cells were allowed to synthesize PGE2 in 1ml of media under incubation at 37°C and 5%CO2 for 1hour. The supernatant was collected and assayed for PGE2 content using the Prostaglandin E2 ELISA Kit-Monoclonal. The PGE2 content was normalized to the total DNA content. Cells were harvested and DNA was quantified as described above.

Immunofluorescent staining

Alterations in the cytoskeleton due to ROCK inhibition were analysed in loaded and static groups using immunofluorescent staining to examine changes in actin stress fibres (phalloidin-tetramethylrhodamine Bisothiocyanate (TRITC) solution; Sigma-Aldrich; 1:1000) and nucleus (DAPI; Sigma Aldrich; 200ng/ml)

Statistical Analysis

A two-sample t-test was used to compare percentage of reduction of Alamar Blue reagent and DNA content of control cells and cells treated with Y-27632 (1010µM). A one way-ANOVA test was used to compare PGE2 synthesis amongst loaded and static cells with/without ROCK inhibition.

3. Results

The viability of MC3T3-E1 cells was not affected when exposed to Y-27632, a pharmacological ROCK inhibitor, at 10M for 1hr. The ability of the cells to reduce Alamar Blue reagent dye (Resazurin) did not show any statistically significant difference *(p value > 0.05)* when treated with Y-27632, Figure 1(A), indicating the non-toxic effects. Furthermore, it was also seen that DNA content of these cells was not significantly different *(p value > 0.05)* either treated or untreated with ROCK inhibitor, Figure 1(B).

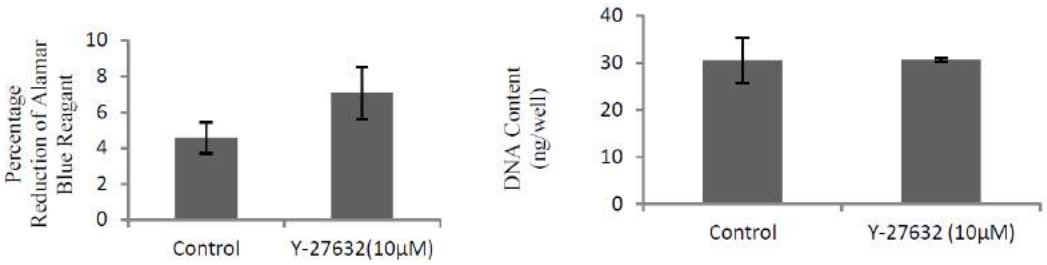

Figure 1*: (A) Percentenage of reduction in Alamar Blue reagant in MC3T3-E1 cells treated with and without, pharmacological ROCK inhibitor, Y-27632 at 10M (B) DNA content of treated and non-treated cells. No statistically significant differences seen (p value > 0.05).*

When ROCK was inhibited using Y-27632 in mechanically stimulated cells, the PGE2 synthesis was highly reduced (p-value <0.05) indicating the negative effect on osteogenesis of these cells. The synthesis of PGE2 by mechanically stimulated and static control cells was also statistically significantly different from each other (p-value <0.05), Figure 2(A). Immunofluoroscent imaging, Figure 2(B), showed extreme disruption of cytoskeleton when flow was applied on ROCK inhibited cells. Also some disruption was visible in inhibitor exposed cells under static condition but static and flow control cells did not seem to have much difference in the development of F-actin stress-fibres as seen in a previous study[12].

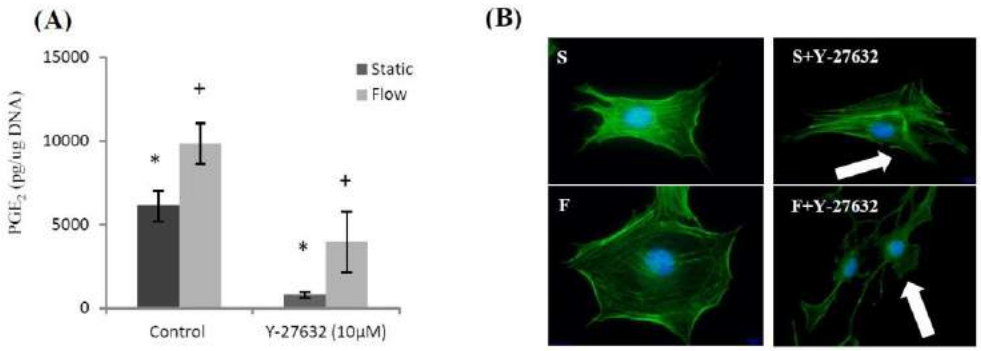

*Figure 2: (A)PGE2 synthesis by mechanically stimulated (flow) and static MC3T3-E1cells following treatment with or without Y-27632. Statistically significant differences were seen,+*p <0.05. (B) Immunofluoroscent imaging of actin-fibres (green) and nucleus (blue) for all conditions, where S is static and F is flow. White arrows indicate where disruption in actin cytoskeleton is seen*

4. Discussion

The results of this study for the first time, show that ROCK inhibition in osteoblasts suppresses the fluid flow induced osteogenic effects, as evident from reduction in PGE2 synthesis. Previously it was shown that ROCK activation may be necessary for fluid flow induced osteogenesis in Mesenchymal Stem Cell (MSCs) [10]. Ongoing studies are evaluating alterations in gene expressions of osteogenic markers such as COX-2, RUNX-2, ALP, RANKL and Osteocalcin. All the results will be compared to similar experiments done with estrogen deficient cells and as ROCK is an important mechanotransduction protein, further experiments are expected to shed some light on targeting th ealtered mechanosensitivity and mechanotransduction of osteoporotic bone cells.

5. References:

1. Brennan, M.A., ; McDermott, A., ; McNamara, L.M. . *The Impact of Shear Stress during Estrogen Withdrawal on Cell Viability and Mineral Production of Osteoblasts*. in *Orthopaedic Research Society*. 2012. San Francisco, USA.
2. Brennan, M.A.G., J. P.; O'Brien, F. J.; McNamara, L. M., *Effects of ageing, prolonged estrogen deficiency and zoledronate on bone tissue mineral distribution.* J Mech Behav Biomed Mater, 2014. **29**: p. 161-70.
3. Voisin, M.M., L. M., *Differential beta3 and beta1 Integrin Expression in Bone Marrow and Cortical Bone of Estrogen Deficient Rats.* Anat Rec, 2015. **298**(9): p. 1548-59.
4. Ogawa, T.T., H; Miyata, Y; Ushitora, Y; Fudaba, Y; Kobayashi, T; Arihiro, K; Okajima, M; Asahara, T, *Rho-Associated Kinase Inhibitor Reduces Tumor Recurrence After Liver Transplantation in a Rat Hepatoma Model.* American journal of transplantation, 2007. **7**(2): p. 347-355.
5. Wyckoff, J.B.P., Sophie E; Gschmeissner, Steve; Condeelis, John S; Sahai, Erik, *ROCK-and myosin-dependent matrix deformation enables protease-independent tumor-cell invasion in vivo.* Current Biology, 2006. **16**(15): p. 1515-1523.
6. Gardinier, J., et al., *P2Y2 receptors regulate osteoblast mechanosensitivity during fluid flow.* Am J Physiol Cell Physiol, 2014. **306**(11): p. C1058-67.
7. Klein-Nulend, J., et al., *Donor age and mechanosensitivity of human bone cells.* Osteoporos Int, 2002. **13**(2): p. 137-46.
8. Kazmers, N.H., et al., *Rho GTPase signaling and PTH 3–34, but not PTH 1–34, maintain the actin cytoskeleton and antagonize bisphosphonate effects in mouse osteoblastic MC3T3-E1 cells.* Bone, 2009. **45**(1): p. 52-60.
9. Street, C.A., et al., *Pharmacological inhibition of Rho-kinase (ROCK) signaling enhances cisplatin resistance in neuroblastoma cells.* International journal of oncology, 2010. **37**(5): p. 1297-1305.
10. Arnsdorf, E.J.T., Padmaja; Kwon, Ronald Y; Jacobs, Christopher R, *Mechanically induced osteogenic differentiation–the role of RhoA, ROCKII and cytoskeletal dynamics.* Journal of cell science, 2009. **122**(4): p. 546-553.
11. Haugh, M.G., T.J. Vaughan, and L.M. McNamara, *The role of integrin α V β 3 in osteocyte mechanotransduction.* Journal of the mechanical behavior of biomedical materials, 2015. **42**: p. 67-75.
12. Malone, A.M., et al., *The role of actin cytoskeleton in oscillatory fluid flow-induced signaling in MC3T3-E1 osteoblasts.* American Journal of Physiology-Cell Physiology, 2007. **292**(5): p. C1830-C1836.

Stem Cell Infiltrated Trabecular-Patterned Scaffolds Induce Extensive Bone Growth during Critical Sized Defect Repair

John A. Szivek, PhD, Andrew M. Wojtanowski, MS, David A. Gonzales, BS, Jordan L. Smith, MD
Orthopedic Research Laboratory, College of Medicine, The University of Arizona, Tucson, Arizona

Introduction: Rapid ingrowth into scaffolds provides substantial advantages when regenerating large bone defects. Inverse trabeculated patterned scaffolds (Figure 1) induce more rapid bone formation compared to identical sized scaffolds with similar sized geometric pores after 6 months in a canine model (1, 2, 3). Based on these results, 3D printed biomimetic scaffolds were produced for long bone segment regeneration in a sheep critical sized defect model (Figure 1). The goal of this study was to determine whether these scaffolds, infiltrated with tricalcium phosphate particles and endogenous stem cells, induce sufficiently rapid bone formation to fill a critical sized defect within 6 months.

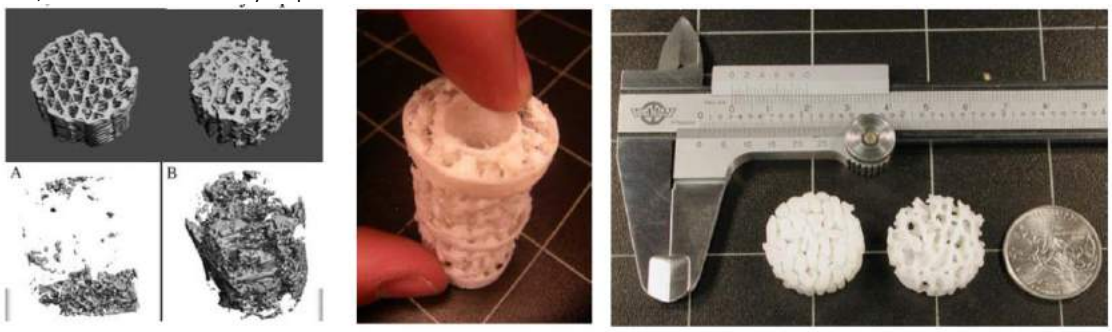

Figure 1: (Left images) A. 3D printed pattern of a simple geometric porous scaffold design and below it a µCT scan of bone ingrowth into the geometric patterned scaffold at 6 months in a dog. B. A biomimetic porous scaffold design and below it a µCT scan of bone ingrowth into the biomimetic pattern at 6 months in a dog. (Middle image) This picture shows a critical sized defect length 3D printed scaffold. (Right images) Biomimetic polybutylene terephthalate scaffolds printed using free form fabrication utilizing µCT data sets collected from trabecular bone and modified to the size of the femoral mid-diaphysis of a sheep. Right scaffold is identical to trabecular bone and left scaffold is identical to the inverse trabecular pattern to induce ingrowth with a trabecular pattern. (4)

Methods: Cylinders of trabecular bone from the femora head and critical defect sized cortical bone samples were collected from adult male sheep. Samples were imaged in a SCANCO µCT 20 at a 12µm resolution. Files were combined and converted to STL files, then exported to build polybutylene terephthalate (PBT) scaffolds in a Stratsys 1650 FDM (3, 4). Structural accuracy was verified by scanning scaffolds in the µCT and comparing scans to the original bone scans. Rosette strain gauges were attached to scaffolds that were compressed to 294 N at 49 N/s and 294 N/s in an MTS. Data was collected with LabView through a NiDaq board and exported to Excel. Stress vs. principal strain curves were drawn and strength and stiffness determined. A previously published latexing process (3,5) was used to coat scaffolds with 4µm tricalcium phosphate particles and scanning electron microscopy (SEM) was used to verify infiltration.
Male sheep underwent two IACUC approved procedures; the 1st was inguinal fat harvesting. Adipose derived stem cells were extracted using our published procedure (3). Cells were fed, passaged and perfused into scaffold pores. Scaffolds were placed 48 hours after perfusion. During surgery, a 42 mm femoral segment was removed and a modified lockable IM rod used to stabilize the scaffold (Figure 2). Sheep were held for 26 weeks. Activity was monitored with 24 hr. video. Monthly radiography and post sacrifice histology were used to determine the extent of tissue ingrowth and rate of bone formation. ANOVA's would determine difference between groups.

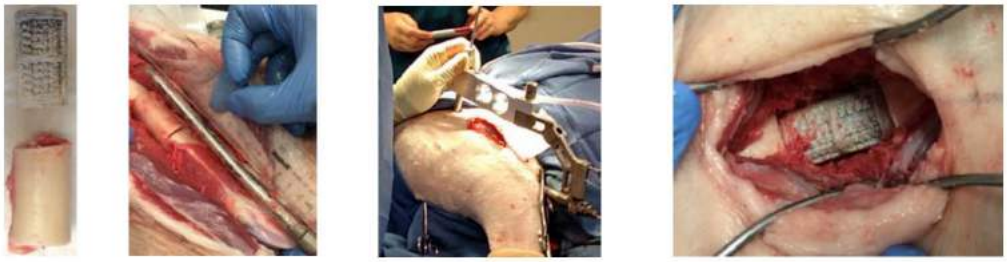

Figure 2: (Left most) Picture of scaffold and bone segment it replaced below it. (Second from left) This picture shows the surgical exposure with the cut segment and intramedullary rod in the image. The rod provided temporary stability while healing occurred. (Middle image) Picture of surgical instrumentation used to lock rod following segment placement. (Right image) Scaffold in place prior to closure.

Results: The final scaffold configuration was 71.6 ± 0.2% porous. Mechanical testing indicated a linear elastic response and a stiffness of 2.8 GPa with a compressive strength of 9.44 ± 0.94 MPa (sufficient to support physiological loads) although scaffolds were only 37% as stiff as sheep bone and 10% the compressive strength. Deposition of TCP was observed inside the pores but cell infiltration was better near outer surfaces and pre- and post- cell counts showed 80% cell depletion following the process of infiltration.
Scaffold placement was uneventful and sheep were load bearing within hours. Activity monitoring indicated the sheep spent 23.8 ±6% of their time standing or walking. After 8 weeks, radiographs showed there was 210 sq. mm. of new bone completely bridging the defect. Post sacrifice radiographs showed extensive bone formation at both the 3 and 6-month time points.

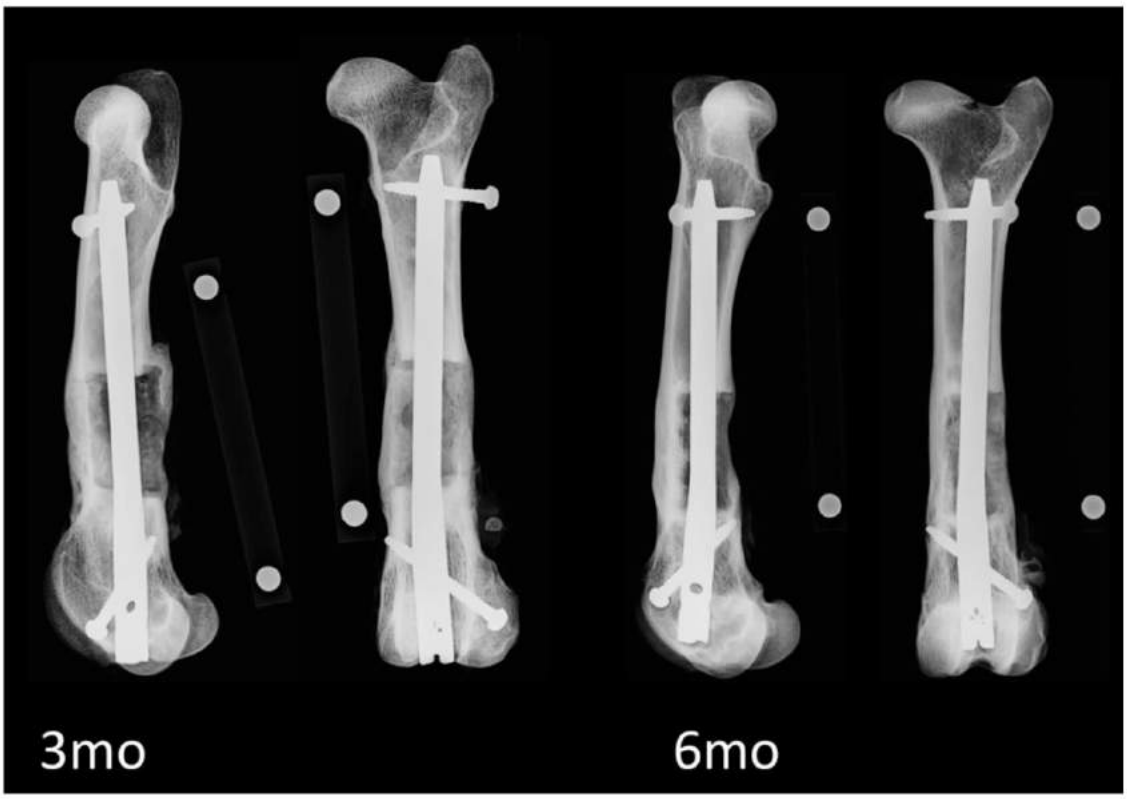

Figure 3: Radiographs of a 3 and a 6 month explanted femur showing extensive bone formation in the region of the scaffold.

MicroCT scans following 3 and 6-month implantation times showed extensive bone formation along the length of each scaffold (Figure 4). The anterior-lateral, anterior, anterior-medial and medial aspects of the defect surface were completely enveloped in bone along the length of the scaffold. Only the posterior lateral aspect of the surface had no visible bone formation, where muscle had originally been attached to the linea aspera of the bone. After 6 months, scans showed better bone infiltration and bone remodeling was apparent along the length of the scaffold (Figure 4).

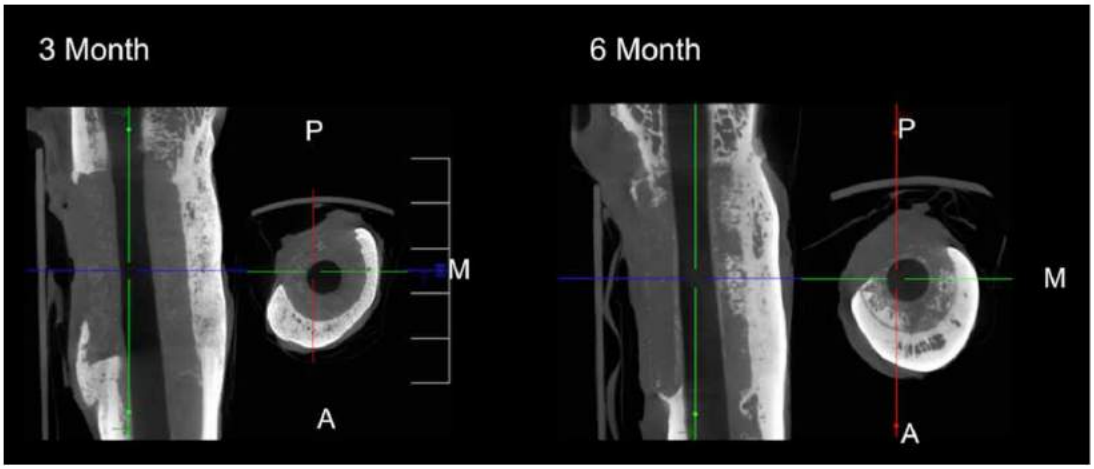

Figure 4: Micro CT's of a 3 and a 6-month explanted femora showing extensive bone formation along the length of the scaffold. There was no bone along the surface where the abductor muscles were attached to the segment that was removed.

Bone areas in experimental limbs were larger in comparison to controls and bone remodeling was reduced excess bone at the 6-month time point. A T-test showed results were significantly different.

Discussion and Conclusions: A long segment regeneration biomimetic scaffold infiltrated with endogenous adult sheep stem cells facilitated rapid bone growth throughout the length of a critical sized defect in a sheep femur even though sheep were relatively inactive. Preliminary results indicate that this design is able to support physiological loads during bone growth as early as 4 weeks. After 3 months the entire length of the scaffold was covered with bone on the anterior and medial surfaces. After 6 months better bone infiltration into the scaffold was noted and bone remodeling was apparent. Little bone formation was noted on the posterior lateral surface in the region coinciding with the location of the linea aspera. In the next stage of this study scaffolds instrumented with sensors (strain gauges) will be used to measure loading of the femur during healing using a published procedure (3, 6).

References:

1. Novel Biomimetic Polymer Scaffold Design enhances Bone Ingrowth, CP Geffre, JA Szivek, JT Ruth, DW DeYoung, B Tellis, DS Margolis, Online Dec 2, DOI: 10.1002/jbm.a.32251 JBMR-A, 2008.
2. Comparison of Bone Ingrowth into Scaffolds with Simple and Novel Biomimetic Porous Architectures, CP Geffre, JA Szivek, DS Margolis, J Invest Med, 56 (1) 242 Suppl., Jan 2008
3. In Vivo Telemetric Determination of Shear and Axial Loads on a Regenerative Cartilage Scaffold following Ligament Disruption, Szivek JA, et al. J Biomed Mater Res–B, DOI: 10.1002/jbm.b.33120, 2014.
4. Trabecular Scaffolds Created Using Micro CT Guided Fused Deposition Modeling, BC Tellis, JA Szivek, CL Bliss, DS Margolis, RK Vaidyanathan, P Calvert, J Mat Science & Engineering-C, Vol. 28/1 pp. 171-178, 2008.
5. TGF-ß1-enhanced TCP-coated Sensate Scaffolds can detect bone bonding, JA Szivek, D Margolis, BK Garrison, E Nelson, RK Vaidyanathan, DW DeYoung, J Biomed Mate Res-B, Vol.: 73B-1, 43-53, 2005.
6. An Instrumented Scaffold can Monitor Loading in the Knee Joint, JA Szivek, et al., J Biomed Mater Res - B, 79B, 218-228, 2006
Acknowledgements: Preliminary research was supported in part by NSF grant # CMMI 0855493 and WAESO.

Development of an *In Vitro* Model for Ligament Wound Healing

Stephanie M. F. Tuft, BS[1,2], Erica E. Morrill, MS[3], Raquel J. Brown, MS[2], Julia T. Oxford, PhD[1,2], Trevor J. Lujan, PhD[2,3]
[1]Department of Biological Sciences, Boise State University Boise, ID, USA
[2]Biomolecular Research Center, Boise State University Boise, ID, USA
[3]Department of Mechanical and Biomedical Engineering, Boise State University Boise, ID, USA

INTRODUCTION. Ligaments provide joint stability through a dense network of collagen fibers that align along the primary loading direction. When a ligament is torn, fibroblasts at the wound site repair the tissue by forming scar tissue, a disorganized or multiaxial network of collagen fibers. Over time, repaired tissue achieves only modest fiber realignment, and after one year its strength is less than half that of healthy tissue. This diminished strength can lead to recurrent ligament sprains, pain, and abnormal stress patterns on the articular surface that can trigger irreversible cartilage degeneration. In order to develop clinical techniques that improve the structural and functional restoration of torn ligament, the mechanical and chemical factors that stimulate matrix remodeling must be identified. A challenge to identifying these factors is the absence of an in vitro model for ligament wound healing. The development and validation of an *in vitro* model would enable the study of mechanical and chemical factors that instruct fibroblasts to align the disorganized scar tissue and strengthen the ligament. Prior studies have used cross-shaped (cruciform) molds to develop fibroblastic collagen gels with variable collagen networks.[1,2] Although the center of these cruciform gels has a multiaxial fibrillar microstructure similar to scar tissue, no study has measured the gene and protein expression by cells within these gels to determine if they are suitable as an *in vitro* wound healing model. The objective of this study is to determine if gels that exhibit a multiaxial fiber architecture will promote the expression of genes and proteins associated with healing ligament.

METHODS. Collagen gels seeded with murine fibroblasts were incubated for 1, 2 or 3 weeks under three loading conditions: stress-free, uniaxial, or biaxial. At each time point, five genes associated with ligament wound healing were measured. Confocal microscopy and imaging software measured fiber alignment. In total, 90 collagen gels were synthesized and tested.

Collagen Gels. Collagen gels were produced by adding Purecol (bovine type I collagen), DMEM, and NIH/3T3 mouse embryonic fibroblast cells in culture media. The collagen gel solution was then neutralized to physiological pH with 0.1 M NaOH and brought to a final volume with 1x PBS. This gave a final cell density of 0.83×10^6 cells/mL per gel and a final type 1 collagen density of 1.5 mg/mL. Teflon cruciform molds were machined with a channel aspect ratio of 1:0.5 (Fig. 1A). The cruciform design generates stress in the gel by resisting gel contraction with fixed glass rods (Fig. 1B).[1,2] The stress environment at the cruciform channel arms (uniaxial stress) differs from the cruciform center (biaxial stress). The gel solution was cast into the cruciform molds at 1.2 mL per mold, and at 2 mL per well in a six-well plate (stress-free). Cells were passaged at 60% confluency using trypsin/EDTA, and the collagen solution was allowed 120 minutes to gel at 37°C. Cell culture media was exchanged every three days. 54 cruciform-shaped cellular gels and 36 stress-free discs were created to allow for a 1 week, 2 week and 3 week time course experiment.

Gene Expression. RNA was extracted from the cells using TRIzol reagent. The control specimens consisted of RNA from cells in a 2D tissue culture flask. RNA concentration was determined by measuring the absorbance at 260 nm. Messenger RNA (mRNA) was used as template for cDNA synthesis and amplified by real time quantitative RT-PCR. Genes of interest were contained within the RT² Profiler™ PCR Array Mouse Extracellular Matrix & Adhesion Molecules. All results were normalized to GAPDH, and expressed as positive fold-changes by comparing to results from the 2D tissue culture flask. The genes targeted for analysis include: collagen type I alpha I (Col1a1), collagen type III alpha I (Col3a1), collagen type V alpha I (Col5a1), integrin alpha 5 (Itga5), and tenascin-C (TnC). The rationale for selecting these genes is that previous animal studies on ligament wound healing found scar tissue at three weeks had a 2.6-fold increase in collagen I and a 1.9-fold increase in collagen III[3], and scar tissue at six weeks had a 4.2 fold increase in collagen V[4] and an increase in TnC[5]. In human ruptured ACL, Itga5 showed a 1.7 fold decrease[6].

Mass Spectrometry: Cellular gels were separated into uniaxial, biaxial, or stress free locations. Proteins were extracted using RIPA buffer protocol. In-solution proteolytic digestion, Nano Liquid chromatography mass spectrometry (nano LC-MS) analysis, and finally peptide spectral matching and protein identification were used to determine which proteins were expressed.

Imaging: Confocal microscopy was used to evaluate the collagen fibril alignment in the stressed and stress-free gels at each time point. The collagen gels were imaged at 63x using the 405 nm laser of a Zeiss 510 scanning confocal microscope and ZEN imaging software (Fig 1C-D). FiberFit software was used to apply a fast-Fourier transform that measured fiber

dispersion (fiber disorder) in the confocal images.[9] A trypan blue/calcein AM assay for live/dead cells was used to determine cell viability.

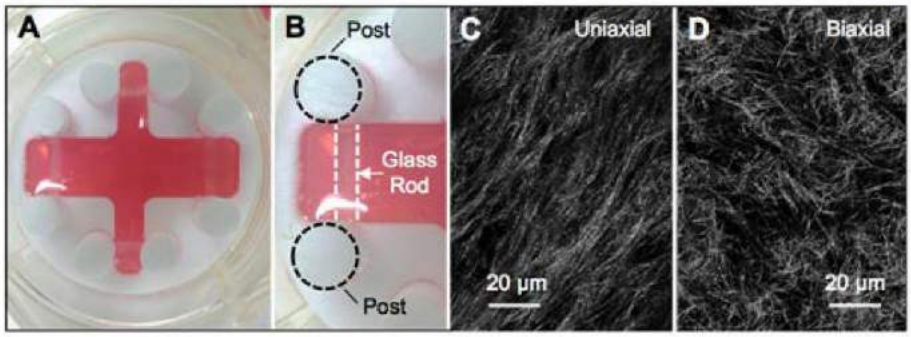

Figure 1: Collagen gels. A) Cruciform. B) Mechanical constraint, C) confocal image of cruciform center and D) cruciform arm.

RESULTS. A gradual increase in collagen was observed for all gels over time (Fig. 2). At three weeks, the stress-free gels had the greatest increase in Col1a1 expression (5.4 fold) and Col5a1 expression (4.8 fold), while the biaxial stressed gels had the greatest increase in Col5a1 expression (12.2 fold). The ratio of Col3a1 to Col1a1 had the greatest increase with time in the stress-free and biaxial gels (Fig. 2D). For all gels, only minor changes occurred over time in the ratio of Col5a1 to Col1a1 (Fig. 2D).

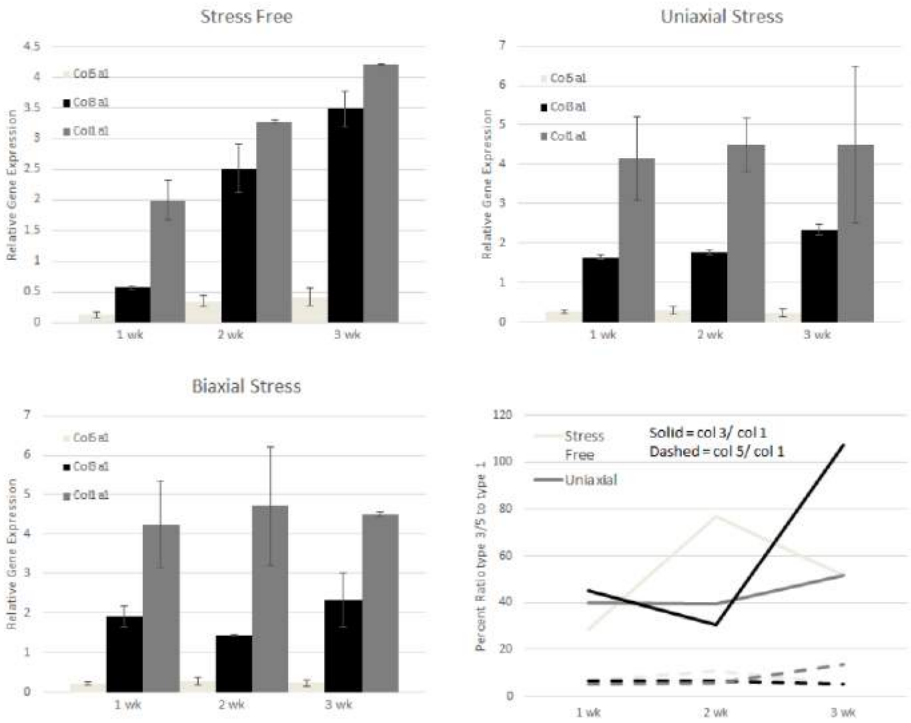

Figure 2: Gene expression when gels are exposed to A) stress-free, B) uniaxial and C) biaxial loads. D) Collagen ratios over time. Values are normalized to GAPDH. Each error bar represents mean ± standard error of the mean (SEM) (n=3).

The increase in expression of Itga5 was lowest (2.7 fold) in the uniaxial stressed gels at two weeks and highest (4.2 fold) in stress-free gels at three weeks. The expression of TnC was greatest in the stress-free gels at week 2 (7.8 fold). Mass spectrometry results show an increase in murine collagen type I, collagen type III and decorin from NIH3T3 cells grown in collagen type-I 3D matrix in both the stress-free and uniaxial-stressed cellular gels. One exception is the decrease in collagen type I from week 1 to week 3 in the uniaxial stressed gels (Fig. 3).

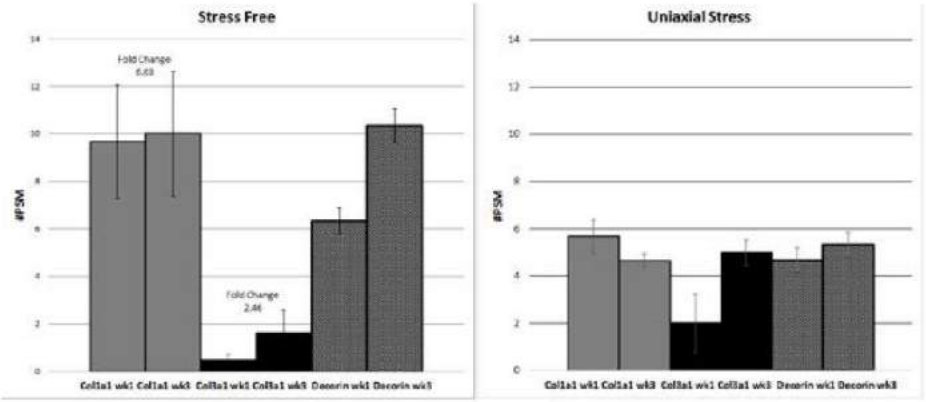

Figure 3: Number of peptide spectral matches (#PSM) for Col1a1, Col3a1 and Decorin. Error bars represent mean ± standard error of the mean (SEM) (n=3). #PSM, have been controlled for bovine collagen type-I and for repeats in #PSM from other proteins.

Image analysis found the uniaxial stressed gels had greater fibril alignment than the biaxial stressed gels (Fig. 1C-D; $p<0.001$). A significant interaction existed, where fibril alignment increased over time in the uniaxial gels and decreased over time in the biaxial gels ($P = 0.02$). Cell viability was robust.

DISCUSSION. This study investigated whether fibroblasts growing in 3D bovine collagen gels could replicate the gene expression observed during ligament wound healing. Based on literature values3, 4, 6, 7, 8, our results indicate that the stress-free gels have a gene expression profile most similar to healing ligament. For example, the stress free gels had gene expressions of Col1a1 and Col5a1 very near to in vivo studies. A close second to the healing ligament profile were the biaxial constructs based on the increase in expressions of the Col1a1, Col3a1, Itga5 genes and their disordered collagen fibril alignment. The uniaxial stressed constructs were least like the healing ligament gene profile and had the most aligned network of collagen fibrils. Based on the proteomics data that mimic that of the gene expression, giving further confirmation that the stress-free cellular gels exhibit healing ligament-like characteristics. Limitations of this work include a small sample size n=3. RNA was normalized to 100 ng per PCR array. Another limitation is that comparable animal studies use different molecular biology techniques. Future work will characterize the molecular constituents using proteomics. To our knowledge, this is the first study to focus on validating an in vitro model for ligament wound healing by examining mRNA expression and collagen fibril alignment in multiaxial collagen gels. Previous animal studies have compared differences in gene expression in fibroblasts from injured and healthy ligament in vivo. Also, studies have mechanically stressed cellular gel constructs but not with the aim of a healing ligament model. Once an in vitro healing ligament model has been validated, it can be used to test the effect of mechanical loading regimes and chemical stimuli on the remodeling and strengthening of the fiber network during healing. This could potentially aid in the development of clinical techniques that restore collagen organization and strengthen the healing ligament.

ACKNOWLEDGEMENTS. The project described was supported by an Institutional Development Award (IDeA) from the National Institute of General Medical Sciences of the National Institutes of Health under Grant #P20GM103408 and #P20GM109095. We also acknowledge support from The Biomolecular Research Center at Boise State with funding from the National Science Foundation, Grants # 0619793 and #0923535; the M. J. Murdock Charitable Trust; Lori and Duane Stueckle, and the Idaho State Board of Education. Its contents are solely the responsibility of the authors and do not necessarily represent the official views of NIH.

REFERENCES

[1] Jhun, C. et al, J Biomech Eng., 131(8): 1-21, 2009.
[2] Sander, E. A. et al, PNAS, 106 (42): 17675-17680, 2009.
[3] Frank, C. B. et al, Osteoarthritis and Cartilage, 7: 130-140, 1999.
[4] Niyibizi, C. et al, Knee Surg, Sports Traumatol, Arthrosc, 8: 281-286, 2000.
[5] Haslauer, C. M. et al, Wound Repair Regen., 22(1): 103-110.
[6] Brune, T. et al, European Cells and Materials, 14: 78-91, 2007.
[7] Chao P. G. et al, Biofabrication, 6: 1-10, 2014.

[8] Neurath M., Zeitschrift fur Orthopadie und Ihre Grenzgebiete, 131(2): 168-172, 1993.
[9] Morrill EE et al., 2015 Proceeding of SB3C, Salt Lake City, UT.

Mechanical LINC between Nucleus and Cytoskeleton Regulates βcatenin Nuclear Access

Gunes Uzer, PhD Guniz Bas, BS, Buer Sen, MD, Janet Rubin, MD
University of North Carolina, USA

Mechanical signals generated during functional loading promote osteoblastogenesis at load bearing sites. βcatenin (βcat) signaling supports osteoblast and inhibits adipocyte recruitment from mesenchymal stem cells (MSC). βcat control of gene expression relies on non-classical nuclear shuttling involving βcat's direct interaction with nuclear pore complexes (NPCs). MSC mechanosensitivity is in-part regulated at the nuclear surface via LINC complexes (Linker of Nucleoskeleton and Cytoskeleton) that integrate the nucleus into the cytoskeleton. As LINC directly binds cytoskeletal actin filaments, NPCs and βcat, it may also have a role in βcat nuclear delivery. Here we hypothesized that LINC complexes regulate nuclear βcat availability in response to mechanical challenge.

To understand the mechanically-induced interaction of βcat with the nuclear envelope, we applied high magnitude strain (HMS, 2%, 0.17Hz) or low intensity vibration (LIV, 0.7g, 90Hz) to murine MSCs and isolated NPC-rich nucleoskeletal (NSk) fractions to probe for βcat. On average, HMS and LIV increased the βcat-NSk association by 2-fold ($p<0.01$). We next asked if LINC connectivity was critical for mechanically-induced βcat-NSk association: un-anchoring the βcat-binding element of LINC, Nesprin-2, via Sun1/2 deletion (SiSUN) decreased both basal NSk-bound βcat (50%, $p<.001$) and mechanically induced βcat-NSk association ($p<0.001$). Further, immunostaining showed that in LINC deficient MSCs where Nesprin-2 was displaced from nuclear envelope, βcat was less tightly localized to nucleus increasing its cytoplasmic staining (1.4-fold, $p<.001$). This suggests that LINC positions βcat at the nuclear envelope, thus providing access to NPC for inward transfer. We tested this possibility by measuring fluorescence recovery of GFP-βcat in the nucleus to quantify the rate of βcat nuclear entry: LINC deficient MSCs showed a 51% recovery delay ($p<.01$), indicating a LINC-dependence of βcat nuclear entry. We next considered if strengthening LINC-mediated connectivity would improve βcat-NSk association. Daily application of LIV x5d increased Nesprin-2 expression by 69% ($p<0.05$), resulting in 49% increase in HMS-induced βcat-NSk association compared to non-LIV group.
In summary, our data indicates that LINC-mediated connectivity enables βcat nuclear transfer. As such, mechanically induced adaptations of LINC complexes may represent a novel avenue for increasing βcat signaling and improving MSC fate decisions.

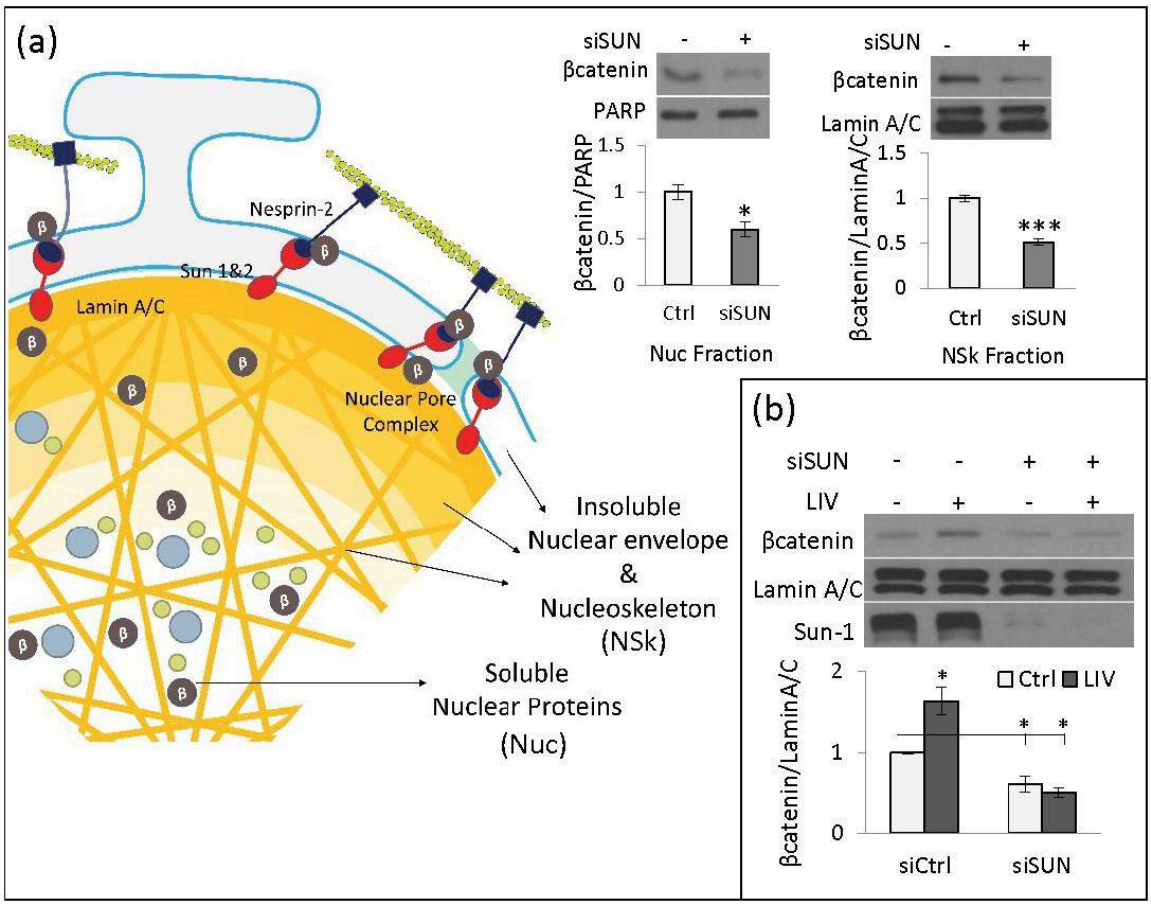

Figure1. a) Separating cell nucleus into soluble nuclear (Nuc) and insoluble nucleoskeletal (NSk) fractions revealed that the Lamin A/C nucleoskeleton and the LINC complex that integrate nucleus into the cell cytoskeleton is also associated with βcatenin. Disabling LINC function using siRNA against Nesprin anchoring protein Sun1/2 (siSUN) reduced nuclear βcatenin levels as well as NsK-βcatenin association. b) Consistent with decreased nuclear levels of βcatenin, siSUN treatment inhibited mechanically induced βcatenin-NSk association, suggesting a LINC-mediated βcatenin control at the nuclear envelope.

7:00 AM – 8:00 AM	**Breakfast & Registration** Support provided by Charles River Laboratories

8:00 AM – 9:45 AM	**Problems in Endocrinology: How Do We Treat Bone, Muscle, and Other Target Organs in Hypophosphatasia?** **Chair: David Thompson, PhD *(D. Thompson Consulting, LLC)*** Introduction: How Do We Treat Bone, Muscle, and Other Affected Organs in Hypophosphatasia? David Thompson, PhD *(D. Thompson Consulting, LLC)* What We Know and Don't Know About Hypophosphatasia José Luis Millán, PhD *(Sanford-Burnham Medical Research Institute)* Muscle Weakness in Hypophosphatasia Michael Whyte, MD *(Washington University)*

10:00 AM – 12:00 PM	**Problems in Orthopaedics: New Materials-based and Ligand-based Strategies to Stimulate Self-Repair of Tendons and Ligaments** **Chair: Michaela Kneissel, PhD *(Novartis)*** The Basis of Tendon Function, Homeostasis, Degeneration, and Regeneration Jess G. Snedeker, PhD *(University Hospital Belgrist)* Molecular Therapies to Augment Intrinsic Tendon Repair Olivier Leupin, PhD (*Novartis Institute for Biomedical Research)* Hydrogel-based Drug Delivery David Mooney, PhD (*Harvard University)* Development of an In Vitro Model for Ligament Wound Healing Stephanie Tuft, BS *(Boise State University)* Lesser Tuberosity Osteotomy and Subscapularis Tenotomy Repair Techniques during Total Shoulder Arthroplasty: A Meta-Analysis of Cadaveric Studies Matthew Kraeutler, MD *(University of Colorado School of Medicine)*

1:30 PM – 3:30 PM	**Career Development Workshop: Tenure and Promotion** **Chair: Marjolein van der Meulen, PhD *(Cornell University)*** Moderator: Marjolein van der Meulen, PhD *(Cornell University)* Panelists: Teresita Bellido, PhD *(Indiana University School of Medicine)* Susan Bloomfield, PhD *(Texas A&M University)* Gary Krishnan, PhD *(Eli Lilly)* David Roodman, MD *(Indiana University School of Medicine)* The discussion will be organized around four topics: 1. Tenure & promotion policies 2. Tenure references/letter writers 3. Dossier materials: CV, statements, papers 4. Other considerations We will start each topic with comments from the panelists, followed by discussion and questions from the participants. Presenter: Gayle Lester, PhD *(Program Director, NIAMS, NIH)*

	Topic: Over view of recent NIH Policies: • Premise and Rigor/Reproducibility • Biosketch and annotated publications

5:30 PM – 8:00 PM	Banquet	Lodge Terrace

Introduction: How Do We Treat Bone, Muscle, and Other Affected Organs in Hypophosphatasia?

David D. Thompson, PhD
D. Thompson Consulting, LLC

Hypophosphatasia (HPP) is the rare, sometimes fatal, inborn-error-of-metabolism caused by deactivating mutation(s) in the gene that encodes the tissue non-specific isoenzyme of alkaline phosphatase (TNSALP).(1,2) Due to diminished function of this important enzyme(3) in HPP, there can be defective mineralization of the skeleton leading to rickets or osteomalacia and associated complications, and in the most severe cases hypercalcemia and hyperphosphatemia with kidney damage from impaired calcium/phosphate regulation.(4)

Important preclinical and clinical research to understand the consequences from deficiency of TNSALP activity has provided new insights into the role of TNSALP in organ systems.(5,6) This appreciation of TNSALP and its deficiency has advanced new therapeutic options for HPP patients.(1)

Clinical Research in HPP

HPP presents across broad-ranging patient ages. Interdependent clinical manifestations can emanate from impaired mineralization of skeletal and dental matrix due to elevated extracellular levels of the TNSALP substrate inorganic pyrophosphate (PPi), a potent inhibitor of mineralization. Significant advancements in understanding the clinical manifestations of HPP have come from non-interventional natural history studies that are the foundation for therapeutic intervention trials for rare diseases.

What have clinical studies in HPP patients revealed about TNSALP, the disease, its morbidity, and therapeutic intervention?

Preclinical Research in HPP

Advances in understanding TNSALP and HPP have also come from development of animal models of HPP. A murine knockout model (designated *Akp2-/-*) was generated by inactivating the TNSALP gene,(5) closely mimics the infantile form of the human disease, and has provided important insights into the physiological role of TNSALP and the pathogenesis of HPP.

What have murine models of HPP revealed about the role of TNSALP?
What has HPP murine models revealed about therapeutic options for HPP?

HPP and Muscle Function

Well-documented in many HPP patients is muscle weakness and impaired physical performance. Any direct role for TNSALP in muscle function is not understood. Preclinical and clinical studies of HPP in this area have advanced our understanding and point to future research directions.

What are the problems with muscle function and physical performance in HPP?
Does TNSALP have a direct role in muscle function?
How have therapeutic interventions in HPP impacted muscle function?

References

1) Whyte MP: Hypophosphatasia: etiology, nosology, pathogenesis, diagnosis and treatment. Nature Reviews Endocrinology 12:233-46, 2016

2) Whyte, MP. Hypophosphatasia. In “Genetics of Bone Biology and Skeletal Disease”. Thakker RV, Whyte MP, Eisman J, Igarashi T (editors). Elsevier (Academic Press), San Diego, CA, pp 337-60, 2013

3) Millan JL, Whyte MP: Alkaline Phosphatase and Hypophosphatasia. Calcif Tissue Int 98:398-416 doi 10.1007/S00223-015-0079-1. PUBmED pmid: 26590809, 2016

4) Whyte MP, Greenberg CR, Salman NJ, Bober MB, McAlister WH, Van Sickle B, Wenkert D, Edgar TS, Bauer ML, Hamdan M, Simmons JH, Bishop N, Lutz RE, McGinn M, Craig S, Moore JN, Taylor JW, Cleveland RH, Cranley WR, Lim R, Thacher TD,

Mayhew JE, Downs M, Millan JL, Skrinar A, Crine P, Landy H: Enzyme replacement therapy in life-threatening hypophosphatasia. New England Journal of Medicine 366: 904-13, 2012
5) Narisawa S, Frohlander N, Millan JL. Inactivation of two mouse alkaline phosphatase genes and establishment of a model of infantile hypophosphatasia. Dev Dyn. 1997 208(3):432-46.

6) Whyte MP, Madson KL, Phillips D, Reeves A, McAlister WH, Yakimoski A, Mack K, Hamilton K, Kagan K, Melian A, Thompson D, Moseley S, Odrljin T, Greenberg CR: Asfotase alfa therapy for children with hypophosphatasia. JCI Insight 1:e85971; 1-10, 2016

7) Whyte MP, Greenberg CR, Ozono K, Riese R, Moseley S, Melian A, Thompson D, Hofmann C: Asfotase alfa treatment improves survival for perinatal and infantile hypophosphatasia. Journal of Clinical Endocrinology and Metabolism, 101: 334-42, 2016

What We Know and Don't Know About Hypophosphatasia

José Luis Millán, PhD
Sanford Burnham Prebys Medical Discovery Institute, La Jolla,
CA 92037. millan@sbpdiscovery.org

Hypophosphatasia (HPP) is the heritable rare disease that results from *ALPL* gene mutations leading to deficient activity of the tissue-nonspecific alkaline phosphatase isozyme (TNAP).[1] HPP features rickets or osteomalacia and hypomineralization and early loss of teeth.[2] These skeletal and dental manifestations are caused by the accumulation of extracellular inorganic pyrophosphate (PPi), a potent mineralization inhibitor and a physiological substrate of TNAP, that impedes the normal propagation of hydroxyapatite (HA) onto the collagenous extracellular matrix (ECM).[1-4] Additionally, phosphorylated osteopontin (OPN), another potent mineralization inhibitor and a substrate of TNAP, binds to HA as soon as it is exposed to the extracellular fluid further restricting the degree of ECM mineralization. Initiation of mineralization however occurs inside chondrocyte- and osteoblast-derived matrix vesicles (MVs) by accumulation of Pi generated intravesicularly by the action of PHOSPHO1 on phosphocholine and also via PiT-1-mediated incorporation of Pi generated extravesicularly by TNAP or NPP1. This mechanism of initiation and progression of skeletal mineralization (illustrated in the Figure), including the fundamental role played by TNAP in the control of the PPi/Pi ratio, is compatible with a wealth of experimental data (reviewed in references **3** and **4** and references therein). Understanding this mechanism has provided the rationale for the current therapeutic intervention for HPP using recombinant mineral-targeted TNAP for enzyme replacement.[5, 6]

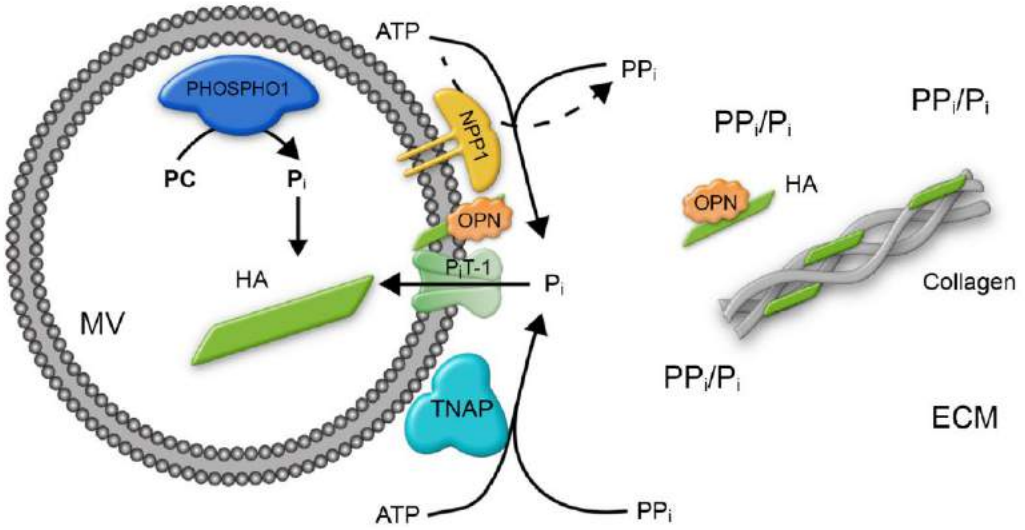

Severely affected HPP patients, as well as *Alpl*$^{-/-}$ mice, suffer from severe seizures that herald a lethal outcome.[1, 2] The seizures are partly, but not entirely, explained by inadequate availability of pyridoxal phosphate, a physiological substrate of TNAP that is a co-factor in the synthesis of neurotransmitters by neuronal cells.[1, 2, 4] Other features of HPP are not yet understood, such as what pathophysiological mechanisms lead to the development of craniosynostosis, nephrocalcinosis, muscle weakness, inflammation and pain. During my presentation I will argue that some of these poorly understood manifestations of HPP are caused at least in part by local changes in the ATP/adenosine ratio as a result of deficient TNAP activity leading to altered purinergic signaling that affects cell behavior and tissue homeostasis.[7]

REFERENCES

1. Millán J.L. *Mammalian Alkaline Phosphatases: From Biology to Applications in Medicine and Biotechnology*. Weinheim, Germany: Wiley-VCH Verlag GmbH & Co.; 2006, pp.
1-322.
2. Whyte, M. P. Hypophosphatasia - aetiology, nosology, pathogenesis, diagnosis and treatment. Nature Rev. Endo. (2016) 12:233-246.
3. Millán J.L. The Role of Phosphatases in the Initiation of Skeletal Mineralization. Calcif. Tissue Int. (2013) 93 (4): 299-306.
4. Millán J. L., Whyte M. P. Alkaline Phosphatase and Hypophosphatasia. Calcif. Tissue Int.
(2016) 98:398–416.

5. Millán J.L., Narisawa S., Lemire I., Loisel T.P., Boileau G., Leonard P., Gramatikova S., Terkeltaub R., Camacho N.P., McKee M.D., Crine P., Whyte M.P. Enzyme replacement therapy for murine hypophosphatasia. J. Bone Miner. Res. (2008) 23(6):777-787.
6. Whyte M.P., Greenberg C.R., Salman N.J., Bober M.B., McAlister W.H., Wenkert D., Van Sickle B.J., Simmons J.H., Edgar T.S., Bauer M.L., Hamdan M.A., Bishop N., Lutz R.E., McGinn M., Craig S., Moore J.N., Taylor J.W., Cleveland R.H., Cranley W.R., Lim R., Thacher T.D., Mayhew J.E., Downs M., Millán J.L., Skrinar A.M., Crine P., Landy H. Enzyme-replacement therapy in life-threatening hypophosphatasia. N. Engl. J. Med. (2012) 366(10):904-913.
7. Millán J. L. What Can We Learn About the Neural Functions of TNAP from Studies on Other Organs and Tissues? Subcell. Biochem. (2015) 76:155-166.

Muscle Weakness in Hypophosphatasia

Michael P. Whyte, MD
Washington University School of Medicine and Shriners Hospital for Children, St. Louis, MO

Hypophosphatasia (HPP) is the inborn-error-of-metabolism characterized by deficient activity of the tissue-nonspecific isoenzyme of alkaline phosphatase (TNSALP).[1] Because TNSALP is a cell-surface protein, its substrates accumulate extracellularly in HPP, including the inhibitor of mineralization inorganic pyrophosphate (PPi).[2] The PPi excess typically leads to tooth loss and can cause rickets during growth or osteomalacia in adult life.[3] Nevertheless, HPP has a remarkably broad ranging expressivity that spans clinically from stillbirth due to absence of skeletal calcification to dental disease or calcific arthropathies alone presenting in adult life.[1,4,5] This range of severity is explained largely by autosomal recessive versus autosomal dominant transmission from among more than 300 predominantly missense mutations scattered throughout the TNSALP (ALPL) gene.[1,6]

In the most severely affected HPP infants, the block in skeletal mineralization results in bone deformity, fracture, and pain, but sometimes also to hypercalcemia, hypercalciuria, and hyperphosphatemia that can cause kidney damage.[7] Two additional natural substrates for TNSALP have been identified from study of HPP patients; phosphoethanolamine and pyridoxal 5′-phosphate (the major circulating form of vitamin B_6). In severely affected newborns and infants with HPP, disturbed vitamin B_6 metabolism can cause vitamin B_6-dependent seizures, seemingly explained by insufficient hydrolysis of the accumulated pyridoxal 5′-phosphate to pyridoxal that can enter the brain for neurotransmitter biosynthesis.[1,3] Damage to other organs in HPP can usually be explained by the underlying skeletal fractures and deformity, sometimes causing fatal pulmonary problems. The calcific arthropathies of HPP reflect the PPi accumulation.[5]

An unexplained feature of HPP, when severe, is muscle weakness that can compromise activities of daily living causing disability.[1,8] This muscle weakness has been considered a "myopathy",[1] but our experience with patients[7,8] and the limited published information (showing unremarkable circulating muscle enzyme levels, nerve conduction studies, and muscle biopsy findings only of deficiency of TNSALP activity) suggests that muscle itself is intact. Accordingly, I see this complication of HPP as muscle weakness without myopathy. How TNSALP deficiency in HPP engenders muscle weakness is an enigma. Preliminary studies suggest that there may be more than three TNSALP natural substrates in HPP. I recall, however, how several key features of severe HPP are recapitulated by toxicity from the first-generation, bisphosphonate disodium 1-hydroxyethylidene diphosphoric acid (etidronate, Didronel®, EHDP). EHDP toxicity features rickets or osteomalacia, hyperphosphatemia, and muscle weakness. In fact, the bisphosphonates have PPi as their parent molecule.

Recent approval of asfotase alfa treatment for pediatric-onset HPP[7-9] has brought attention to this orphan disease, including its muscle weakness. Infants and children given this recombinant, bone-targeted, first-in-class, enzyme replacement treatment can show rapid improvement in their weakness[8,9] that sometimes impresses treating clinicians as occurring too fast to be accounted for by better skeletal mineralization. Perhaps rapid hydrolysis of extracellular PPi with the onset of asfotase alfa treatment implicates PPi in the muscle weakness. However, this requires study.

References

1) Whyte MP: Hypophosphatasia: etiology, nosology, pathogenesis, diagnosis and treatment. Nature Reviews Endocrinology 12:233-46, 2016

2) Millan JL, Whyte MP: Alkaline Phosphatase and Hypophosphatasia. Calcif Tissue Int 98:398-416 doi 10.1007/S00223-015-0079-1. PUBmED pmid: 26590809, 2016

3) Whyte, MP. Hypophosphatasia. In "Genetics of Bone Biology and Skeletal Disease". Thakker RV, Whyte MP, Eisman J, Igarashi T (editors). Elsevier (Academic Press), San Diego, CA, pp 337-60, 2013

4) Wenkert D, McAlister WH, Coburn SP, Zerega JA, Ryan LM, Ericson KL, Hersh JH, Mumm S, Whyte MP: Hypophosphatasia: non-lethal disease despite skeletal presentation in utero (17 new cases and literature review). Journal of Bone and Mineral Research 26: 2389-98, 2011

5) Guañabens N, Mumm S, Möller I, González-Roca E, Peris P, Demertzis JL, Whyte MP: Calcific periarthritis as the only clinical manifestation of hypophosphatasia in middle-aged sisters. Journal of Bone Mineral Research 29: 929-34, 2014

6) Whyte MP, Zhang F, Wenkert D, McAlister WH, Mack KE, Benigno MC, Coburn SP, Wagy S, Griffin DM, Ericson KL, Mumm S: Hypophosphatasia: validation and expansion of the clinical nosology for children from 25 years experience with 173 pediatric patients. Bone 75:229-39, 2015

7) Whyte MP, Greenberg CR, Salman NJ, Bober MB, McAlister WH, Van Sickle B, Wenkert D, Edgar TS, Bauer ML, Hamdan M, Simmons JH, Bishop N, Lutz RE, McGinn M, Craig S, Moore JN, Taylor JW, Cleveland RH, Cranley WR, Lim R, Thacher TD, Mayhew JE, Downs M, Millan JL, Skrinar A, Crine P, Landy H: Enzyme replacement therapy in life-threatening hypophosphatasia. New England Journal of Medicine 366: 904-13, 2012

8) Whyte MP, Madson KL, Phillips D, Reeves A, McAlister WH, Yakimoski A, Mack K, Hamilton K, Kagan K, Melian A, Thompson D, Moseley S, Odrljin T, Greenberg CR: Asfotase alfa therapy for children with hypophosphatasia. JCI Insight 1:e85971; 1-10, 2016

9) Whyte MP, Greenberg CR, Ozono K, Riese R, Moseley S, Melian A, Thompson D, Hofmann C: Asfotase alfa treatment improves survival for perinatal and infantile hypophosphatasia. Journal of Clinical Endocrinology and Metabolism, 101: 334-42, 2016

The Basis of Tendon Function, Homeostasis, Degeneration, and Regeneration

Jess G. Snedeker PhD
University and ETH Zurich, Zurich, Switzerland

Motivation:

Chronic degenerative tendon disease and related injuries are widespread and largely unsolved clinical problems. Plausible estimates suggest that diminished regenerative capacity of tendon and ligament lies behind more than 50% of all musculoskeletal related medical visits and lost workdays – statistics with enormous socio-economic implications.

Collective efforts to isolate, identify, and clinically address the physiological barriers to tendon regeneration are still in their infancy, hindered by a subcritical mass of resources that has until now been invested in tendon research. To guide strategic focus in the development of effective therapies, many gaps in our knowledge must first be overcome.

What is accepted as truth, and what remains unclear:

Tendon repair is limited by available regenerative capacity, with an age-dependent propensity for dysfunctional extracellular matrix synthesis and assembly. Although the various mechanisms of tissue damage and damage accumulation remain unclear, fibrosis-like tendon extracellular matrix repair is widely viewed to be a central factor in the onset and progression of chronic degenerative disease.

As with many tissues, our understanding of tendon physiology is largely built on data from relatively non-physiological experimental models. Despite the often questionable clinical relevance of these models, in vitro and in vivo studies have fairly uniformly indicated a central importance of dynamic mechanical loads in tendon cell regulation. Nonetheless, the precise mechanisms of tendon cell mechano-transduction remain poorly understood, as does the cellular signaling and tissue regulation downstream of various mechanical stimuli. Further the relative importance of cell-cell contacts and cell-matrix contact in tendon homeostasis is poorly apprehended, and the cellular coordination of repair secondary to physiologically relevant matrix damage remains virtually undescribed.
On the other hand, the multi-scale structure of healthy tendon is well characterized. How this structure relates to organ level function is also fairly well understood – with the notable exceptions of the functional location of cellular subpopulations, basic understanding of cellular nutrient supply and metabolism in accordance with tissue oxygen level, and mechanisms for tendon nociception. Also to be noted is the still unfathomed mechanical and biological complexity of structure-function in the tendon extracellular matrix at subcellular size scales. For instance, important aspects of collagen assembly remain unclear including the role of various small collagens and a wide range of fibrillar collagen binding proteins and peptides. Finally, degenerative changes in the extracellular matrix can be diverse and difficult to interpret in the context of tendon cell behavior and tissue homeostasis.

Questions this lecture will address:

This lecture will address many of the topics mentioned above, specifically focusing on three questions: How does multi-scale tendon structure relate to multi-scale function? What is / how does tendon damage? What is / how does tendon repair?

Structure-function will be discussed in terms of energy storing and positional tendons (organ level), the fascicle as the basic functional muscle/tendon unit (tissue level), the collagen fiber and sheath as the basic cellular unit structures (cell level), and molecular constituents of the tendon ECM (protein level). Tendon damage will be discussed in the context of mechanical disruption and accumulation of this damage, molecular inflammation and vascular involvement, and progression to chronically adverse tendon cell activity and tissue disrepair. Finally, what little is known about tendon repair will be discussed, specifically matrix synthesis and turnover, intrinsic vs extrinsic repair, the matrix modeling and remodeling that occurs in acute vs. chronic scenarios, and considerations of the role of nociception and vascularity.

Molecular Therapies to Augment Intrinsic Tendon Repair

Olivier Leupin, PhD
Musculoskeletal Diseases, Novartis Institutes of BioMedical Research (NIBR), Basel, Switzerland

Tendinopathy induced by degenerative changes and/or overuse resulting in tendon tears and tendon rupture is a common cause of morbidity in the general population with a prevalence as high as 45%. Tendinopathy is an unresolved problem in the workplace, in both elite and recreational athletes and in the aging population. There is a high unmet medical need for improvement of tendon repair and regeneration, since such treatments have the potential to shorten the lengthy healing time and to reduce the re-rupture rate.
Imbalances in tendon remodeling in response to mechanical stress, aging and/or drugs such as statins and fluoroquinolones lead to tissue degeneration characterized by overlapping histological, cellular and molecular changes (e.g. disorganized fibril structure, rounding of cell nuclei, and increased expression of catabolic proteases). The normal interplay between tenocytes, tendon stem cells and cells recruited from the circulation to regenerate and repair tendons is affected in conditions of tendinopathy. Tenocytes represent an attractive cell population to identify novel mechanisms to improve intrinsic tendon regeneration and repair. We hypothesize that cell modifications leading to early recruitment, proliferation and maturation of tenocytes are complementary to the regenerative activity of tendon stem cells.
The presentation aims to illustrate various clinical and scientific approaches leading to a better understanding of the intrinsic tendon healing mechanisms.

Hydrogel-based Drug Delivery

David Mooney, PhD
School of Engineering and Wyss Institute, Harvard University

Classic enteral and parenteral drug delivery, and even material-based delivery systems currently used in the clinic, typically require high drug dosages or repeated administration to stimulate a therapeutic effect, which can lower overall efficacy and patient compliance, and result in severe side effects. Further, these strategies typically lead to a low percentage of the drug reaching the target tissue site. The delivery of peptide and protein drugs is often particularly difficult due to their short half-lives in the body. Hydrogel delivery systems can potentially address these issues due to their ability to protect labile therapeutic agents from degradation, tunable physical properties, and controlled degradation. Hydrogels have physical similarities to the native extracellular matrix of many tissues, in that both are water swollen polymer networks. Hydrogels can provide spatial and temporal control over the release of various therapeutic agents, including small-molecule drugs, macromolecular drugs, and cells. A number of mechanisms, at distinct size scales, underlie the design of hydrogel drug delivery systems, and different mechanisms are often combined to provide the desired rate and duration of drug release. Further, one can modulate the release rate of drugs in real time using ultrasound and other stimuli that transiently alter the hydrogel structure and enhance diffusion and/or induce convective currents; nearly digital drug release is possible with certain systems.

Development of an I*n Vitro* Model for Ligament Wound Healing

Stephanie M. F. Tuft, BS[1,2], Erica E. Morrill, MS[3], Raquel J. Brown, MS[2], Julia T. Oxford, PhD[1,2], Trevor J. Lujan, PhD[2,3]
[1]Department of Biological Sciences, Boise State University Boise, ID, USA
[2]Biomolecular Research Center, Boise State University Boise, ID, USA
[3]Department of Mechanical and Biomedical Engineering, Boise State University Boise, ID, USA

INTRODUCTION. Ligaments provide joint stability through a dense network of collagen fibers that align along the primary loading direction. When a ligament is torn, fibroblasts at the wound site repair the tissue by forming scar tissue, a disorganized or multiaxial network of collagen fibers. Over time, repaired tissue achieves only modest fiber realignment, and after one year its strength is less than half that of healthy tissue. This diminished strength can lead to recurrent ligament sprains, pain, and abnormal stress patterns on the articular surface that can trigger irreversible cartilage degeneration. In order to develop clinical techniques that improve the structural and functional restoration of torn ligament, the mechanical and chemical factors that stimulate matrix remodeling must be identified. A challenge to identifying these factors is the absence of an in vitro model for ligament wound healing. The development and validation of an *in vitro* model would enable the study of mechanical and chemical factors that instruct fibroblasts to align the disorganized scar tissue and strengthen the ligament. Prior studies have used cross-shaped (cruciform) molds to develop fibroblastic collagen gels with variable collagen networks.[1,2] Although the center of these cruciform gels has a multiaxial fibrillar microstructure similar to scar tissue, no study has measured the gene and protein expression by cells within these gels to determine if they are suitable as an *in vitro* wound healing model. The objective of this study is to determine if gels that exhibit a multiaxial fiber architecture will promote the expression of genes and proteins associated with healing ligament.

METHODS. Collagen gels seeded with murine fibroblasts were incubated for 1, 2 or 3 weeks under three loading conditions: stress-free, uniaxial, or biaxial. At each time point, five genes associated with ligament wound healing were measured. Confocal microscopy and imaging software measured fiber alignment. In total, 90 collagen gels were synthesized and tested.

Collagen Gels. Collagen gels were produced by adding Purecol (bovine type I collagen), DMEM, and NIH/3T3 mouse embryonic fibroblast cells in culture media. The collagen gel solution was then neutralized to physiological pH with 0.1 M NaOH and brought to a final volume with 1x PBS. This gave a final cell density of 0.83×10^6 cells/mL per gel and a final type 1 collagen density of 1.5 mg/mL. Teflon cruciform molds were machined with a channel aspect ratio of 1:0.5 (Fig. 1A). The cruciform design generates stress in the gel by resisting gel contraction with fixed glass rods (Fig. 1B).[1,2] The stress environment at the cruciform channel arms (uniaxial stress) differs from the cruciform center (biaxial stress). The gel solution was cast into the cruciform molds at 1.2 mL per mold, and at 2 mL per well in a six-well plate (stress-free). Cells were passaged at 60% confluency using trypsin/EDTA, and the collagen solution was allowed 120 minutes to gel at 37°C. Cell culture media was exchanged every three days. 54 cruciform-shaped cellular gels and 36 stress-free discs were created to allow for a 1 week, 2 week and 3 week time course experiment.

Gene Expression. RNA was extracted from the cells using TRIzol reagent. The control specimens consisted of RNA from cells in a 2D tissue culture flask. RNA concentration was determined by measuring the absorbance at 260 nm. Messenger RNA (mRNA) was used as template for cDNA synthesis and amplified by real time quantitative RT-PCR. Genes of interest were contained within the RT² Profiler™ PCR Array Mouse Extracellular Matrix & Adhesion Molecules. All results were normalized to GAPDH, and expressed as positive fold-changes by comparing to results from the 2D tissue culture flask. The genes targeted for analysis include: collagen type I alpha I (Col1a1), collagen type III alpha I (Col3a1), collagen type V alpha I (Col5a1), integrin alpha 5 (Itga5), and tenascin-C (TnC). The rationale for selecting these genes is that previous animal studies on ligament wound healing found scar tissue at three weeks had a 2.6-fold increase in collagen I and a 1.9-fold increase in collagen III[3], and scar tissue at six weeks had a 4.2 fold increase in collagen V[4] and an increase in TnC[5]. In human ruptured ACL, Itga5 showed a 1.7 fold decrease[6].

Mass Spectrometry: Cellular gels were separated into uniaxial, biaxial, or stress free locations. Proteins were extracted using RIPA buffer protocol. In-solution proteolytic digestion, Nano Liquid chromatography mass spectrometry (nano LC-MS) analysis, and finally peptide spectral matching and protein identification were used to determine which proteins were expressed.

Imaging: Confocal microscopy was used to evaluate the collagen fibril alignment in the stressed and stress-free gels at each time point. The collagen gels were imaged at 63x using the 405 nm laser of a Zeiss 510 scanning confocal microscope and ZEN imaging software (Fig 1C-D). FiberFit software was used to apply a fast-Fourier transform that measured fiber

dispersion (fiber disorder) in the confocal images.[9] A trypan blue/calcein AM assay for live/dead cells was used to determine cell viability.

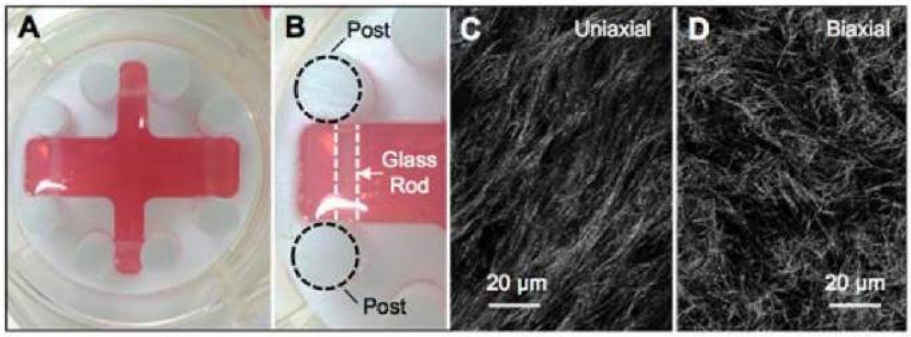

Figure 1: Collagen gels. A) Cruciform. B) Mechanical constraint, C) confocal image of cruciform center and D) cruciform arm.

RESULTS. A gradual increase in collagen was observed for all gels over time (Fig. 2). At three weeks, the stress-free gels had the greatest increase in Col1a1 expression (5.4 fold) and Col5a1 expression (4.8 fold), while the biaxial stressed gels had the greatest increase in Col5a1 expression (12.2 fold). The ratio of Col3a1 to Col1a1 had the greatest increase with time in the stress-free and biaxial gels (Fig. 2D). For all gels, only minor changes occurred over time in the ratio of Col5a1 to Col1a1 (Fig. 2D).

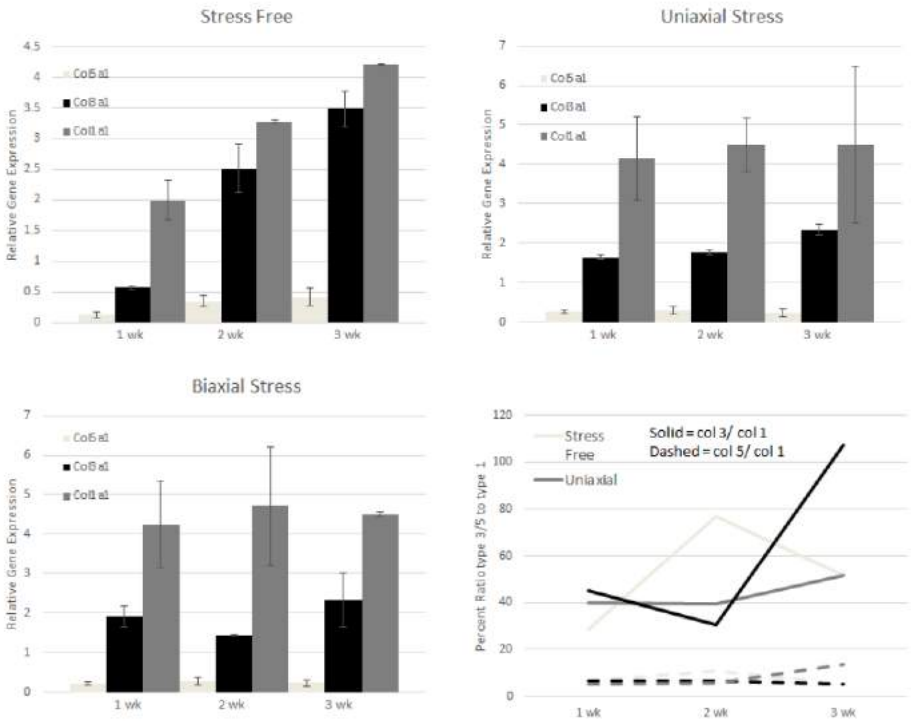

Figure 2: Gene expression when gels are exposed to A) stress-free, B) uniaxial and C) biaxial loads. D) Collagen ratios over time. Values are normalized to GAPDH. Each error bar represents mean ± standard error of the mean (SEM) (n=3).

The increase in expression of Itga5 was lowest (2.7 fold) in the uniaxial stressed gels at two weeks and highest (4.2 fold) in stress-free gels at three weeks. The expression of TnC was greatest in the stress-free gels at week 2 (7.8 fold). Mass spectrometry results show an increase in murine collagen type I, collagen type III and decorin from NIH3T3 cells grown in collagen type-I 3D matrix in both the stress-free and uniaxial-stressed cellular gels. One exception is the decrease in collagen type I from week 1 to week 3 in the uniaxial stressed gels (Fig. 3).

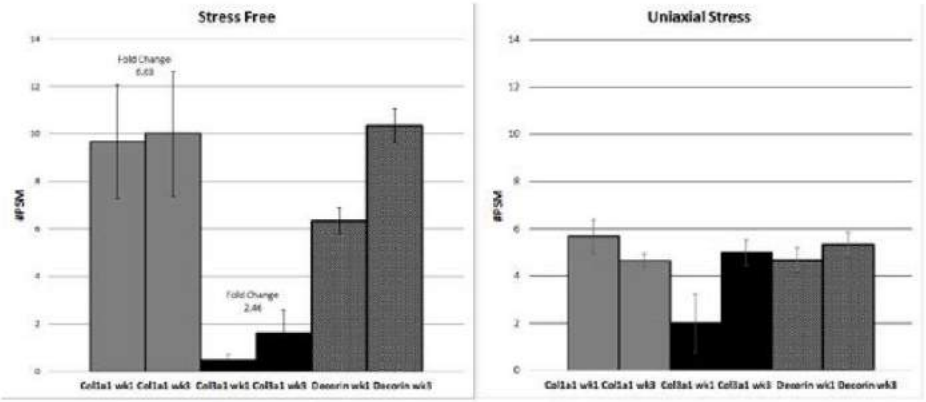

Figure 3: Number of peptide spectral matches (#PSM) for Col1a1, Col3a1 and Decorin. Error bars represent mean ± standard error of the mean (SEM) (n=3). #PSM, have been controlled for bovine collagen type-I and for repeats in #PSM from other proteins.

Image analysis found the uniaxial stressed gels had greater fibril alignment than the biaxial stressed gels (Fig. 1C-D; $p<0.001$). A significant interaction existed, where fibril alignment increased over time in the uniaxial gels and decreased over time in the biaxial gels ($P = 0.02$). Cell viability was robust.

DISCUSSION. This study investigated whether fibroblasts growing in 3D bovine collagen gels could replicate the gene expression observed during ligament wound healing. Based on literature values3, 4, 6, 7, 8, our results indicate that the stress-free gels have a gene expression profile most similar to healing ligament. For example, the stress free gels had gene expressions of Col1a1 and Col5a1 very near to in vivo studies. A close second to the healing ligament profile were the biaxial constructs based on the increase in expressions of the Col1a1, Col3a1, Itga5 genes and their disordered collagen fibril alignment. The uniaxial stressed constructs were least like the healing ligament gene profile and had the most aligned network of collagen fibrils. Based on the proteomics data that mimic that of the gene expression, giving further confirmation that the stress-free cellular gels exhibit healing ligament-like characteristics. Limitations of this work include a small sample size n=3. RNA was normalized to 100 ng per PCR array. Another limitation is that comparable animal studies use different molecular biology techniques. Future work will characterize the molecular constituents using proteomics. To our knowledge, this is the first study to focus on validating an in vitro model for ligament wound healing by examining mRNA expression and collagen fibril alignment in multiaxial collagen gels. Previous animal studies have compared differences in gene expression in fibroblasts from injured and healthy ligament in vivo. Also, studies have mechanically stressed cellular gel constructs but not with the aim of a healing ligament model. Once an in vitro healing ligament model has been validated, it can be used to test the effect of mechanical loading regimes and chemical stimuli on the remodeling and strengthening of the fiber network during healing. This could potentially aid in the development of clinical techniques that restore collagen organization and strengthen the healing ligament.

ACKNOWLEDGEMENTS. The project described was supported by an Institutional Development Award (IDeA) from the National Institute of General Medical Sciences of the National Institutes of Health under Grant #P20GM103408 and #P20GM109095. We also acknowledge support from The Biomolecular Research Center at Boise State with funding from the National Science Foundation, Grants # 0619793 and #0923535; the M. J. Murdock Charitable Trust; Lori and Duane Stueckle, and the Idaho State Board of Education. Its contents are solely the responsibility of the authors and do not necessarily represent the official views of NIH.

REFERENCES

[1] Jhun, C. et al, J Biomech Eng., 131(8): 1-21, 2009.
[2] Sander, E. A. et al, PNAS, 106 (42): 17675-17680, 2009.
[3] Frank, C. B. et al, Osteoarthritis and Cartilage, 7: 130-140, 1999.
[4] Niyibizi, C. et al, Knee Surg, Sports Traumatol, Arthrosc, 8: 281-286, 2000.
[5] Haslauer, C. M. et al, Wound Repair Regen., 22(1): 103-110.
[6] Brune, T. et al, European Cells and Materials, 14: 78-91, 2007.
[7] Chao P. G. et al, Biofabrication, 6: 1-10, 2014.

[8] Neurath M., Zeitschrift fur Orthopadie und Ihre Grenzgebiete, 131(2): 168-172, 1993.
[9] Morrill EE et al., 2015 Proceeding of SB3C, Salt Lake City, UT.

Lesser Tuberosity Osteotomy and Subscapularis Tenotomy Repair Techniques during Total Shoulder Arthroplasty: A Meta-Analysis of Cadaveric Studies

Matthew J. Kraeutler, MD, John B. Schrock, BA, Darby A. Houck, Gina G. Provenzano, BSc, Eric C. McCarty, MD, Jonathan T. Bravman, MD
University of Colorado School of Medicine, Boulder, CO

Introduction: Numerous techniques have been used to mobilize and repair the subscapularis tendon during total shoulder arthroplasty (TSA). The purpose of this study is to perform a detailed comparison of subscapularis tenotomy (Figure 1) and lesser tuberosity osteotomy (LTO) (Figure 2) repairs during TSA.

Methods: Two independent reviewers searched two databases (PubMed and the Cochrane Library) to find cadaveric studies comparing the biomechanical strength of various subscapularis repair techniques following TSA. The following search terms were used: subscapularis, subscapularis repair, arthroplasty, total shoulder, biomechanics, lesser tuberosity osteotomy, and subscapularis tenotomy. Articles that compared at least two repair techniques with similar biomechanical methods were included.

Results: An initial literature search resulted in 145 studies. A title and abstract review resulted in five studies which analyzed outcomes of subscapularis tenotomy (total n = 29) or LTO using a single- or dual-row suture technique (total n = 46). Load to failure was significantly higher in the LTO group (443 ± 231 N) than the tenotomy group (350 ± 113 N) ($p = 0.047$) (Table 1). Tenotomy (n = 19) and LTO (n = 31) had average cyclic displacements of 1.7 ± 1.3 mm and 2.1 ± 1.6 mm, respectively ($p = 0.36$). Mode of failure was significantly different between the two groups ($p < 0.0001$), with soft tissue failure accounting for most tenotomy repairs (97%) and bone failure accounting for the majority of LTO repairs (72%).

Discussion and Conclusion: Based on current biomechanical data, LTO is a stronger repair than a subscapularis tenotomy at "time-zero" in terms of load to failure. However, cyclic displacement did not differ statistically between the two techniques.

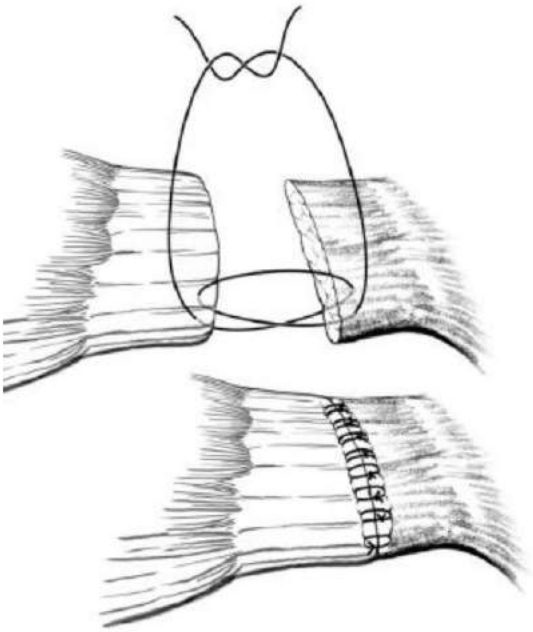

Figure 1: Subscapularis tenotomy repair technique with eight sutures placed in a figure-of-eight fashion.1 Reprinted from Giuseffi SA, Wongtriratanachai P, Omae H, Cil A, Zobitz ME, An KN, et al. Biomechanical comparison of lesser tuberosity osteotomy versus subscapularis tenotomy in total shoulder arthroplasty. J Shoulder Elbow Surg 2012;21(8):1087-1095

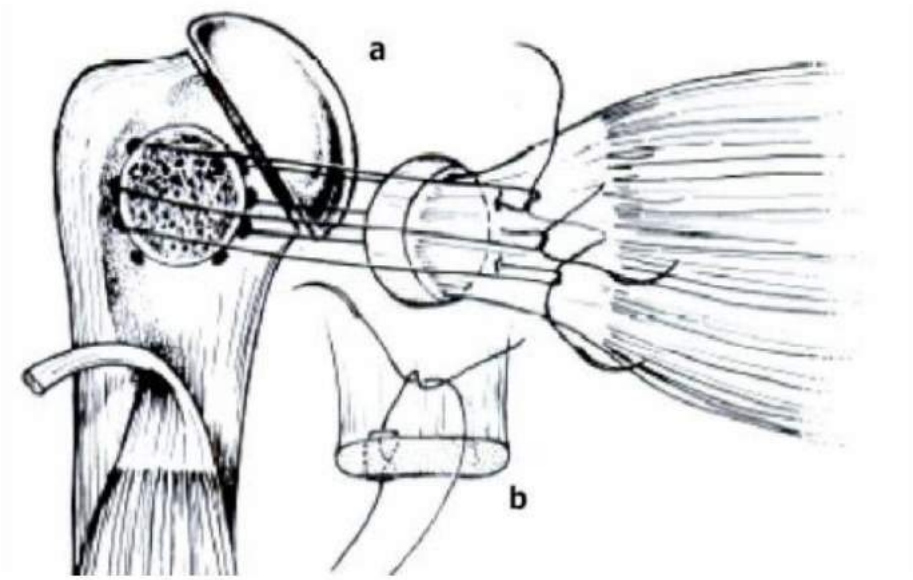

Figure 2: Lesser tuberosity osteotomy subscapularis repair technique.2 Reprinted from Ponce BA, Ahluwalia RS, Mazzocca AD, Gobezie RG, Warner JJ, Millett PJ. Biomechanical and clinical evaluation of a novel lesser tuberosity repair technique in total shoulder arthroplasty. J Bone Joint Surg Am 2005;87 suppl 2:1-8.

Table 1. Load to failure and cyclic displacement outcomes. Data are given as a mean ± SD. LTO = lesser tuberosity osteotomy. *Double-row LTO. †Single-row LTO. [α]Thick osteotomy bony wafer. [β]Thin osteotomy bony wafer.

		Load to failure (N)		Displacement (mm)	
Study	**n**	**Tenotomy (n = 29)**	**LTO (n = 46)**	**Tenotomy (n = 19)**	**LTO (n = 31)**
Fishman et al, 2014[3]	10	300 ± 92	375 ± 125	-	-
Giuseffi et al, 2012[1]	20	439 ± 96	447 ± 89	0.8 ± 0.2	1.8 ± 0.6
Krishnan et al, 2009[4*]	15	252 ± 99	466 ± 158	-	-
Krishnan et al, 2009[4†]		-	430 ± 202	-	-
Ponce et al, 2005[2]	18	334 ± 88	738 ± 261	2.7 ± 1.2	0.9 ± 0.5
Schmidt et al, 2014[5α]	12	-	249 ± 150	-	2.4 ± 1.1
Schmidt et al, 2015[5β]		-	234 ± 97	-	4.2 ± 2.3
Total	75	350 ± 113	443 ± 231	1.7 ± 1.3	2.1 ± 1.6
p-value		*0.047*		0.36	

References:

1. Giuseffi SA, Wongtriratanachai P, Omae H, Cil A, Zobitz ME, An KN, Sperling JW, Steinmann SP. Biomechanical comparison of lesser tuberosity osteotomy versus subscapularis tenotomy in total shoulder arthroplasty. J Shoulder Elbow Surg. 2012;21(8):1087-1095.
2. Ponce BA, Ahluwalia RS, Mazzocca AD, Gobezie RG, Warner JJ, Millett PJ. Biomechanical and clinical evaluation of a novel lesser tuberosity repair technique in total shoulder arthroplasty. J Bone Joint Surg Am. 2005;87 Suppl 2:1-8.
3. Fishman MP, Budge MD, Moravek JE Jr, Mayer M, Kurdziel MD, Baker KC, Wiater JM. Biomechanical testing of small versus large lesser tuberosity osteotomies: effect on gap formation and ultimate failure load. J Shoulder Elbow Surg. 2014;23(4):470-476.
4. Krishnan SG, Stewart DG, Reineck JR, Lin KC, Buzzell JE, Burkhead WZ. Subscapularis repair after shoulder arthroplasty: biomechanical and clinical validation of a novel technique. J Shoulder Elbow Surg. 2009;18(2):184-192.
5. Schmidt CC, Jarrett CD, Brown BT, DeGravelle M Jr, Sawardeker P, Weir DM, Latona CR, Miller MC. Effect of lesser tuberosity osteotomy size and repair construct during total shoulder arthroplasty. J Shoulder Elbow Surg. 2014;23(1):117-127.

7:00 AM – 8:00 AM	**Breakfast & Registration** Support provided by Charles River Laboratories

8:00 AM – 9:00 AM	**ASBMR/Harold M. Frost Young Investigator Awards Presentation**
	Multiscale Mechanics and Mechano-adaptation in Mouse Bone Alessandra Carriero, PhD (*Florida Institute of Technology)*
	Inducible Deletion of β-Catenin in Nucleus Pulposus Cells Demonstrates the Degenerative Mechanism During Tail Compression of Mouse Intervertebral Discs Nilsson Holguin, PhD *(Washington University in St. Louis)*
	Glutaminase Acts in Osteoblasts to Regulate Bone Formation Courtney Karner, PhD *(Duke University)*

9:15 AM – 10:15 AM	**Debate: Is Osteoporosis Over Diagnosed?** **Chair: Steve Cummings, MD *(University of California, San Francisco)***
	Is Osteoporosis Over- or Under-diagnosed? Steve Cummings, MD *(University California, San Francisco)*
	We are Overdiagnosis Osteoporosis - For the Motion Teppo Järvinen, MD, PhD (*University of Helsinki)*
	Is Osteoporosis Over Diagnosed? - Against the Motion Munro Peacock, MD *(Indiana University)*

10:15 AM – 12:00 PM	**Poster Viewing**

2:00 PM – 4:00 PM	**Orienteering**

7:30 PM – 10:00 PM	**ASBMR/Harold M. Frost Young Investigator Awards Presentations**
	The Therapeutic Potential of Endothelial Progenitor Cells in Bone Regeneration Yohei Kawakami, MD, PhD *(Kobe University Graduate School of Medicine)*
	Stem Cells of The Suture Mesenchyme In Craniofacial Bone Development, Repair And Regeneration Takamitsu Maruyama, PhD (*University of Rochester Medical Center)*
	Blood Flow Regulates Function of Endothelium and Bone Formation in the Skeletal System Saravana Ramasamy, PhD *(Max Planck Institute for Molecular Biomedicine)*
	CRISPR/Cas9-generated Mouse Model of Autosomal-dominant Hypocalcemia Harboring the Activating G Protein Alpha 11 Mutation Arg60Cys and Use of Calcilytics and a Gαq/Gα11-specific Inhibitor Kelly Lauter Roszko, MD, PhD *(Endocrine Unit, Massachusetts General Hospital)*
	Anabolic and Anti-resorptive Modulation of Bone Homeostasis by the Epigenetic Modulator Sulforaphane, an Naturally Occurring Isothyiocyanate Roman Thaler, PhD *(Mayo Clinic)*
	Sensory Nerve Signals Mediate Skeletal Adaptation to Mechanical Loads Ryan Tomlinson, PhD *(John Hopkins Medicine)*

Multiscale Mechanics and Mechano-adaptation in Mouse Bone

Alessandra Carriero, PhD
Department of Biomedical Engineering, Florida Institute of Technology, Melbourne FL 32901

Composition and structure of the bone over many length-scales are responsible for its strength, toughness, and ability to adapt to mechanical loads. Aging and disease alter bone composition, disrupt its hierarchical structure and change the loads acting on it, therefore increasing bone's vulnerability to fractures and deformities. My research examines the relation between composition, structure and mechanics of mouse bone model of aging and disease with the aim to (i) develop multiscale pipelines to understand factors affecting bone mechanics and adaptation, improving reproducibility in preclinical testing, and (ii) aid in the development of new treatment for bone fragility and deformities.

Multi-scale mechanics: I developed a novel multidisciplinary approach for investigating mechanisms of fracture in murine bone. Using mouse models of osteogenesis imperfecta with genetic defects of the collagen, my research reveals how small scale molecular abnormalities ramify at larger length scales, causing whole bone fragility. Using interdisciplinary methods, I assess composition, structure, and mechanics from the molecular level to the whole-bone organ level. The use of such a multiscale study allows to detect the salient damage modes and corresponding toughening mechanisms in mouse bones. The application of this pipeline to other mouse bones, models of disease and knock-out genes, will improve our understanding of the interaction between biology and fracture, thus offering insights for more effective treatment strategies for bone frailty.

Mechano-adaptation: Bone adapts its shape and structure in response to the applied loads. My research combines clinical studies, computational modeling and animal experiments to examine how mechanical forces influence bone shape, structure, and function. Particularly, my studies on mouse bone investigate how bone mechano-adaptation is spatially coordinated in aging and disease. I developed new methods to examine 3D bone adaptation and strain mapping across the entire cortical bone surface in mouse bone. These methods will now make it possible to more precisely match strain, as well as other mechanical stimuli investigated with 3D finite element analysis, to the ensuing changes in cellular osteogenic/anti-resorptive adaptive activity between various mouse bones analyzed. Unraveling how gender, aging and disease influence bone mechanoadaptive responses will aid to develop treatment therapies focused on maintaining normal bone mass.

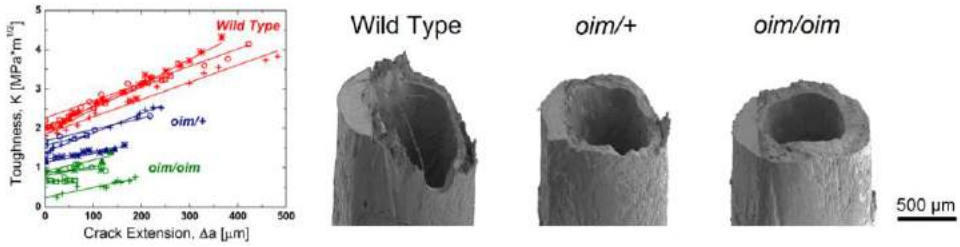

Figure 1 Right) Crack-resistance curve for WT and oim mouse bones [Carriero et al. JBMR 2014] Left) Fracture surface for WT and oim bones [Carriero et al. JBMR 2014]

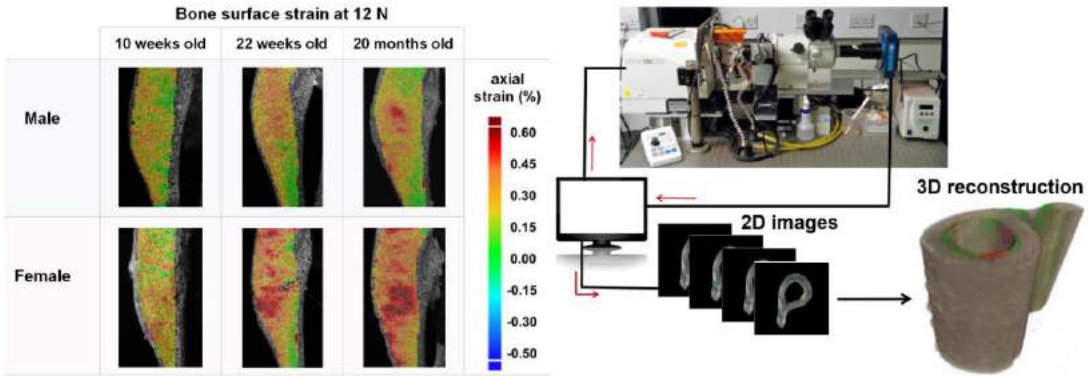

Figure 2 Right) Strain map on male and female mouse bone at 10 w.o., 22 w.o. and 20 m.o. Left) Method for 3D histology of bone adptation: a microtrome and a fluorescence microscope are connected to a PC for automatic slice and view of the bone block. Images are acquired with a camera and saved on the PC. Composite images from different filters were put together in 2D first and then in 3D for the volumetric reconstruction of the bone adaptation (grey is bone, green is calcein and red is alizarin label). Resolution is 1-2 um in image 5um axial.

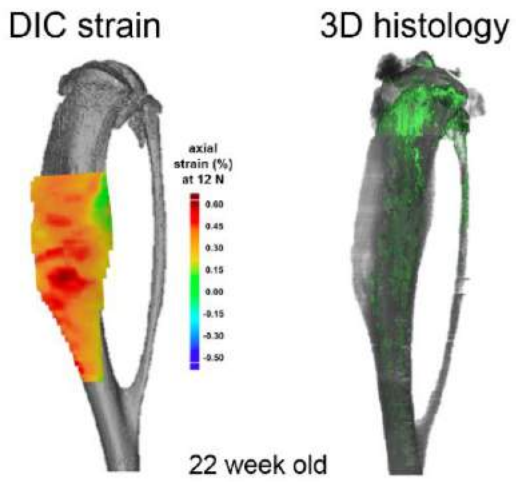

Figure 3 Axial strain map at 12 N and 3D histology reconstruction of the bone and adaptation to load (green) for a 22 w.o. mouse bone. Bone adaptation results from a loading regime of 12N for 40 cycles, 3 times a week for 2 weeks.

Inducible Deletion of β-Catenin in Nucleus Pulposus Cells Demonstrates the Degenerative Mechanism During Tail Compression of Mouse Intervertebral Discs.

Nilsson Holguin, PhD, Matthew Silva, PhD
Washington University School of Medicine, St. Louis, MO

The canonical Wnt pathway is putatively involved in the catabolism of intervertebral discs, where Wnt signaling decreases with mouse aging (a factor of degeneration), but β-catenin (β-Cat), a transcription factor, is promoted in patients with degeneration. Therefore, it is unclear whether disc degeneration is associated with decreased Wnt signaling concomitant to increased β-Cat or if the discrepancy is due species differences. *We hypothesized that tail compression, a model degeneration, reduces Wnt signaling in the nucleus pulposus of mouse discs despite increased β-Cat and that suppression of β-Cat in the nucleus pulposus is a degenerative mechanism.*

We determined the induction of Wnt signaling by 1 week of tail compression of CC7-8 and CC8-9 in 5 mo and 12 mo TOPGAL mice (Wnt-reporter; n=6/age). Gene expression was determined in another set of TOPGAL mice (n=6-8/age). Discs CC10-11 and CC11-12 served as internal controls. To determine the effect of reduced Wnt signaling, β-Cat-floxed mice were bred with SHH-CreER^{T2} to inducibly knockout β-Cat when 4mo mice are dosed with tamoxifen (β-Cat cKO, n=6-10). Histology (L1-L3), qPCR (L3-L5) and mechanical testing (L6-S1) was determined in each animal 3 and 11 weeks after 5 daily doses of tamoxifen. Floxed mice served as controls (CTL, n=5).

One week of chronic compression of tail intervertebral discs applied to young-adult and aged TOPGAL animals initiated a cascade of degenerative changes (Fig.1A, B), which included reduced Wnt signaling (Fig.1A', B', C) in the nucleus pulposus cells of both young-adult and aged animals, despite accumulation of β-Catenin (Fig. 1A", B", D). To mimic the suppression of Wnt signaling in the nucleus pulposus by static compression while obviating neighboring tissues, transcription factor β-Catenin was knocked out in nucleus pulposus cells. These short-term conditional KO discs had less proteoglycan in the nucleus pulposus (Fig.1E), were imbalanced toward aggrecan degradation as determined by gene expression (Fig.1F) and mechanically less stiff (Fig.1G). Long-term KO in adult discs were also less stiff but not less than short-term deletion (Fig.1G), suggesting that the effects of reducing Wnt signaling has a limit. Overall, these data suggest that degenerative-inducing loads reduce Wnt signaling, which has functional consequences, and that the disc may cope by increasing β-catenin. Therefore, clarity of this pathway in the disc may offer therapeutics for the disc under harmful conditions or aging.

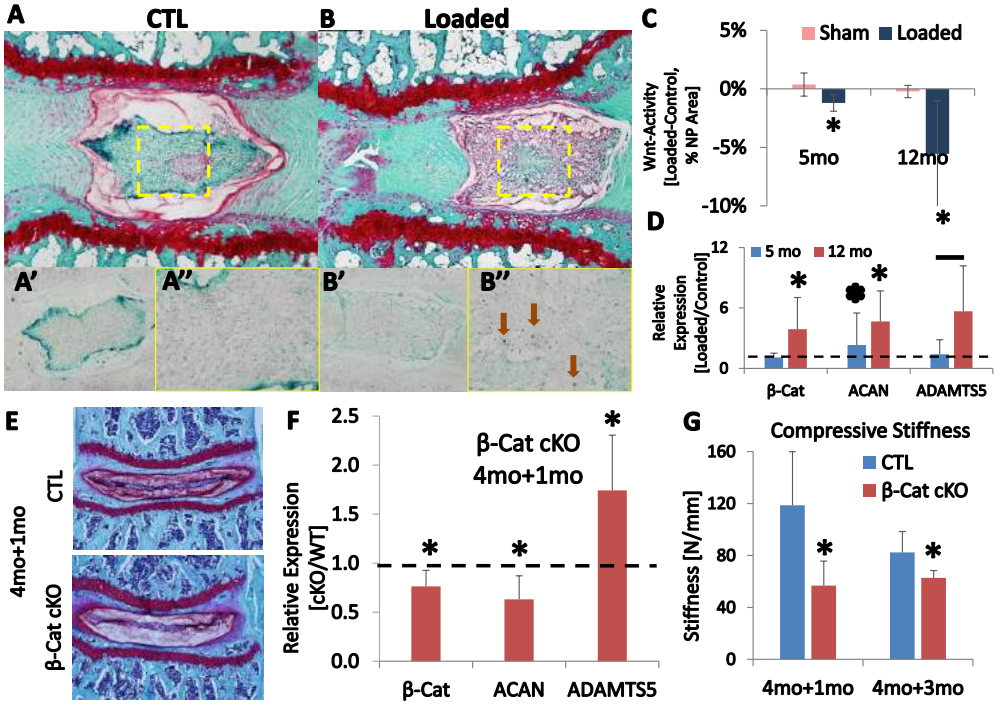

Figure 1. *LacZ (Blue) and Safranin-O (Red) staining of (a) Control (CTL) and (B) Loaded disc in 10X magnification. 20X magnification of LacZ staining of nucleus pulposus of (A') CTL and (B') Loaded disc. 40X magnification of LacZ and IHC of β-catenin (Brown arrow) of (A") CTL and (B") Loaded disc. (C) Reduced Wnt-activity (Blue) with loading in 5 mo and 12 mo discs. (D) Aging enhances gene expression response to compression. 1 mo of β-catenin suppression in Shh-expressing cells reduced (E) nucleus pulposus proteoglycan and gene expression of (F) aggrecan and ADAMTS5. (G) 1 mo and 3 mo of β-catenin suppression accelerated reduction of the compressive stiffness of the intervertebral disc. *P<0.05 CTL vs Loaded or CTL vs* β-Cat cKO.

Glutaminase Acts in Osteoblasts to Regulate Bone Formation

Courtney M. Karner, PhD, Yilin Yu, BA, Everett Knudsen, Fanxin Long, PhD
Duke University, Durham, NC

Wnt signaling has emerged as a critical regulator of osteoblast differentiation and bone formation. A defining feature of osteoblasts is their capacity to produce large amounts of extracellular matrix proteins. Wnt signaling stimulates bone formation by increasing both the number of osteoblasts and their protein-synthesis activity. Increased protein synthesis is very demanding, both energetically and synthetically. How osteoblasts meet these increased energetic and biosynthetic demands is not well understood. We have recently discovered that glutamine metabolism is a critical mediator for Wnt to stimulate osteoblast differentiation and activity. Glutamine is a conditionally essential amino acid that can be metabolized into alpha-ketoglutarate to replenish the TCA (tricarboxylic acid) cycle metabolites, a process termed glutamine anaplerosis. The enzyme glutaminase (GLS) catalyzes the deamination of glutamine to form glutamate, the rate-limiting step in glutamine anaplerosis. During osteoblast differentiation, Wnt stimulates GLS activity and glutamine anaplerosis through the TCA cycle in order to meet the energetic requirements of protein synthesis. Here we show GLS is required for physiological bone formation both *in vitro* and *in vivo*. Using Crispr/Cas9 technology we show GLS protein expression is required for osteoblast differentiation and mineralization in multiple *in vitro* models. Genetic deletion of a floxed *Gls* allele ($Gls^{fl/fl}$) in Prx1Cre positive mesenchymal progenitor cells significantly reduces bone mass *in vivo.* This is due to a significant reduction in both osteoblast numbers and individual osteoblast activity. Likewise, GLS deletion in Sp7 positive osteoblast precursors reduces bone mass. The low bone mass phenotype in Sp7Cre;$Gls^{fl/fl}$ mice is due primarily to decreased osteoblast activity with no effect on osteoblast numbers. Finally, pharmacological inhibition of GLS activity suppresses excessive bone formation in a mouse model for human osteosclerosis caused by hyperactive Wnt signaling. Collectively, these data indicate that GLS functions in mesenchymal progenitors to promote osteoblast differentiation while acting in differentiated osteoblasts to stimulate robust bone forming activity. Thus, the manipulation of GLS activity may provide a valuable therapeutic approach for normalizing deranged protein anabolism associated with human bone diseases.

Is Osteoporosis Over- or Under-Diagnosed?

Steven R. Cummings, MD
S.F. Coordinating Center

The diagnosis of osteoporosis (from the Greek for "porous bone") started out in the 19th century as a name for a pathologic condition observed in patients and autopsies. About a century later it became a clinical diagnosis for vertebral fractures in early postmenopausal women. Riggs and Melton extended the diagnosis to include two types of osteoporosis, Type 1 manifest as vertebral fractures early after menopause and Type 2 as a deficit of bone mass manifest as hip fractures late in life. The development and application of measurements of bone mass by densitometry eventually led to definitions based on statistical definitions based on comparisons to normal values and associations with risk of fracture. Clinical practice and epidemiologic research needed a categorical definition which led to a fundamentally arbitrary diagnosis of osteoporosis based on femoral neck BMD: a T-score ≤ -2.5. This cut-point was essentially based on an estimated 15% prevalence of "osteoporosis" in postmenopausal women that seemed not too high and not too low but just right. The prevalence expanded by defining "osteoporosis" by a T-score ≤ -2.5 at any site that could be measured by any form of bone measurement.

A few studies showed that bone density did not account for the whole of the risk of fractures, giving birth to the general concept of "bone quality." These developments led to a consensus definition from the 2001 NIH Consensus Conference:

"Osteoporosis is defined as a skeletal disorder characterized by compromised bone strength predisposing a person to an increased risk of fracture. Bone strength primarily reflects the integration of bone density and bone quality."

The development of bisphosphonates "for osteoporosis" needed entry criteria for the clinical trials that adopted both prevalence of a vertebral fracture or a T-score <-2.5. The enrollment criteria defined the FDA sanctioned that definition as the indication for treatment of osteoporosis.

Data about risk factors for fracture showed that risk was not congruent with the diagnosis of 'osteoporosis' – many people with high BMD had a low risk of fractures while others had lower BMDs but a high risk of fractures based on characteristics unrelated to properties of bone. Algorithms, particularly FRAX, were adopted for standardized estimates of fracture risk and, logically, indications for treatment were based on fracture risk. The risk, 'treatment threshold,' was defined by a cost-effectiveness analysis for the use of alendronate. These were incorporated into guidelines for when to treat patients with drugs to reduce fracture risk. However, in the U.S. reimbursement for evaluation and treatment of patients continued to rely on the diagnosis of osteoporosis by T-score. This discrepancy led to the recent proposal by the National Bone Health Alliance to define "osteoporosis" by the NOF guideline-based indications for treatment.

Thus, the prevalence of 'osteoporosis' has it's roots in the clinical diagnosis of vertebral fracture, bone densitometry with a committee decision about a reasonable prevalence of osteoporotic BMD, criteria for enrollment in clinical trials leading to the FDA indication, epidemiologic studies of risk factors for fracture, cost-effectiveness analysis of alendronate that led to treatment guidelines. These sources of a definition of 'osteoporosis' have given rise to the debate about whether osteoporosis is over- or under-diagnosed.

We are Overdiagnosis Osteoporosis - For the Motion

Teppo LN Järvinen, MD, PhD[1]
[1] *Department of Orthopaedics and Traumatology, University of Helsinki and Helsinki University Central Hospital, Helsinki, Finland*

Distinguishing the sick from the healthy has always been a fundamental challenge for medicine. A chief concern has been to guard against missing disease, with the focus on problems of underdiagnosis and undertreatment (1). Early detection and subsequent treatment to prevent imminent adverse events is the crux of such strategy. For such strategy to be viable, one is required to a) identify factors that place individuals at "high risk" of a certain event, b) provide means to reduce this risk effectively, c) show that the net adverse effects of the suggested strategy do not exceed the net adverse effects of actual events to be prevented, and d) assess that the costs of providing prevention do not (excessively) exceed the costs of treating the actual events. Since preventive treatment are always targeted at asymptomatic individuals, the evidence-base supporting the strategy needs to be exceptionally sound, as it is possible that patients get exposed to unnecessary harms of treatments and patients (and physicians) misconceive being at "high risk" of a disease as a disease of its own right, and are therefore exposed to adverse psychological effects of disease labelling.

Current prevention strategy for low-trauma fractures among older people rest on the notions that fractures are mainly caused by osteoporosis (pathophysiology), that patients at high risk can be identified (screening), and that the risk is amenable to bone-targeted pharmacotherapy (treatment). However, all these three notions can be disputed.

Pathophysiology: Fractures are primarily caused by falls (2), also in the case of vertebral fractures (3). Most fracture patients have fallen, but actually do not have osteoporosis. A large population-based study of women aged 65 years or more showed that 85% of all low-trauma fractures were not attributable to osteoporosis (4). Moreover, although BMD is on average associated with risk of fracture (5), the added discriminatory capacity of BMD to clinical risk factors remains modest (6). High propensity of falling, in turn, is attributable to aging-related decline in physical functioning and general frailty. Thus a simple question "Do you have impaired balance" can predict about 40% of all hip fractures, (7) whereas osteoporosis predicts less than 30% (4).

Screening: currently available fracture risk prediction strategies including bone densitometry and prediction tools are unable to identify a large proportion of patients who will sustain a fracture, whereas many of those with high fracture risk score will not sustain a fracture (2, 8, 9). Thus, accurate identification of fracture-prone *individuals* is not possible on the basis of DXA-defined osteoporosis or the available fracture prediction tools (10-12).

Treatment: the evidence on the viability of bone-targeted pharmacotherapy in preventing hip fracture is mainly limited to women aged 65 to 80, while the proof of hip fracture-preventing efficacy in women over 80 years of age and in men at all ages is meagre or absent (11, 12). Further, the anti-hip fracture efficacy shown in clinical trials vanishes in real-life studies, possibly (partly) due to discouracingly poor compliance/persistence (~30% at 2 years after the initiation of therapy) (13). Many osteoporosis drugs have also been associated with increased risks of serious adverse events (14, 15). There are also considerable uncertainties related to the efficacy of drug therapy in preventing clinical vertebral fractures, whereas the efficacy for preventing other fractures (relative risk reductions of 20–25%) remains moderate, particularly in terms of the low absolute risk reduction of fractures with the treatment.

Advocates of the prevailing osteoporosis-based prevention and treatment strategy for fractures argue that BMD and fracture risk calculators predict fracture risk as accurately as blood pressure predicts stroke, and considerably better than serum cholesterol predicts coronary artery disease (5, 16, 17). This is true. However, it is rarely noted that this strategy also leads to labelling the majority of otherwise asymptomatic older people as sick and subjecting them to long-term medication to prevent relatively rare morbid events. A disease label can have both positive and negative consequences (18, 19): In a survey assessing how the results of bone densitometry affected women's decisions about measures to prevent fractures and whether labelling women as having below-normal BMD had adverse effects (20), women who reported that their BMD values were below normal were much more likely to take measures to prevent fractures compared with women with normal results, to start hormone therapy, and to take precautions to avoid falling. All this can be considered beneficial for health. However, unfortunately the surveyed women often reported declined physical activity: fear of falling was more prevalent among those reporting low BMD and they also limited their activities to avoid falling.

REFERENCES

1. Moynihan R, Glasziou P, Woloshin S, Schwartz L, Santa J, Godlee F. Winding back the harms of too much medicine. Bmj. 2013;346:f1271.
2. Jarvinen TL, Sievanen H, Khan KM, Heinonen A, Kannus P. Shifting the focus in fracture prevention from osteoporosis to falls. Bmj. 2008;336(7636):124-6.
3. Oudshoorn C, Hartholt KA, Zillikens MC, Panneman MJ, van der Velde N, Colin EM, et al. Emergency department visits due to vertebral fractures in the Netherlands, 1986-2008: Steep increase in the oldest old, strong association with falls. Injury. 2011.
4. Stone KL, Seeley DG, Lui LY, Cauley JA, Ensrud K, Browner WS, et al. BMD at multiple sites and risk of fracture of multiple types: long-term results from the Study of Osteoporotic Fractures. Journal of bone and mineral research : the official journal of the American Society for Bone and Mineral Research. 2003;18(11):1947-54.
5. Marshall D, Johnell O, Wedel H. Meta-analysis of how well measures of bone mineral density predict occurrence of osteoporotic fractures. Bmj. 1996;312(7041):1254-9.
6. Black DM, Steinbuch M, Palermo L, Dargent-Molina P, Lindsay R, Hoseyni MS, et al. An assessment tool for predicting fracture risk in postmenopausal women. Osteoporos Int. 2001;12(7):519-28.
7. Wagner H, Melhus H, Gedeborg R, Pedersen NL, Michaelsson K. Simply ask them about their balance--future fracture risk in a nationwide cohort study of twins. American journal of epidemiology. 2009;169(2):143-9.
8. Collins GS, Michaelsson K. Fracture risk assessment: state of the art, methodologically unsound, or poorly reported? Current osteoporosis reports. 2012;10(3):199-207.
9. Sanders KM, Nicholson GC, Watts JJ, Pasco JA, Henry MJ, Kotowicz MA, et al. Half the burden of fragility fractures in the community occur in women without osteoporosis. When is fracture prevention cost-effective? Bone. 2006;38(5):694-700.
10. Jarvinen TL, Jokihaara J, Guy P, Alonso-Coello P, Collins GS, Michaelsson K, et al. Conflicts at the heart of the FRAX tool. CMAJ : Canadian Medical Association journal = journal de l'Association medicale canadienne. 2014;186(3):165-7.
11. Jarvinen TL, Michaelsson K, Aspenberg P, Sievanen H. Osteoporosis: the emperor has no clothes. Journal of internal medicine. 2015;277(6):662-73.
12. Jarvinen TL, Michaelsson K, Jokihaara J, Collins GS, Perry TL, Mintzes B, et al. Overdiagnosis of bone fragility in the quest to prevent hip fracture. Bmj. 2015;350:h2088.
13. Yeaw J, Benner JS, Walt JG, Sian S, Smith DB. Comparing adherence and persistence across 6 chronic medication classes. Journal of managed care pharmacy : JMCP. 2009;15(9):728-40.
14. Schilcher J, Koeppen V, Aspenberg P, Michaelsson K. Risk of atypical femoral fracture during and after bisphosphonate use. N Engl J Med. 2014;371(10):974-6.
15. Ulmner M, Jarnbring F, Torring O. Osteonecrosis of the jaw in Sweden associated with the oral use of bisphosphonate. J Oral Maxillofac Surg. 2014;72(1):76-82.
16. (WHO) WHO. Assessment of fracture risk and its application to screening for postmenopausal osteoporosis: Report of a WHO study group. WHO Technical Report Series, Report No. 843. WHO, Geneva, Switzerland. 1994.
17. Cooper C, Aihie A. Osteoporosis: recent advances in pathogenesis and treatment. Q J Med. 1994;87(4):203-9.
18. Callard F, Bracken P, David AS, Sartorius N. Has psychiatric diagnosis labelled rather than enabled patients? Bmj. 2013;347:f4312.
19. Haynes RB, Sackett DL, Taylor DW, Gibson ES, Johnson AL. Increased absenteeism from work after detection and labeling of hypertensive patients. The New England journal of medicine. 1978;299(14):741-4.
20. Rubin SM, Cummings SR. Results of bone densitometry affect women's decisions about taking measures to prevent fractures. Annals of internal medicine. 1992;116(12 Pt 1):990-5.

Is Osteoporosis Over Diagnosed? – Against the Motion

Munro Peacock, MD
Indiana University, Indianapolis, IN

Osteoporotic fracture is common and its occurrence depends in part on bone mass, with the incidence higher in women than men and in American whites than in American blacks (1). The occurrence of the three main fractures, wrist, spine and hip rises markedly with age (2). The risk of having one type of fracture increases the risk of having another type, suggesting some common etiological factors, although the wrist starts to increase in the 5th decade, the spine in the 6th and the hip in the 7th decade. Hip fracture caries a particularly high morbidity and mortality and is the most expensive fracture to manage. The cost of management of patients with fracture currently exceeds that of many other common age-related diseases including cancer, respiratory disease, and cardiovascular disease (3;4). Thus, there is no disagreement that the successful prevention and treatment of osteoporotic fracture is a major health care problem. However, there is ongoing disagreement on the diagnosis (5-7) and treatment (8-10).

Osteoporosis was originally defined as too little bone of normal composition by histology and later bone mass measurement. Expansion of the definition to include bone microarchitecture and unquantifiable quality (11), has added much to the literature but little to clinical diagnosis, treatment and management of the disease. Osteoporosis can be caused by a number of underlying pathological conditions, such as vitamin D and calcium deficiency, and severe primary hyperparathyroidism which if cured can often reverse bone mineral density back to normal. However, osteoporosis is also an inevitable physiological feature of aging, and by the age of 80 years the populations mean bone mineral density has decreased by about four standard deviations from peak bone density as a young adult. Both pathological and physiological low bone mass result in fracture and by general usage, they are diagnosed as the same disease, osteoporosis, arguably an unfortunate historical decision. Because of the universal loss of bone with age and its normal distribution around the mean, the classification of low bone mass as a disease was questioned by some earlier investigators (12). Its relation to fracture particularly that at the hip was also questioned when cross sectional studies demonstrated that the diagnosis by bone mineral density of hip fracture patients from subjects who had not yet had a fracture, was largely valueless in the individual because of the large overlap in bone mass measurement between fracture and non- fracture subjects(13) . Further, the value of bone mineral density in diagnosing and predicting fracture was questioned when it was shown in longitudinal studies that the increased incidence of fracture was predicted by advancing chronological age rather than a decrease in measured bone mineral density (14). Never the less, because bone mineral density accounts for about 70% of bone strength and can be measurement relatively precisely clinically, it continues to play a central role in diagnosing osteoporosis, and is the major target for therapeutic intervention.

Fracture is a stochastic event that results from the inability of the skeleton to resist physical trauma. The term 'fragility fracture' is increasingly often used to describe osteoporotic fracture on the misguided, or perhaps misguiding, assumption that trauma can be readily quantitated from patient history. Although severe trauma such as falling down a flight of stairs can be distinguished from a fall to the ground from tripping, the term obscures the fact that a person with underlying low bone mass has increased risk of fracture both to mild and not so mild trauma. Research into prevention of falls and trauma although clearly a major factor in fracture (15) has not received the resources that have been applied to drug treatment of low bone mineral density (16)

Drug therapy is currently the mainstay of management to prevent fracture in both patients who have had a fracture or who have low bone mineral density and considered at increased risk of fracture. However, although drug treatment reduces the incidence of fracture (17), most patients are not treated or have poor compliance (8). Further, no drug reduces the rate to much below 50% (17). The beneficial effect on BMD and bone strength through which the reduction in fracture incidence occurs, disappears when the drug is stopped and the BMD eventually returns to the patient's baseline value. This highlights two important facts. Drug therapy needs to be life-long and in the absence of a specific underlying disease, BMD appears to be an intrinsic characteristic of the individual which drug therapy does not reset.

If the burden of fracture on the health resources of the general population and the individual patient is to be reduced, subjects at risk of fracture need to be diagnosed. Drugs must be developed that effectively stop fracture and permanently reset bone mass at a higher level. In addition, and particularly if such drugs are not forth coming, novel modes of intervention on other etiological causes of fracture must be developed. Such targets will need to involve muscle strength, agility, balance, and other body systems that help to reduce falls and trauma.

Reference List

1. Kellie SE, Brody JA 1990 Sex-specific and race-specific hip fracture rates. Am J Public Health 80:326-328

2. Horsman A, Marshall DH, Peacock M 1985 A stochastic model of age-related bone loss and fractures. Clin Orthop 195:207-215

3. Singer A, Exuzides A, Spangler L, O'Malley C, Colby C, Johnston K, Agodoa I, Baker J, Kagan R 2015 Burden of illness for osteoporotic fractures compared with other serious diseases among postmenopausal women in the United States. Mayo Clin Proc 90:53-62

4. Hopkins RB, Tarride JE, Leslie WD, Metge C, Lix LM, Morin S, Finlayson G, Azimaee M, Pullenayegum E, Goeree R, Adachi JD, Papaioannou A, Thabane L 2013 Estimating the excess costs for patients with incident fractures, prevalent fractures, and nonfracture osteoporosis. Osteoporos Int 24:581-593

5. Jarvinen TL, Michaelsson K, Aspenberg P, Sievanen H 2015 Osteoporosis: the emperor has no clothes. J Intern Med 277:662-673

6. Kanis JA, McCloskey EV, Harvey NC, Johansson H, Leslie WD 2015 Intervention Thresholds and the Diagnosis of Osteoporosis. J Bone Miner Res 30:1747-1753

7. Compston J 2015 Overdiagnosis of osteoporosis: fact or fallacy? Osteoporos Int 26:2051-2054

8. Liu Z, Weaver J, de PA, Li Z, Martin J, Allen K, Hui S, Imel EA 2016 Disparities in osteoporosis treatments. Osteoporos Int 27:509-519

9. Imel EA, Eckert G, Modi A, Li Z, Martin J, de PA, Allen K, Johnston CC, Hui SL, Liu Z 2016 Proportion of osteoporotic women remaining at risk for fracture despite adherence to oral bisphosphonates. Bone 83:267-275

10. Miller PD 2016 Underdiagnoses and Undertreatment of Osteoporosis: The Battle to Be Won. J Clin Endocrinol Metab 101:852-859

11. NIH Consensus Development Panel on Osteoporosis Prevention, Diagnosis, and Therapy, March 7-29, 2000: highlights of the conference 2001 South Med J 94:569-573

12. Newton-John HF, Morgan DB 1970 The loss of bone with age, osteoporosis, and fractures. Clin Orthop Relat Res 71:229-252

13. Cummings SR 1985 Are patients with hip fractures more osteoporotic? Review of the evidence. Am J Med 78:487-494

14. Hui SL, Slemenda CW, Johnston CC, Jr. 1988 Age and bone mass as predictors of fracture in a prospective study. J Clin Invest 81:1804-1809

15. TINETTI M, Speechley M 1989 Prevention of Falls among the Elderly. N Eng J Med 320(16):1055-1059

16. Gillespie LD, Robertson MC, Gillespie WJ, Lamb SE, Gates S, Cumming RG, Rowe BH 2009 Interventions for preventing falls in older people living in the community. Cochrane Database Syst RevCD007146

17. Black DM, Rosen CJ 2016 Postmenopausal Osteoporosis. N Engl J Med 374:2096-2097

The Therapeutic Potential of Endothelial Progenitor Cells in Bone Regeneration

Yohei Kawakami, MD, PhD
Kobe University Graduate School of Medicine, Kobe, Japan

Failures in fracture healing are mainly caused by a lack of neovascularization. The therapeutic potential of endothelial progenitor cells (EPCs) in fracture healing has been demonstrated with mechanistic insight of vasculogenesis/angiogenesis and osteogenesis enhancement at sites of fracture. We have previously demonstrated that local transplantation of G-CSF-mobilized peripheral blood (GM-PB) CD34+ cells, an endothelial/hematopoietic progenitor enriched cell population, contributed to fracture healing. Based on these preclinical achievements, we have started a phase I/II clinical trial of local transplantation of GM-PB CD34+cells in patients with nonunion fracture and fracture healing was significantly accelerated radiographically and symptomatically following cell therapy. However, the scarcity of CD34+ cells in PB and the biological side effect of G-CSF administration and apheresis still remain to be possible problems in clinical settings. In terms of expanding clinical application, we demonstrated that local transplantation of culture expanded bone marrow (BM) CD34+ cells exhibited striking therapeutic efficacy for non-union fracture promoting neovascularization and osteogenesis in sites of fracture even in the same number of freshly isolated BM CD34+ cells or GM-PB CD34+ cells using a rat unhealing fracture model.

Recently, we explored the relationship of SDF-1/CXCR4 pathway in Tie2-lineage cells (including EPCs) and fracture healing. CXC chemokine receptor 4 (CXCR4) is a specific receptor for stromal derived-factor 1 (SDF-1). SDF-1/CXCR-4 interaction is reported to play an important role in vascular development. We demonstrated that EPC SDF-1/CXCR4 axis plays an important role in bone fracture healing using Tie2-Cre^{ER} CXCR4 conditional knockout mice. Our results also indicated that mobilization and incorporation of EPCs in bone fracture healing process was regulated through SDF-1/CXCR4 pathway. The bone fracture healing delayed and formed callus diminished in CXCR4 deficient mice compared with wild type mice. An attenuation of angiogenesis and osteogenesis at fracture site in CXCR4 deficient mice could be considered a cause of this impair in fracture repair.

(Figure) Moreover, the promotion of EPC CXCR4/SDF-1 axis leads to the acceleration of bone fracture healing and might be served as a novel therapeutic application for genetic bone disease and bone injuries.

Figure

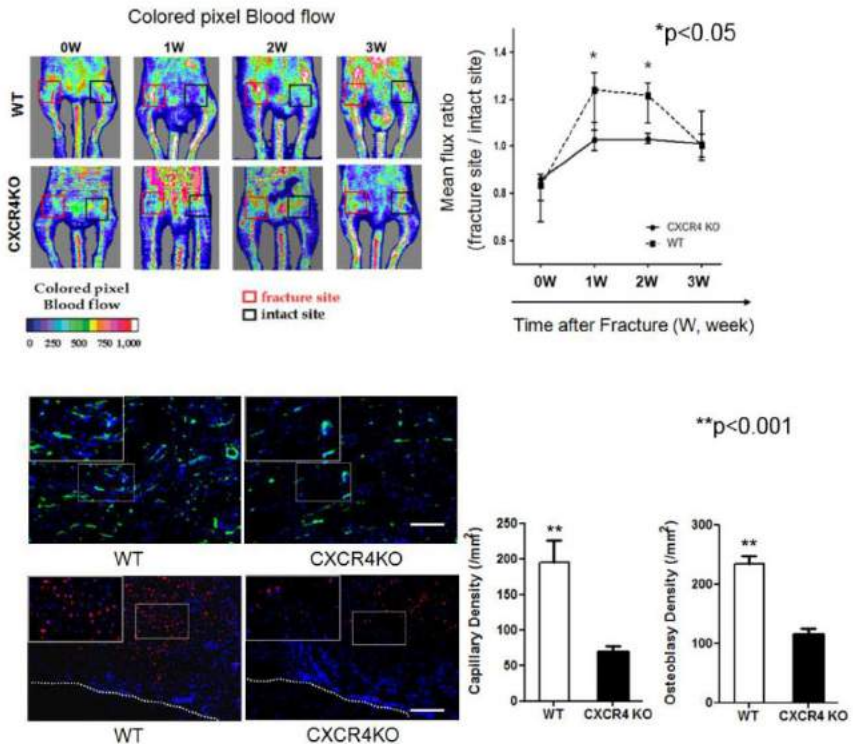

Stem Cells of The Suture Mesenchyme In Craniofacial Bone Development, Repair And Regeneration

Takamitsu Maruyama, PhD[2, 3, 6], Jaeim Jeong, BS[2], Tzong-Jen Sheu[4] and Wei Hsu, PhD[1, 2, 5, 6]
[1]Department of Biomedical Genetics, [2]Center for Oral Biology, [3]Department of Dentistry, [4]Center for Musculoskeletal Research, [5]Wilmot Cancer Institute, [6]Stem Cell and Regenerative Medicine Institute, University of Rochester, Rochester, NY 14642

Development of the skeleton is mediated through two distinct ossification mechanisms. Craniofacial bones are formed mainly through intramembranous ossification, a mechanism different from endochondral ossification required for development of the body skeleton. The skeletal structures are quite distinct between the two, thus they are likely to have their unique stem cell populations. The sutures serve as the growth center critical for healthy development of the craniofacial skeleton. Defects in suture morphogenesis cause its premature closure, resulting in development of craniosynostosis, a devastating disease affecting 1 in ~2,500 individuals. The suture mesenchyme has been postulated to act as the niche of skeletal stem cells essential for calvarial morphogenesis. However, very limited knowledge is available for suture biology and suture stem cells (SuSCs) have yet to be isolated. Here we report the first evidence for identification and isolation of a stem cell population residing in the suture midline. Genetic labeling of SuSCs shows their ability to self-renew and continually give rise to mature cell types over a 1-year monitoring period. They maintain their localization in the niches constantly produce skeletogenic descendants during calvarial development and homeostastic maintenance. Upon injury, SuSCs expand drastically surrounding the skeletogenic mesenchyme, migrate to the damaged site and contribute directly to skeletal repair in a cell autonomous fashion. The regeneration, pluripotency and frequency of SuSCs are also determined using limiting dilution transplantation. In vivo clonal expansion analysis demonstrates a single SuSC capable of generating bones. Furthermore, SuSC transplantation into injured calvaria facilitates the healing processes through direct engraftments. Our findings demonstrate SuSCs are bona fide skeletal stem cells ideally suited for cell-based craniofacial bone therapy as they possess abilities to engraft, differentiate into skeletogenic cell types, generate bones and enhance repair processes. Future study of SuSCs also promises new insights into pathogenic mechanisms of skeletal disease.

Blood Flow Regulates Function of Endothelium and Bone Formation in the Skeletal System

Saravana K. Ramasamy, PhD, Anjali P. Kusumbe, PhD, Ralf H. Adams
Max Planck Institute for Molecular Biomedicine, Roentgenstrasse 20, Muenster-48149, Germany

Blood flow has been linked to bone repair and maintenance, however fundamental aspects of hemodynamics in bone endothelial cell function and osteogenesis remain little understood. In this study, we show that the bone vasculature generates a peculiar blood flow pattern, which critically regulates skeletal angiogenesis. Intravital imaging of bone vasculature reveals that vessel growth in murine bone involves the extension and anastomotic fusion of endothelial buds. Impaired blood flow leads to defective endothelial buds, thus reduced angiogenesis and osteogenesis, and downregulation of Notch signaling in endothelial cells. In aged mice, skeletal blood flow and endothelial Notch activity were also reduced leading to decreased angiogenesis and osteogenesis, which was reverted by genetic reactivation of Notch in the endothelium.
Administration of Alendronate also led to enhanced blood flow and angiogenesis in aged mice. We propose that blood flow and endothelial Notch signaling are key factors controlling ageing processes in the skeletal system.

CRISPR/Cas9-generated Mouse Model of Autosomal-dominant Hypocalcemia Harboring the Activating G Protein Alpha 11 Mutation Arg60Cys and Use of Calcilytics and a Gαq/Gα11-specific Inhibitor

Kelly Lauter Roszko, MD, PhD, Bi Ruiye, Sarah A Howles, Hans Bräuner-Osborne, Xiaofeng Xiong, Fadil M. Hannan, M. Andrew Nesbit, Rajesh V. Thakker, Kristian Strømgaard, PhD Tom Gardella, Michael Mannstadt
Endocrine Unit, Massachusetts General Hospital, Boston, MA

Parathyroid hormone (PTH) acts to maintain extracellular calcium in a tightly regulated range. Inadequate PTH levels result in hypocalcemia and hyperphosphatemia. Activating mutations in *GNA11*, encoding Gα11, have recently been implicated in autosomal dominant hypocalcemia type 2 (ADH2) and are thought to activate the CASR pathway.
One such mutation, uncovered in a family with ADH2, is the heterozygous missense mutation c.178C→ T leading to the replacement of arginine 60 with cysteine in the GTPase domain.
We expressed wildtype (WT) Arg60 and mutant Cys60 Gα11 in HEK293 cells stably expressing the CASR and measured the intracellular calcium response to changes in extracellular calcium concentrations. This showed a leftward shift of the concentration response curve in the cells expressing mutant Gα11, consistent with an increased sensitivity to calcium (Fig 1).
We used CRISPR/Cas9 to create a mouse model of the Arg60Cys mutation. Compared to littermates WT for Gα11, 9-week-old mice heterozygous and homozygous for R60C were hypocalcemic (iCal=1.26±0.03, 1.20±0.04, and 1.12±0.05 mmol/L). Compared to
WT animals, PTH was inappropriate in heterozygous and homozygous animals
(PTH=123±60, 124±17, and 62±18 pg/mL). We explored the effect of calcilytics on these mice by injecting 30 mg/kg of NPS2143 IP; 4 hours after injection, serum calcium was increased in mice WT, heterozygous and homozygous for R60C (1.38±0.12; 1.29±0.04; and 1.25±0.09 mmol/L). Serum PTH increased in all animal groups (Fig 2).
We tested the effects of the specific Gα11/Gαq inhibitor YM-254890. A single dose of
YM-254890 given IP at 0.15mg/kg led to an increase in calcium in WT mice, and in mice heterozygous for R60C (calcium increased from 1.22±0.03 to 1.27±0.02; and 1.19±0.03 to 1.23±0.03) (Fig 3). Published crystallography studies predict that YM-254890 inhibits
WT Gα11, but not Gα11 R60C. Further studies are needed to test whether the observed effects of YM-254890 are due to the effect on WT Gα11.
In summary, we have used CRISPR/Cas9 to create a mouse with the p.Arg60Cys mutation found in humans with ADH2. Our mouse model mimics the biochemical findings of the human disease, namely hypocalcemia and inadequate PTH. We have used the mouse model to show efficacy of treatment with a calcilytic. A Gα11/Gαq inhibitor increased serum calcium in WT animals, and in mice heterozygous for R60C and is therefore an important new tool to explore pathways affected by mutations in Gα11 and a potential treatment.

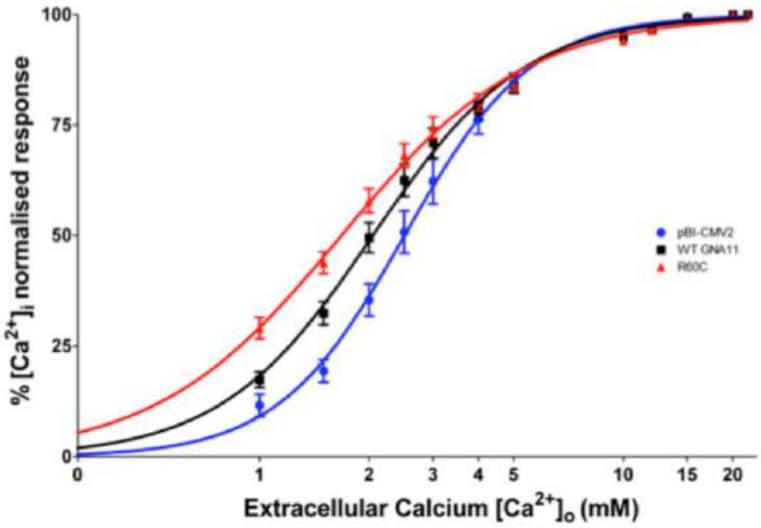

Figure 1. Either wildtype Arg 60 Gα11, mutant Cys60 Gα11, or empty vector was expressed in HEK 293 cells stably expressing the calcium sensing receptor. Intracellular calcium concentration was measured in response to changes in extracellular calcium. This revealed a leftward shift of the curve, consistent with an increased sensitivity to extracellular calcium in the cells expressing mutant Cys 60 Gα11.

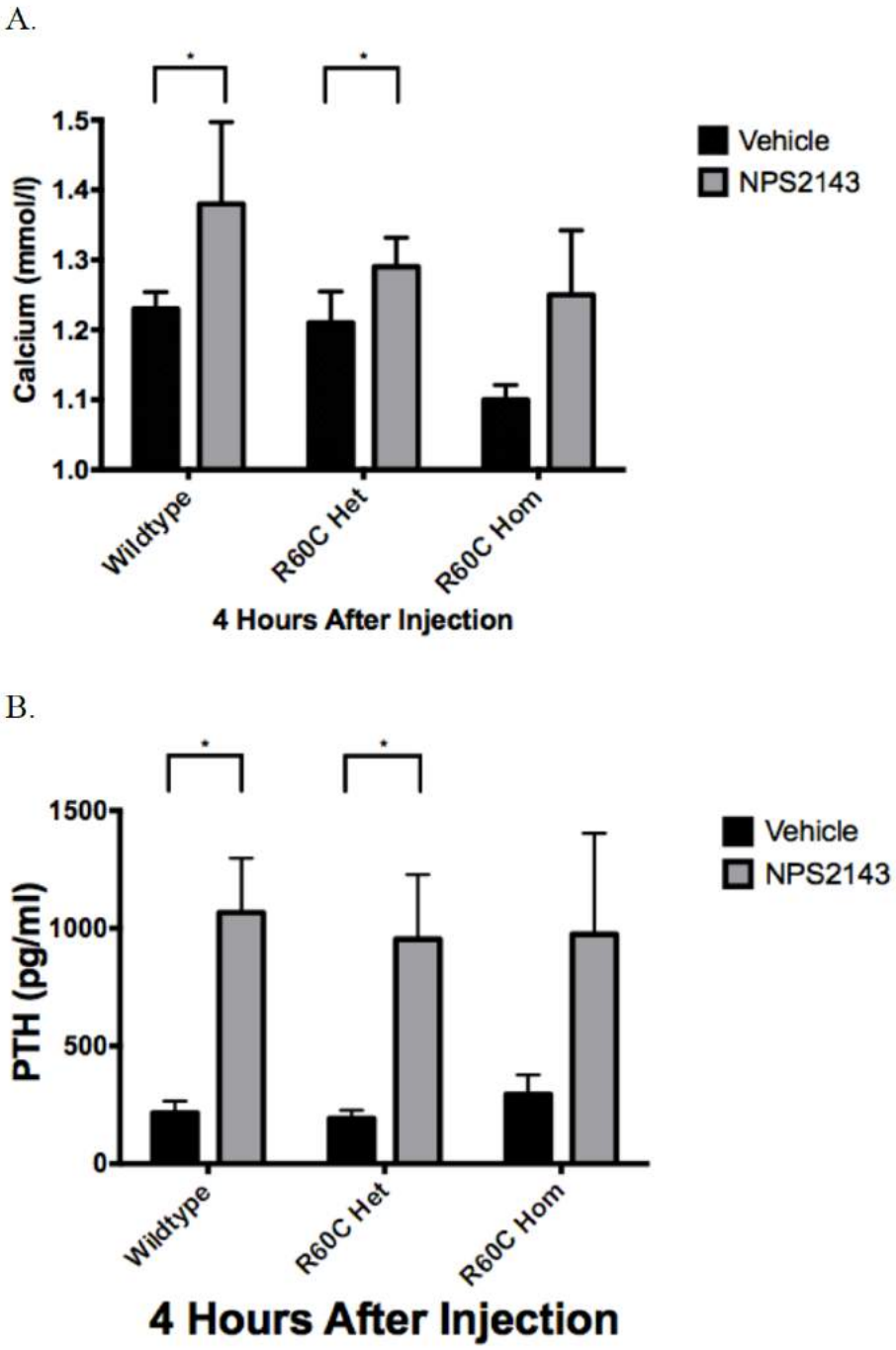

Figure 2. a) Nine week old mice heterozygous and homozygous for Gα11 R60C were hypocalcemic at baseline as compared to wildtype littermates. The serum calcium increased in all groups four hours after injection of the calcilytic NPS2143. There was a significant increase in the calcium in the wildtype and heterozygous mice as compared to vehicle treated littermates. The serum calcium returned to baseline 24 hours after injection in all groups. b) The PTH was inappropriate at baseline in the hypocalcemic Gα11 R60C heterozygous and homozygous mice. PTH increased at one hour in mice injected with NPS2143 and remained elevated four hours after the injection. At four hours,

there was a significant increase in the PTH in wildtype and heterozygous mice as compared to their vehicle treated littermates.

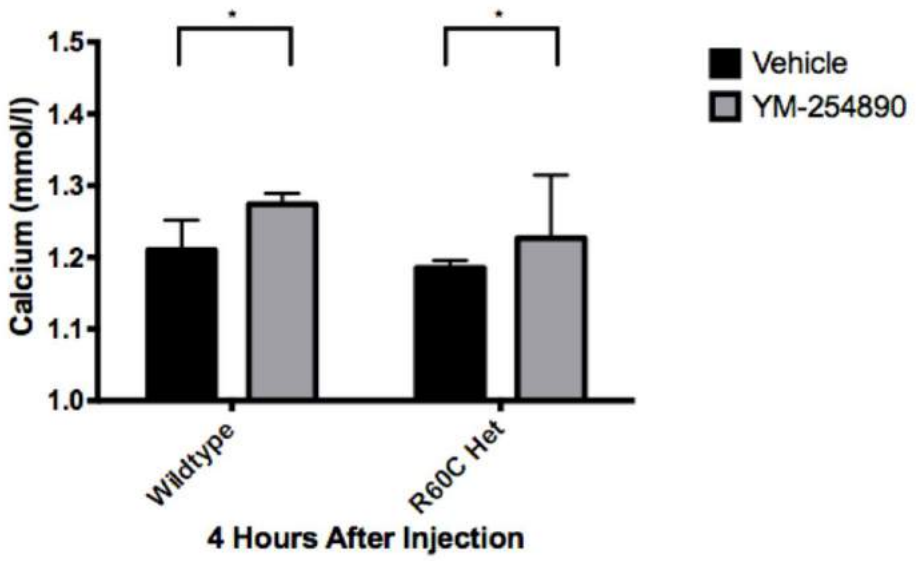

Figure 3. Mice heterozygous for Gα11 R60C were hypocalcemic at baseline. The calcium significantly increased in both wild type and heterozygous mice four hours after injection of the Gα11 inhibitor YM-254890 in comparison to vehicle treated controls. The calcium remained elevated at 24 hours and returned to baseline by 48 hours.

Anabolic and Anti-resorptive Modulation of Bone Homeostasis by the Epigenetic Modulator Sulforaphane, a Naturally Occurring Isothiocyanate

Roman Thaler, PhD
Mayo Clinic, Rochester, MN

Bone degenerative pathologies like osteoporosis may be initiated by age-related shifts in anabolic and catabolic responses that control bone homeostasis. We show that sulforaphane (SFN), a naturally occurring isothiocyanate, promotes osteoblast differentiation by epigenetic mechanisms. SFN enhances active DNA demethylation via Tet1 and Tet2 and promotes pre-osteoblastic differentiation by enhancing extracellular matrix mineralization and by increasing the expression of osteoblastic markers (Runx2, Col1a1, Bglap2, Sp7, Atf4, and Alpl). SFN decreases the expression of the osteoclast activator receptor activator of nuclear factor-κB ligand (RANKL) in osteocytes and mouse calvarial explants and preferentially induces apoptosis in pre-osteoclastic cells via up-regulation of theTet1/Fas/Caspase 8 and Caspase 3/7 pathway. These mechanistic effects correlate with higher bone volume (∼20%) in both normal and ovariectomized mice treated with SFN for 5 weeks compared with untreated mice as determined by microcomputed tomography. This effect is due to a higher trabecular number in these mice. Importantly, no shifts in mineral density distribution are observed upon SFN treatment as measured by quantitative backscattered electron imaging. Further analysis demonstrates that SFN shows similar effects in human mesenchymal stem cells (MSCs), promoting osteogenic but inhibiting adipogenic differentiation by epigenetic mechanisms like active DNA demethylation and histone modifications. Moreover, already after short SFN treatment, MSCs memorize the pro-osteoblastic and anti-adipogenic commitment which endures over several cell divisions. Our data indicate that the food-derived compound SFN epigenetically stimulates osteoblast activity and diminishes osteoclast bone resorption, shifting the balance of bone homeostasis and favoring bone acquisition and/or mitigation of bone resorption in vivo. Furthermore, in human MSCs SNF epigenetically programs these cells into a more osteogenic commitment. Thus, SFN is a member of a new class of epigenetic compounds that could be considered for novel strategies to counteract osteoporosis.

Sensory Nerve Signals Mediate Skeletal Adaptation to Mechanical Loads

Ryan E. Tomlinson, PhD, Zhi Li, PhD, Ryan C. Riddle, PhD, Thomas L. Clemens, PhD
Johns Hopkins University, Baltimore, MD, USA
Baltimore Veterans Administration Medical Center, Baltimore, MD, USA

A critical process required for endochondral bone formation is the invasion of TrkA sensory nerves whose axons are guided to sites of bone formation by retrograde signaling of the neurotrophic factor NGF. As a direct consequence of this developmental process, TrkA sensory nerves densely innervate the periosteal and endosteal surfaces of adult bone, a privileged location for the perception of mechanical signals. Therefore, we hypothesized that NGF-TrkA signaling in sensory nerves is required for skeletal adaptation to the mechanical loads imposed by axial compression of the forelimb. In loaded limbs from NGF-eGFP reporter mice, osteocalcin+ osteoblasts on the periosteal and endosteal surfaces of bone had robust NGF expression 1 and 3 hours after loading, which returned to baseline by 24 hours. However, NGF expression was not observed in osteocytes at any time point or position in the bone. A similar time course of NGF activation was observed after *in vitro* stretching of primary osteoblasts from NGF-eGFP neonates. To selectively disrupt NGF-TrkA signaling, we used mice harboring TrkAF592A knockin alleles that render the endogenous TrkA kinase sensitive to inhibition by the membrane-permeable molecule 1NMPP1. Unlike NGF or TrkA null mice that die perinatally, TrkA-F592A mice live to adulthood and display a normal skeletal phenotype. Following 3 consecutive days of loading, inhibition of TrkA signaling significantly decreased both periosteal and endosteal load-induced bone formation, primarily by decreasing the extent of mineralizing surfaces. To further explore our hypothesis, exogenous NGF was administered to mice 1 hour before loading, which induced thermal hyperalgesia lasting for at least 3 days. Consistent with TrkA inhibition, exogenous NGF significantly increased both periosteal and endosteal loadinduced bone formation by increasing the extent of mineralizing surfaces. Finally, TrkA-F592A mice were subjected to an ulnar stress fracture generated by a single bout of fatigue loading. In this setting, inhibition of TrkA signaling decreased both the innervation and vascularization of the woven bone callus, resulting in significantly diminished woven bone formation 7 days after loading. In total, these results show for the first time that osteoblasts on the bone surface release NGF in response to mechanical load to activate TrkA sensory nerves. Moreover, NGFdependent TrkA signals by sensory nerves are necessary for optimal load-induced bone formation.

7:00 AM – 8:00 AM	**Breakfast & Registration** Support provided by Charles River Laboratories

8:00 AM – 11:00 AM	**Problem: How Can Bone and Muscle Health Be Maintained in Cancer Survivors?** ***Chair: G. David Roodman, MD, PhD (Indiana University)***
	The Skeletal Significance of Monoclonal Gammopathy of Undetermined Significance Matthew Drake, MD, PhD *(Mayo Clinic)*
	Problem: How Can Bone Health Be Maintained in Cancer Survivors? G. David Roodman, MD, PhD *(Indiana University)*
	Maintaining Muscle Health in Cancer Survivors: What is the Target and Is Exercise Enough? Kerri Winters-Stone, PhD, FACSM *(Oregon Health and Science University)*

11:15 AM – 12:00 PM	**Poster Viewing**

12:30 PM – 5:00 PM	**Guided Hike to Pioneer Cabin** Attendees meet at the back door or the Sun Valley Inn at 12:15 PM

7:30 PM – 10:00 PM	**Problem: How Do We Advance the Muscle-Bone Signaling Story?** ***Chair: Sue Bloomfield, PhD, FACSM (Texas A&M University)***
	Advancing the Muscle-bone Signaling Story: Using *in vivo* Models Sue Bloomfield, PhD, FACSM *(Texas A&M University)*
	How Muscle Force Production Affects Bone (or Does it?) Gordon Warren, PhD *(Georgia State University)*
	Exosomes and Microvesicles: New Candidate Mediators for Signaling between Muscle and Bone Mark Hamrick, PhD *(Georgia Regents University)*

The Skeletal Significance of Monoclonal Gammopathy of Undetermined Significance

Matthew T. Drake, MD, PhD
Division of Endocrinology, Department of Medicine; Mayo Clinic, Rochester, MN, 55905

Fractures resulting from age-associated bone loss are common and are expected to increase with the aging population. This age-associated increase in fracture risk is paralleled by the increased risk for developing a monoclonal gammopathy, a spectrum of plasma cell disorders heralded by monoclonal gammopathy of undetermined significance (MGUS). MGUS is a frequent finding identified during routine clinical care. It affects more than 3% of adults aged > 50 years, equal to ~3.5 million US residents. Further, MGUS increases with age, affecting nearly 8% of adults by age 85 (1). As originally described, the 'undetermined significance' portion of the term MGUS reflected the uncertainty in identifying patients with a benign stable plasma cell disorder from those patients destined to progress to the hematologic malignancy multiple myeloma. However, there is now clear epidemiologic evidence that rather than being of condition of 'undetermined significance', patients with MGUS have a significantly increased fracture risk (2,3). Potential etiologies for this increased fracture risk have until recently, however, been poorly understood.

While fracture incidence is increased in MGUS, DXA imaging has provided conflicting results as to whether MGUS subjects have decreased bone mass. DXA limitations include the extrapolation of a two-dimensional (areal) measurement of bone mineral content to derive a three-dimensional volumetric density, as well as the inability to accurately assess bone structure and to differentiate between cortical and trabecular bone compartments. Recent imaging studies using high resolution peripheral quantitative CT clearly show that patients with MGUS have substantial trabecular and cortical microarchitectural deterioration and associated deficits in biomechanical bone strength (4,5), factors which are likely important contributors to the increased skeletal fragility seen in these patients. Further, circulating levels at least two cytokines (the osteoclast-activating factor CCL3/MIP-1α and the osteoblast-inhibitory factor DKK1) with well-recognized roles in bone disease in the closely related monoclonal gammopathy multiple myeloma are also increased in patients with MGUS (4). Collectively, this evolving evidence strongly suggests that care providers need to shift the paradigm from one in which MGUS is considered to be a disorder of 'undetermined significance' to one of 'skeletal significance' in order to ultimately limit skeletal deterioration and fractures in this high-risk population (6).

References

1. Kyle RA, Rajkumar SV 2007 Monoclonal gammopathy of undetermined significance and smoldering multiple myeloma. Hematol Oncol Clin North Am 21(6):1093-1113, ix.
2. Melton LJ, 3rd, Rajkumar SV, Khosla S, Achenbach SJ, Oberg AL, Kyle RA 2004 Fracture risk in monoclonal gammopathy of undetermined significance. J Bone Miner Res 19(1):25-30.
3. Kristinsson SY, Tang M, Pfeiffer RM, Bjorkholm M, Blimark C, Mellqvist UH, Wahlin A, Turesson I, Landgren O 2010 Monoclonal gammopathy of undetermined significance and risk of skeletal fractures: a population-based study. Blood 116(15):2651-2655.
4. Ng AC, Khosla S, Charatcharoenwitthaya N, Kumar SK, Achenbach SJ, Holets MF, McCready LK, Melton LJ, 3rd, Kyle RA, Rajkumar SV, Drake MT 2011 Bone microstructural changes revealed by high-resolution peripheral quantitative computed tomography imaging and elevated DKK1 and MIP-1alpha levels in patients with MGUS. Blood 118(25):6529-6534.
5. Farr JN, Zhang W, Kumar SK, Jacques RM, Ng AC, McCready LK, Rajkumar SV, Drake MT 2013 Altered cortical microarchitecture in patients with monoclonal gammopathy of undetermined significance. Blood.
6. Drake MT 2014 Unveiling skeletal fragility in patients diagnosed with MGUS: No longer a condition of undetermined significance? J Bone Miner Res 29(12):2529-2533.

Problem: How Can Bone Health Be Maintained in Cancer Survivors?

G. David Roodman MD, PhD
Indiana University School of Medicine

Cancer survivors are defined as individuals "living with or beyond cancer". These are patients who have completed initial treatment of their cancer or have no apparent evidence of active disease. This definition includes people living with progressive disease or who may be receiving anticancer treatment but are not in the terminal phases of the disease. Thus, the definition of a cancer survivor is any person diagnosed with cancer from the time of diagnosis until his or her death. This is a very different definition from one that only uses patients who have been cured of their cancer or will die of other causes than their cancer.
Cancer survivors comprise about 4% of the US population and represent more than 14,500,000 people. Patients with any type of cancer can be at risk for musculoskeletal complications from their treatment or their disease. For example, women with breast cancer experience early menopause secondary to chemotherapy, and/or surgery that can directly impact musculoskeletal health. Increased levels of osteoporosis occur in both men and women who are cancer survivors. However, the majority of cancer survivors are women with breast cancer. This is because breast cancer is the most common noncutaneous malignancy in women, and over 90% of women with breast cancer survive at least 5 years from diagnosis. Further, lifestyle factors, such as smoking, alcohol, use of corticosteroids and anticonvulsants for other conditions as well as inactivity that results in weight gain or lack of weight-bearing exercise, further increases the risk of musculoskeletal complications in cancer survivors.

In this session, we will discuss the extent of the problem, focus on particular malignancies and discuss approaches to musculoskeletal health in cancer survivors. I will discuss bone health in cancer survivors. Dr. Matthew Drake will discuss how to maintain bone health in patients with monoclonal gammopathy of undetermined significance, a premalignant condition that occurs in 4% of the population over the age of 55 and in up to 8 percent of the population aged 80. Dr. Kerri Winters will discuss maintaining muscle health in cancer survivors.

Multiple factors contribute to the skeletal sequelae of cancer and cancer therapy. These include hypogonadism, androgen deprivation therapy, estrogen suppression, effects of glucocorticoids on osteoblast, osteocytes and osteoclasts, chemotherapeutic agents such as methotrexate, platinum - containing compounds, cyclophosphamide, doxorubicin and high-dose chemotherapy or radiation therapy used in stem cell transplantation for patients with hematologic malignancies or refractory testicular cancer. Vitamin D deficiency is also common among cancer survivors and cranial radiation can have a direct effect on pituitary function. Further, patients can develop hypoparathyroidism and have skeletal malformations secondary to radiation therapy or surgery. However, the primary cause of cancer induced bone loss is hypogonadism, which can result from chemotherapy, radiation therapy, surgical castration or hormonal therapy. The risk of chemotherapy induced in ovarian failure increases with age because of the decreased number and quality of ovarian follicles. Even in patients without chemotherapy-induced ovarian failure, natural menopause occurs earlier than those not receiving chemotherapy. Further, androgen deprivation therapy or treatment with aromatase inhibitors exacerbates normal bone loss that occurs with aging. In addition, anabolic agents are seldom used in cancer patients because of fear that anabolic agents such as parathyroid hormone can simulate recurrence or growth of residual cancer cells. This is because some cancers express functional PTH receptors. This is especially important for patients with multiple myeloma who do not heal their lytic bone even when in complete remission. Thus, multiple factors combine to have dramatic effects on bone health in cancer survivors and management of these problems is an important area of investigation.

As stated above, women with breast cancer represent the largest single population cancer survivors. It is estimated that $18.1 billion is expended for treatment of breast cancer in the United States and almost $8 billion of these expenditures are for survivorship care. However, there is no universally accepted standardized follow-up for these patients, especially patients with early-stage breast cancer who have completed active chemotherapy or hormonal therapy. Further, it is unclear if oncologists or primary care physicians should follow these patients. Results of randomized trials have shown that patients assigned to care by family physicians had similar health outcomes in terms of recurrence rates, mortality rates and rates of serious clinical events (including pathologic fracture or hypercalcemia) as patients followed by oncologists. Maintaining bone health in breast cancer survivors is important since between 63 to 96% of premenopausal women who receive adjuvant chemotherapy develop ovarian insufficiency within a year of treatment. Chemotherapy

induced ovarian failure results in bone loss as early as 6 months to one year from the initiation of chemotherapy, with highly significant decreases in bone mineral density in the spine or femur within 6 months of starting chemotherapy when compared to patients who maintain ovarian function.

Numerous guidelines have been proposed to help physicians provide appropriate care for breast cancer survivors. The National Comprehensive Cancer Network and the American Society of Clinical Oncology have recently developed guidelines to assist clinicians in the overall care of these patients. Bone targeted therapies have been used in multiple clinical trials to treat or prevent skeletal related events in breast cancer patients. The ABCSG – 12 trial, Z-FAST, and the Z0-fast trials have all shown that bone targeted agents such as bisphosphonates prevent cancer treatment induced bone loss, and that early zoledronic acid treatment increased bone mineral density at the lumbar spine and hip. Interestingly, Gnant et al reported that the addition of zoledronic acid to tamoxifen or anastrozole therapy blocked treatment induced bone loss and skeletal related events. However, which breast cancer patients should receive adjuvant bisphosphonate therapy remains controversial. The Z0-FAST trials supported the use of adjuvant bisphosphonates in patients receiving letrozole, but the AZURE trial did not support the routine use of zoledronic acid in the adjuvant setting for all breast cancer patients, because there was no significant benefit of adjuvant zoledronic acid treatment found for disease-free survival or overall survival. However, the Azure trial did show a survival advantage for bisphosphonate treatment in postmenopausal women regardless if menopause was natural or treatment induced. Similarly to the ABCSG-12 trial, a metaanalysis of 36 trials of adjuvant bisphosphonate therapy in breast cancer patients found no benefit in premenopausal women. However, adjuvant bisphosphonates reduced bone metastasis and improved survival in women who had low levels of reproductive hormones. A more recent trial comparing denosumab to zoledronate therapy for patients with breast cancer bone metastasis found that denosumab was superior in decreasing skeletal -related events, and demonstrated a survival advantage compared to patients receiving zoledronic acid. At the recent ASCO meeting results of the MA-17R trial were presented in which patients were initially treated with tamoxifen or letrozole for 5 years followed by 5 years of letrozole or placebo. The study found that longer treatment with an aromatase inhibitor improved disease-free survival but, the incidence of osteoporosis and fracture was increased significantly, (14% of 9% and 11% of 6%; $p<.001$). A value analysis of the health benefits versus costs of this trial showed that there was very little value supporting generalization of the results of this trial to all breast cancer survivors.

In addition to bone targeted treatments, breast cancer patients can reduce their risk of skeletal issues through lifestyle modifications. Lifestyle changes such as increasing physical activity, modifying diet, weight management, smoking and alcohol cessation or moderation, or other changes that influence comorbidities in these patients, ultimately impact overall survival and have a major impact on bone health in breast cancer patients. Thus, breast cancer survivors face multiple complex issues including maintaining bone health and quality of life.

In men with prostate cancer, androgen deprivation therapy has proven to be effective treatment for locally advanced metastatic prostate cancer. Androgen deprivation therapy is accomplished by treating the patients with GNRH agonists or orchiectomy. Patients receiving androgen deprivation therapy have a decrease in BMD of 2.4% in the 1st year and 7.6% in the 2nd year. Bone loss was greater in patients who were 75 years of age or more, did not engage in regular physical activity and were obese. Bisphosphonates have been shown to improve bone mineral density in prostate cancer patients and denosumab has been shown to increase survival of patients with prostate cancer who are refractory to hormonal therapy.

Adult survivors of childhood cancers also have skeletal issues resulting from their anti-cancer therapy. Many of these effects can occur late. These include decreased bone mineral density, osteonecrosis, slippage of the capital femoral epiphyses and hormone related growth disturbances. In addition, both radiation therapy and surgery for childhood cancers can cause spinal malalignment, spinal growth retardation, limb discrepancies, skull-hypoplasia and craniofacial deformities. Further treatment with L-aspariginase, methotrexate or vincristine have late effects on muscle strength.

Thus maintaining bone health in cancer survivors though the use of bisphosphonates or denosumab, lifestyle changes and increasing exercise levels is critically important, development of safe bone anabolic agents for these patients should be a research priority.

Selected references:

1. Stava CJ, Jimenez C, Hu MI, Vassilopoulou-Sellin R. Skeletal sequelae of cancer and cancer treatment. J. Cancer Surviv. 2009 10.1007/s11764-009-0083-4. PubMed PMID: 19412668
2. Lustberg MB, Reinbolt RE, Shapiro CL. Bone health in adult cancer survivorship. J. Clinical Oncol. 2012 Oct 20;30(30):3665-74. doi: 10.1200/JCO.2012.42.2097. PubMed PMID:23008309
3. Gawade PL, Hudson MM, Kaste SC, Neglia JP, Wasilewski-Masker K, Constine LS, Robison LL, Ness KK. A systematic review of selected musculoskeletal late effects in survivors of childhood cancer. Curr Pediatr Rev. 2014;10(4):249-62. Review. PubMed PMID: 25403639; PubMed Central PMCID: PMC4336580.
4. Melisko ME, Gradishar WJ, Moy B. Issues in Breast Cancer Survivorship: Optimal Care, Bone Health, and Lifestyle Modifications. Am Soc Clin Oncol Educ Book. 2016;35:e22-9. doi: 0.14694/EDBK_159203. PubMed PMID: 27249727.
5. Chen Z1, Maricic M, Bassford TL, Pettinger M, Ritenbaugh C, Lopez AM, Barad DH, Gass M, Leboff MS. Fracture risk among breast cancer survivors: results from the Women's Health Initiative Observational Study Arch Intern Med. 2005 Mar 14;165(5):552-8. PubMed PMID: 15767532

Maintaining Muscle Health in Cancer Survivors: What is the Target and Is Exercise Enough?

Kerri Winters-Stone, PhD, FACSM, Knight Cancer Institute and School of Nursing, Oregon Health & Science University

Cancer treatment can result in loss of muscle mass that results in sarcopenia and weakness that may impact physical functioning and survival. The mechanisms underlying muscle loss can be diverse depending on cancer type, treatment and host factors, such as age. Prostate cancer survivors are at particular risk for muscle loss due to the use of androgen deprivation therapy in disease management that is aimed to reduce testosterone to castrate levels. ADT leads to muscle loss of 2% to 4% as soon as 6 months into treatment[1-3] and is associated with weakness, disability and falls[4]. In bladder cancer patients, sarcopenia is associated with significantly worse 5-year cancer specific survival[5] and in breast cancer survivors faster functional decline post treatment is associated with significantly shortened survival[6]. Exercise, particularly resistance training, is a candidate approach to reverse cancer treatment associated muscle loss and has been modestly studied in some cancer populations. A recent review of progressive resistance training studies identified only six RCTs in varied cancer populations and training effects that produced a net change of -0.1 to 1.5 kg in lean muscle mass, with a mean difference of 0.7 kg between exercise and control groups[7]. The clinical significance of this amount of lean mass change in cancer survivors remains unknown. Though it is expected that increases in muscle mass translate to increases in muscle strength, we know from studies in aging adults that hypertrophy may not be a requisite adaptation to improve muscle strength. In our resistance training trials in breast and prostate cancer survivors we have not observed significant increases in muscle mass between strength trained survivors and untrained controls; however, our functional strength training program consistently increases lower body muscle strength by 15%-25% above control levels.[8-11] In our trial of prostate cancer survivors on androgen deprivation therapy, muscle mass did not increase from strength training but improvements in muscle strength translated directly to reductions in mobility disability[11]. Though exercise may appear to be a universal treatment approach for reversing muscle loss questions remain around therapeutic and clinical significance of observed changes, optimal training programs, integration into clinical care, and exercise tolerance and adherence. In this presentation and discussion we will address which target outcome of muscle health: mass, strength, function or some other characteristic is appropriate for a given cancer survivor population n and research question and whether exercise is the appropriate countermeasure. Other approaches to prevent muscle mass and/or improve strength and function will be highlighted including pharmacologic therapy, nutritional interventions alone or in combination with prescribed exercise, and alternative stimuli such as whole body vibration.

1. Haseen F, Murray LJ, Cardwell CR, O'Sullivan JM, Cantwell MM. The effect of androgen deprivation therapy on body composition in men with prostate cancer: Systematic review and meta-analysis. J Cancer Surviv. 2010;4: 128-139.
2. Smith MR, Saad F, Egerdie B, et al. Sarcopenia during androgen-deprivation therapy for prostate cancer. J Clin Oncol. 2012;30: 3271-3276.
3. Chang D, Joseph DJ, Ebert MA, et al. Effect of androgen deprivation therapy on muscle attenuation in men with prostate cancer. J Med Imaging Radiat Oncol. 2014;58: 223-228.
4. Moe EL BC, Garg B, Dobek JC, Doggett R, Graff JN, Beer TM, Winters-Stone KM.
Falls and Frailty in Prostate Cancer Survivors on Androgen Deprivation Therapy.
American Society of Clinical Oncology Cancer Survivorship Symposium. San Francisco, CA, 2016.
5. Psutka SP, Carrasco A, Schmit GD, et al. Sarcopenia in patients with bladder cancer undergoing radical cystectomy: Impact on cancer-specific and all-cause mortality.
Cancer. 2014;120: 2910-2918.
6. Sehl M, Lu X, Silliman R, Ganz PA. Decline in physical functioning in first 2 years after breast cancer diagnosis predicts 10-year survival in older women. J Cancer Surviv. 2013;7: 20-31.
7. Lønbro S. The effect of progressive resistance training on lean body mass in posttreatment cancer patients – A systematic review. Radiotherapy and Oncology. 2014;110: 71-80.
8. Winters-Stone K, Dobek, J, Nail, L, Bennett, JA, Naik, A, Schwartz, A. Strength training stops bone loss and builds muscle in postmenopausal breast cancer survivors: a randomized controlled trial. Breast Cancer Res Treat. 2011;27: 447-456.
9. Winters-Stone KM, Dobek J, Bennett JA, Nail LM, Leo MC, Schwartz A. The effect of resistance training on muscle strength and physical function in older, postmenopausal breast cancer survivors: a randomized controlled trial. J Cancer Surviv. 2012;6: 189-199.
10. Winters-Stone KM, Dobek J, Nail LM, et al. Impact + resistance training improves bone health and body composition in prematurely menopausal breast cancer survivors: a randomized controlled trial. Osteoporos Int. 2013;24: 1637-1646.

11. Winters-Stone KM, Dobek JC, Bennett JA, et al. Resistance training reduces disability in prostate cancer survivors on androgen deprivation therapy: evidence from a randomized controlled trial. Arch Phys Med Rehabil. 2015;96: 7-14.

Advancing the Muscle-bone Signaling Story: Using *in vivo* Models

Susan Bloomfield, PhD, FACSM
Dept. of Health & Kinesiology, Texas A&M University, College Station, TX

Clever approaches to induce external loading of bone in multiple species dating back to the 1960's defined in detail the relative importance of strain magnitude, strain rate and distribution of strain on bone's anabolic response to loading (5). A burst of research activity in the last decade produced intriguing data about signaling between osteocytes and muscle cells that might explain the impact of skeletal muscle on bone beyond mechanical loading (and even some impact of bone-specific molecules on skeletal muscle). However, nearly all these data derive from cell culture models in which media from one cell type is transferred to the other set of cells or co-culture. By design, these cultured cells are isolated from multiple factors that those cells are exposed to *in vivo*: neural input, changes in blood flow and hence oxygen/nutrient exposure, circulating endocrine or paracrine factors, and exosome-associated miRNA's. However, to define the physiological relevance of any one candidate signaling factor to muscle-bone signaling, we need models in which bone retains not only its intimate physical relationship to skeletal muscle, with shared circulation intact, but also exposure to the fully integrated physiological response to exercise (2).

A number of experimental live animal models exist for studying muscle-bone signaling and each has its advantages/disadvantages. These include stimulated muscle contractions in the anesthetized animal, which allows for precise control of the type, frequency and intensity of muscle contraction (e.g., 3, 8). Purely voluntary exercise with running wheels (4) or elevated food/water to induce standing or climbing minimize stress to the animal but make quantification of the muscle stimulus difficult and may not generate the higher force contractions necessary to muscle-bone signaling. Various paradigms for endurance and resistance training (e.g., 1, 7) exist, each with its own challenges and advantages.

A good example of studies on muscle-bone signaling that utilize the full integrative exercise response are found in a paper published this summer; the results suggest that osteocalcin, an osteoblast protein, plays in important role in skeletal muscle metabolism during endurance exercise by enhancing muscle uptake of free fatty acids and glucose(6). Further, osteocalcin released during exercise appears to promote release of interleukin-6 from contracting skeletal muscle. Notably, the outcomes were generated using a series of genetic models, so whether these signaling interactions are biologically important in genetically intact organisms remains to be defined.

References:

1. Boudreaux RD, Metzger CE, Macias BR, Shirazi-Fard Y, Hogan HA, Bloomfield SA. Bone loss during partial weightbearing (1/6th gravity) is mitigated by resistance and aerobic exercise in mice. *Acta Astronautica* 99: 71-77, 2014.
2. Hawley JA, Hargreaves M, Joyner MJ, Zierath JR. Integrative biology of exercise. *Cell* 159: 738-749, 2014.
3. Hubal MJ, Ingalls CP, Allen MR, Wenke JC, Hogan HA, Bloomfield SA. Effects of eccentric exercise ttraining on cortical bone and muscle strength in the estrogen deficient mouse. *J Appl Physiol* 98: 1674-11681, 2005
4. Lightfoot JT, Turner MJ, Daves M, Vordermark A, Kleeberger SR. Genetic influence on daily wheel running activity level. *Physiol. Genomics* 19:270-276, 2004.
5. Meakin LB, Price JS, Lanyon LE. The contribution of experimental in vivo models to understanding the mechanisms of adaptation to mechanical loading in bone. *Front Endocrinol (Lausanne)* 5:154, 2014.
6. Mera P, Laue K, Ferron M, et al. Osteocalcin signaling in myofibers is necessary and sufficient for optimum adaptation to exercise. Cell Metabolism 2016. http://dx.doi.org/10.1016/j.cmet.2016.05.004.
7. Swift JM, Gasier HG, Wiggs MP, Hogan HA, Fluckey JA, Bloomfield SA. Increased training loads do not magnify cancellous bone gains with rodent jump resistance exercise. *J Appl Physiol* 109:1600-1607, 2010.
8. Swift JM, Hogan HA, Nilsson MI, Sumner LR, Bloomfield SA. Simulated resistance training during hindlimb unloading abolishes disuse bone loss and maintains muscle strength. *J Bone Miner Res* 25: 564-574, 2010.

In vitro models

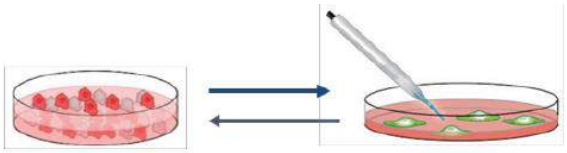

External loading models

+ Deformation of bone tissue; tight control of μE magnitude, rate, # cycles

+ Intact muscle:bone unit (bone, muscle, periosteum)

Stimulated muscle contractions

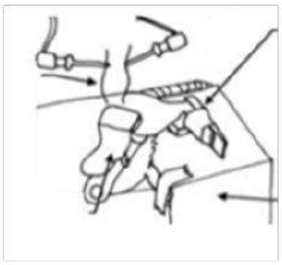

+ Active muscle contraction; tight control of contraction type, intensity, duration

+ Myokine, exosome(?) release

Conscious animal exercise: resistance/endurance modes

+ Integrated response: increased blood flow, altered endocrine factors (insulin, IGF-I, PTH, osteocalcin), sympatho-adrenal activation

How Muscle Force Production Affects Bone (or Does it?)

Gordon Warren, PhD
Georgia State University, Atlanta, GA

According to Wolff's Law [1-3], the structural and mechanical adaptations made by bone should result primarily from the loads imposed upon the bone. Most of this loading (i.e., >70%) comes from forces exerted by skeletal muscle rather than from forces external to the body [4]. Thus, the adaptive responses made by bone should largely be dependent on the level of muscle contractile activity. This talk will initially review the factors modulating muscle force production in both the conscious human/animal and in the anesthetized animal preparation used in conjunction with electrical stimulation. Factors such as muscle size, muscle fiber type, contraction type, contraction velocity, motor unit recruitment, rate coding, stimulation frequency, pulse duration, train duration, impact of injury, etc. will be discussed. The second part of the talk will review the mutability of the mechanical relationship between muscle and bone. We will review experimental manipulations (e.g., increased/decreased activity, estrogen, muscle disease, aging) that we have used in several studies in an attempt to disrupt the muscle-bone mechanical relationship [5-10]. The take-home point from this part of the talk should be that the muscle-bone mechanical relationship is mutable, meaning that the structural and mechanical properties of bone are not solely determined by muscle loads.

References

1. Wolff, J., Concerning the interrelationship between form and function of the individual parts of the organism. By Julius Wolff, 1900. Clin Orthop Relat Res, 1988(228): p. 2-11.
2. Wolff, J., The classic: on the inner architecture of bones and its importance for bone growth. 1870. Clin Orthop Relat Res, 2010. 468(4): p. 1056-65.
3. Wolff, J., The classic: On the significance of the architecture of the spongy substance for the question of bone growth: a preliminary publication. 1869. Clin Orthop Relat Res, 2011. 469(11): p. 3077-8.
4. Lu, T.W., et al., Influence of muscle activity on the forces in the femur: an in vivo study. J Biomech, 1997. 30(11-12): p. 1101-6.
5. Novotny, S.A., et al., Low intensity, high frequency vibration training to improve musculoskeletal function in a mouse model of Duchenne muscular dystrophy. PLoS One,
2014. 9(8): p. e104339.

Exosomes and Microvesicles: New Candidate Mediators for Signaling between Muscle and Bone

Mark W. Hamrick, PhD
Department of Cellular Biology & Anatomy, Medical College of Georgia, Augusta University, Augusta, GA 30912.
mhamrick@augusta.edu.

Muscle-bone interactions are complex and can include a variety of cellular, molecular, and physiological mechanisms. These interactions range from muscle-induced mechanical loads on bone to changes in bone intramedullary pressure in response to muscle contraction. Muscle and bone cells also secrete growth factors and cytokines, which may circulate and impact different organs and tissues in both normal and pathological conditions. Recently, extracellular vesicles (EVs) including exosomes and microvesicles have received considerable attention as key mediators of cell-cell communication. These small (50-200 nm) membrane-bound particles are released by a most cell types. Importantly, EVs carry membrane-bound cargo including proteins, mRNAs, and microRNAs, and EVs can deliver this cargo to target cells via endocytosis and membrane fusion. EVs are most well recognized in cancer biology for seeding future sites of metastasis and serving as potential biomarkers of tumor progression, but other studies have highlighted a potential therapeutic role for stem cell-derived EVs in treating tissue ischemia. We have recently investigated a potential role for exosomes and microvesicles in aging bone. EVs can be isolated from bone marrow interstitial fluid, and in vitro these EVs are endocytosed by myoblasts (Fig. 1). Aged, bone-derived EVs can suppress the expression of myogenic genes, suggesting that the EVs are biologically active and can impact transcription of specific genes in recipient cells.

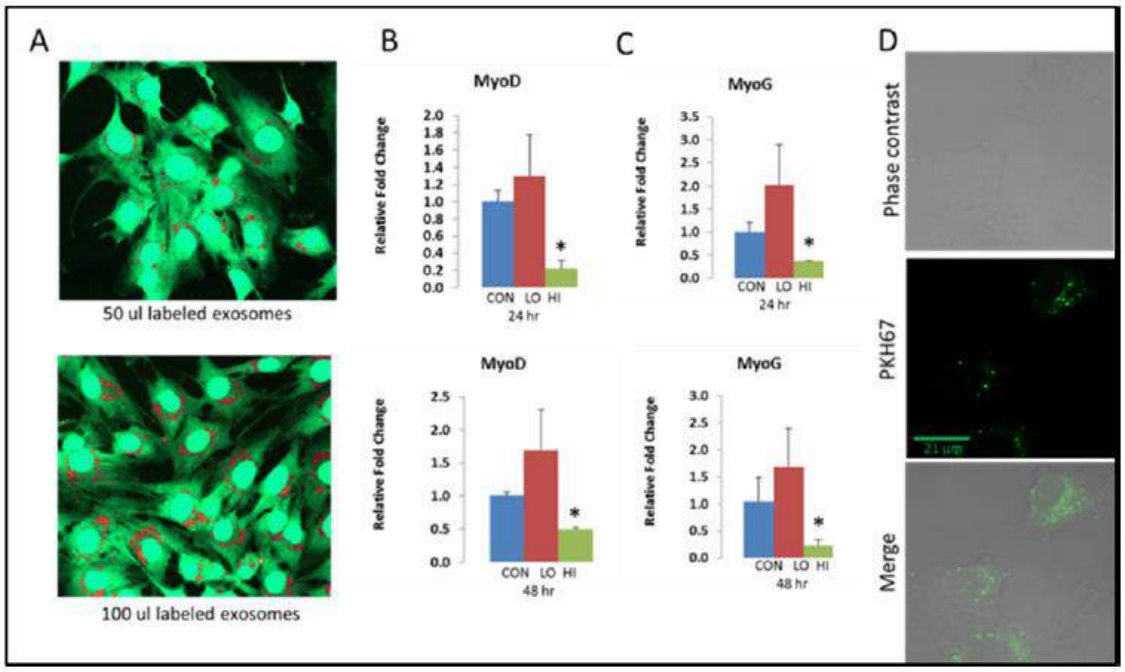

Figure 1. Myoprogenitor cells accumulate bone-derived EVs. A. Mouse C2C12 myoprogenitor cells treated with aged mouse bone marrow exosomes labeled with Exo-Red to stain mRNA and miRNA. RTPCR shows that the myogenic markers B. MyoD and C. Myogenin (MyoG) are downregulated with higher exosome concentrations at both 24 and 48 hours. LO=50µg/ml, HI=250µg/ml. *P

EVs can be tracked in vivo by DiR labeling and infrared imaging using IVIS/Xenogen or Ami X imaging systems. Our own experiments indicate that bone-derived EVs injected via tail vein in mice are distributed to most organs and tissues, including muscle, within 24 hours. Organs can also be imaged using this approach ex vivo to confirm EV distribution, and even localized in frozen tissue sections (Fig. 2).

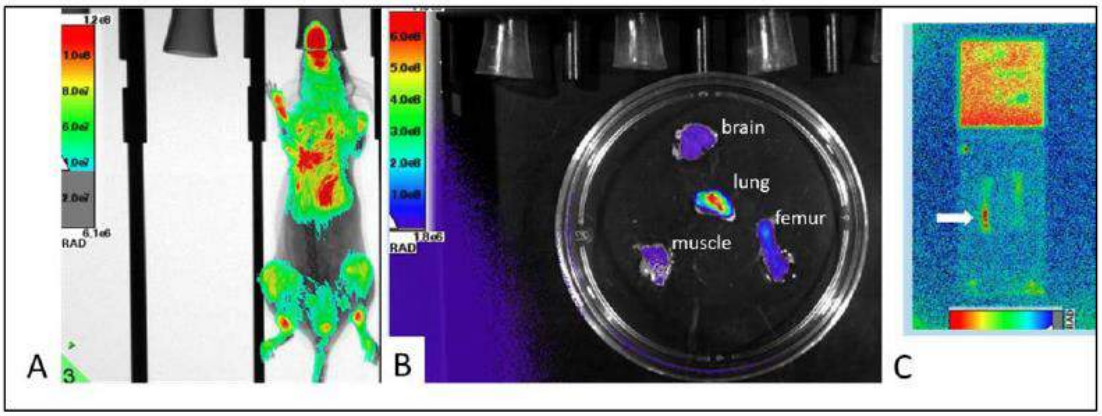

Figure 2. Biodistribution of DiR-labeled, bone-derived extracellular vesicles (3.0 mg/ml, 100 µl volume) 24 hrs after i.v. (tail vein) injection in vivo (A) and ex vivo (B) from the same mouse. Femur shown in (C) is a frozen section of the same femur in (B). Imaging was performed using Ami X instrument 24 hrs postinjection.

Muscle cells also produce EVs in vitro and in vivo, and EV release is stimulated by a rise in intracellular calcium, a key step in muscle contraction. Muscle-derived EVs can be isolated from serum using alpha-sarcoglycan immunocapture (Guescini et al., 2015), which facilitates the identification of muscle-derived proteins and microRNAs carried by circulating EVs to bone or other organs and tissues. Cre-lox technology now facilitates in vivo tracking of EVs derived from specific cell types. For example, Cre-expressing hematopoietic cells secrete EVs carrying Cre mRNA (but not protein), and neurons that endocytose these Cre+ EVs can be recognized using ROSA reporters such as Td-tomato or LacZ (Ridder et al., 2014). Another approach that has been used successfully in tumor cells utilizes Cre-reporter cells that switch from (DsRed+) to (eGFP+) expression once these cells receive EVs from Cre+ cells (Zomer et al., 2016). This technology should prove to be a powerful tool for studying muscle-bone interactions, since it would be possible to study differences in gene expression or function between cell populations that take up EVs secreted by specific tissue types.

References:

Guescini M et al. (2015) Muscle releases alpha-sarcoglycan positive extracellular vesicles carrying miRNAs in the bloodstream. PLoS One. 10(5):e0125094.

Ridder K et al. (2014) Extracellular vesicle-mediated transfer of genetic information between the hematopoietic system and the brain in response to inflammation. PLoS Biol. 3;12(6):e1001874. Zomer A et al. (2016) Studying extracellular vesicle transfer by a Cre-loxP method. Nat Protoc. 11(1):87- 101.